Applications of Fungal Prenyltransferases in the Chemoenzymatic Synthesis

Anwendungen von pilzlichen Prenyltransferasen in der Chemoenzymatischen Synthese

Dissertation

zur

Erlangung des Doktorgrades

der Naturwissenschaften

(Dr. rer. nat.)

dem

Fachbereich Pharmazie

der Philipps-Universität Marburg

vorgelegt von

Kang Zhou

aus **Hunan, China**

Marburg/Lahn **Jahr 2017**

Erstgutachter: **Prof. Dr. Shu-Ming Li**

Zweitgutachter: **Prof. Dr. Peter Kolb**

Eingereicht am **21. März 2017**

Tag der mündlichen Prüfung am **05. Mai 2017**

Hochschulkennziffer: 1180

Dedicated to my family

Table of contents

List of publications

Kang Zhou, Carsten Wunsch, Jungui Dai, and Shu-Ming Li (2017). *Gem*-diprenylation of acylphloroglucinols by a fungal prenyltransferase of the dimethylallyltryptophan synthase superfamily. *Org. Lett.,* 19 (2): 388–391

Wei Zhao, Aili Fan, Sylwia Tarcz, **Kang Zhou**, Wen-BingYin, Xiao-Qing Liu, and Shu-Ming Li (2017). Mutation on Gly115 and Tyr205 of the cyclic dipeptide *C2*-prenyltransferase FtmPT1 increases its catalytic activity toward hydroxynaphthalenes. *Appl Microbiol Biot*echnol, 101: 1989–1998

Kang Zhou, Wei Zhao, Xiao-Qing Liu, and Shu-Ming Li (2016). Saturation mutagenesis on Tyr205 of the cyclic dipeptide *C2*-prenyltransferase FtmPT1 results in mutants with strongly increased *C3*-prenylating activity. *Appl Microbiol Biotechnol,* 100 (23):9943-9953

Kang Zhou, Xia Yu, Xiulan Xie, and Shu-Ming Li (2015). Complementary flavonoid prenylations by fungal indole prenyltransferases. *J. Nat. Prod.,* 78 (9): 2229–2235

Kang Zhou, Lena Ludwig, and Shu-Ming Li (2015). Friedel-Crafts alkylation of acylphloroglucinols catalyzed by a fungal indole prenyltransferase. *J. Nat. Prod.*, 78 (4): 929–933

Share of author contributions

Publication (status)	Authors	Estimated equity ratio [%]
Gem-diprenylation of acylphloroglucinols by a fungal prenyltransferase of the dimethylallyltryptophan synthase superfamily. *Org. Lett.*, (published)	Zhou, K.; Wunsch, C.; Dai, J.; Li, S.-M.	50
Mutation on Gly115 and Tyr205 of the cyclic dipeptide *C2*-prenyltransferase FtmPT1 increases its catalytic activity toward hydroxynaphthalenes. *Appl Microbiol Biot*echnol. (published)	Zhao, W.; Fan, A.; Tarcz, S.; Zhou, K.; Yin, W.-B.; Liu, X.-Q; Li, S.-M.	15
Saturation mutagenesis on Tyr205 of the cyclic dipeptide *C2*-prenyltransferase FtmPT1 results in mutants with strongly increased *C3*-prenylating activity. *Appl Microbiol Biot*echnol. (published)	Zhou, K.; Zhao, W.; Liu, X.-Q; Li, S.-M.	45
Complementary flavonoid prenylations by fungal indole prenyltransferases. *J. Nat. Prod.* (published)	Zhou, K.; Yu, X.; Xie, X.; Li, S.-M.	60
Friedel-Crafts alkylation of acylphloroglucinols catalyzed by a fungal indole prenyltransferase. *J. Nat. Prod.* (published)	Zhou, K.; Ludwig, L.; Li, S.-M.	65

………………………………….   ………………………………….

Signature candidate   **Signature supervisor**

Abbreviations

For units of measurements, the international system of units and units derived thereof have been used. Acronyms and abbreviations are explained in detail in the corresponding passage in the text.

2D NMR	two dimensional nuclear magnetic resonance
4HB	4-hydroxybenzoate
5-DMATS	5-dimethylallyl tryptophan synthase
5-DMATS$_{Sc}$	5-dimethylallyltryptophan synthase from *Streptomyces coelicolor*
6-DMATS	6-dimethylallyl tryptophan synthase
6-DMATS$_{Sa}$	6-dimethylallyltryptophan synthase from *Streptomyces ambofaciens*
6-DMATS$_{Sv}$	6-dimethylallyltryptophan synthase from *Streptomyces violaceusniger*
7-DMATS	7-dimethylallyl tryptophan synthase
APs	acylphloroglucinols
AnaPT	indole diterpene prenyltransferase anaPT
AtaPT	*Aspergillus terreus* aromatic prenyltransferase
A. fumigatus	*Aspergillus fumigatus*
A. terreus	*Aspergillus terreus*
br	broad (NMR signal)
CD$_3$OD	deuterated methanol
CDCl$_3$	deuterated chloroform
CoA	coenzyme A
CCL	carboxyl CoA ligase
CHS	chalcone synthase
Comp.	compound
Conc.	concentration
COSY	correlation spectroscopy
Cyclo-L-Trp- L-Leu	*cyclo*-L-tryptophanyl-L-leucinyl
Cyclo-L-Trp-L-Pro	*cyclo*-L-tryptophanyl-L-prolinyl
D$_2$O	deuterium oxide
d	doublet
DCM	dichloromethane
DMA	dimethylallyl

DMAPP	dimethylallyl diphosphate
DMATS	dimethylallyltryptophan synthase
DMSO-d_6	deuterated dimethyl sulfoxid
DNA	deoxyribonucleic acid
EI-MS	electron impact mass spectrometry
ESI-MS	electrospray ionization spectrometry
E. coli	*Escherichia coli*
FPP	farnesyl diphosphate
GPP	geranyl diphosphate
GGPP	geranylgeranyl diphosphate
His$_5$	pentahistidine
His$_6$	hexahistidine
His$_8$	octahistidine
HMBC	heteronuclear multiple bond correlation
HPLC	high performance liquid chromatography
HR	high resolution
HSQC	heteronuclear single quantum coherence
Hz	hertz
HIPT-1	aromatic prenyltransferase from *Humulus lupulus*
HIPT1L	aromatic prenyltransferase HIPT
HIPT2	aromatic prenyltransferase HIPT
H. lupulus	*Humulus lupulus*
H. monopetalus	*Hexalobus monopetalus*
IPP	isopentenyl diphosphate
IPTG	isopropyl β-thiogalactopyranoside
J	coupling constant
k_{cat}	turnover number
kDa	kilo Dalton
K_M	Michaelis-Menten constant
LB	lysogeny broth
m	multiplet
MAPP	monomethylallyl diphosphate (also methylallyl diphosphate)
MHz	mega hertz
MVA	mevalonate

MS	mass spectrometry
multi	multiplicity
n × C5	number of C5 units, minimum 1
Ni-NTA	nickel-nitrilotriacetic acid
NMR	nuclear magnetic resonance
NOESY	nuclear overhauser effect spectroscopy
NRPS	non-ribosomal peptide synthase
N. fischeri	*Neosatorya fischeri*
A_{600}	absorption at 600 nm
PT	prenyltransferase
PKS	polyketide synthase
PIBP	phlorisobutyrophenone
PIVP	phlorisovalerophenone
PBZP	phlorbenzophenone
PPi	inorganic diphosphate
ppm	parts per million
q	quartet
rel. conv.	relative conversion
RP	reverse phase
rpm	revolutions per minute
s	singlet
SDS	sodium dodecyl sulfate
SDS-PAGE	sodium dodecyl sulfate polyacrylamide gel electrophoresis
sp.	species (sing.)
spp.	species (pl.)
syn.	synonymous
t	triplet
TB	Terrific-Broth
TBA	tetrabutylammonium
Tris	2-amino-2-(hydroxymethyl)-propan-1,3-diol
v/v	volume per volume
VPS	valerophenone synthase
× g	gravitational acceleration

Summary

Plants, bacteria, and fungi provide diverse structures derived from their primary and the secondary metabolism. Representative substances from secondary metabolite pathways are flavonoids, coumarins, xanthones, and indole alkaloids. The attachment of isoprene units (n × C5) such as dimethylallyl (DMAPP), geranyl (GPP), or farnesyl (FPP) moieties to the backbones of aromatic secondary metabolites is a further step for the broad diversification. Prenylated natural products often exhibit stronger pharmacological activities than their non-prenylated precursors. The prenyltransferases (PTs) accomplish these prenyl transfer reactions in nature. Therefore, the investigation on the applications of prenyltransferases could be used for structural modification of aromatic substances to produce biologically active compounds.

Prenylated acylphloroglucinols (APs), which have remarkable chemical structures and intriguing biological and pharmacological activities, are characteristic constituents of several plant families. Main structural features of prenylated APs are highly oxygenated and densely decorated with prenyl moieties, such as dimethylallyl and geranyl moieties. Phlorisobutyrophenone (PIBP), phlorisovalerophenone (PIVP), and phlorbenzophenone (PBZP) serve as precursors of most prenylated APs. In the first part of this thesis, the acceptance of APs catalyzed by thirteen fungal prenyltransferases in the presence of DMAPP was elucidated. Nine regular prenylated products were obtained from the reactions with AnaPT. The results indicated that AnaPT catalyzes the same prenylation of PIBP and PIVP as the membrane-bound prenyltransferases like HlPT-1 involved in the biosynthesis of the prenylated APs in plants, but with much higher conversion yields than HlPT-1. However, only monoprenylated derivatives were obtained in the presence of DMAPP and the conversion yields of PIBP, PIVP, and PBZP with GPP as prenyl donor were very low in AnaPT reactions. Recently, a fungal prenyltransferase AtaPT was demonstrated to carry an unprecedented promiscuity toward diverse drug-like aromatic acceptors and prenyl donors including DMAPP, GPP, and FPP. On the availability of AtaPT, we investigated the behavior of AtaPT toward PIBP, PIVP, and PBZP. Twenty-one prenylated APs were isolated and their structures were elucidated by NMR and MS analyses. Total conversion yields were calculated for the three APs with AtaPT and DMAPP, which are significantly higher than those of AnaPT. *C*-prenylated products are in consistent with the AnaPT products. *O*-

prenylated products were also obtained from the reaction mixtures of PIBP and PIVP. Also *Gem*-diprenylated derivatives were identified in the reaction mixtures of these substrates respectively. *C*-monoprenylated products were converted into *gem*-diprenylated derivatives as predominant products in the presence of DMAPP. GPP and FPP also served as good prenyl donors for the reaction of AtaPT. Only one *C*-prenylated derivative and one *O*-prenylated derivative each were identified from these incubation mixtures.

Subsequently, prenylation of different flavonoids including flavanones and isoflavones by AnaPT at C-6 of the A ring or C-3′ of the B ring was demonstrated. Twelve prenylated flavonoids from incubation mixtures of flavonoids with AnaPT in the presence of DMAPP were produced. Previous studies found that 7-DMATS accepted chalcones, isoflavonoids, and flavanones much better than flavones and flavonols and mainly catalyzed prenylation at C-6. AnaPT and 7-DMATS show different substrate preferences and prenylation positions.

In the third part of this thesis, we identified a key amino acid residue Tyr205 in FtmPT1 for the interaction with its aromatic substrate brevianamide F. Saturation mutagenesis on this position resulted in all nineteen possible mutants. FtmPT1_Y205N and FtmPT1_Y205L differ from FtmPT1 in behaviors toward four *cyclo*-Trp-Pro isomers. Regularly *C2*-prenylated derivatives were detected as main products of FtmPT1 reactions with all these isomers. In contrast, the reversely *C3*-prenylated products were found to be the main products in Y205N and Y205L reactions with *cyclo*-D-Trp-D-Pro, *cyclo*-D-Trp-L-Pro, and *cyclo*-L-Trp-D-Pro, while regularly *C2*- and *C3*-prenylated derivatives were identified in their reaction mixtures with *cyclo*-L-Trp-L-Pro. These results indicated that the isomers are in different positions and orientations in the reaction chamber and Tyr205 is important for the prenyl transfer reaction, but can be replaced by other amino acids.

The results obtained during this thesis demonstrate that AtaPT and AnaPT could be promising candidates for production of prenylated APs like β-bitter acids by synthetic biology. AnaPT and 7-DMATS could be used complementarily for prenylation of flavonoids. The mutants of FtmPT1 can be used for production of regularly *C3*-prenylated brevianamide F in synthetic biology.

Zusammenfassung

Pflanzen, Bakterien und Pilze produzieren vielseitige primäre und sekundäre Stoffwechselprodukte. Beispiele der Sekundärstoffe sind Flavonoide, Coumarine, Xanthone und Indolalkaloide. Das Anhängen von Isopreneinheiten (n x C5), wie Dimethylallyl (DMAPP), Geranyl (GPP) oder Farnesyl (FPP) an aromatischen Grundstrukturen des Sekundärmetabolismus ist ein weiterer Schritt in der Diversifizierung dieser Stoffe. Die prenylierten Naturstoffe zeigen häufig stärkere pharmakologische Aktivitäten als ihre nicht-prenylierten Vorgänger. In der Natur wird die Übertragung der Prenyleinheit von Prenyltransferasen realisiert. Aus diesem Grund können Prenyltransferasen genutzt werden, um aromatische Substanzen zu modifizieren und somit neue biologisch aktive Stoffe herzustellen.

Prenylierte Acylphloroglucinole (APs), die sich durch bemerkenswerte chemische Strukturen und verblüffende biologische und pharmakologische Aktivitäten auszeichnen, sind charakteristische Sekundärstoffe verschiedener Pflanzenfamilien. Wichtige Strukturmerkmale von prenylierten APs sind hoch oxidiert und dicht verziert mit Prenylgruppen, wie Dimehylallyl- und Geranyleinheiten. Phlorisobutyrophenone (PIBP), Phlorisovaerophenone (PIVP) und Phlorbenzophenon (PBZP) sind die Vorstufen der meisten prenylierten APs. Im ersten Teil dieser Arbeit wurde die Akzeptanz der APs durch dreizehn pilzliche Prenyltransferasen in der Gegenwart von DMAPP untersucht. Neun regulär prenylierte Produkte wurden durch Einsatz von AnaPT erhalten. Die Ergebnisse weisen darauf hin, dass AnaPT dieselben Prenylierungen von PIBP und PIVP wie die membrangebundenen Prenyltransferasen, wie z.B. HIPT-1, katalysiert, welche in die Biosynthese von prenylierten APs in Pflanzen involviert sind. Die Umsatzrate mit AnaPT sind jedoch deutlich höher als mit HIPT-1. Allerdings wurden nur monoprenylierte Derivate in Gegenwart von DMAPP erhalten und die Umsatzraten von PIBP, PIVP und PBZP mit GPP als Prenyldonor waren sehr gering. Vor Kurzem wurde mit der pilzlichen Prenyltransferase AtaPT eine außergewöhnliche Promiskuität gegenüber diversen Arzneimittel-relevanten aromatischen Akzeptoren und Prenyldonoren, darunter DMAPP, GPP, und FPP, nachgewiesen. Daraufhin untersuchten wir das Verhalten von AtaPT gegenüber PIBP, PIVP und PBZP. Einundzwanzig prenylierte APs wurden isoliert und ihre Strukturen mittels NMR und MS aufgeklärt. Die Umsetzungen der drei APs wurden mit AtaPT und DMAPP bestimmt und waren deutlich höher als die mit AnaPT. Gleiche C-prenylierte Produkte wie AnaP-

3

ZUSAMMENFASSUNG

Reaktionen wurden identifiziert. *O*-prenylierte Produkte wurden aus den Reaktionen mit PIBP und PIVP erhalten. Auch *Gem*-diprenylierte Derivate konnten in den Reaktionsgemischen identifiziert werden. *C*-monoprenylierte Produkte wurden in Anwesenheit von DMAPP hauptsächlich zu *gem*-diprenylierte Derivate umgesetzt. GPP und FPP waren auch gute Prenyldonoren der AtaPT-Reaktionen. Nur ein einziges *C*-prenyliertes und ein *O*-prenyliertes Derivat konnten aus diesen Reaktionen identifiziert werden.

Anschließend wurden Prenylierungen verschiedener Flavonoide, darunter Flavanone und Isoflavone durch AnaPT am C-6 des A-Rings und dem C-3´ des B-Rings untersucht. Zwölf prenylierte Flavonoide wurden in den Reaktionsgemischen von Flavonoiden und AnaPT in der Gegenwart von DMAPP produziert. Es ist bekannt, dass 7-DMATS Chalcone, Isoflavonoide und Flavanone deutlich besser als Flavone oder Flavonole akzeptiert und hauptsächlich die Prenylierung am C-6 katalysiert. AnaPT und 7-DMATS zeigen unterschiedliche Substratpräferenzen und Prenylierungspositionen.

Im dritten Teil dieser Arbeit wurden die für die Interaktion von FtmPT1 mit dem aromatischen Substrat Brevianamide F Schlüssel-Aminosäure Tyr205 identifiziert. Mittels Sättigungsmutagenese an dieser Position wurden Mutanten von allen übrigen 19 Aminosäuren hergestellt. FtmPT1_Y205N und FtmPT1_Y205L unterscheiden sich von FtmPT1 in ihrem Verhalten gegenüber den vier *cyclo*-Trp-Pro Isomeren. Regulär C2-prenylierte Derivate wurden als Hauptprodukte der FtmPT1 mit diesen Isomeren identifiziert. Dagegen waren revers *C3*-prenylierte Produkte die Hauptprodukte von Y205N und Y205L mit *cyclo*-D-Trp-D-Pro, *cyclo*-D-Trp-L-Pro und *cyclo*-L-Trp-D-Pro, während regulär *C2*- und *C3*-prenylierte Derivate mit *cyclo*-L-Trp-L-Pro nachgewiesen wurden. Diese Ergebnisse lassen darauf schließen, dass die Isomere in unterschiedlichen Positionen und Orientierungen im aktiven Zentrum vorliegen und Tyr205 für die Reaktion zwar wichtig ist, jedoch durch andere Aminosäuren ersetzt werden kann.

Die Ergebnisse dieser Arbeit zeigen, dass AtaPT und AnaPT vielversprechend Kandidaten für die Produktion von prenylierten APs, wie beispielsweise β-Bittersäuren im Rahmen der synthetischen Biologie sein können. AnaPT und 7-DMATS könnten komplementär für die Prenylierung der Flavonoide genutzt werden. Die Mutanten der FtmPT1 können für die Produktion von regulär *C3*-prenyliertem Brevianamid F in der synthetischen Biologie genutzt werden.

1. Introduction

1.1. Prenylated aromatic secondary metabolites

Prenylated aromatic secondary metabolites are distributed throughout all kingdoms of life. These compounds fulfil various roles in their plant, bacterial or fungal hosts and the prenyl residue is a key element for the presented biological and pharmacological activities (Botta et al. 2005b; Chen et al. 2014a; El-Seedi et al. 2010; Heide 2009a; Li 2010; Liu et al. 2015; Sunassee and Davies-Coleman 2012). The basic chemical structures of these metabolites emerge from different biosynthetic pathways and form various substance classes, including acylphloroglucinols (APs), flavonoids, indole alkaloids, naphthalenes, quinones, xanthones, and coumarins (Figure 1-1, A). The distinctive prenyl moieties play an important role in the structural diversity of these natural products, due to various prenylation positions forming C-C, C-O or C-N bonds on the aromatic nucleus and different patterns (regular or reverse) as well as lengths of the prenyl chain from dimethylallyl diphosphate (DMAPP, C5 unit), geranyl diphosphate (GPP, C10 unit), farnrsyl diphosphate (FPP, C15 unit), to geranylgeranyl pyrophosphate (GGPP, C20 unit) (Figure 1-1, B) (Heide 2009a; Winkelblech et al. 2015a). In addition, the prenylated compounds can be further modified by rearrangement, cyclization, oxidation, and hydroxylation reactions (Heide 2009a; Raju et al 2011). The prenylated aromatic metabolites are classified into prenylated acylphloroglucinols, flavonoids, indole alkaloids, naphthalenes, quinones, xanthones, and coumarins. The prenylated acylphloroglucinols, flavonoids, and indole alkaloids are described and summarized in this thesis in details.
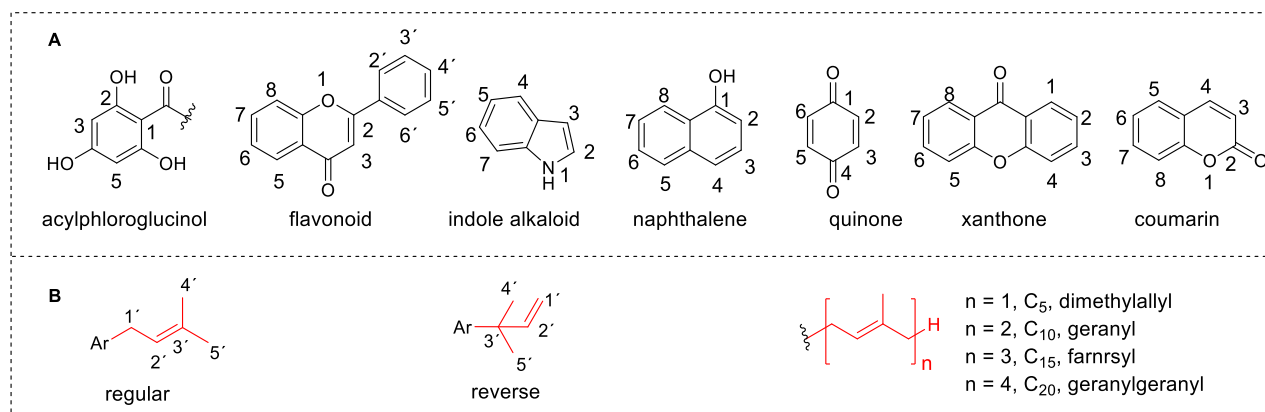

Figure 1-1. (A) Aromatic scaffold with numbering; (B) Examples of regular and reverse prenyl patterns and different lengths of prenyl moieties.

1.1.1. Prenylated acylphloroglucinols

Prenylated acylphloroglucinols (APs) are characteristic constituents of plant families including Clusiaceae, Hypericaceae, and Cannabaceae. Prenylated APs are classified into monocyclic polyprenylated acylphloroglucinols (MPAPs) and polycyclic polyprenylated acylphloroglucinols (PPAPs) (Ciochina and Grossman 2006). Two classes of MPAPs are found in hops, α-acids and β-acids. The PPAPs feature a highly oxygenated and densely substituted bicyclo[3.3.1]nonane-2,4,9-trione or bicyclo[3.2.1]octane-2,4,8-trione core decorated with C_5H_9 or $C_{10}H_{17}$ (dimethylallyl, geranyl, etc.) side chains. The PPAPs can be divided into three classes: type A PPAPs have a C-1 acyl group and an adjacent C-8 quaternary center, type B PPAPs have a C-3 acyl group, and the rare type C PPAPs have a C-1 acyl group and a distant C-6 quaternary center (Figure 1-2). Secondary cyclizations involving the β-diketone and pendant olefinic groups may occur to afford adamantanes, pyrano-fused, or other cyclized structures (Ciochina and Grossman 2006).
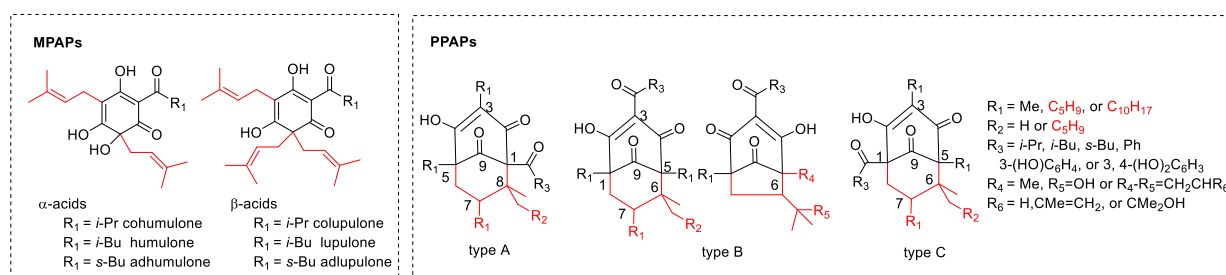

Figure 1-2. Main structures and classification of prenylated APs.

Prenylated APs exhibit various biological activities including antibacterial, antifungal, anti-inflammatory, antioxidant, and cytotoxic effects and are considered as a source of new drug lead from plant sources. As shown in Figure 1-3, lindbergins E and lindbergins F showed significant leishmanicidal activity (Socolsky et al. 2016). Psorothatin C from *Psorothamnus fremontii* was active against methicillin-resistant *Staphylococcus aureus* and vancomycin-resistant *Enterococcus faecium* (Yu et al. 2015b). Clusianone and its 7-epimer from the family Clusiaceae exhibited anti-HIV and antitumor activities (Garnsey et al. 2011; Nagalingam et al. 2016; Piccinelli et al. 2005; Sales et al. 2015). Yojironin E and petiolin J exhibited moderate antimicrobial activity (Tanaka et al. 2010; Tanaka et al. 2011). Yojironin E also showed cytotoxicity against murine lymphoma P388 cells and human epidermoid carcinoma KB cells *in vitro* (Tanaka et al. 2011). α- and β-Bitter acids (Figure 1-2) from *H. lupulus* (Cannabinaceae), commonly known as hops, were used in folk medicine as an antibacterial (in the form of wound powders and salves), a tranquilizer (sleep inducer), and a

diuretic and to ameliorate the symptoms of menopause. Perhaps more importantly, the female inflorescences (hop cones) of hops were also used in beer production (Van Cleemput et al. 2009). Different approaches were developed for the production of prenylated APs, including the isolation from plants (Nagalingam et al. 2016; Piccinelli et al. 2005; Sales et al. 2015; Socolsky et al. 2016; Van Cleemput et al. 2009; Yu et al. 2015b), chemical synthesis (Garnsey et al. 2011; Qi and Porco 2007; Shimizu et al. 2010; Tsukano et al. 2007), and chemoenzymatic synthesis (Li et al. 2015a; Tsurumaru et al. 2012).
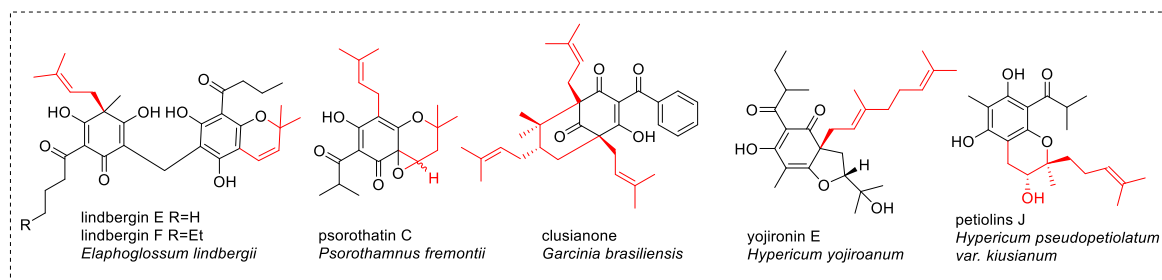

Figure 1-3. Examples of prenylated APs.

1.1.2. Prenylated flavonoids

Flavonoids are valuable natural products distributed mainly in plant kingdom. Chemically, flavonoids have the general structure of a 15-carbon skeleton, which consists of two phenyl rings (A and B) and heterocyclic ring (C) (Figure 1-4) (Sandhar et al. 2011). This carbon structure can be abbreviated C6-C3-C6. Based on their structures, they are categorized into flavones, isoflavonoids, neoflavonoids, flavonols, flavanone, flavanonols, flavans, and anthocyanidines (Figure 1-4) (Botta et al. 2009; Sandhar et al. 2011). Flavonoids have a wide range of biological and pharmacological activities *in vitro*-studies, including anti-inflammatory, antiviral, antithrombogenic, antifungal, and antitumor activities (Agrawal 2011). They are also considered as potential candidates for treatment of neurodegenerative and vasodilatory diseases (Sandhar et al. 2011). Prenylations at the two benzene rings often increase the lipophilicity of flavonoids, which results in an increased affinity to biological membranes and an improved interaction with target proteins (Botta et al. 2005b; Chen et al. 2014a).
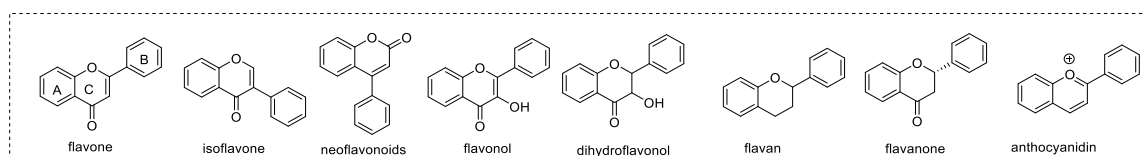

Figure 1-4. Main structures of flavonoids.

An example of prenylated flavonoids is licoflavonol (Figure 1-5), which is a novel natural inhibitor of *Salmonella* type III secretion system (T3SS) that secreted effector proteins to facilitate invasion into host cells. And it could be a promising candidate for novel type of anti-virulence drugs (Guo et al. 2016). Abyssinone-V 4′-methyl ether inhibited pneumococcal neuraminidase (NA), pneumococcal growth, and biofilm formation, without harming lung epithelial cells (Grienke et al. 2016). Sanggenol A and abyssinone-V 4′-methyl ether disrupted the synergism between influenza A virus and NA *in vitro*, hence functioning as dual-acting anti-infectives (Grienke et al. 2016). Kuwanon E and kuwanon C showed anti-inflammatory activity (Zelová et al. 2014). The higher toxicity of kuwanon C in comparison to kuwanon E could be caused by the presence of two prenyl moieties in contrast to only one geranyl group in kuwanon E, as well as by the positions at which these were attached to the flavonoid skeleton (Zelová et al. 2014).
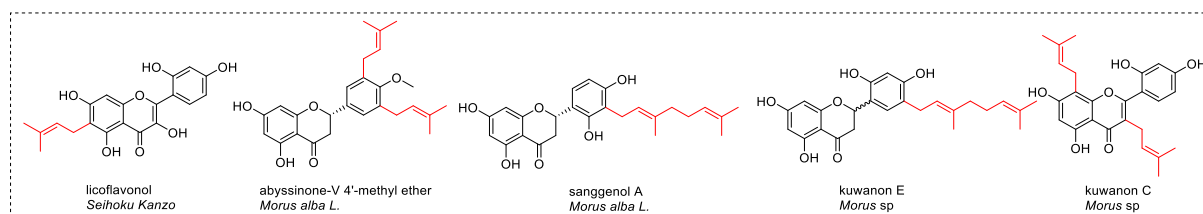

Figure 1-5. Examples of prenylated flavonoids.

1.1.3. Prenylated indole alkaloids

Alkaloids are a group of naturally occurring chemical compounds that mostly contain basic nitrogen atoms. Indole alkaloids are a class of alkaloids containing a structural moiety of indole. Many indole alkaloids contain isoprene groups and are thus called terpene indole or secologanin tryptamine alkaloids, which belong to one of the largest classes of alkaloids. Many of them possess significant physiological activity and some of them were used as medicine (Li 2010; Tanner 2015). The amino acid tryptophan is the biogenetic precursor of indole alkaloids. The indole structure is derived from L-tryptophan and its precursors (Li 2010; Tanner 2015).

Prenylated indole alkaloids comprise a large family of biologically active natural products produced by plants, fungi, and bacteria (Tanner 2015). These alkaloids generally contain a diketopiperazine or a bicyclo[2.2.2]diazaoctane ring as a core structure, and are biogenetically derived from tryptophan, a second amino acid, and one or two isoprene units (Tanner 2015). The prenyl carbons may reside on the periphery, or may ultimately be

embedded within the core of the alkaloid product. Thus, they may serve either to increase the lipophilicity of the alkaloids or to provide a carbon skeleton that is integral to the structure (Li 2010; Tanner 2015). These natural products attract attention in consequence to their strong biological and pharmacological effects (Li 2010; Wallwey and Li 2011). Therefore, diverse approaches were used to obtain such compounds, including the isolation from natural sources (Chang et al. 2016; Mireku et al. 2016; Tsukamoto et al. 2009a; Tsukamoto et al. 2009b), chemical synthesis (Mercado-Marin et al. 2016; Robins et al. 2016; Simpkins et al. 2013; Sunderhaus et al. 2013), and chemoenzymatic synthesis (Ding et al. 2010; Li 2010). One part of my thesis deals with enzymes for *C2*- and *C3*-prenylation of indole alkaloids. Therefore more details on *C2*-, *C3*- and other prenylated indole alkaloids are described below.

1.1.3.1. *C2*-prenylated indole alkaloids

Prenylated indole alkaloids in this group carry one prenyl moiety at position C-2 on the indole ring (Figure 1-6). For example, deoxybrevianamide E, a *C2*-reverse prenylated brevianamide F, obtained from a marine-derived fungus, *Aspergillus* sp. (Kato et al. 2007; Steyn 1971). Talathermophilin A and talathermophilin B were isolated from a thermophilic fungus *Talaromyces thermophilus* strain. The ratio of the two talathermophilins in the culture broths was unexpectedly rather constant, suggesting that talathermophilins might be of special function for the extremophilic fungus (Chu et al. 2010). Asterriquinone C-1 (ARQ C1) and ARQ analogues from *Aspergillus* sp. were effective in inhibiting the growth of several transplantable animal tumor *in vivo* (Shimizu et al. 1982a; Shimizu et al. 1982b).
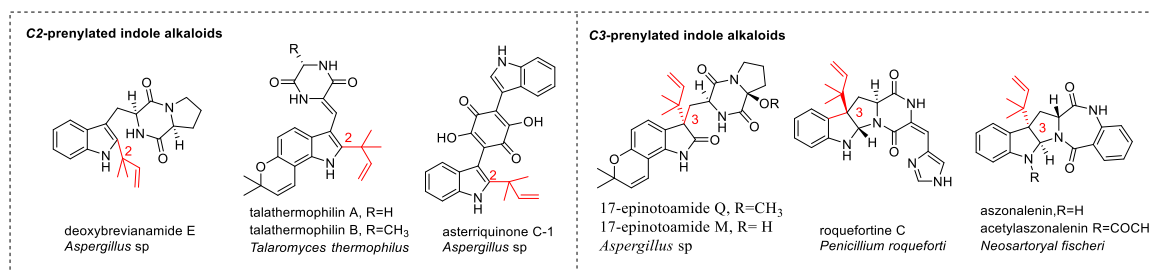

Figure 1-6. Examples of *C2*- and *C3*-prenylated indole alkaloids.

1.1.3.2. *C3*-prenylated indole alkaloids

Most of *C3*-prenylated indole alkaloids represent a characteristic fused multicyclic ring system with the prenyl moiety at the position C-3 on the indole ring (Figure 1-6). Most of these compounds are reversely *C3*-prenylated derivatives of cyclic dipeptides. For example, 17-epinotoamide Q and 17-epinotoamide M were isolated from a marine-derived *Aspergillus* sp. (Chen et al. 2013a). Roquefortine C identified from *Penicillium* strains is a cyclic

dipeptide derivative of tryptophan and histidine (O'Brien et al. 2006; Ohmomo et al. 1977). The mycotoxin acetylaszonalenin and its non-acetylated form aszonalenin were identified in various fungal strains, e.g. *N. fischeri* (Ellestad et al. 1973; Wakana et al. 2006; Yin et al. 2009b).Their stereoisomers *epi*-aszonalenins A and C were isolated from *Aspergillus novofumigatus* (Rank et al. 2006). These four compounds are derived from the amino acids tryptophan and anthranilic acid.

1.1.3.3. Other prenylated indole alkaloids

Besides positions C-2 and C-3, the prenyl moiety can be connected to positions C-4, C-5, C-6, C-7, and N-1 on the indole ring in nature (Figure 1-7). The tremorgenic mycotoxin aflatrem was *C4*-prenylated indole alkaloid from *Aspergillus flavus* (Cole et al. 1981; Gallagher and Wilson 1978), which is a monoprenylated derivative of the indole diterpene. Iso-notoamide B was isolated from the marine-derived endophytic fungus *Paecilomyces variotii*, which is an example of *C5*-prenylation, forming the fused dimethyldihydropyran ring at C-5 and C-6 of the indole ring (Zhang et al. 2015). Semicochliodinol B from *Chrysosporium merdarium* is prenylated bisindolylbenzoquinone with prenyl moieties substituted at position C-6 on indole ring, which exhibited inhibitory activity against HIV-1 protease (Fredenhagen et al. 1997). Penipalines A and B were isolated from the deep-sea-sediment derived fungus *Penicillium paneum* and were identified as *C7*-prenylated indole alkaloids. Penipaline B showed potent cytotoxic activities against A-549 and HCT-116 cell lines (Li et al. 2014). Asterriquinone contains one reverse prenyl moiety at the position N-1 on each tryptophanyl moiety, which showed inhibitory activity against tumour cells (Yamamoto et al. 1976a; Yamamoto et al. 1976b).
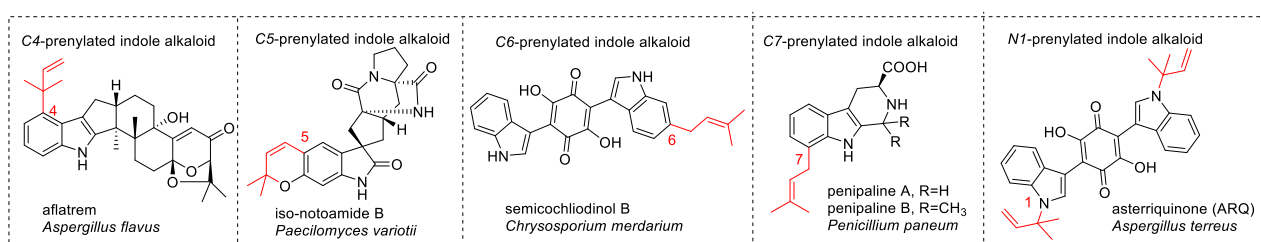

Figure 1-7. Examples of C-4, C-5, C-6, C-7, and N-1 prenylated indole alkaloids.

1.2. Biosynthetic pathways of prenylated acylphloroglucinols, prenylated flavonids, and fumitremorgins

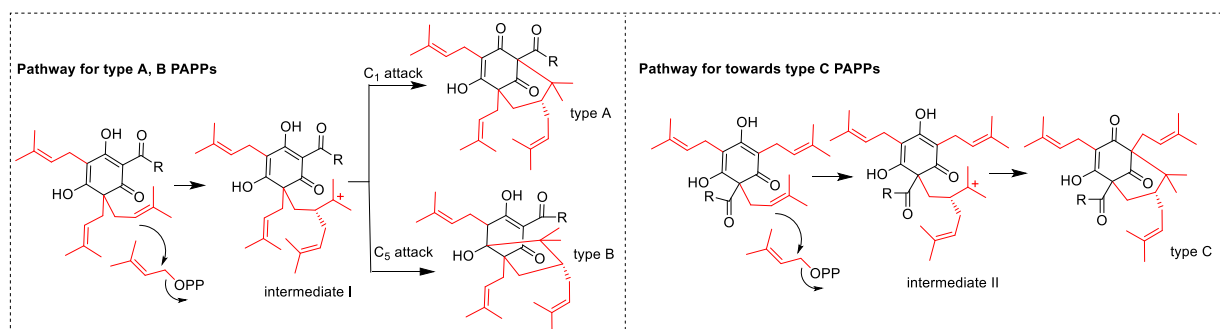### 1.2.1. Biosynthetic pathway of prenylated acylphloroglucinols

Early labelling experiments provided evidence for a polyketide-type biosynthesis for monocyclic polyprenylated acylphloroglucinols (MPAPs) (bitter acids) that involves one acyl-CoA and three malonyl-CoA units (Scheme 1-1) (Okada et al. 2004; Paniego et al. 1999). The acylphloroglucinol cores, phlorisovalerophenone (PIVP) and phlorisobutyrophenone (PIBP), were formed by condensation of three malonyl-CoA-derived acetate units with isovaleryl-CoA or isobutyryl-CoA as the starter units (Okada et al. 2004; Paniego et al. 1999). The enzyme valerophenone synthase (VPS), which was involved in the formation of PIVP in the biosynthesis of humulone, had been characterized (Scheme 1-1) (Okada and Ito 2001; Zhao et al. 2016). Recently, dual functional CHS (chalcone synthase)/VPS had also been reported. A CHS, FvCHS2-1 from strawberry was identified to be responsible for acylphloroglucinol synthesis in strawberry fruit (Song et al. 2016a). Several plants from the families Clusiaceae and Hypericaceae also used benzoyl-CoA as start unit and produced phlorbenzophenone and derivatives thereof, such as grandone (Hu and Sim 2000; Tian et al. 2014; Wu et al. 2014; Zhang et al. 2014). The prenylation or geranylation of this compound occured through an enzyme-catalyzed addition of dimethylallyl or geranyl pyrophosphate to the phloroglucinol moiety. Li et al. identified two membrane-bound prenyltransferases HIPT1L and HIPT2 from *H. lupulus* in 2015. Co-expression of different genes in *Saccharomyces cerevisiae* revealed that HIPT1L and HIPT2 catalyzed three sequential prenylations in the β-bitter acid biosynthetic pathway (Scheme 1-1). HIPT1L was confirmed to be an orthologue of HIPT1 (Tsurumaru et al. 2012). HIPT2 was only active, when it was co-expressed with HIPT1L. This led to the hypothesis that HIPT1L and HIPT2 formed a metabolon as the catalytic unit (Li et al. 2015a).
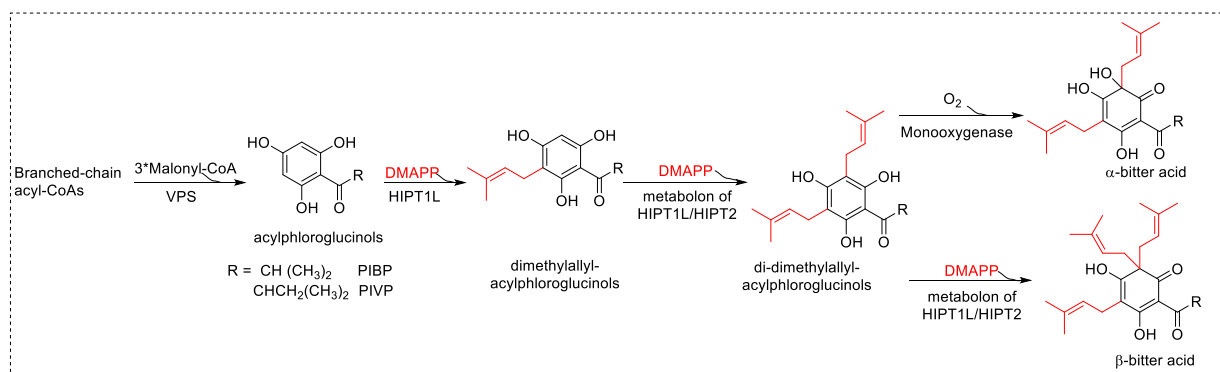
Scheme 1-1. The proposed biosynthetic pathway for MPAPs

PPAPs are biosynthetically derived from the less complex MPAPs. The hypothesized biosynthetic pathway of PPAPs is shown in Scheme 1-2 (Adam et al. 2002; Ciochina and

Grossman 2006; Cuesta-Rubio et al. 2001). MPAPs were cyclized to both type A and type B PPAPs via a precursor. Attack of one of the geminal prenyl groups of a MPAP on prenyl pyrophosphate gave the tertiary carbocation. Attack of C-1 of intermediated I on the pendant carbocation (or the corresponding pyrophosphate) would provide a type A PPAP, whereas attack of C-5 would provide a type B PPAP. The most likely scheme for the biosynthesis of the type C PPAPs, in contrast, would require that the initial MPAP have its quaternary center bear the acyl group (Adam et al. 2002; Ciochina and Grossman 2006; Cuesta-Rubio et al. 2001).

Scheme 1-2. The proposed biosynthetic pathway for PPAPs

## 1.2.2. Biosynthetic pathway of prenylated flavonoids

Flavonoids are derived from a chalcone precursor, the product of the condensation of cinnamoyl-CoA or 4-coumaroyl CoA (a product of the central phenylpropanoid pathway) and three molecules of malonyl-CoA by the enzyme chalcone synthase (CHS) (Scheme 1-3) (Dixon and Steele 1999; Koes et al. 1994; Nguyen et al. 2013; Pandey et al. 2016; Song et al. 2016b). The reactions to anthocyanins were catalyzed by chalcone isomerase (CHI), flavanone 3-hydroxylase (FHT), dihydroflavonol 4-reductase (DFR), anthocyanidin synthase (ANS) and flavonoid 3-O-glucosyltransferase (FGT). Most of the post modifications of flavonoids were carried out by enzymes such as glycosyltransferases (GTs), O-methyltransferases (OMTs), cytochrome P450s (CYP), and prenyltransferases (PTs), which modified flavonoid and isoflavonoid skeletons (Pandey et al. 2016; Sasaki et al. 2008; Shen et al. 2012; Yazaki et al. 2009).
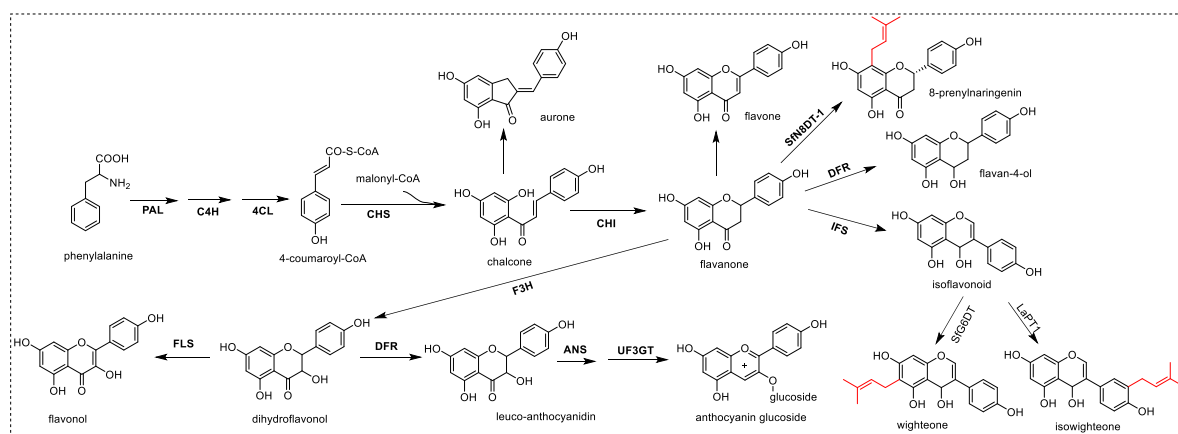
Scheme 1-3. The proposed biosynthetic pathway for prenylated flavonoids
PAL, phenylalanine ammonia-lyase; C4H, cinnamate 4-hydroxy; 4CL, 4-coumaroyl-coenzyme A ligase; CHS, chalcone synthase; CHI, chalcone flavanone isomerase; F3H, flavanone 3β-hydroxylase; DFR, dihydroflavonol 4-reductase; FLS, flavonol synthase; IFS, isoflavonoid synthase; AS, anthocyanin synthase; UF3GT, UDP-glucose: flavonoid 3-O-glucosyltransferase; SdN8DT-1, naringenin 8-dimethylallyltransferase 1; SfG6DT, genistein 6-dimethylallyltransferase; LaPT1, plastid-localized 5-hydroxyisoflavone prenyltransferase.

1.2.3. Biosynthetic pathway of fumitremorgins

The gene clusters for the biosynthesis of fumitremorgin-type indole alkaloids were identified in *A. fumigatus* and *N. fischeri* (Grundmann and Li 2005; Li 2011; Steffan et al. 2009). The biosynthesis of these compounds started with the formation of brevianamide F from L-tryptophan and L-proline by the nonribosomal peptide synthetase (NRPS) FtmPS, followed by a prenylation reaction catalyzed by FtmPT1 to produce tryprostatin B (Scheme 1-4) (Grundmann and Li 2005; Maiya et al. 2006). The cytochrome P450 enzyme FtmP450-1 and the putative methyltransferase FtmMT catalyzed the addition of small functional groups, i.e. hydroxyl and methyl groups, resulting in the formation of tryprostatin A (Kato et al. 2009). The second cytochrome P450 enzyme FtmP450-2 was responsible for cyclization of tryprostatin A, and the hydroxylation was catalyzed by the third cytochrome P450 enzyme FtmP450-3 consequently for the production of 12,13-dihydroxyfumitremorgin C (Kato et al. 2009; Tang et al. 2017). The identification of three cytochrome P450 genes was carried out by gene disruption (Kato et al. 2009). The second prenyltransferase FtmPT2 was proven to catalyze the conversion of 12,13 dihydroxyfumitremorgin C to fumitremorgin B (Grundmann et al. 2008). The non-heme Fe(II) α-ketoglutarate-dependent dioxygenase FtmOx1 catalyzed the formation of verruculogen from fumitremorgin B (Steffan et al. 2009). The final step of this biosynthetic pathway was the *O*-prenylation of verruculogen to fumitremorgin A by FtmPT3 in *N. fischeri* (Mundt et al. 2012).
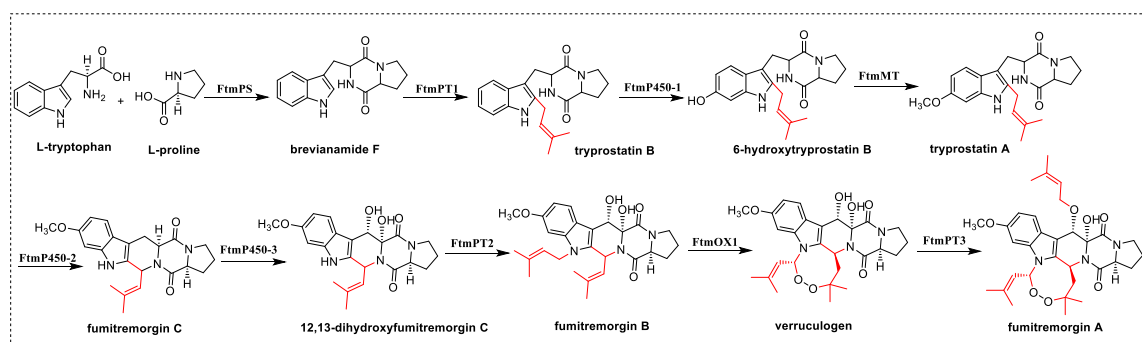
Scheme 1-4. The proposed biosynthetic pathway for fumitremorgins

1.3. Prenyltransferases

Prenyltransferases (PTs) attach isoprenoid moieties derived from allylic isoprenyl diphosphates to acceptor molecules. The prenyl diphosphates originate from the terpenoid biosynthetic pathway and therefore consist of n × C5 units, e.g. dimethylallyl diphosphate (DMAPP; n=1), geranyl diphosphate (GPP; n=2), farnesyl diphosphate (FPP; n=3) or geranylgeranyl diphosphate (GGPP; n=4) (Figure 1-1, B) (Heide 2009a; Winkelblech et al. 2015a). These enzymes catalyze the cleavage of a prenyl moiety from its diphosphate and the subsequent transfer of the resulting isoprene carbocation onto other isoprenoid moieties, amino acids or aromatic and a few non-aromatic structures. According to their sequences, structures, biochemical properties, and functions, PTs can be classified into different subgroups, like *trans*- and *cis* -PTs, peptide, protein, and tRNA PTs and aromatic PTs (Heide 2009a; Winkelblech et al. 2015a). The aromatic PTs will be described in this thesis in details.

Aromatic prenyltransferases catalyze the transfer reactions of prenyl moieties onto aromatic acceptors, such as indole derivatives, flavonoids, naphthalenes, phenolic acids, coumarins, phenazines, or phenols. Aromatic prenylations are important steps in the biosynthesis of natural products in both primary and secondary metabolism. Particularly, the latter leads to a diversity of chemical structures in plants, fungi, and bacteria (Botta et al. 2005a; Heide 2009a; Winkelblech et al. 2015a). The acceptance of aromatic compounds by these enzymes is one explicit feature to divide the diverse prenyltransferases into distinct enzyme groups. Furthermore, discrimination characteristics are their native organisms and if the proteins are soluble in the cytosol or membrane bound. Dependency on divalent metal ions is an additional criterion. Moreover, aromatic prenyltransferases may present certain amino acid motifs or exhibit distinct tertiary structures (Botta et al. 2005a; Heide 2009a; Winkelblech et al. 2015a). There are several possibilities to categorize prenyltransferases based on the

described properties. Prenyltransferases comprises the membrance-bound prenyltransferases, including UbiA superfamily and aromatic prenyltransferases of plant secondary metabolism; soluble prenyltransferases, including the CloQ/NphB group and the DMATS superfamily (Heide 2009a; Winkelblech et al. 2015a). These groups or super families are described in the following paragraphs.

1.3.1. Membrance-bound prenyltransferases for aromatic substrates

Membrane-bound prenyltransferases play an important role in diversifying secondary metabolites. These enzymes are responsible for synthesizing potentially active molecules (Yazaki et al. 2009). The best-studied prenyltransferase is 4-hydroxybenzoate (4HB) polyprenyltransferase, which is responsible for an essential step in the biosynthesis of ubiquinones. Ubiquinone (also known as coenzyme Q) is a ubiquitous lipid soluble redox cofactor that is an essential component of electron transfer chains dependent on the predominant isoprenoid chain length of ubiquinones in the respective organism (Heide 2009a). The 4HB polyprenyltransferases usually showed a broad substrate specificity for the isoprenoid substrate, accepting short chain isoprenoids like FPP and GPP, but not DMAPP and *cis*-prenyl diphosphates (Saleh et al. 2009b). UbiA transfered prenyl moieties of different size (usually 30–50 carbons) to position 3 of 4HB (Figure 1-8, A). The UbiA homologue UBIAD1 was discovered in human cells and was involved in the vitamin K biosynthesis, which is important for maintaining vascular homeostasis (Hegarty et al. 2013; Nakagawa et al. 2010). The crystal structures of an archaeal UbiA in its apo and substrate-bound states were reported, which gave detailed information about the reaction mechanism of this type of prenyltransferases (Cheng and Li 2014). Flavin prenyltransferase UbiX linked a dimethylallyl moiety to the flavin N5 and C6 atoms and added a fourth non-aromatic ring to the flavin isoalloxazine group (Figure1-8, A) (Aussel et al. 2014; White et al. 2015). All prenyltransferases of lipoquinone biosynthesis comprise an aspartate-rich motif (e.g. NDxxDxxxD). Most of their activity is absolutely dependent on the presence of Mg^{2+} or similar cations like Mn^{2+}, Co^{2+}, or Ni^{2+}. However, UbiX is metal-independent and requires dimethylallyl monophosphate as substrate (Aussel et al. 2014; White et al. 2015).
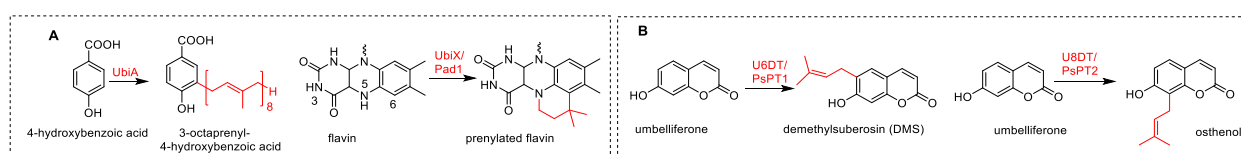

Figure 1-8. Examples of membrance-bound prenyltransferases reactions.

Umbelliferone dimethylallyltransferase (UDT) is a prenyltransferase that is specific for the first reaction step in the furanocoumarin (FC) biosynthetic pathway (Figure 1-8, B). This enzyme plays a critical role in FC structural diversification because its regiospecificity determines the final form of the isomer, that is, dimethylallylation at the C-6 or C-8 position leading to linear or angular FCs, respectively (Dhillon and Brown 1976; Ellis and Brown 1974; Hamerski et al. 1990). Two new UDT enzymes, prenyltransferase PsPT1 and PsPT2, were discovered and characterized as two membrane-bound prenyltransferases that synthesized demethylsuberosin (linear FC intermediate) and osthenol (angular FC intermediate), respectively, in parsnip (Munakata et al. 2016).

In prenylflavonoid and prenylisoflavonoid biosynthesis, prenylation is also carried out by membrane-bound prenyltransferases (Sasaki et al. 2011; Yazaki et al. 2009). SfN8DT-1, the first identified flavonoid-specific prenyltransferase, was shown to be responsible for the prenylation of a very few select flavanones at C-8 (Scheme 1-3) (Sasaki et al. 2008). G4DT was found to act specifically on a pterocarpan substrate glycinol (Akashi et al. 2009). SfFPT displayed high catalytic efficiency with high regiospecificity acting on C-8 of structurally different types of flavonoids and exhibited strict stereospecificity for levorotatory flavanones to produce (2*S*)-prenylflavanones (Chen et al. 2013b). SfG6DT was found to specifically prenylate the isoflavone genistein at C-6 (Scheme 1-3) (Sasaki et al. 2011). The chalcone-specific prenyltransferase SfiLDT was shown to prenylate isoliquiritigenin (Sasaki et al. 2011). LaPT1 catalyzed the prenylation of the B-ring of isoflavones, such as genistein (Scheme 1-3) and 2´-hydroxygenistein (Sasaki et al. 2011; Shen et al. 2012; Yazaki et al. 2009). Recently, two isoliquiritigenin 3-dimethylallyltransferases MaIDT and CtIDT had been identified in *Morus alba* and *Cudrania tricuspidata,* respectively (Wang et al. 2014).

The overproduction of the membrane-bound prenyltransferase HIPT-1 from *H. lupulus* and its biochemical characterization were reported (Scheme 1-1) (Tsurumaru et al. 2012). This enzyme catalyzed the prenylation of PIVP in the presence of DMAPP and also accepted PIBP as prenylation acceptor. Two membrane-bound prenyltransferases HIPT1L and HIPT2 from *H. lupulus* were identified (Li et al. 2015a). HIPT1L and HIPT2 catalyzed three sequential prenylation steps in the β-bitter acid pathway. HIPT1L was confirmed to be an orthologue of HIPT1 identified by Tsurumaru et al.

1.3.2. Soluble prenyltransferases for aromatic substrates

1.3.2.1. Prenyltransferases of the CloQ/NphB group

The enzyme CloQ from *Streptomyces roseochromogenes* catalyzed the prenylation of 4-hydroxyphenylpyruvic acid in the clorobiocin biosynthesis (Figure 1-9) (Pojer et al. 2003). On the basis of sequence similarity with CloQ, NphB (initially termed Orf2) from the biosynthetic gene cluster of the meroterpenoid (prenylated polyoetide) naphterpin in a *Steptomyces* strain was identified as an aromatic prenyltransferase (Kuzuyama et al. 2005). Orf2 catalyzed the prenylation of 1,6-DHN (1,6-dihydroxynaphthalene) to produce two prenylated products, 1,6-DHN-P1 and 1,6-DHN-P2 in the presence of GPP (Figure 1-9) (Kuzuyama et al. 2005). SCO7190, an NphB homologue found in *Streptomyces coelicolor*, catalyzed the attachment of DMAPP onto 1,6-DHN (Kumano et al. 2008). Both EpzP and PpzP from *Streptomyces* sp. catalyzed the *C*-prenylation of 5,10-dihydrophenazine-1-carboxylic acid (Figure 1-9) (Saleh et al. 2009a; Seeger et al. 2011; Zocher et al. 2012). These enzymes are restricted to the transfer of C5 or C10 isoprene units. DzmP, the first farnesyl diphosphate prenyltransferase of the CloQ/NphB group, had been characterized from the bacterium *Micromonospora* sp. and was involved in the biosynthesis of diazepinomicin (Bonitz et al. 2013). In contrast to the membrane bound enzymes of the UbiA superfamily, this group comprised soluble enzymes found in bacteria and fungi (Heide 2009b). All enzymes of this group did not depend on divalent metal ions (Kuzuyama et al. 2005; Tello et al. 2008). Recent computational studies further elucidated and strengthened the metal ion independent prenylation mechanism of these enzymes (Bayse and Merz 2014). No aspartate rich (N/D)DxxD motif was present in these enzymes and with the exception of NphB (Kuzuyama et al. 2005; Tello et al. 2008). Crystallization of NphB revealed a new tertiary structure with an α-β-β-α (ABBA) barrel fold. This protein structure is also termed prenyltransferase (PT) barrel, which allows another classification into the ABBA prenyltransferase family (Kuzuyama et al. 2005; Tello et al. 2008).
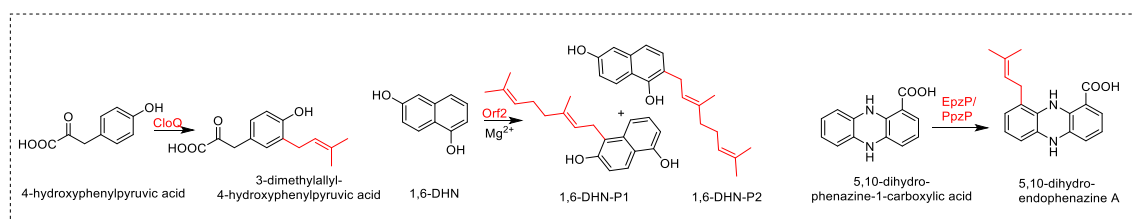

Figure 1-9. Examples of CloQ/NphB group prenyltransferases reactions.

1.3.2.2. Ezymes of the DMATS superfamily
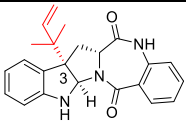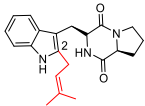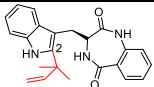
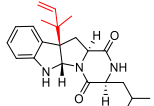## Bacterial prenyltransferases of the LtxC group
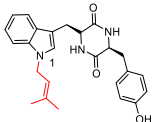
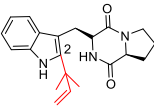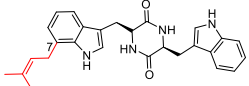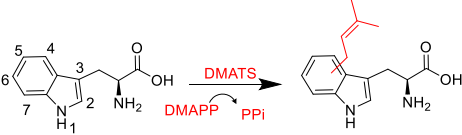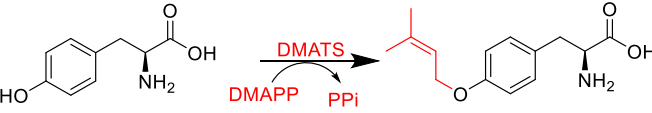Members of the LtxC group prenylate indole-containing substrates. These enzymes carry no aspartate rich motif and are divalent metal ion independent (Edwards and Gerwick 2004). They are predominantly expressed in bacterial hosts. Due to their common features and relatively high sequence similarity with fungal DMAT synthases, this group of prenyltransferases could likely be integrated into the DMATS superfamily. LtxC from *Lyngbya majuscula* was a member of the lyngbyatoxin A−C biosynthetic pathway and geranylated the precursor (−)-indolactam V at position C-7 to lyngbyatoxin A (Edwards and Gerwick 2004). TleC, a LtxC homologous prenyltransferase, and MpnD catalyzed the 'reverse' prenylation of (-)-indolactam V at the C-7 position of the indole ring with geranyl pyrophosphate or dimethylallyl pyrophosphate to produce lyngbyatoxin or pendolmycin, respectively (Awakawa et al. 2014; Ma et al. 2012; Takahashi et al. 2010). Recent studies on TleC and MpnD revealed a high flexibility toward prenyl donors with different chain length (C5–C25) (Mori et al. 2016). In the actinobacterium *Salinispora* sp.*,* the reverse L-tryptophan *N*-prenyltransferase, CymD was involved in the biosynthesis of the anti-inflammatory and anti-bacterial cyclic peptides cyclomarin and cyclomarazine, respectively (Schultz et al. 2008; Schultz et al. 2010). ComX pheromone was produced by *Bacillus subtilis* and related bacilli (Magnuson et al. 1994). The tryptophan residue of ComX pheromone was modified by ComQ with either a geranyl or a farnesyl group in the α formation at the C-3 position of tryptophan residue, resulting in the formation of a tricyclic structure, including a newly formed pyrrolidine ring. KgpF modified the tryptophan derivative with a dimethylallyl group at the 3 position of its indole ring, resulting in the β formation of a tricyclic structure with the same scaffold as ComX pheromones (Okada et al. 2005; Okada et al. 2007; Okada et al. 2016). FamD1 and FamD2, from the cyanobacterium *Fischerella ambigua*, played critical roles in fusing indole isonitrile with GPP to generate tri- or tetracyclic hapalindoles and prenylating tetracyclic hapalindoles with dimethylallyl pyrophosphate (DMAPP) to form the ambiguines (Li et al. 2015b). Two additional 6-DMAT synthases, namely 6-DMATS$_{sa}$ and 6-DMATS$_{sv}$, were identified from *Streptomyces* spp. L-Tryptophan and derivatives were well accepted by both enzymes in the presence of DMAPP or GPP (Winkelblech and Li 2014).

Fungal prenyltransferases

Prenyltransferases of the **dim**ethyl**a**llyl**t**ryptophan **s**ynthase (DMATS) superfamily are found predominantly in fungi of the genera of *Aspergillus*, *Penicillium*, and *Claviceps* (Williams et al. 2000). The enzymes are soluble proteins and carry no aspartate rich motifs. They catalyze

mainly the formation of prenylated indole derivatives and no divalent metal ions are required for the catalytic reaction (Winkelblech et al. 2015a; Yu and Li 2012). Most of these enzymes show broad substrate promiscuity while retaining a strong specificity regarding the prenylation position. The 4-DMATS (the first DMATS) was obtained from *Claviceps* sp. in 1992. It catalyzed the *C4*-prenylation of L-tryptophan and was involved in the biosynthesis of ergot alkaloids (Gebler and Poulter 2009). Later the corresponding gene *dmaW* was isolated, its amino acid sequence was elucidated and the prenyl transfer reaction was proved in yeast transformants, 4-DMATS is also termed DmaW (Tsai et al. 1995). Prenyltransferases that transfer the isoprene residue selectively to one of the carbon atoms (C-2, C-3, C-4, C-5, C-6, C-7) or the nitrogen atom (N-1) of the indole ring, in regular or reverse orientation, have been reported in recent years (Table 1-1) (Li 2010; Yu and Li 2012). AstPT and TdiB as well as ArdB accepted a bisindolyl benzoquinone and a cyclic tripeptide as substrates, respectively (Haynes et al. 2013; Schneider et al. 2008; Tarcz et al. 2014a). XptB combined xanthones with a DMA residue (Pockrandt et al. 2012). VrtC is the first DMATS, which utilized GPP instead of DMAPP and moreover transfered the prenyl moiety onto a tetracyclic ring system (Chooi et al. 2010). In addition, NscD catalyzed the addition of the dimethylallyl group to the aromatic C-5 of viridicatumtoxin (Chooi et al. 2012; Chooi et al. 2013). Beside the numerous indole prenyltransferases, several prenyltransferases used non-indole substrates e.g. the tyrosine *O*-prenyltransferase SirD from *Leptosphaeria maculans* and TyrPT from *Aspergillus niger* (Table 1-1) (Fan et al. 2014; Kremer and Li 2010). One example for a prenyltransferase from DMATS superfamily, PAPT from *Phomopsis amygdali* used a non-aromatic derivative for *O*-prenylation in the glucose moiety (Noike et al. 2012). Two aromatic prenyltransferases (PenI and PenG) played an iterative prenylation mechanism for installing the 10-carbon unit present in the gene cluster of penigequinolones from *Penicillium thymicola* (Zou et al. 2015). FoPT1, a highly regiospecificity prenyltransferase, catalyzed the prenylation of flavonoids to produce only *C6*-prenylated flvonoids (Yang et al. 2016). Recently, a soluble prenyltransferase AtaPT from *A. terreus* strain was demonstrated to carry an unprecedented promiscuity toward 72 drug-like acceptors and prenyl donors including DMAPP, GPP, and FPP (Chen et al. 2017).

Table 1-1. PTs of the DMATS superfamily used in this thesis

Prenyltransferases		Organism	Prenylated substrate, position and pattern	
Cyclic dipeptide prenyltransferases	AnaPT (Yin et al. 2009b)	*N. fischeri*	*cyclo*-D-Trp-Ant, C-3, reverse	
	AtaPT (Chen et al. 2017)	*A. terreus*	drug-like aromatic acceptors	mono-, di-, and/or tri-prenylated products
	FtmPT1 (Grundmann and Li 2005)	*A. fumigatus*	*cyclo*-L-Trp-L-Pro, C-2, regular	
	CdpC2PT (Mundt and Li 2013)	*N.fischeri*	*cyclo*-D-Trp-Ant, C-2, reverse	
	CdpC3PT (Yin et al. 2010b)	*N. fischeri*	*cyclo*-L-Trp-L-Leu, C-3, reverse	
	CdpNPT (Yin et al. 2007)	*A. fumigatus*	*cyclo*-L-Trp-L-Tyr, N-1, regular	
	BrePT (Yin et al. 2013)	*A. versicolor*	*cyclo*-L-Trp-L-Pro, C-2, reverse	
	CTrpPT (Zou et al. 2010)	*A. oryzae*	*cyclo*-L-Trp-L-Trp, C-7, regular	
Tryptophan prenyltransferases				
	7-DMATS (Kremer et al. 2007)	*A. fumigatus*	L-Trp	C-7, regular
	6-DMATS$_{Sa}$ (Winkelblech and Li 2014)	*Streptomyces ambofaciens*	L-Trp	C-6, regular
	5-DMATS (Yu et al. 2012b)	*Aspergillus clavatus*	L-Trp	C-5, regular
	FgaPT2 (Unsöld and Li 2005)	*A. fumigatus*	L-Trp	C-4, regular
Tyrosine prenyltransferases				
	SirD (Zou et al. 2011)	*L. maculans.*	L-Tyr	*O*-regular
	TyrPT (Fan et al. 2014)	*Aspergillus niger*	L-Tyr	*O*-regular

1.4. Chemoenzymatic synthesis of prenylated aromatic compounds

Prenylation improves the affinity of a compound to biomembranes and the interaction of the substance with proteins, leading to dramatically increased biological activities (Botta et al. 2005b). Therefore, it is attractive for scientists to use prenyltransferases as strategies for regioselective chemoenzymatic synthesis of prenylated derivatives. Aromatic prenyltransferases, especially the soluble indole prenyltransferases of the DMATS superfamily, show promising flexibility towards their aromatic substrates and catalyze highly regioselective and stereoselective prenyltransfer reactions. These features provide evidence for the potential of aromatic prenyltransferases as biocatalysts for chemoenzymatic synthesis. Many series of prenylated derivatives have been successfully synthesized by these enzymes. Details are described below.

1.4.1. Chemoenzymatic synthesis of prenylated indole alkaloids and other prenylated derivatives

The fungal L-tryptophan prenyltransferases FgaPT2, 5-DMATS, and 7-DMATS catalyzed the regiospecific regular *C4-*, *C5-*, and *C7*-prenylation of several simple indole derivatives in the presence of DMAPP, respectively (Kremer and Li 2008; Steffan et al. 2007; Yu et al. 2012a). The bacterial prenyltransferases IptA and its homologues 6-DMATS$_{sa}$ and 6-DMATS$_{sv}$ catalyzed the formation of several *C6*-prenylated indole derivatives. The latter two enzymes also utilized GPP as prenyl donor (Takahashi et al. 2010; Winkelblech and Li 2014). Furthermore, the significantly modified indole derivatives DMA-indoleacetonitriles and DMA-indolocarbazoles were obtained *in vitro* using purified recombinant bacterial and fungal prenyltransferases, respectively (Ozaki et al. 2013; Yu et al. 2012a). Cyclic dipeptide prenyltransferases in turn can be used as biocatalyst for the formation of different prenylated dipeptides. FtmPT1 catalyzed the prenylations of tryptophan-containing cyclic dipeptides to produce not only *C2-*, but also *C3*-regulars prenylated products (Wollinsky et al. 2012). Recent investigations have also shown that FtmPT1 was able to prenylate a non-aromatic carbon atom using the indole derivative indolylbutenone (Chen et al. 2012). Investigation on AnaPT, CdpNPT, and CdpC3PT revealed that these enzymes produced stereospecific *C3*-prenylated cyclic dipeptides (Yin et al. 2009a; Yu et al. 2013). An unnatural cyclic dipeptide, *cyclo*-L-homotryptophan-D-valine, were accepted by eight prenyltransferases, including five

cyclic dipeptide prenyltransferases, BrePT, FtmPT1, CdpC3PT, CdpNPT, and AnaPT as well as three tryptophan prenyltransferases, FgaPT2, 5-DMATS, and 7-DMATS, forming one prenyl moiety at each position of the indole nucleus and one diprenylated derivatives (Fan and Li 2013). Tryptophan prenyltransferases could also use tripeptide derivatives, ardeemin fumiquinazoline (FQ), as prenylation substrates, which provided a possibility for the synthesis of prenylated analogues of ardeemin FQ (Mai et al. 2016).

Not only compounds containing an indole moiety, but also other aromatic compounds could be used as substrates. L-Tyrosine and derivatives could be prenylated by the L-tyrosine prenyltransferases SirD (Rudolf and Poulter 2013) and TyrPT (Fan et al. 2014). Recent studies on the xanthone prenyltransferase XptB and the benzoquinone prenyltransferase AstPT broaden the availability of *O*-prenylated, *O*-geranylated, and *O*-farnesylated xanthones (Pockrandt et al. 2012; Tarcz et al. 2014b). *C*- as well as *O*-, mono- and di-prenylated hydroxynaphthalenes were also formed using the L-tryptophan prenyltransferases or cyclic dipeptide prenyltransferases (Winkelblech and Li 2014; Yu et al. 2011). Dimethylallyl and geranyl moieties have been attached to different flavonoid substrates, in the presence of diverse prenyltransferases, such as 7-DMATS, NphB, NovQ, and FoPT1 (Kumano et al. 2008; Ozaki et al. 2009; Yang et al. 2016; Yu and Li 2011). LynF was able to prenylate several other nonnatural substrates, including N-acetyl- and N-boc-modified D- or L-Tyr, as well as several other linear and cyclic polypeptides (McIntosh et al. 2011). The regiospecific 2-prenylation of a variety of structurally diverse hydroxyxanthones was catalyzed by MaIDT, which is a plant flavonoid prenyltransferase with substrate flexibility from *Morus alba* (Wang et al. 2016).

1.4.2. Chemoenzymatic synthesis of aromatic substrates by altering the prenyl donors

In the last years, the potential usage of DMATS enzymes as biocatalysts was expanded significantly by their acceptance of different prenyl donors. In addition to their remarkable high flexibility toward aromatic substrates, recent studies manifested that several members of this family accept not only DMAPP, but also other alkyl donors, such as GPP and FPP. Meanwhile, it was demonstrated that the unnatural DMAPP analogous like monomethylallyl (MAPP), 2-pentenyl (2-pentenyl-PP), and benzyl diphosphate (benzyl-PP) could also be used for alkylation or benzylation of tryptophan and tryptophan-containing cyclic dipeptides by a

number of DMATS enzymes (Liebhold et al. 2012; Liebhold et al. 2013; Liebhold and Li 2013; Winkelblech et al. 2015b; Yu et al. 2015a).

1.4.3. Chemoenzymatic synthesis of aromatic substrates with enzymes from saturation mutagenesis experiments

Enzymes have been successfully improved for many years by mutation and selection. Many improvements have been made to this technology. Existing approaches to improve single proteins or parts thereof include modelling based point mutagenesis, cassette library mutagenesis, and random point mutagenesis, mutator strains, and UV or chemical mutagenesis, which introduce (partially) random mutations either into a selected small region of a gene or throughout a gene (Powell et al. 2001). As refer to PTs, crystal structures of DMATS enzymes provide not only detailed insights into the reaction mechanism of the prenyl transfer reactions, but also basic information for protein engineering to create new biocatalysts with desirable features (Jost et al. 2010). Due to the difficulty of high throughput screening (HTS) for PT mutants, rational design based on the available crystal structure is more efficient and preferred. In the last years, structures of several DMATSs including FgaPT2 (Metzger et al. 2009), FtmPT1 (Jost et al. 2010), CdpNPT (Schuller et al. 2012), AnaPT (Yu et al. 2013), and AtaPT (Chen et al. 2017) were determined and used as basis for understanding the catalytic mechanism and for creation of new biocatalysts. Comparing these structures revealed that these enzymes share similar folds consisting of five repeating "αββα" (ABBA) barrel fold. Their active sites are located in the center of the barrel. The amino acid residues in the DMAPP binding sites seem to be fairly conserved, while the binding sites of the aromatic substrates differ from each other. FtmPT1 catalyzed the prenylation of brevianamide F in the biosynthesis of fumitremorgin-type alkaloids which showed diverse pharmacological activities and are promising candidates for the development of antitumor agents (Grundmann and Li 2005) (Figures 1-10). The overall three-dimensional structure of FtmPT1 was formed by a central core of 10 antiparallel β-strands that are surrounded by a ring of 10 partially solvent exposed α-helices. FtmPT1 exists as a dimer in solution and also forms dimers in the crystal (Figure 1-11, A). Based on the structure of FtmPT1, a modifiable reaction chamber was identified and a mutant FtmPT1_G115T was obtained. The mutant still accepted brevianamide F as substrate, but catalyzed mainly a reversely *syn-cis C3* prenylation instead of the regularly *C2*-prenylation (Jost et al. 2010) (Figures 1-10 and 1-11, B).
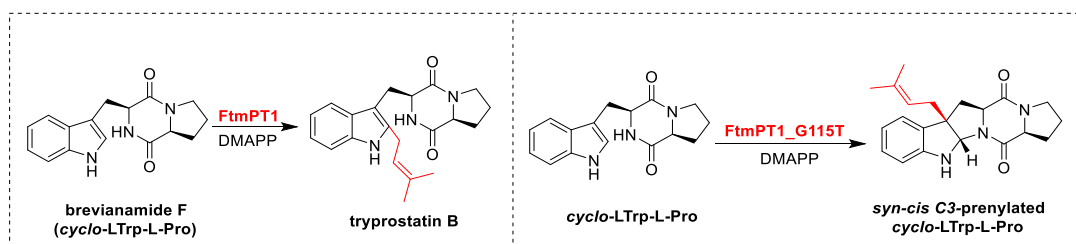
Figure 1-10. Reactions catalyzed by FtmPT1 and its Gly115 mutant
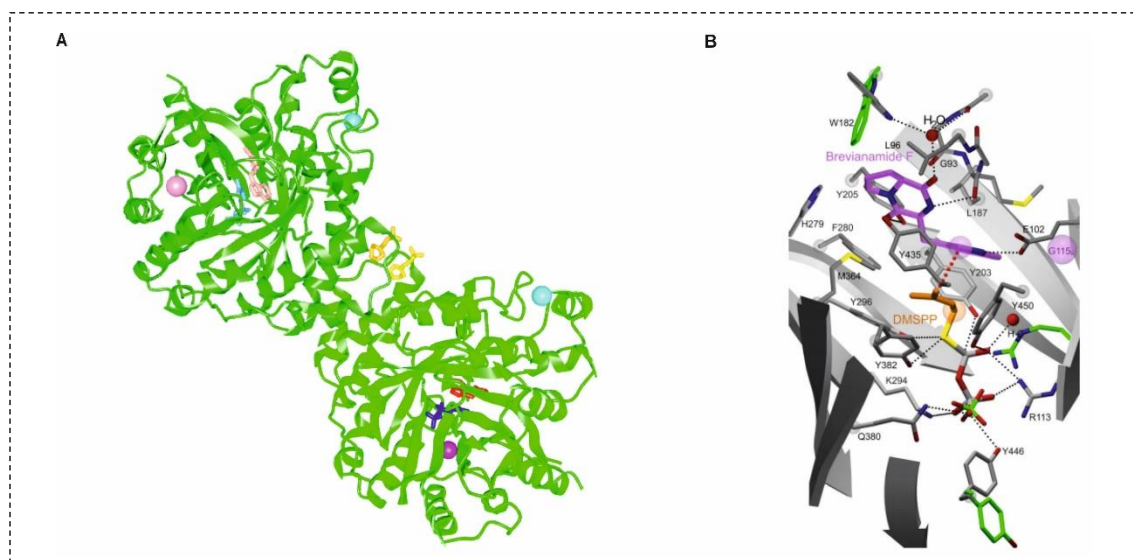

Figure 1-11. Crystal structure of brevianamide F prenyltransferase complexed with brevianamide F and dimethylallyl S-thiolodiphosphate (A) and cross section of the active site of FtmPT1 with the bound substrates, brevianamide F (violet), around DMSPP (orange), and G115 is indicated as a violet sphere (B) (adopted from Jost et al., 2010).

Structure-based engineering of EpzP resulted in a novel phenazine PT with conformational changes at *C*-termini and increased its catalytic turnover rate (Zocher et al. 2012). FgaPT2 from *A. fumigatus* catalyzed *C4*-prenylation of L-tryptophan (Unsöld and Li 2005). With high protein amount, FgaPT2 was able to catalyze the *C4*-prenylation of five tryptophan-containing cyclic dipeptides (Steffan et al. 2007) and *C3*-prenylation of tyrosine (Fan et al. 2015b). Lys174 was proposed to abstract one proton from the intermediate cation and to rearomatization for end products (Metzger et al. 2009). Saturation mutagenesis on Lys174 led to creation of 17 mutants, and FgaPT2_K174F exhibited much higher catalytic efficiency towards L-tyrosine than FgaPT2, while its activity towards L-tryptophan was almost abolished (Fan et al. 2015b). Arg244 was proposed to bind the hydroxylate group of tryptophan (Metzger et al. 2009). Site-directed mutagenesis on Arg244 led to identification of 13 mutants, which display differentially increased enzyme activities for tryptophan-containing cyclic dipeptides, with up to 76-fold turnover number of that of FgaPT2 (Fan and Li 2016).

24

2. Aims of this thesis

The following issues have been addressed in this thesis:

2.1. Biochemical investigations on the acceptance of acylphloroglucinols in the presence of DMAPP, GPP, and FPP catalyzed by fungal prenyltransferases

Different approaches and agents were developed for synthesis of the prenylated APs. Chemical prenylation usually has some limitations, such as different reactivities of C-atoms on APs, difficulty to construct quaternary centers, and extensive oxygen functionality. In contrast, prenylation catalyzed by enzymes, i.e., prenyltransferases, provides a more environment-friendly and safer alternative. Three membrane-bound prenyltransferases HIPT-1, HIPT1L, and HIPT2 from *H. lupulus* were demonstrated to catalyze the prenylations in the β-bitter acid pathway. However, most membrane-bound proteins were difficult to overproduce and purify than soluble enzymes. These features prohibit their potential use as biocatalysts for chemoenzymatic synthesis for production of prenylated APs. Therefore, there is a need to find alternative enzymes with better properties. The aim of this project was to test the acceptance of APs by fungal prenyltransferases, which are soluble proteins and can be readily overproduced in *E. coli* with significantly higher yields. The following experiments were carried out:

➢ Overproduction and purification of the tryptophan-containing cyclic dipeptide, tryptophan, and tyrosine prenyltransferases.

➢ Analysis of enzymatic conversion of APs and analogues in the presence of different prenyl donors (DMAPP, GPP, and FPP) by HPLC.

➢ Isolation of enzymatic products for structure elucidation by LC-MS and NMR.

➢ Determination of kinetic parameters of identified reactions.

2.2. Chemoenzymatic synthesis of prenylated flavonoids by fungal prenyltransferases

Fungal prenyltransferases of the DMATS superfamily show no sequence similarity to known aromatic prenyltransferases of the CloQ/NphB group and the UbiA superfamily. However, recent studies indicated that prenyltransferases of the DMATS superfamily share structure

similarity with those of the CloQ/NphB group. In a previous study, it was demonstrated that the recombinant indole prenyltransferase 7-DMATS accepted several flavonoids and mainly catalyzed prenylations at C-6. These results encouraged us to find more prenyltransferases with different substrate specificities and prenylation positions on the flavonoid skeleton. The following experiments were carried out:

> Enzyme assays of flavonoids with fungal prenyltransferases.
> Analysis and isolation of enzyme products by HPLC, and structure elucidation by NMR and MS analyses.
> Determination of kinetic parameters for selected substrates.

2.3. Creation of FtmPT1 mutants with strongly increased activity for production of *C3*-prenylated *cyclo*-Trp-Pro stereoisomers by saturation mutagenesis

The fungal indole prenyltransferase FtmPT1 catalyzed prenylation of *cyclo*-L-Trp-L-Pro (brevianamide F) at position C-2 of the indole nucleus to produce a regular product tryprostatin B in the presence of DMAPP, and it was involved in the biosynthesis of fumitremorgins. Analysis of the substrate-bound structure of FtmPT1 revealed that several amino acid residues including Gly115 and Tyr205 were involved in the binding of brevianamide F. Mutation of Gly115 in FtmPT1 redirected the prenylation of brevianamide F from regular *C2*- to reverse *C3*-prenylation. Brevianamide F formed a hydrogen bond via its carbonyl oxygen in the diketopiperazine moiety with the hydroxyl group of Tyr205 near the center of the PT barrel (Jost et al. 2010) (Figure 1-11). We proposed that the location and orientation of brevianamide F in the reaction chamber can be influenced by replacement of Tyr205 with other amino acids, which could result in the formation of mutants with different enzyme activities. The following experiments were carried out:

> Molecular modeling-guided site-directed mutagenesis experiments.
> Enzyme assays of FtmPT1 and mutants with four *cyclo*-Trp-Pro stereoisomers.
> Comparison of enzyme activities and structure elucidation by LC-MS and NMR.
> Determination of kinetic parameters for selected substrates.

3. Results and discussion

3.1. Biochemical investigations on the acceptance of acylphloroglucinols in the presence of DMAPP, GPP, and FPP catalyzed by fungal prenyltransferases

Up to now, three membrane-bound prenyltransferases HlPT-1, HlPT1L, and HlPT2 from *H. lupulus* were reported to elaborate skeletons of APs (Li et al. 2015a; Tsurumaru et al. 2012). HlPT-1 catalyzed the prenylation of phlorisobutyrophenone (**1**) and phlorisovalerophenone (**2**) in the presence of DMAPP. Co-expression of different genes revealed that HlPT1L and HlPT2 catalyzed three sequential prenylation steps in the β-bitter acid pathway (Li et al. 2015a; Tsurumaru et al. 2012). In this study, we tested the acceptance of APs by fungal prenyltransferases of the DMATS superfamily.

DMAPP, GPP, and FPP were prepared according to the method described for GPP (Woodside et al. 1988) by Lena Ludwig and Dr. Edyta Stec. **1**, **2**, and phlorbenzophenone (**3**) were synthesized by Lena Ludwig according to protocols described previously (George et al. 2010) and incubated with thirteen purified soluble prenyltransferases, including seven cyclic dipeptide prenyltransferases (AnaPT (Yin et al. 2009b), FtmPT1 (Grundmann and Li 2005), CdpC2PT (Mundt and Li 2013), CdpC3PT (Yin et al. 2010b), CdpNPT (Yin et al. 2007), BrePT (Yin et al. 2013), and CTrpPT (Zou et al. 2010)), four tryptophan prenyltransferases (5-DMATS (Yu et al. 2012b), 6-DMATS$_{Sa}$ (Winkelblech and Li 2014), 7-DMATS (Kremer et al. 2007), and FgaPT2 (Unsöld and Li 2005)), and two tyrosine prenyltransferases (SirD (Zou et al. 2011) and TyrPT (Fan et al. 2014)). HPLC analysis of the incubation mixtures revealed that AnaPT showed higher activities towards these compounds than other tested enzymes. The tryptophan prenyltransferase 7-DMATS from *A. fumigatus* (Kremer et al. 2007) showed slightly lower activities than AnaPT. These results encouraged us to test the acceptance of phloroglucinol (**4**) and its carboxylic acid (**5**), orsellinic acid (**6**) and 6-methylsalicylic acid (**7**) as substrates. All of these substances were accepted with 50 μg AnaPT at 37°C for 6 h (Scheme 3-1). Nine enzyme products of AnaPT were isolated on HPLC and their structures were elucidated by HRESI-MS and NMR analyses, including ^{1}H-NMR and ^{1}H-^{1}H spatial correlations in nuclear overhauser effect spectroscopy (NOESY). The results showed that the soluble fungal indole prenyltransferase AnaPT catalyzed the same reaction of APs as the membrane-bound prenyltransferases involved in the biosynthesis

of the prenylated APs in plants like HIPT-1. AnaPT also prenylated hydroxylated benzoic acids, such as **6** and **7**, which are typical PKS products of microorganisms. Therefore, prenylated and hydroxylated benzoic acids could be produced by introducing *anaPT* into the producers of **6** and **7** or by coexpression of the responsible PKS genes with *anaPT* in suitable hosts.

**Scheme 3-1.** Prenyl transfer reactions of (*R*)-benzodiazepinedione and **1−7** catalyzed by AnaPT (modified from Zhou et al., 2015).
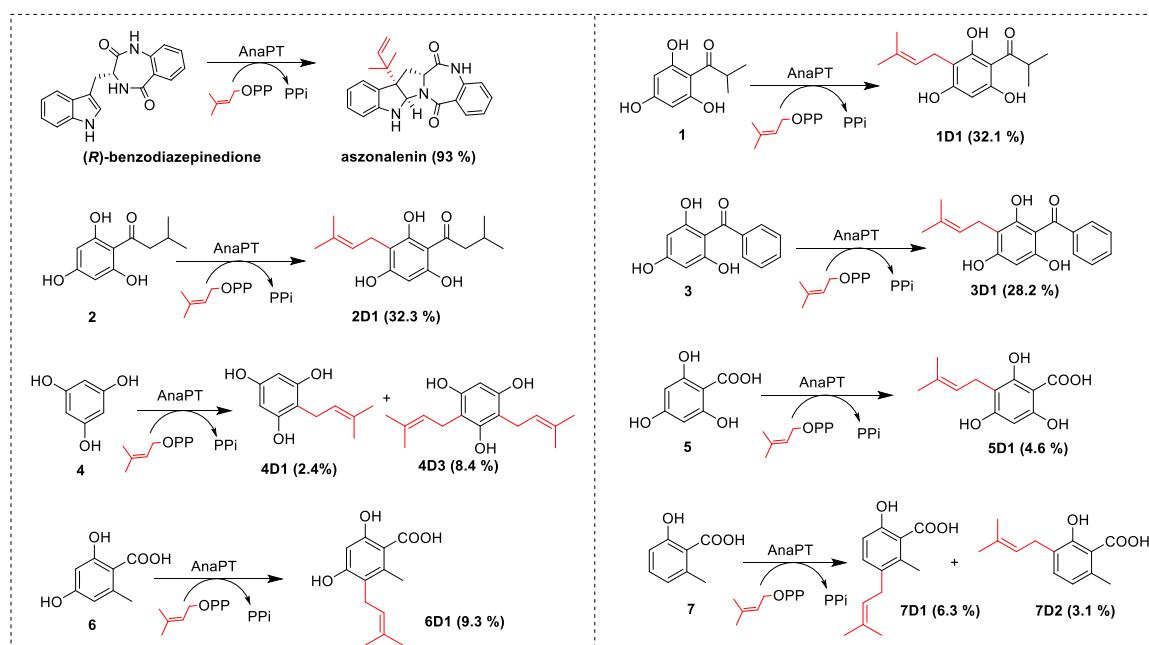
The observed activities of AnaPT toward **1–3** were much higher than that of a microsomal fraction containing the overproduced prenyltransferase from the glandular trichomes of hops. However, only monoprenylated derivatives were obtained in the presence of DMAPP and the conversion yields of **1–3** with GPP as prenyl donor were very low. Recently, a soluble prenyltransferase AtaPT from *A. terreus* strain was demonstrated to carry an unprecedented promiscuity toward diverse drug-like aromatic acceptors and prenyl donors including DMAPP, GPP, and FPP (Chen et al. 2017). AtaPT shares high sequence identity with the hypothetical protein EAU34068 encoded by ATEG_04999 from *A. terreus* NIH2624 and differs at only three residues, i.e. at 290 (Thr in AtaPT and Lys in EAU34068), 292 (Ala versus Glu), and 373 (Asn versus Ser). Among the tested aromatic substrates, AtaPT also consumed **3** in the presence of DMAPP, GPP, and FPP, although no noteworthy sequence homology exits between AtaPT and HIPT1L and HIPT2. These reactions were not studied in detail (Chen et al. 2017). The coding sequence of ATEG_04999 orthologue from *A. terreus*

DSM 1958 was amplified by PCR and cloned into the expression vector pQE-70, resulting in the expression construct pCaW7, which carried out by Dr. Carsten Wunsch. Gene expression in *E. coli* and purification of the soluble protein resulted in a predominant band on SDS-PAGE with a migration above the 45 kDa size marker, corresponding well to the calculated mass of 48.7 kDa for AtaPT-His$_6$. Protein yield was calculated to be 29 mg of purified protein per liter of culture.
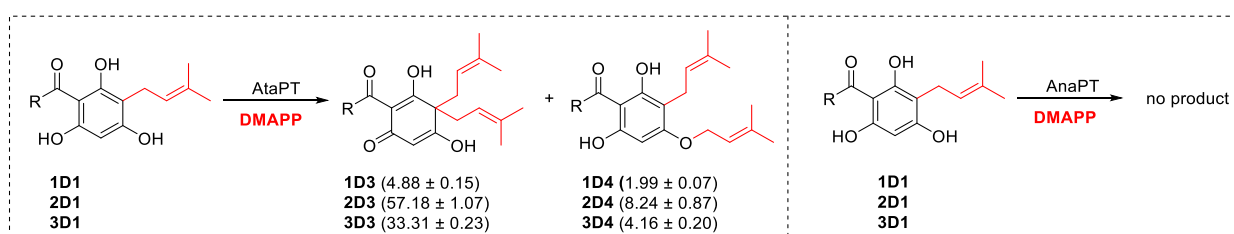
Total conversion yields of 64.3 ± 2.4, 23.7 ± 1.2, and $27.4 \pm 0.2\%$ were calculated for **1–3** after incubation with 20 µg protein at 37°C for 2 h in the presence of DMAPP, respectively (Scheme 3-2). These values were higher than those obtained from AnaPT with conversion yields of 3.6 ± 0.8, 4.3 ± 0.8, and $7.7 \pm 0.5\%$ respectively in the same conditions. Interestingly, two main products were observed from the reaction mixtures of AtaPT with **1–3**. LC-MS analysis revealed that the [M+H]$^+$ ions of the unknown product peaks are 136 Da larger than their respective substrates, indicating that the diprenylations of **1–3** had taken place. These results encouraged us to investigate into the structures of the diprenyl derivatives. To elucidate the structures, nine enzyme products were isolated from the incubation mixtures of **1–3** with AtaPT and DMAPP and were subjected to NMR analysis. They were proven to be *C*-dimethylallyl products **1D1–3D1**, *gem*-diprenylated derivatives **1D3–3D3**, *O*-dimethylallyl derivatives **1D2** and **2D2**, and *C*- and -*O*-di-dimethylally product **2D4** (Scheme 3-2).

Scheme 3-2. Prenyl transfer reactions of **1–3** catalyzed by AtaPT (modified from Zhou et al., 2017).
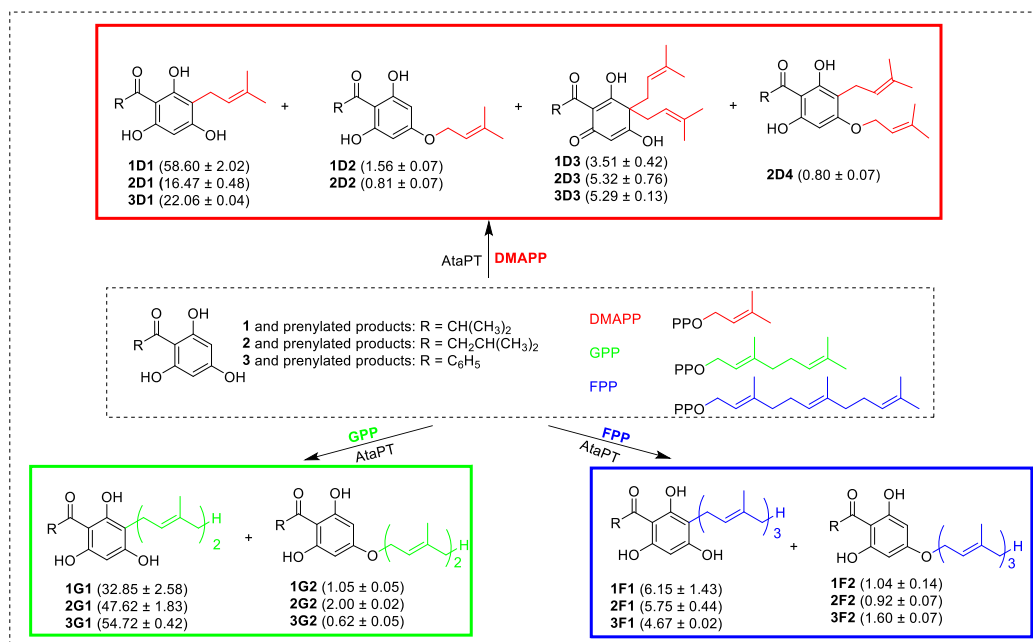
More interestingly, AtaPT also accepted *C*-monoprenylated products **1D1–3D1** as substrates. After incubation with 50 μg protein at 37°C for 2 h in the presence of DMAPP. HPLC, LC-MS, and NMR analyses revealed that *gem*-diprenylated derivatives **1D3–3D3** were observed as predominant products from extract of the incubation mixtures with product yields of 4.88 ± 0.15, 57.18 ± 1.07, and 33.31 ± 0.23%, respectively. A minor diprenylated product each with longer retention time was detected. No product was detected in the incubation mixtures of **1D1−3D1** with AnaPT and DMAPP under the same conditions (Scheme 3-3).

Scheme 3-3. Results of the incubation of dimethylallyl APs catalyzed by AtaPT or AnaPT (modified from Zhou et al., 2017).

In addition geranyl diphosphates (GPP) and farnesyl diphosphates (FPP) were also accepted by AtaPT as prenyl donors, forming monoprenylated acylphloroglucinols with C-C or C-O bonds. The conversion yields of *C*-prenylated products were 32.9 ± 2.6, 47.6 ± 1.8, and 54.7 ± 0.4% were calculated for **1−3** after incubation with 20 μg protein at 37°C for 2 h in the presence of GPP (Scheme 3-2), which were much higher than that of AnaPT. FPP was also used as a donor, but the conversion yields of the three substrates **1−3** were lower than that of DMAPP or GPP as donors under the same condition. These prenylated products were identified as *C*-geranyl derivatives **1G1–3G1**, *O*-geranyl products **1G2–3G2**, *C*-farnesyl derivatives **1F1–3F1**, and *O*-farnesyl products **1F2–3F2** (Scheme 3-2). The *O*-prenylated derivatives were identified as minor products with conversion yields in the range of 0.5-2.0%.

No product was detected by LC-MS analysis after incubation of **1D2** and **2D2** with 50 μg AtaPT and DMAPP at 37°C for 2 h. Incubation of **1D1–3D1** with AtaPT and GPP or FPP did not result in product formation under the same conditions. No diprenylated product was detected in the incubation mixtures of AtaPT with **1−3** and GPP or FPP in the same conditions, which was confirmed by incubation of their *C*-monoprenylated derivatives (Scheme 3-4). Product formation was not observed neither for the reaction mixtures of **1G1–3G1** with AtaPT in the presence of GPP, nor for those of **1F1–3F1** with FPP.

Scheme 3-4. Results of the incubations of monoprenylated APs with AtaPT (modified from Zhou et al., 2017).
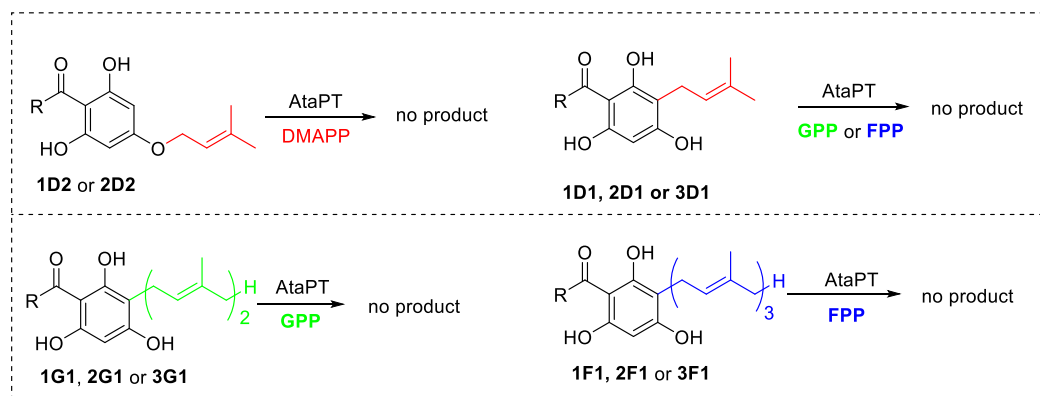
To get more information on the catalytic efficiency of the tetrameric AtaPT, kinetic parameters including Michaelis−Menten constants (K_M) and turnover numbers (k_{cat}) were determined at pH 7.5 for **1**, **2**, and **3** in the presence of DMAPP, GPP, and FPP as well as DMAPP with **1** and GPP with **3**. The catalytic efficiency of AtaPT toward **1** is 32-fold of that of AnaPT in the presence of DMAPP. **1** was better consumed by AtaPT in the presence of DMAPP and FPP than **2** and **3**. **3** was the most efficiently consumed substrate in the presence of GPP. The determined k_{cat}/K_M values for **1**−**3** are in the range of 170−300 $s^{-1}M^{-1}$ in the presence of GPP and between 17 and 37 $s^{-1}M^{-1}$ in the presence of FPP. With **1** as acceptor, a 95-fold k_{cat}/K_M value of that of AnaPT was determined for DMAPP with AtaPT.

In this study, we provided the first example of *gem*-diprenylation of APs by a member of the dimethylallyltryptophan synthase superfamily and an alternative synthesis method of *gem*-diprenylation of APs. AtaPT could be an interesting candidate for production of polyprenylated APs like β-bitter acids by synthetic biological method.

For detailed information about this work, please see the publications (sections 4.1 and 4.2)

Kang Zhou, Lena Ludwig, and Shu-Ming Li (2015). Friedel-Crafts alkylation of acylphloroglucinols catalyzed by a fungal indole prenyltransferase. *J. Nat. Prod.*, *78* (4): 929–933

Kang Zhou, Carsten Wunsch, Jungui Dai, and Shu-Ming Li (2017). *Gem*-diprenylation of acylphloroglucinols by a fungal prenyltransferase of the dimethylallyltryptophan synthase superfamily. *Org. Lett.* 19 (2): 388–391

3.2. Chemoenzymatic synthesis of prenylated flavonoids by fungal prenyltransferases

Prenylated flavonoids are a group of compounds predominantly found in plants (Botta et al. 2005b; Botta et al. 2009; Chen et al. 2014a). Due to their broad pharmacological activities (Botta et al. 2005b; Botta et al. 2009; Grienke et al. 2016; van de Schans et al. 2015; Wätjen et al. 2007), various strategies have been developed for both regioselective chemical and chemoenzymatic synthesis of prenylated flavonoids, especially for *C*-prenylated derivatives (Hossain et al. 2006; Tischer and Metz 2007; Yang et al. 2016; Yazaki et al. 2009). In previous studies, prenylated flavonoids have been produced by using recombinant enzymes (Kumano et al. 2008; Ozaki et al. 2009; Sasaki et al. 2008; Sasaki et al. 2011). However, only a few of such derivatives carry a dimethylallyl moiety at position C-6. In a former work, it was demonstrated that the recombinant indole prenyltransferase 7-DMATS accepted chalcones, isoflavonoids, and flavanones much better than flavones and flavonols and mainly catalyzed prenylation at C-6 of the ring A. Preliminary results indicated that AnaPT could be a good candidate for prenylations other than those of 7-DMATS (Yu and Li 2011).

AnaPT was then incubated with twenty-one flavonoids and analogues in the presence of DMAPP. Naringenin (**1a**), 7-hydroxyflavanone (**2a**), eriodictyol (**3a**), hesperetin (**4a**), silibinin (**5a**), phloretin (**6a**), apigenin (**7a**), genistein (**8a**), and biochanin A (**9a**) were better substrates than other substrates. HPLC analysis showed that the retention time of the major enzyme product of AnaPT with **1a** was 9 min, which was 1 min shorter than that of the *C6*-prenylated **1a** obtained from the 7-DMATS assay with 40 μg AnaPT at 37°C for 2h (Figure 3-1).

To get more information of enzyme products catalyzed by 7-DMATS and AnaPT, we extended the reaction time to 16h. As shown in Figure 3-1, AnaPT displayed a clearly different substrate preference from that of 7-DMATS. AnaPT accepted **1a**, **2a**, **5a**, **7a**, and **9a** better than 7-DMATS, while **3a**, **4a**, **6a**, and **8a** were better substrates for 7-DMATS. The major products of AnaPT and 7-DMATS reactions clearly differed in some cases from each other. For example, the main product **1b** in the 7-DMATS reaction with **1a** was only detected as a minor product in its reaction mixture with AnaPT. Instead, a product **1c** with a yield of 54.2% was the main product. Eriodictyol (**3a**) was much better accepted by 7-DMATS and several products including **3b**, **3c**, and **3d** with comparable yields were observed, whereas **3c** with a product yield of 16.4% was the main product of the AnaPT reaction. Silibinin (**5a**), a

hepatoprotective flavanonol from the medicinal plant *Silybum marianum* (Biedermann et al. 2014), was accepted by AnaPT with a product yield of 11.3%, whereas HPLC analysis showed that no product formation was observed from the incubation mixture of **5a** with 7-DMATS. Phloretin (**6a**) was converted by 7-DMATS to one predominate product **6b**, while a number of products including **6b**, **6c**, and **6d** were detected in its reaction mixture with AnaPT. These results indicated that different prenyl transfer reactions catalyzed by the two enzymes.

To investigate the prenylated positions and patterns of these substrates, twelve enzyme products **1b**, **1c**, **2b**, **3c**, **5b**, **6b**, **6c**, **6d**, **7b**, **8b**, **8c**, and **9b** were isolated by preparative HPLC from incubation mixtures of **1a-3a**, **5a-9a** with AnaPT and DMAPP, respectively. The ^{1}H NMR spectrum of **5b** was very similar to that of its substrate silybin (Lee and Liu 2003) and showed additional signals for a dimethylallyl moiety. HSQC and HMBC spectra were further proved the prenylation of the 7-hydroxy group (Figure 3-1). Comparing the ^{1}H-NMR spectra of **6c** and **6d** (Yu and Li 2011) with that of **6a** revealed that **6c** is a *C3′*-monoprenylated derivative and **6d** bears the two prenyl moieties at C-6 and C-3′ (Figure 3-1). Compounds **1b**, **1c**, **2b**, **3c**, **6b**, **7b**, **8b**, **8c**, and **9b** were identified as known compounds by ^{1}H-NMR and HR-EI-MS analyses and literature search, including *C6*-prenylated derivatives (**1b**, **2b**, **6b**, **7b**, **8b**, and **9b**), *C3′*-prenylated derivatives (**1c** and **3c**), and *C6*, *C3′*-diprenylated product (**8c**) (Figure 3-1).

AnaPT displayed in several cases different behaviors regarding the prenylation positions from those of 7-DMATS reported previously (Yu and Li 2011). For **1a**, **3a**, and **6a**, 7-DMATS preferred for a prenylation at C-6 of A-ring and *C6*-prenylated derivatives **1b**, **3b**, and **6b** were detected as predominant or one of the main products. In contrast, *C3′*-prenylation of B-ring was observed as main reactions in the assays of these compounds with AnaPT.

To get information on the catalytic efficiencies of AnaPT towards flavonoids, kinetic parameters were determined for the nine substrates. The K_M and k_{cat} values for flavonoids were determined to be in the range of 0.10-0.90 mM and 3-170 s^{-1}, respectively. These data provided evidence that AnaPT, the soluble indole prenyltransferases, could also be used for production of prenylated flavonoids in microorganisms by synthetic biological approaches.
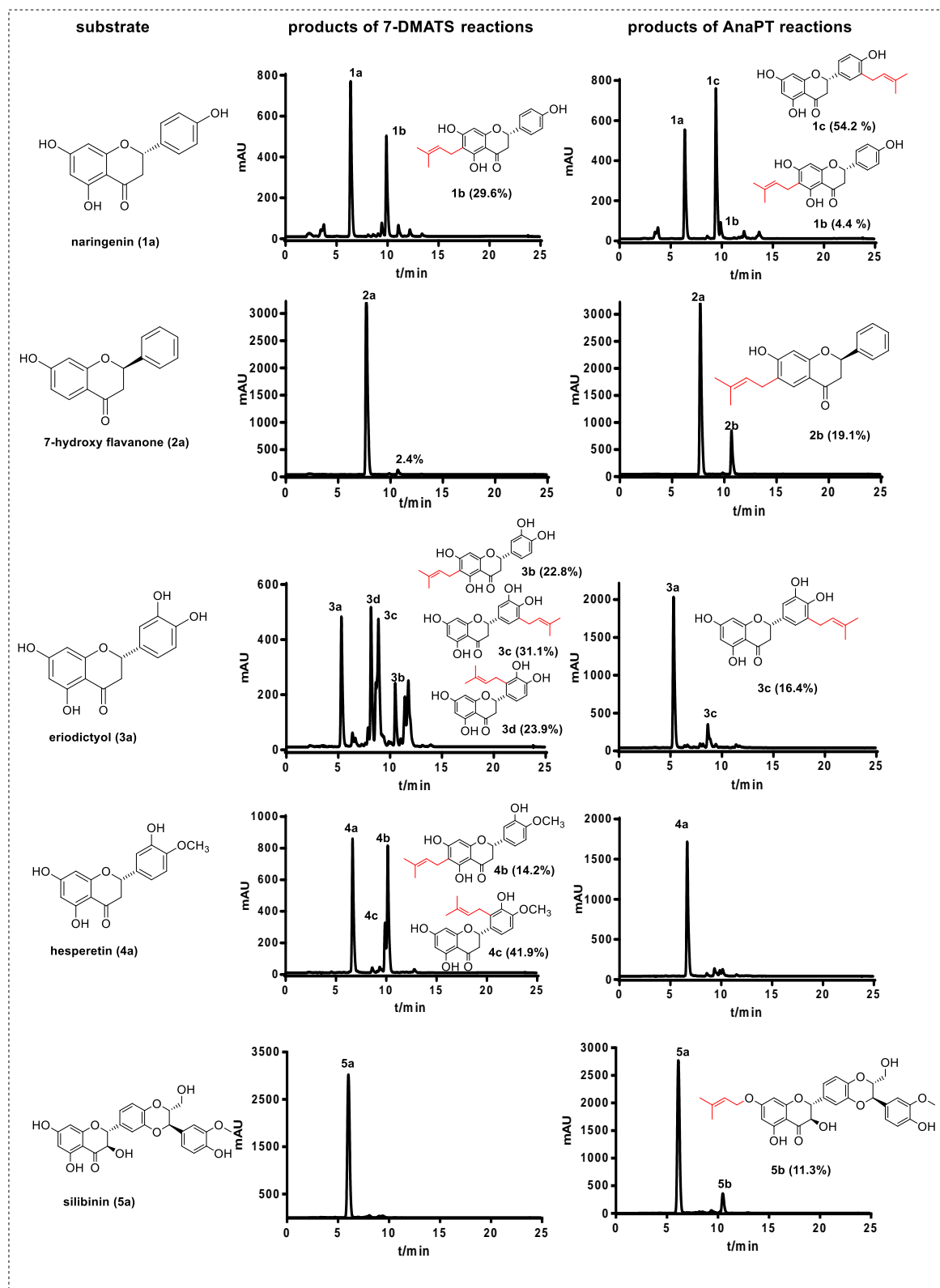
Figure 3-1. HPLC analysis of reaction mixtures of 7-DMATS and AnaPT (modified from Zhou et al., 2015).
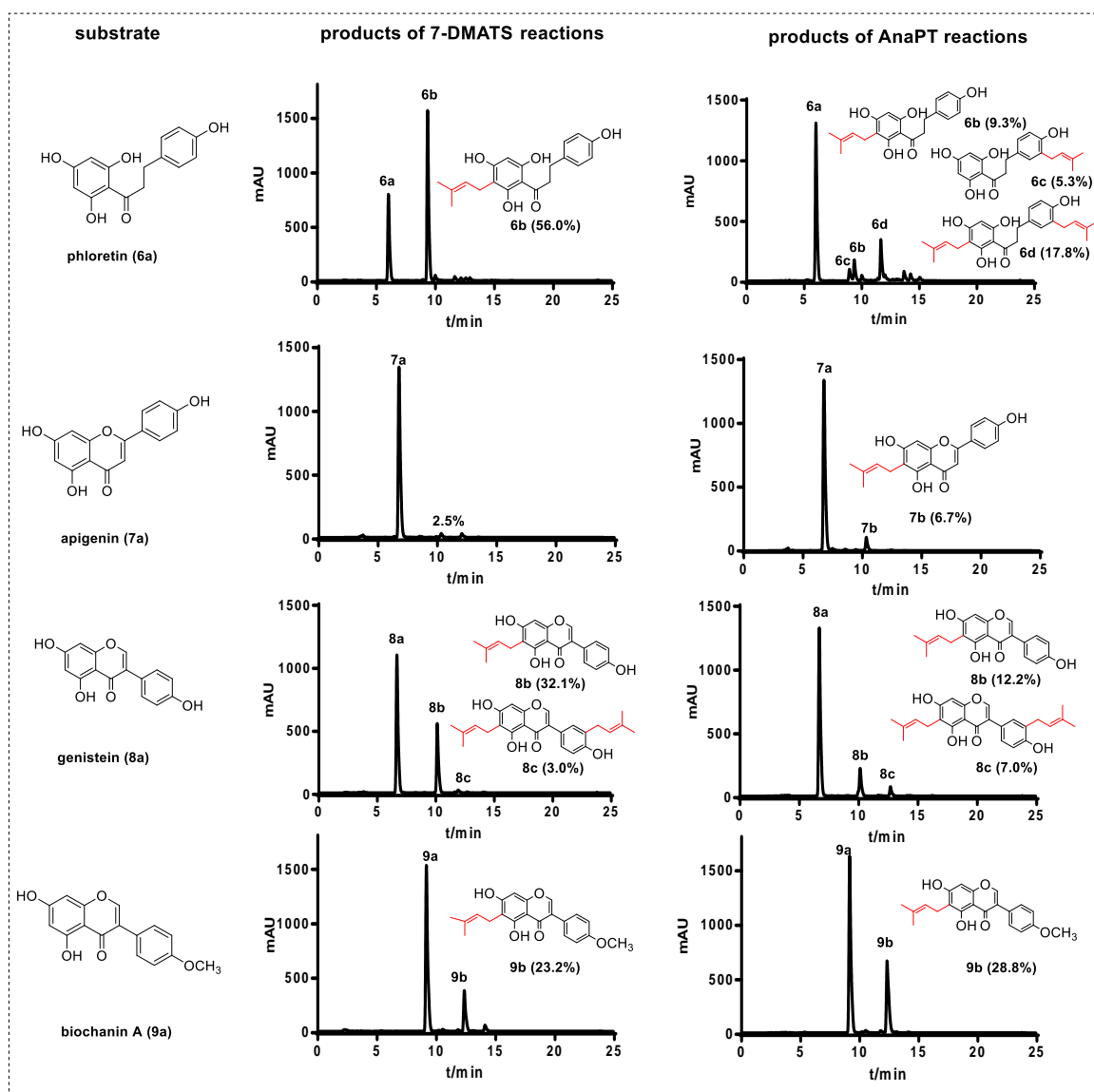
Figure 3-1 (continued)

For detailed information about this work, please see the publication (section 4.3)

Kang Zhou, Xia Yu, Xiulan Xie, and Shu-Ming Li (2015). Complementary flavonoid prenylations by fungal indole prenyltransferases. *J. Nat. Prod.,* 78 (9): 2229–2235

3.3. Creation of FtmPT1 mutants with strongly increased activity for production of *C3*-prenylated *cyclo*-Trp-Pro stereoisomers by saturation mutagenesis

The indole prenyltransferase FtmPT1 from *A. fumigatus* used DMAPP as prenyl donor and *cyclo*-L-Trp-L-Pro as acceptor and catalyzed predominantly a regular *C2*-prenylattion
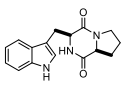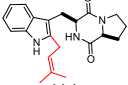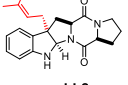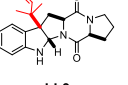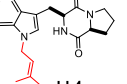
(Grundmann and Li 2005; Li 2011; Wollinsky et al. 2012). AnaPT, CdpNPT, and CdpC3PT acted as reverse *C3*-prenyltransferases on different cyclic dipeptides, leading to the formation of prenylated pyrrolo[2,3-b]indoles with *anti-cis* or *syn-cis* configuration of the ring systems (Fan et al. 2015a; Schuller et al. 2012; Winkelblech et al. 2015a; Yin et al. 2009b; Yin et al. 2010a; Yu et al. 2013). The indole prenyltransferase ArdB from *A. fischeri* catalyzed reverse *C3*-prenylation of a tripeptide derivative (Haynes et al. 2013). A prenyltransferase was identified in the producer of nocardioazines and proven to be responsible for a regular *C3*-prenylation of *cyclo*-ʟ-Trp-ʟ-Trp (Alqahtani et al. 2015). In comparison to reverse *C3*-prenyltransferases, there is still a deficiency with the availability of regular *C3*-prenyltransferases for application in the chemoenzymatic synthesis or synthetic biology.
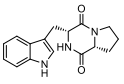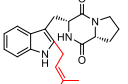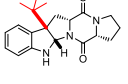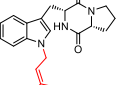
Crystal structures of unliganded FtmPT1 and its ternary complex with brevianamide F and DMSPP were solved and used as basis to understand the catalytic mechanism. Prenyl transfer reaction was performed in a hydrophobic reaction chamber at the center of the barrel (Jost et al. 2010). Several amino acid residues including Gly115 and Tyr205 were proposed to be involved in the binding of brevianamide F. Mutation of Gly115 to Thr in FtmPT1 redirects the prenylation of brevianamide F from regular *C2*- to reverse *C3*.

Saturation mutagenesis experiments were carried out on the amino acid Tyr205. Nineteen single and one double mutants of FtmPT1 were obtained. Single mutants were constructed by Wei Zhao and Dr. Sylwia Tarcz. Five mutants Y205C, Y205L, Y205N, Y205I, and Y205S showed similar enzyme activity as the wildtype with substrate consumption of more than 90% under the tested conditions. Five mutants Y205H, Y205Q, Y205V, Y205G, and Y205E showed lower enzyme activity with substrate consumption between 46.9 and 76.4%. Other mutants like Y205A, Y205R, Y205K, Y205D, and Y205P accepted brevianamide F with significantly reduced activities. In addition to the regularly *C2*-prenylated derivative **LL1** and the regularly *C3*-prenylated **LL2**, product peaks **LL3** at 34.8 min and **LL4** at 35.8 min were also detected in the reaction mixtures of most mutants (Scheme 3-5). Among these mutants, Y205L and Y205N showed high activity toward *cyclo*-ʟ-Trp-ʟ-Pro. Therefore, behaviors of Y205N and Y205L toward *cyclo*-Trp-Pro stereoisomers were tested. Y205N converted *cyclo*-ᴅ-Trp-ᴅ-Pro, *cyclo*-ʟ-Trp-ᴅ-Pro, and *cyclo*-ᴅ-Trp-ʟ-Pro mainly to one dominant peak each (**DD3**, **LD3**, or **DL3**), identified as reversely *C3*-prenylated derivatives, with product yields of 21.6 ± 1.1, 41.1 ± 1.9, and 32.5 ± 1.1%, respectively. Regularly *C2*-prenylated derivatives **DD1**, **LD1**, and **DL1** were minor products of *cyclo*-ᴅ-Trp-ᴅ-Pro, *cyclo*-ʟ-Trp-ᴅ-Pro, and

cyclo-D-Trp-L-Pro reactions, respectively. **DD1** was also identified as the predominant product of Y205L with *cyclo*-D-Trp-D-Pro, with a product yield of 60.5 ± 3.0%.
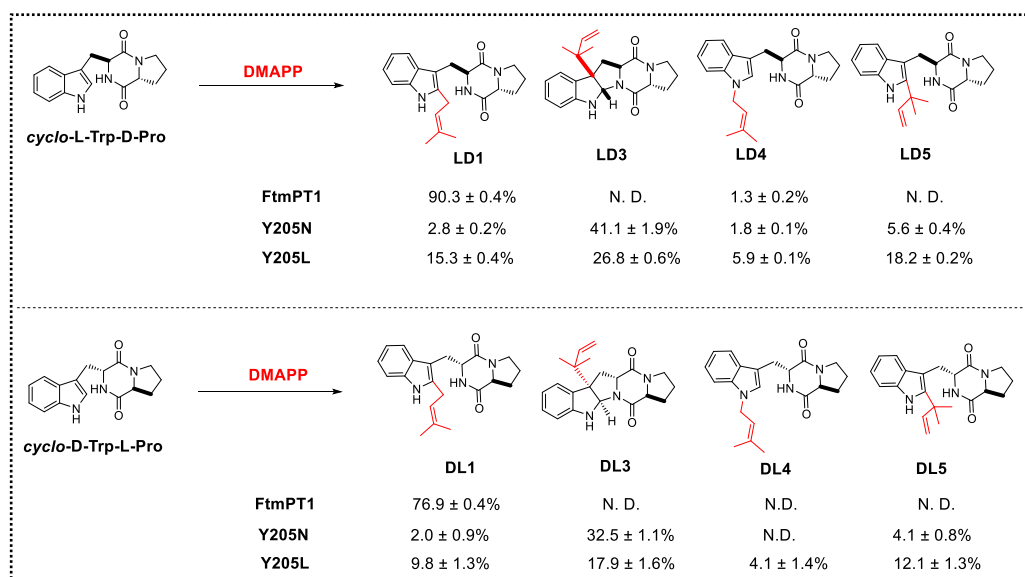
Scheme 3-5. Prenyl transfer reactions of *cyclo*-L-Trp-L-Pro and *cyclo*-D-Trp-D-Pro catalyzed by FtmPT1, Y205N, and Y205L (modified from Zhou et al., 2016).

	LL1	LL2	LL3	LL4
FtmPT1	96.2 ± 0.2%	N. D.	N. D.	2.0 ± 0.2%
Y205N	51.6 ± 0.1%	35.6 ± 0.2%	2.8 ± 0.2%	4.4 ± 0.1%
Y205L	53.5 ± 0.1%	31.8 ± 0.1%	1.6 ± 0.2%	7.6 ± 0.1%

	DD1	DD3	DD4
FtmPT1	27.5 ± 0.2%	N. D.	9.5 ± 0.3%
Y205N	3.1 ± 0.1%	21.6 ± 1.1%	N. D.
Y205L	6.1 ± 0.2%	60.5 ± 3.0%	3.1 ± 0.1%

The two enantiomers *cyclo*-L-Trp-D-Pro and *cyclo*-D-Trp-L-Pro were converted by Y205L to two similar complex product mixtures (Scheme 3-6). Detailed inspection of the HPLC chromatograms indicated the presence of **LD1** and **LD3** as well as **DL1** and **DL3** with the same retention times as those in the incubation mixtures of *cyclo*-L-Trp-D-Pro and *cyclo*-D-Trp-L-Pro with FtmPT1 and/or Y205N. **LD5** and **LD4** as well as **DL5** and **DL4** showed the same retention times as those of the reversely *C2*- and regularly *N1*-prenylated derivatives, which were obtained from the incubation mixtures of *cyclo*-L-Trp-D-Pro with BrePT (Yin et al. 2013) and CdpNPT (Yu et al. 2013), respectively. According to ^{1}H-NMR of the incubation mixtures of *cyclo*-L-Trp-D-Pro and *cyclo*-D-Trp-L-Pro with Y205N or Y205L, signals for dimethylallyl moieties of **LD5** and **LD4** as well as **DL5** and **DL4** were observed, which also proved the structures of enzyme products.

Scheme 3-6. Prenyl transfer reactions of *cyclo*-L-Trp-D-Pro and *cyclo*-D-Trp-L-Pro catalyzed by FtmPT1, Y205N, and Y205L (modified from Zhou et al., 2016).

	LD1	LD3	LD4	LD5
FtmPT1	90.3 ± 0.4%	N. D.	1.3 ± 0.2%	N. D.
Y205N	2.8 ± 0.2%	41.1 ± 1.9%	1.8 ± 0.1%	5.6 ± 0.4%
Y205L	15.3 ± 0.4%	26.8 ± 0.6%	5.9 ± 0.1%	18.2 ± 0.2%

	DL1	DL3	DL4	DL5
FtmPT1	76.9 ± 0.4%	N. D.	N.D.	N. D.
Y205N	2.0 ± 0.9%	32.5 ± 1.1%	N.D.	4.1 ± 0.8%
Y205L	9.8 ± 1.3%	17.9 ± 1.6%	4.1 ± 1.4%	12.1 ± 1.3%

It was demonstrated that mutation on Gly115 to Thr led to change the prenylation pattern and position, i.e. from regular *C2*-prenylation catalyzed by FtmPT1 to reverse *C3*-prenylation catalyzed by FtmPT1_G115T. A plasmid pKZ27 for overproduction of the double mutant FtmPT1_G115T_Y205N was constructed. HPLC analysis of the incubation mixture of *cyclo*-L-Trp-L-Pro with 5 µg enzyme at 37°C for 2 h revealed a drastic reduction of the enzyme activity. A very small product peak with a retention time corresponding to that of **LL2** was observed in the chromatogram. These resulted indicated that both positions could not be altered at the meantime. Similar results were also obtained for G115T_Y205N with *cyclo*-D-Trp-D-Pro, *cyclo*-L-Trp-D-Pro, or *cyclo*-D-Trp-L-Pro.

These results demonstrated that Y205N and Y205L could be used for production of regularly *C3*-prenylated brevianamide F in the chemoenzymatic synthesis and synthetic biology. More specific enzymes for regular *C3*-prenylation should be created in the future, e.g. by mutagenesis of mutants obtained in this study.

For detailed information about this work, please see the publication (section 4.4)

Kang Zhou, Wei Zhao, Xiao-Qing Liu, and Shu-Ming Li (2016). Saturation mutagenesis on Tyr205 of the cyclic dipeptide *C2*-prenyltransferase FtmPT1 results in mutants with strongly increased *C3*-prenylating activity. *Appl Microbiol Biotechnol,* 100 (23):9943-9953

4.   Publications

4.1. Friedel-Crafts alkylation of acylphloroglucinols catalyzed by a fungal indole prenyltransferase

Friedel–Crafts Alkylation of Acylphloroglucinols Catalyzed by a Fungal Indole Prenyltransferase

Kang Zhou, Lena Ludwig, and Shu-Ming Li*

Institut für Pharmazeutische Biologie und Biotechnologie, Philipps-Universität Marburg, Marburg 35037, Germany

Ⓢ Supporting Information

ABSTRACT: Naturally occurring prenylated acylphloroglucinol derivatives are plant metabolites with diverse biological and pharmacological activities. Prenylation of acylphloroglucinols plays an important role in the formation of these intriguing natural products and is catalyzed in plants by membrane-bound enzymes. In this study, we demonstrate the prenylation of such compounds by a soluble fungal prenyltransferase AnaPT involved in the biosynthesis of prenylated indole alkaloids. The observed activities of AnaPT toward these substrates are much higher than that of a microsomal fraction containing an overproduced prenyltransferase from the plant hop.
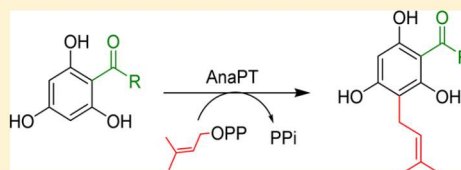
Polyprenylated acylphloroglucinols are found in a limited number of plant families including Clusiaceae, Hypericaceae, and Cannabaceae.[1−5] Their fascinating chemical structures and intriguing biological activities have attracted increasing attention. Hyperforin, a polyprenylated acylphloroglucinol (Scheme S1, Supporting Information), and the naphthodianthrone hypericin are considered as active constituents in extracts of *Hypericum perforatum* (St John's wort, Hypericaceae) used for treatment of depression in Europe and the USA.[2] Humulone (α-acid) and lupulone (β-acid, Scheme S1, Supporting Information) are prenylated acylphloroglucinols in hop cones, the female flowers of *Humulus lupulus* (Cannabaceae), and are responsible for the bitter taste and pharmacological effects.[3] Hops are used primarily as a flavoring and stabilizing agent in beer. In traditional medicines, hops are also used as mild sedative drugs.[3]

Biogenetically, the acylphloroglucinol cores in hyperforin and lupulone are formed by condensation of three malonyl-CoA molecules with different start units, isobutyryl-CoA in the case of the hyperforin precursor phlorisobutyrophenone (1a) and isovaleryl-CoA in the case of the lupulone precursor phlorisovalerophenone (2a). This key step is catalyzed by a polyketide synthase (PKS) and followed by an alkylation on the benzene ring catalyzed by prenyltransferases (Scheme S1, Supporting Information).[1,6,7] Several plants from the families Clusiaceae and Hypericaceae also use benzoyl-CoA as start unit and produce phlorbenzophenone (3a) and derivatives thereof such as grandone (Scheme S1, Supporting Information).[4,5,8,9]

In sharp contrast to many new prenylated acylphloroglucinol derivatives reported in 2014,[1,5,8] little is known about the enzymes related to the biosynthesis of these compounds. Until now, only one recombinant enzyme involved in their biosynthesis, the prenyltransferase HIPT-1 from *Humulus lupulus*, was investigated biochemically.[6] The membrane-bound HIPT-1 was overproduced in baculovirus-infected insect cells[6] and the microsomal fraction of the protein extract was used for enzyme assays. It catalyzed the prenylation of

phlorisovalerophenone (2a) in the presence of dimethylallyl diphosphate (DMAPP) and also accepted phlorisobutyrophenone (1a) as prenylation substrate. Its catalytic activities for both substrates were very low, being 11 pmol per mg of microsomal fraction per minute for phlorisovalerophenone (2a), and 29.5% of that for phlorisobutyrophenone (1a). Like most membrane-bound proteins, HIPT-1 is more difficult to overproduce and purify than soluble enzymes. These features strongly prohibit its potential use as a biocatalyst for chemoenzymatic synthesis for production of prenylated acylphloroglucinols. Therefore, there is a need to find alternative enzymes with better properties. In this study, we tested the acceptance of such acylphloroglucinols by prenyltransferases of the DMATS superfamily from fungi, which are soluble proteins and can be easily overproduced in *Escherichia coli* with significantly higher yields.[10]

Phlorisobutyrophenone (1a), phlorisovalerophenone (2a), and phlorbenzophenone (3a) were synthesized according to protocols described previously[11−13] (Scheme 1) and incubated with 13 purified soluble fungal prenyltransferases including four tryptophan, seven cyclic dipeptide, and two tyrosine prenyltransferases. HPLC analysis of the incubation mixtures revealed that AnaPT from *Neosartorya fischeri*, which catalyzes the C3-

Scheme 1. Synthesis of Acylphloroglucinols

R=CH(CH₃)₂ phlorisobutyrophenone (1a, 70.8 %)

R=CH₂CH(CH₃)₂ phlorisovalerophenone (2a, 67.1 %)
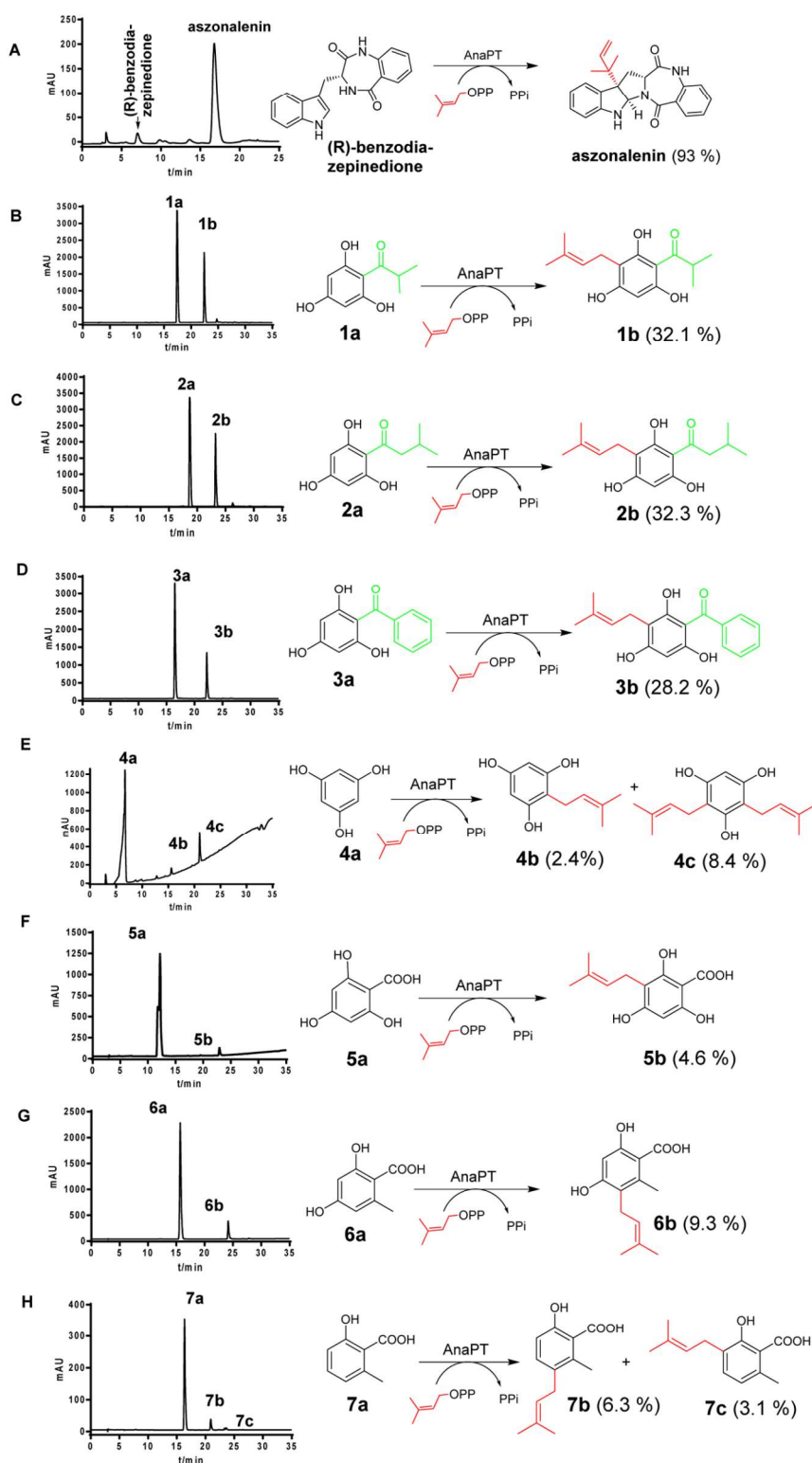
R=C₆H₅ phlorbenzophenone (3a, 65.8%)
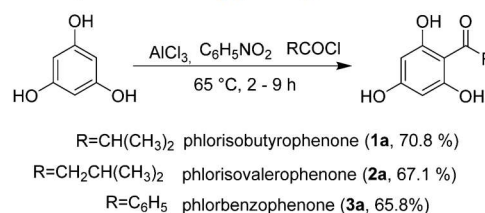
Figure 1. HPLC chromatograms and prenyl transfer reactions catalyzed by AnaPT. Different wavelengths were used for illustration of product formation: 230 nm (**4a**), 254 nm ((R)-benzodiazepinedione and **5a**), 266 nm (**6a**), 291 nm (**1a**, **2a**, and **7a**), and 306 nm (**3a**).

prenylation of (R)-benzodiazepinedione (Figure 1A) and is involved in the biosynthesis of acetylaszonalenine,[14] showed higher activities toward these compounds than other tested enzymes (Table S1, Supporting Information). Conversion

yields between 12% and 14% were achieved for these substrates after incubation with 5 μg of AnaPT in 100 μL assay at 37 °C for 16 h. No product formation was detected with heat-inactivated AnaPT (data not shown). Using 50 μg of protein,

41

Table 1. ^{1}H NMR Data (500 MHz) of the Enzyme Products 5b, 6b, 7b, and 7c in Methanol-d_4^{a}

Pos.	5b $\delta_{H,}$ (*J* in Hz)	6b $\delta_{H,}$ (*J* in Hz)	7b $\delta_{H,}$ (*J* in Hz)	7c $\delta_{H,}$ (*J* in Hz)
3	/	6.13, s	6.97, d (8.4)	/
4	/	/	6.57, d (8.4)	6.91, d (8.4)
5	5.73, s	/	/	6.50, d (8.4)
7	/	2.50, s	2.46, s	2.53, s
1′	3.16, d (7.0)	3.28, d (7.0)	3.24, d (7.0)	3.24, d (6.9)
2′	5.20, m	5.02, m	5.16, m	5.32, m
4′	1.63, s	1.66, s	1.71, s	1.70, s
5′	1.73, s	1.75, s	1.72, s	1.73, s

^{a}Chemical shifts (δ) are given in ppm and coupling constants (*J*) in Hz.

we found product formation to be nearly linear in the first 6 h (Figure S1, Supporting Information). Conversion yields of 32.1%, 32.3%, and 28.2% were calculated for **1a**, **2a**, and **3a**, respectively, after incubation with 50 μg of protein at 37 °C for 6 h (Figure 1). Under this condition, 93% of (*R*)-benzodiazepinedinone was converted to aszonalenin (Figure 1A). The tryptophan prenyltransferase 7-DMATS from *Aspergillus fumigatus*[15] showed slightly lower activities than AnaPT, with product yields of about 10% in the assays of **1a** and **2a** with 5 μg of protein (Table S1, Supporting Information). Compound **1a** was accepted by CdpC3PT from *Neosartorya fischeri*[16] with a conversion yield of 5.7% (Table S1, Supporting Information).

These results encouraged us to test the acceptance of phloroglucinol (**4a**) and its carboxylic acid **5a**, as well as orsellinic acid (**6a**) and 6-methylsalicylic acid (**7a**), as substrates. The latter two compounds were identified as PKS products in different microorganisms.[17−19] As shown in Figure 1, all of these substances were accepted by AnaPT. Conversion yields of 4.6−10.8% were observed using 50 μg of AnaPT after incubation at 37 °C for 6 h. It is obvious that acylphloroglucinols **1a**−**3a** are better substrates for AnaPT than **4a**−**7a**. Interestingly, **6a** with a methyl instead of a hydroxy group in **5a** was a better substrate for AnaPT (Figure 1F,G). Detailed inspection of the HPLC chromatograms B−H in Figure 1 revealed the presence of one predominant product each in the incubation mixtures of **1a**−**3a**, **5a**, and **6a**. Compounds **4a** and **7a** were converted to at least two products.

In a previous study,[20] we demonstrated that AnaPT also used geranyl diphosphate (GPP) as prenyl donor. Therefore, **1a**−**7a** were incubated with 50 μg of AnaPT in the presence of GPP. Indeed, product formation was observed in all incubation mixtures, but with relatively lower activities than with DMAPP for a given aromatic substrate. After incubation for 16 h, conversion yields of 6−10% were obtained for **1a**−**3a** and less than 5% for other substrates (Figure S2, Supporting Information).

To elucidate the structures, nine enzyme products, **1b**, **2b**, **3b**, **4b**, **4c**, **5b**, **6b**, **7b**, and **7c**, were isolated from the incubation mixtures of **1a**−**7a** with AnaPT and DMAPP and subjected to NMR and HR-EI-MS analysis (Table 1 and Tables S2 and S3 and Figures S3−S14, Supporting Information). In addition, **1b** was also isolated from the incubation mixtures of **1a** with CdpC3PT or 7-DMATS. The spectra of **1b** from the three different incubation mixtures are nearly identical, proving the same product of different enzymes. With the exception of **4c**, the M$^+$ ions of the isolated products are 68 Da larger than the respective substrates (Table S2, Supporting Information), proving the monoprenylation of these compounds. The M$^+$ ion of **4c** is 136 Da larger than that of **4a**, proving the diprenylation in its structure. This conclusion was confirmed by their molecular formula deduced from HR-MS analysis (Table S2, Supporting Information). The signals at δ3.16−3.29 (d, 2H −CH$_2$−), 5.02−5.32 (m, 1H, −C=CH), 1.61−1.71 (s, 3H, −C=C−CH$_3$), and 1.72−1.76 ppm (s, 3H, −C=C−CH$_3$) in the ^{1}H NMR spectra of the isolated products confirmed the presence of regular dimethylallyl moieties in their structures. The resonance of the methylene group in the range of 3.16−3.29 ppm proved their attachment to aromatic carbon atoms.[21] Comparison of the NMR data with those of previously reported compounds led to identification of the structures of **1b**,[22] **2b**,[22] **3b**,[23] **4b**,[24] and **4c**[24] as shown in Figure 1. The structures of **5b**, **6b**, **7b**, and **7c** have not been reported prior to this study.

Only one singlet for an aromatic proton at δ5.73 ppm was found in the ^{1}H NMR spectrum of **5b**, which proved unequivocally the attachment of the prenyl moiety at C-3 of the benzene ring (Table 1, Figure 1F). One singlet for an aromatic proton (δ6.13 ppm) was also observed in the ^{1}H NMR spectrum of **6b**, confirming the prenylation at C-3 or C-5 of the benzene ring. Coupling between CH$_3$ at C-6 and H-5 was observed in the ^{1}H NMR spectrum of **6a** (data not shown). No coupling between the signal for this methyl group at δ2.50 ppm with the singlet at δ6.13 ppm was observed in the ^{1}H NMR spectrum of **6b**, indicating a prenylation at C-5. The NOESY correlation of the signal at δ2.50 ppm with that of H-

1′ of the prenyl moiety at δ3.28 ppm proved unequivocally the prenylation at C-5, as shown in Figure 1. The ^{1}H NMR spectrum of **7b** showed two doublets at δ6.97 (1H, d, J = 8.4 Hz, ArH-3) and δ6.57 ppm (1H, d, J = 8.4 Hz, ArH-4), and the NOESY correlation of the signal at δ2.46 ppm for CH$_3$ at C-6 with that of H-1′ of the prenyl moiety at 3.24 (d, J = 7.8 Hz) confirmed the prenyl moiety at C-5 of the benzene ring. The spectrum of **7c** also showed signals of two aromatic protons at δ6.91 (1H, d, J = 7.5 Hz, ArH-3) and δ6.50 (1H, d, J = 7.5 Hz, ArH-4). NOESY correlation was observed for the signal of CH$_3$ at C-6 with that of H-5, suggesting the prenylation at C-3 in **7c** (Figure 1H).

In summary, our data provide evidence that the soluble fungal indole prenyltransferase AnaPT catalyzed the same prenylation reaction of acylphloroglucinols as the membrane-bound prenyltransferases involved in the biosynthesis of the prenylated acylphloroglucinols in plants like HIPT-1,[6] but with much higher conversion yields than HIPT-1. To the best of our knowledge, this is the first report on the prenylation of acylphloroglucinols by microbial enzymes. Furthermore, AnaPT also prenylated hydroxylated benzoic acids such as orsellinic acid (**6a**) and 6-methylsalicylic acid (**7a**), which are typical PKS products of microorganisms.[17−19] Therefore, prenylated and hydroxylated benzoic acids could be produced by introducing *anaPT* into the producers of **6a** and **7a** or by coexpression of the responsible PKS genes[17−19] with *anaPT* in suitable hosts. Thus, this work extends significantly the substrate and catalytic promiscuity of the prenyltransferases of the DMATS superfamily as well as their potential applications.

To get more insights into the catalytic efficiency of the tetrameric AnaPT[14,25] toward acylphloroglucinols and hydroxybenzoic acids, kinetic parameters including Michaelis−Menten constants (K_M) and turnover numbers (k_{cat}) were determined at pH 7.5 for (R)-benzodiazepinedinone, **1a−7a**, and DMAPP by Hanes−Woolf, Eadie−Hofstee, and Lineweaver−Burk plots and were compared with each other (Figures S15−24, Supporting Information). As given in Table 2, AnaPT displayed

Table 2. Kinetic Parameters of AnaPT toward Selected Substrates

substrate	K_M [mM]	V_{max} (nmol mg protein^{-1} min^{-1})	k_{cat} [s^{-1}]	k_{cat}/K_M [s^{-1} M^{-1}]
(R)-benzodiazepinedione	0.22	526	1.72	7818
1a	0.22	3.71	0.012	54.5
2a	0.33	5.07	0.017	51.5
3a	0.24	4.54	0.015	62.5
4a	1.64	0.71	0.0023	1.4
5a	0.87	1.21	0.0040	4.8
6a	0.42	3.54	0.012	28.6
7a	0.52	1.11	0.0037	7.1
DMAPP with **1a**	0.21	2.56	0.0084	40.0
DMAPP with **2a**	0.38	3.29	0.011	28.9

similar affinity to **1a−3a** as to its natural aromatic substrate (R)-benzodiazepinedinone,[14] while **4a−7a** showed lower affinity to AnaPT. With **1a** as aromatic substrate, a slightly higher K_M value was determined for DMAPP than in the presence of (R)-benzodiazepinedinone,[14] while a significantly higher K_M value was obtained in the presence of **2a**. As expected, the turnover numbers of AnaPT for **1a−3a** are very low, only 0.7−1.0% of

that of (R)-benzodiazepinedione determined in this study. Undoubtedly, catalytic efficiency of AnaPT toward acylphloroglucinols should be improved in the future by suitable approaches such as mutagenesis experiments. However, it should be mentioned that the turnover number of AnaPT toward its natural substrate is much higher (up to 10-fold) than most prenyltransferases of the DMATS superfamily to their natural substrates. The determined V_{max} values for **1a−3a** are in the range of 3.7−5.1 nmol mg protein^{-1} min^{-1}. Therefore, it can be concluded that AnaPT is already an interesting candidate as a biocatalyst for prenylation of phloroglucinol analogues, especially of acylphloroglucinols.

■ **EXPERIMENTAL SECTION**

General Experimental Procedures. Phloroglucinol (**4a**) was obtained from Acros Organics, 2,4,6-trihydroxybenzoic acid (**5a**) and orsellinic acid (**6a**) from Alfa Aesar, and 6-methylsalicylic acid (**7a**) from Chempur. NMR spectra were recorded on a JEOL ECA-500 spectrometer, processed with MestReNova 5.2.2. Chemical shifts were referenced to the signal of acetone-d_6 at 2.05 ppm or methanol-d_4 at 3.31 ppm. The enzyme products were also analyzed by electron impact mass spectrometry (EI-MS) on an Auto SPEC (Micromass Co. UK Ltd.).

Synthesis of DMAPP, GPP, and Acylphloroglucinols 1a, 2a, and 3a. The triammonium salts of dimethylallyl diphosphate (DMAPP) and geranyl diphosphate (GPP) were synthesized according to the method described for geranyl diphosphate by Woodside et al.[26] Compounds **1a**, **2a**, and **3a** in yields of 70.8%, 67.1%, and 65.8% were prepared by Friedel−Crafts acylations of phloroglucinol with isobutyryl chloride,[11] methylbutanal chloride,[13] and benzoyl chloride[12] in the presence of AlCl$_3$, respectively (Scheme 1).

Overproduction and Purification of the Recombinant AnaPT and Enzyme Assay. Protein overproduction and purification were carried out as described previously.[14] The enzyme assays (100 μL) contained **1a−7a** (1 mM), CaCl$_2$ (5 mM), DMAPP/GPP (2 mM), glycerol (1.0−6% v/v), dimethyl sulfoxide (DMSO, 5% v/v), 50 mM Tris-HCl (pH 7.5), and purified recombinant protein (5−50 μg). The reaction mixtures were incubated at 37 °C for different times and terminated by addition of 100 μL of methanol. The protein was removed by centrifugation at 13000 rpm for 20 min. Assays for isolation of the enzyme products were carried out in large scale (10−15 mL) containing aromatic substrates (1 mM), DMAPP (2 mM), CaCl$_2$ (5 mM), glycerol (1.0−9.9% v/v), DMSO (5% v/v), 50 mM Tris-HCl (pH 7.5), and 5 mg of recombinant protein per 10 mL assay. After incubation for 16 h at 37 °C, the reaction mixtures of **1a−3a** were extracted 3−4 times with a double volume of ethyl acetate. The organic phases were combined and evaporated. The residues were dissolved in methanol (0.5−1.0 mL) and purified by HPLC. The reaction mixtures of **4a−7a** were terminated by addition of a double volume of methanol. Protein was removed by centrifugation at 6000 rpm for 30 min. The supernatants were collected, concentrated, and dried on a rotary evaporator. The residues were dissolved in methanol (0.5−1.0 mL) and after centrifugation, the supernatants were purified on HPLC. Assays for determination of kinetic parameters (100 μL) contained CaCl$_2$ (5 mM), glycerol (1.0−9.9% v/v), DMSO (5% v/v), 50 mM Tris-HCl (pH 7.5), DMAPP (2 mM), 50 μg of AnaPT, and (R)-benzodiazepinedinone or **1a−7a** at final concentrations of up to 20.0 mM. For determination of the kinetic parameters of DMAPP, **1a** or **2a** at a final concentration of 1 mM and DMAPP of up to 5.0 mM were used. The reaction mixtures were incubated for 60 min ((R)-benzodiazepinedinone), 120 min (**1a**, **2a**, **3a**, **5a**, DMAPP, and **6a**), or 240 min (**4a** and **7a**). Product formation was found to be linear within such incubation times (Figure S1, Supporting Information). The reactions were then terminated with 100 μL of methanol. Protein was removed by centrifugation at 13000 rpm for 20 min.

Analysis of Enzyme Products by HPLC and Structure Elucidation by NMR and MS Analysis. An Agilent HPLC series

1200 was used for analysis and isolation of the enzyme products. A Multospher 120 RP-18 column (250 mm × 4 mm, 5 μm C+S Chromatographie Service, Langerwehe, Germany) was applied for analysis at a flow rate of 1 mL/min, and a Multospher 120 RP18 column (250 mm × 10 mm, 5 μm) was used for isolation at a flow rate of 2.5 mL/min. Water containing 0.5% trifluoroacetic acid (solvent A) and acetonitrile containing 0.5% trifluoroacetic acid (solvent B), were used as solvents. A linear gradient of 2−100% (v/v) solvent B in 30 min was used for analysis of the enzymatic products. The column was then washed with 100% solvent B for 5 min and equilibrated with 2% solvent B for another 5 min. Detection was carried out on a photodiode array detector. Solvents for isolation of the enzyme products are water (solvent C) and acetonitrile (solvent D) without acid. The enzyme products were isolated with a linear gradient of 10−100% D in C in 25 min. After each run, the column was equilibrated with 10% solvent D for 5 min. Analysis of product from (*R*)-benzodiazepinedione by HPLC was carried out as described previously.[14]

■ ASSOCIATED CONTENT

Ⓢ Supporting Information

Examples of polyprenylated acylphloroglucinols and their biosynthetic origins, results of different enzyme assays as tables or HPLC chromatograms, MS and ^{1}H NMR data, NMR spectra, and, kinetic parameters. This material is available free of charge via the Internet at http://pubs.acs.org.

■ AUTHOR INFORMATION

Corresponding Author

*E-mail: shuming.li@staff.uni-marburg.de.

Notes

The authors declare no competing financial interest.

■ ACKNOWLEDGMENTS

■ REFERENCES

(1) Yang, X. W.; Ding, Y.; Zhang, J. J.; Liu, X.; Yang, L. X.; Li, X. N.; Ferreira, D.; Walker, L. A.; Xu, G. *Org. Lett.* **2014**, *16*, 2434−2437.
(2) Russo, E.; Scicchitano, F.; Whalley, B. J.; Mazzitello, C.; Ciriaco, M.; Esposito, S.; Patanè, M.; Upton, R.; Pugliese, M.; Chimirri, S.; et al. *Phytother. Res.* **2014**, *28*, 643−655.
(3) Van Cleemput, M.; Cattoor, K.; De Bosscher, K.; Haegeman, G.; De Keukeleire, D.; Heyerick, A. *J. Nat. Prod.* **2009**, *72*, 1220−1230.
(4) Wu, S.-B.; Long, C.; Kennelly, E. *J. Nat. Prod. Rep.* **2014**, *31*, 1158−1174.
(5) Zhang, J. J.; Yang, J.; Liao, Y.; Yang, X. W.; Ma, J. Z.; Xiao, Q. L.; Yang, L. X.; Xu, G. *Org. Lett.* **2014**, *16*, 4912−4915.
(6) Tsurumaru, Y.; Sasaki, K.; Miyawaki, T.; Uto, Y.; Momma, T.; Umemoto, N.; Momose, M.; Yazaki, K. *Biochem. Biophys. Res. Commun.* **2012**, *417*, 393−398.
(7) Adam, P.; Arigoni, D.; Bacher, A.; Eisenreich, W. *J. Med. Chem.* **2002**, *45*, 4786−4793.
(8) Tian, W. J.; Yu, Y.; Yao, X. J.; Chen, H. F.; Dai, Y.; Zhang, X. K.; Yao, X. S. *Org. Lett.* **2014**, *16*, 3448−3451.
(9) Hu, L.-H.; Sim, K.-Y. *Tetrahedron* **2000**, *56*, 1379−1386.
(10) Yu, X.; Li, S.-M. *Methods Enzymol.* **2012**, *516*, 259−278.
(11) George, J.-H.; Hesse, M.-D.; Baldwin, E.; dlington, R.-M. *Org. Lett.* **2010**, *12*, 3532−3535.
(12) Pepper, H. P.; Lam, H. C.; Bloch, W. M.; George, J. H. *Org. Lett.* **2012**, *14*, 5162−5164.

(13) Morkunas, M.; Dube, L.; Gotz, F.; Maier, M.-E. *Tetrahedron* **2013**, *69*, 8559−8563.
(14) Yin, W.-B.; Grundmann, A.; Cheng, J.; Li, S.-M. *J. Biol. Chem.* **2009**, *284*, 100−109.
(15) Kremer, A.; Westrich, L.; Li, S.-M. *Microbiology* **2007**, *153*, 3409−3416.
(16) Yin, W.-B.; Yu, X.; Xie, X.-L.; Li, S.-M. *Org. Biomol. Chem.* **2010**, *8*, 2430−2438.
(17) Ding, W.; Lei, C.; He, Q.; Zhang, Q.; Bi, Y.; Liu, W. *Chem. Biol.* **2010**, *17*, 495−503.
(18) Lu, P.; Zhang, A.; Dennis, L. M.; Dahl-Roshak, A. M.; Xia, Y. Q.; Arison, B.; An, Z.; Tkacz, J. S. *Mol. Genet. Genomics* **2005**, *273*, 207−216.
(19) Lackner, G.; Bohnert, M.; Wick, J.; Hoffmeister, D. *Chem. Biol.* **2013**, *20*, 1101−1106.
(20) Pockrandt, D.; Li, S.-M. *ChemBioChem* **2013**, *14*, 2023−2028.
(21) Yu, X.; Xie, X.; Li, S.-M. *Appl. Microbiol. Biotechnol.* **2011**, *92*, 737−748.
(22) Boubakir, Z.; Beuerle, T.; Liu, B.; Beerhues, L. *Phytochemistry* **2005**, *66*, 51−57.
(23) Fung, S.-Y.; Brussee, J.; van der Hoeven, R. A. M.; Niessen, W.-M. A.; Scheffer, J.-J. C.; Verpoorte, R. *J. Nat. Prod.* **1994**, *57*, 452−459.
(24) Osorio, M.; Aravena, J.; Vergara, A.; Taborga, L.; Baeza, E.; Catalan, K.; Gonzalez, C.; Carvajal, M.; Carrasco, H.; Espinoza, L. *Molecules* **2012**, *17*, 556−570.
(25) Yu, X.; Zocher, G.; Xie, X.; Liebhold, M.; Schütz, S.; Stehle, T.; Li, S.-M. *Chem. Biol.* **2013**, *20*, 1492−1501.
(26) Woodside, A. B.; Huang, Z.; Poulter, C. D. *Org. Synth.* **1988**, *66*, 211−215.

Friedel-Crafts Alkylation of Acylphloroglucinols Catalyzed by a Fungal Indole Prenyltransferase

Kang Zhou, Lena Ludwig and Shu-Ming Li[*]

Institut für Pharmazeutische Biologie und Biotechnologie, Philipps-Universität Marburg, Deutschhausstrasse 17a,

35037 Marburg, Germany. Fax: (49)-6421-2825365; Email: shuming.li@staff.uni-marburg.de

Content

Table S1: Conversions of 1a-3a by 13 purified fungal prenyltransferases

Prenyltransferases		Conversion yield (%)		
		1a	2a	3a
Cyclic dipeptide Prenyltransferases	CdpC2PT[1]	1.23	2.39	2.43
	CdpC3PT[2]	5.66	0.46	1.41
	AnaPT[3]	14.07	14.38	12.74
	CdpNPT[4]	0.65	0.27	0.47
	FtmPT1[5]	0.23	1.16	0.72
	BrePT[6]	0.24	0.41	<0.01
	CTrpPT[7]	0.13	0.25	<0.01
Tryptophan prenyltransferases	6-DMATS$_{Sa}$[8]	0.55	0.39	<0.01
	7-DMATS[9]	10.08	10.09	5.84
	5-DMATS[10]	<0.01	<0.01	<0.01
	FgaPT2[11]	6.45	0.96	0.49
Tyrosine prenyltransferases	SirD[12]	0.15	0.43	<0.01
	TyrPT[13]	0.14	0.12	<0.01

The enzyme assays (100 µL) contained **1a-3a** (1 mM), $CaCl_2$ (5 mM), DMAPP (2 mM), 50 mM Tris-HCl (pH 7.5), glycerol (1.0–6 % v/v), dimethyl sulfoxide (DMSO, 5 % v/v) and purified recombinant proteins (40 µg of FgaPT2 or 5-DMATS and 5µg of other enzymes). The reaction mixtures were incubated at 37°C for 16h.

Table S2: HR-EI-MS data of enzyme products

Product	Chemical formula	Calculated M_r	Measured (M^+)	Deviation (ppm)
1b	$C_{15}H_{20}O_4$	264.1362	264.1369	2.6
2b	$C_{16}H_{22}O_4$	278.1518	278.1515	1.1
3b	$C_{18}H_{18}O_4$	298.1205	298.1246	13.7
4b	$C_{11}H_{14}O_3$	194.0943	194.0952	4.6
4c	$C_{16}H_{22}O_3$	262.1569	262.1548	8.0
5b	$C_{12}H_{14}O_5$	238.0841	238.0836	2.1
6b	$C_{13}H_{16}O_4$	236.1048	236.1055	3.0
7b	$C_{13}H_{16}O_3$	220.1099	220.1093	2.7
7c	$C_{13}H_{16}O_3$	220.1099	220.1098	0.5

Table S3. ¹H NMR data (500 MHz) of enzyme products (known compounds) in acetone-D$_6$ (1b, 2b, and 3b) or methanol-D$_4$ (4b, and 4c)

Comp	1b	2b	3b	4b	4c
Pos.	δ_H (*J* in Hz)	δ_H, (*J* in Hz)	δ_H, (*J* in Hz)	δ_H, (*J* in Hz)	δ_H, (*J* in Hz)
3	/	/	/	5.81, s	/
5	6.06, s	6.07, s	6.04, s	5.81, s	/
6	/	/	/	/	5.93, s
8	3.98, sept (6.6)	2.94, d (6.7)	/	/	/
9	1.12, d, (6.6)	2.23, m	7.59, m	/	/
10	1.12, d, (6.6)	0.94, d (6.7)	7.40, m	/	/
11	/	0.94, d (6.7)	7.47, tt (7.4, 1.3)	/	/
12	/	/	7.40, m	/	/
13	/	/	7.59, m	/	/
1'	3.22, d (6.8)	3.23, d (7.1)	3.29, d (7.1)	3.14, d (7.2)	3.23, d (7.2)
2'	5.20, m	5.22, m	5.27, m	5.17, m	5.17, m
4'	1.61, s	1.61, s	1.65, s	1.62, s	1.65, s
5'	1.72, s	1.73, s	1.76, s	1.71, s	1.74, s
1"					3.23, d (7.2)
2"					5.17, m
4"					1.65, s
5"					1.74, s

Chemical shifts (δ) are given in ppm and coupling constants (*J*) in Hz.
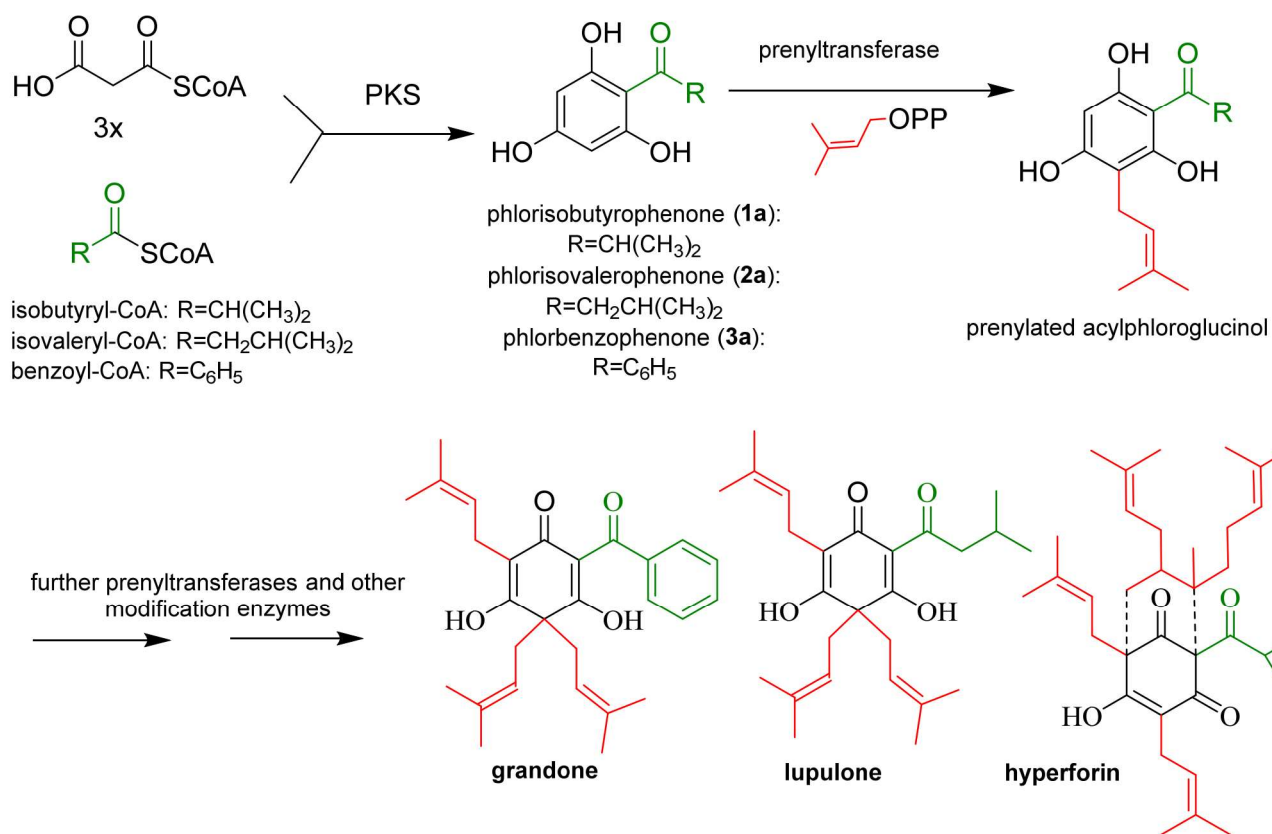
Scheme S1: Examples of polyprenylated acylphloroglucinols and their biosynthetic origins

5
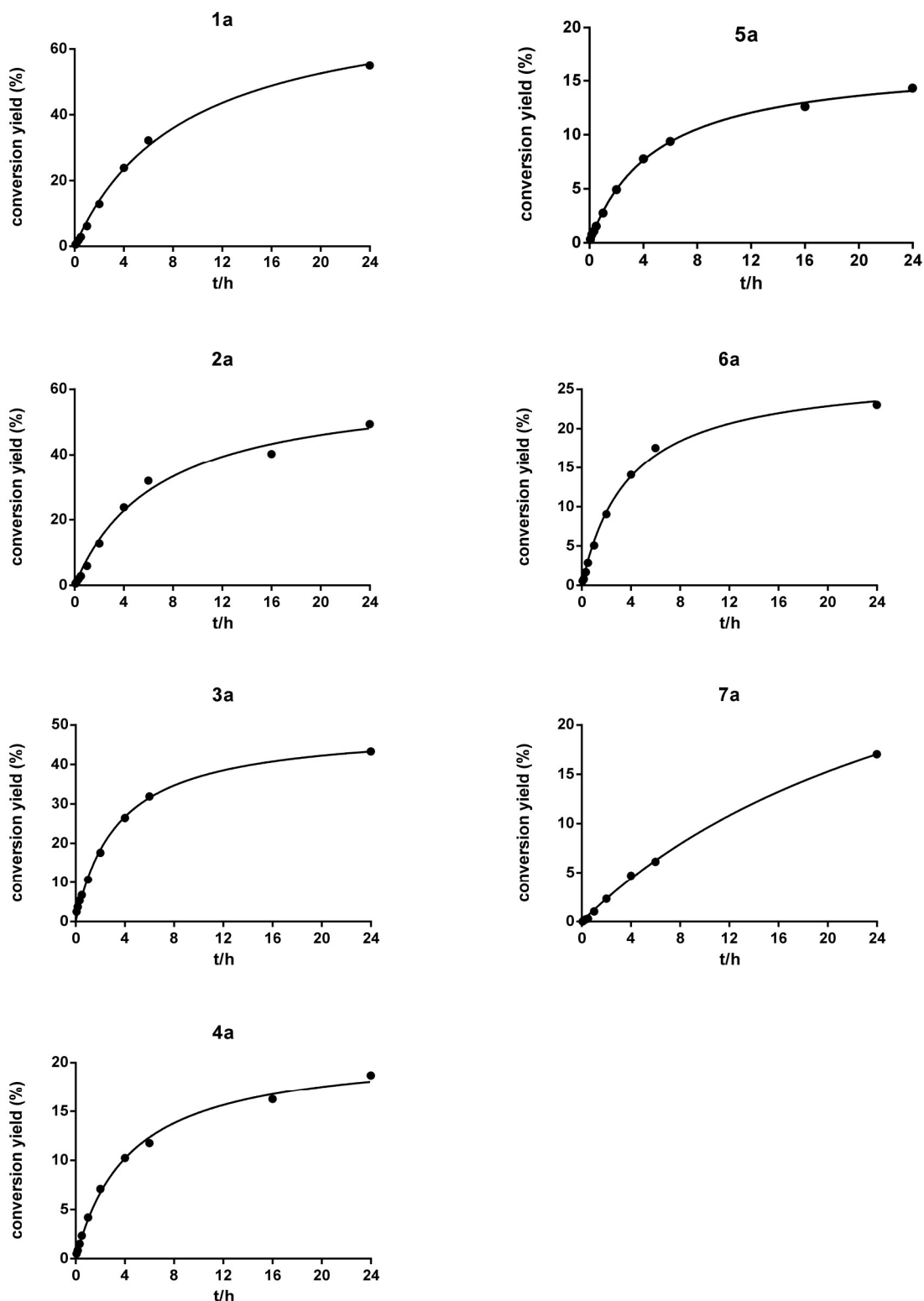
Figure S1: Dependence of the product formation of 1a-7a on incubation times in the presence of DMAPP.

The enzyme assays (100 µL) contained **1a-7a** (1 mM), $CaCl_2$ (5 mM), DMAPP (2 mM), 50 mM Tris-HCl (pH 7.5), glycerol (1.0-6 % v/v), dimethyl sulfoxide (DMSO, 5 % v/v), and 50 µg purified AnaPT. The reaction mixtures were incubated at 37 °C.
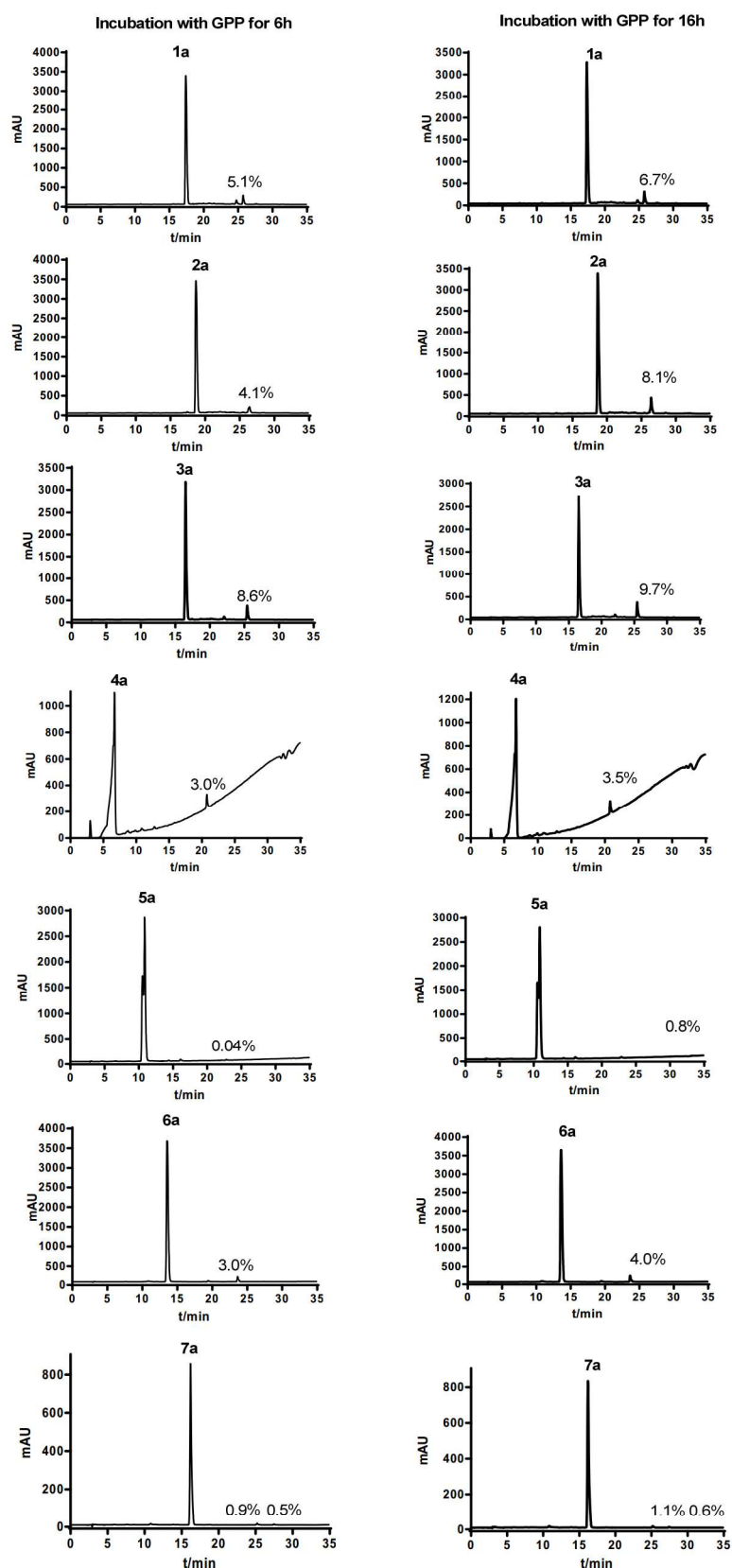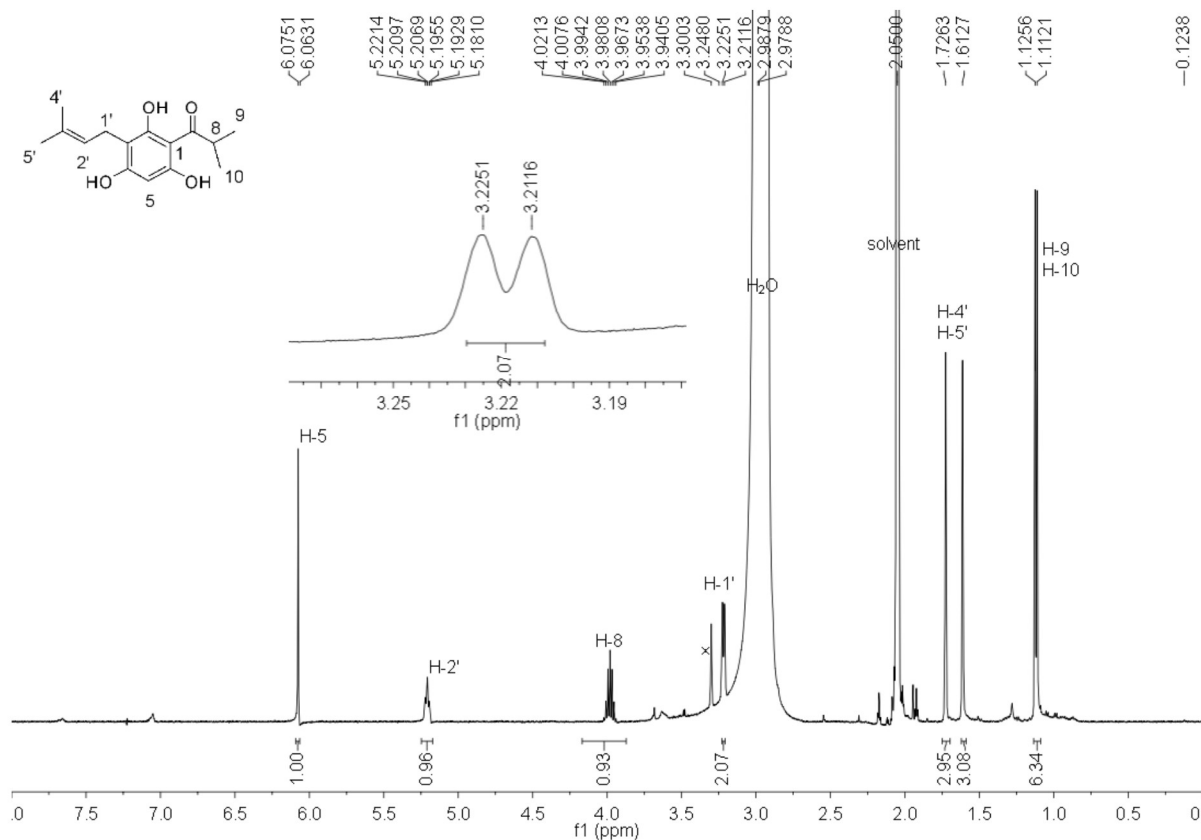
Figure S2: HPLC chromatograms of the incubation mixtures of 1a-7a with AnaPT in the presence of GPP.

The enzyme assays (100 μL) contained **1a-7a** (1 mM), CaCl$_2$ (5 mM), GPP (2 mM), 50 mM Tris-HCl (pH 7.5), glycerol (1.0-6 % v/v), dimethyl sulfoxide (DMSO, 5 % v/v), and 50 μg purified AnaPT. The reaction mixtures were incubated at 37 °C for 6 or 16 h

7

Figure S3: ^{1}H NMR spectrum of 1b in acetone-D$_6$ (500 MHz)
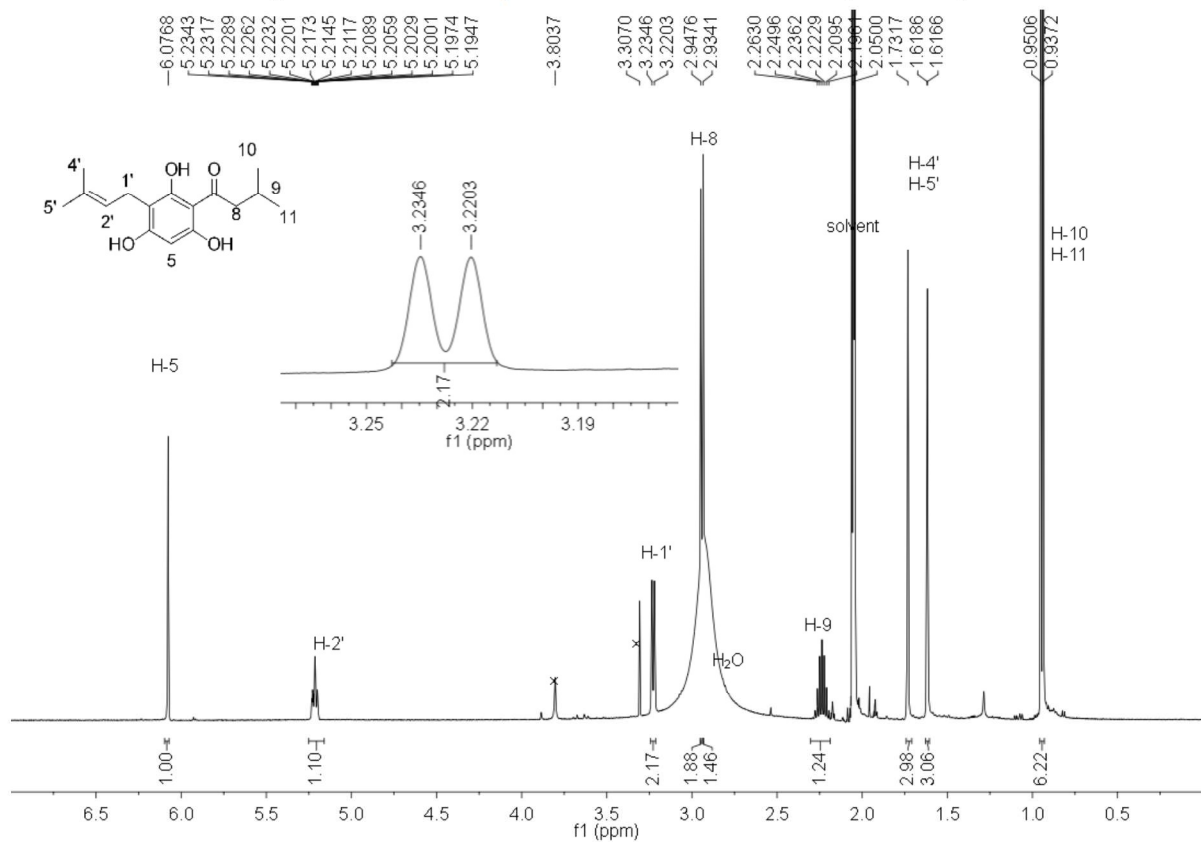
Figure S4: ^{1}H NMR spectrum of 2b in acetone-D$_6$ (500 MHz)

8
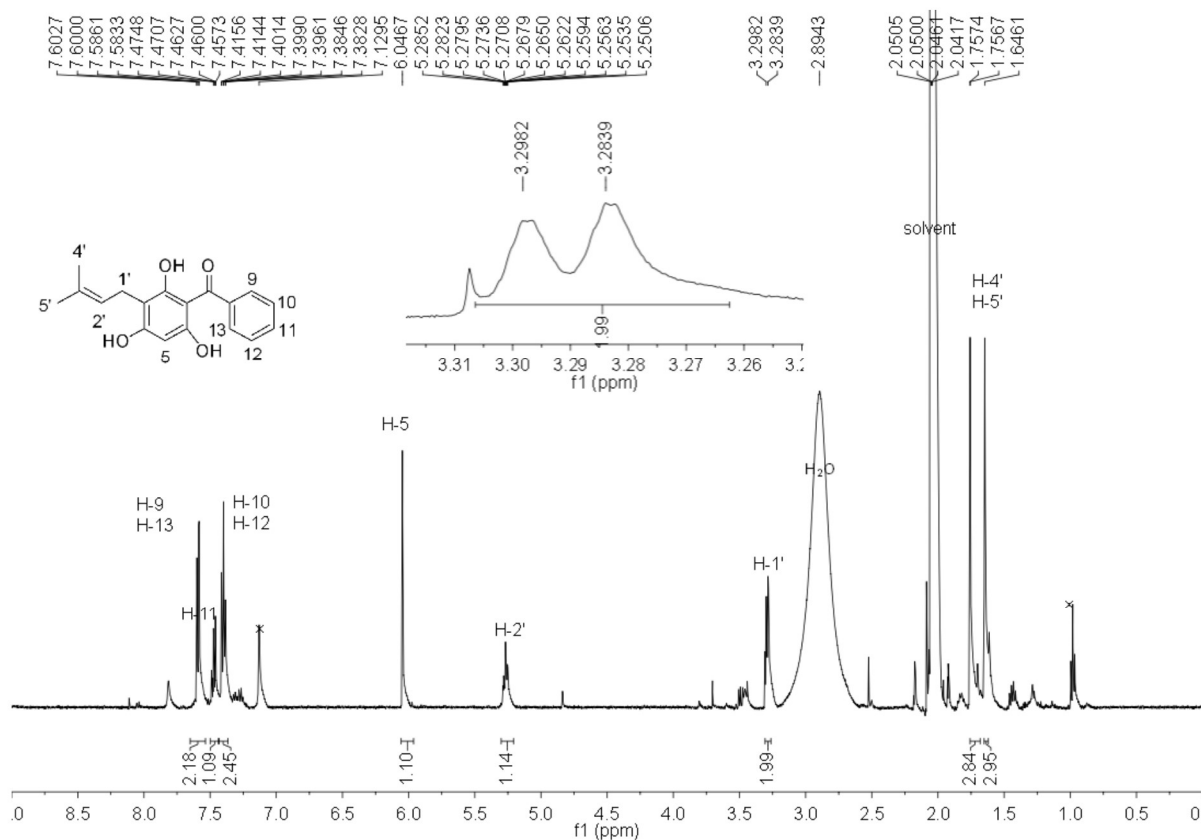
Figure S5: ¹H NMR spectrum of 3b in acetone-D₆ (500 MHz)
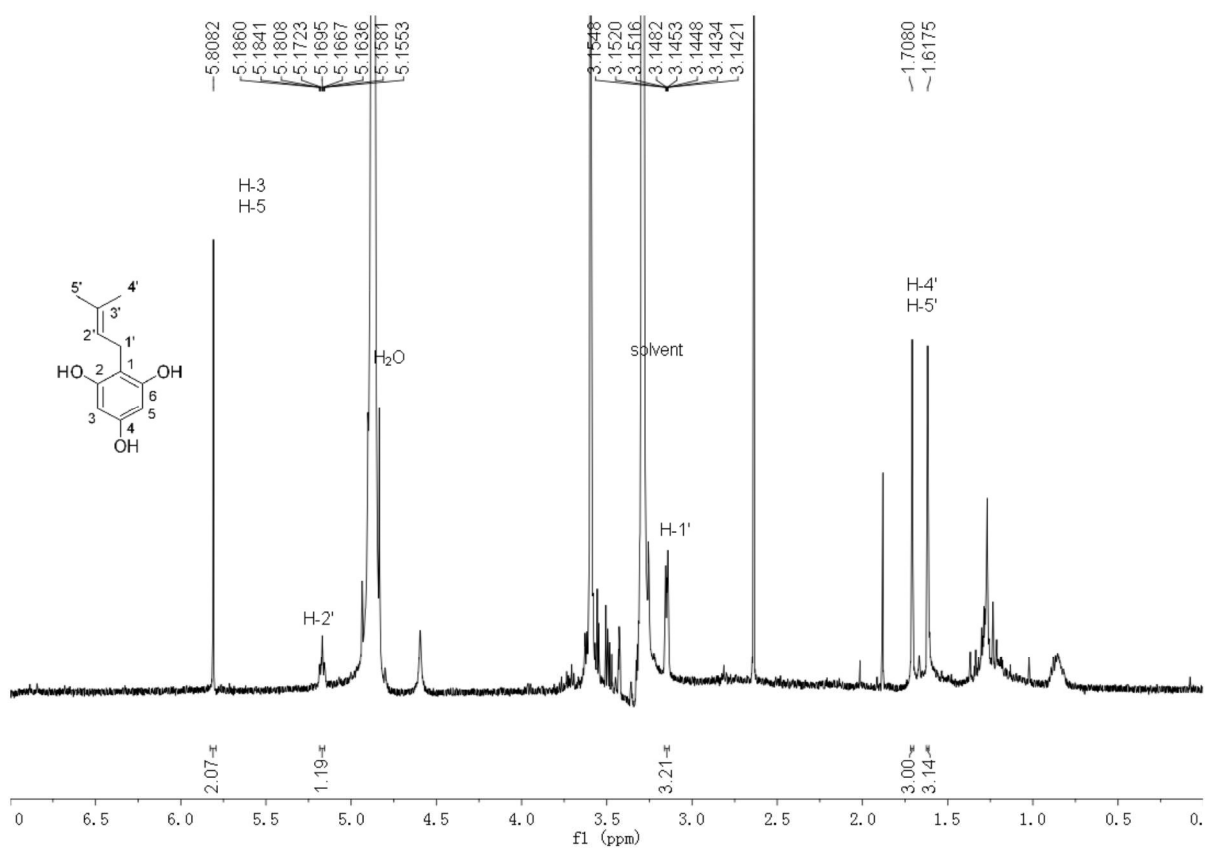
Figure S6: ¹H NMR spectrum of 4b in methanol-D₄ (500 MHz)

9

53
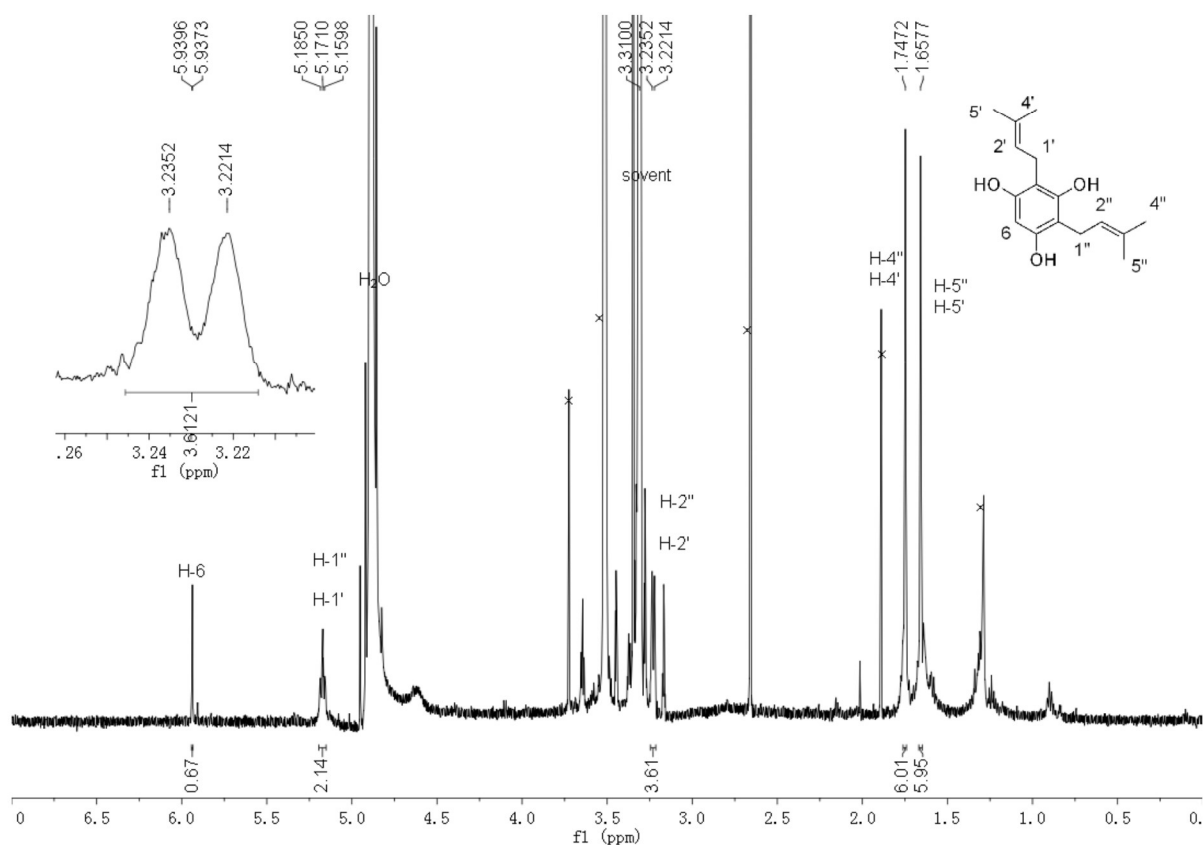
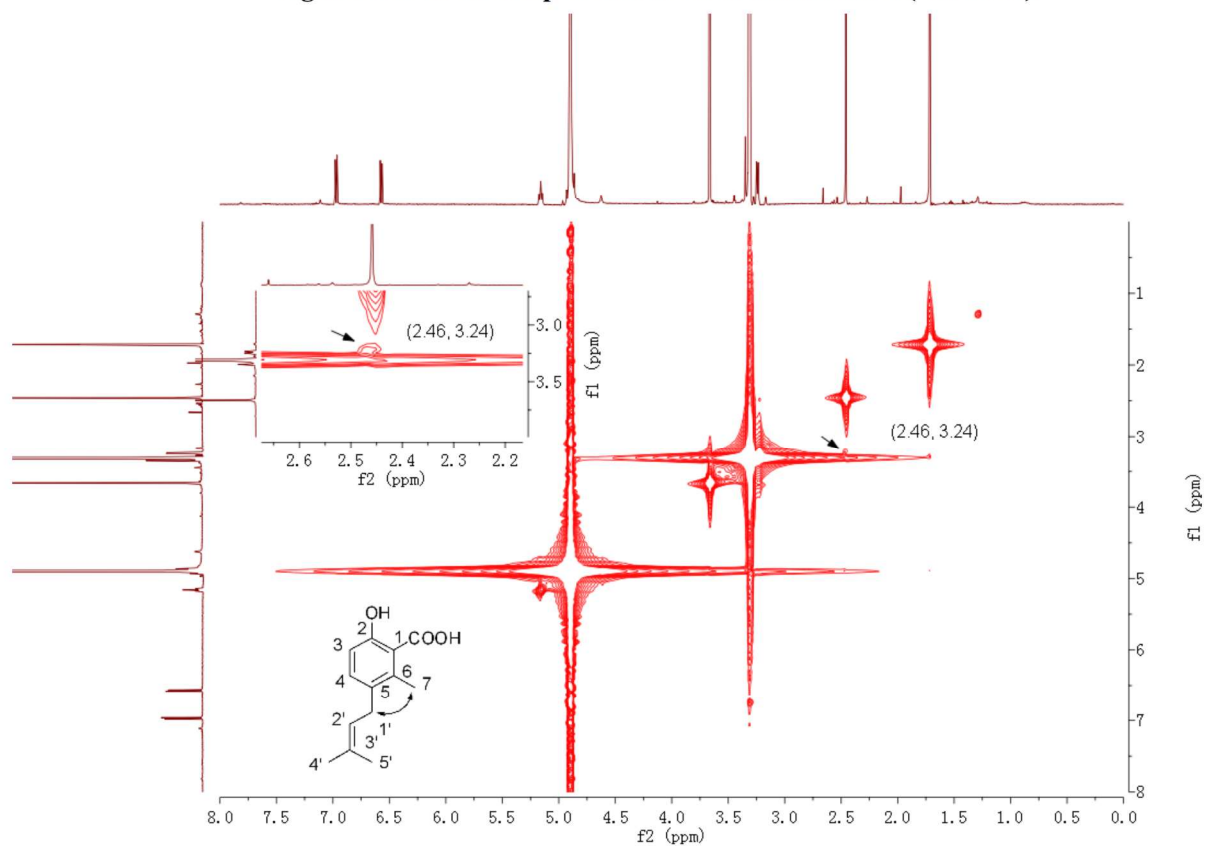**Figure S7: ^{1}H NMR spectrum of 4c in methanol-D$_4$ (500 MHz)**
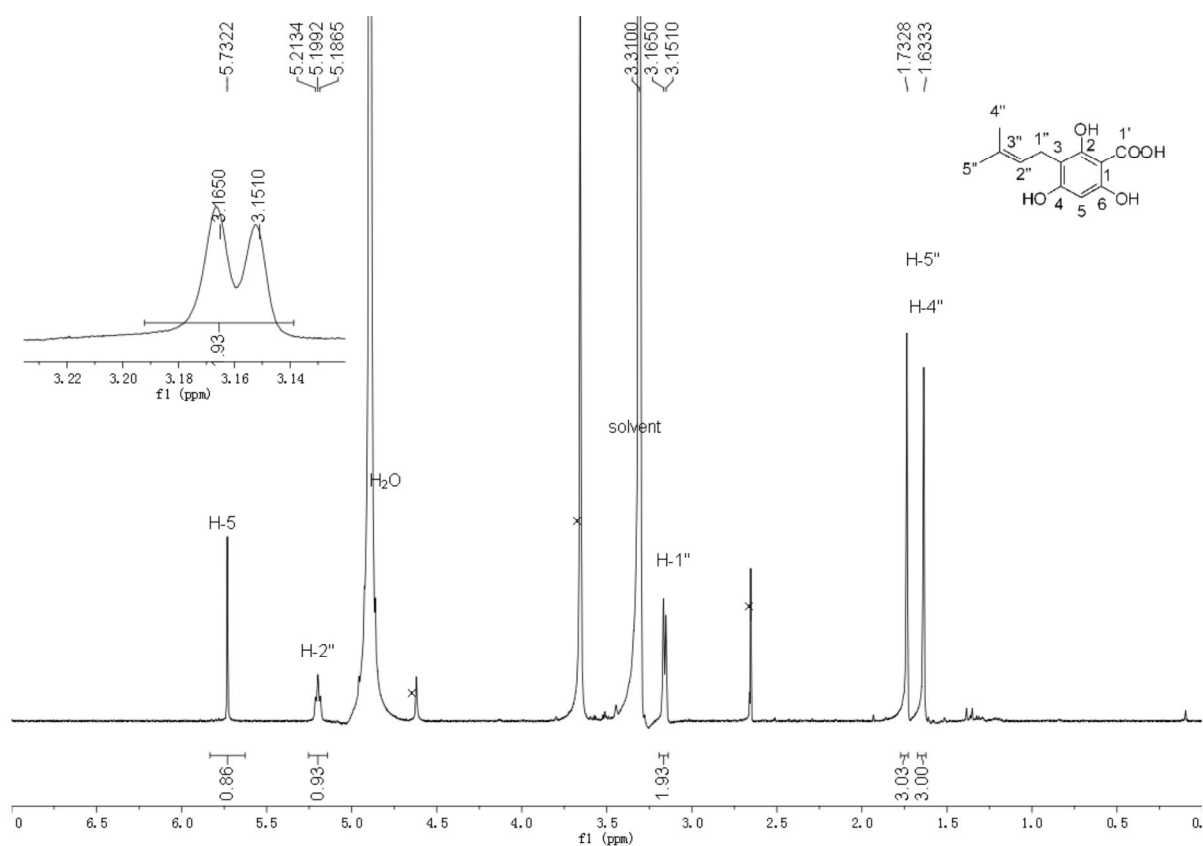
Figure S8: ^{1}H NMR spectrum of 5b in methanol-D$_4$ (500 MHz)

10
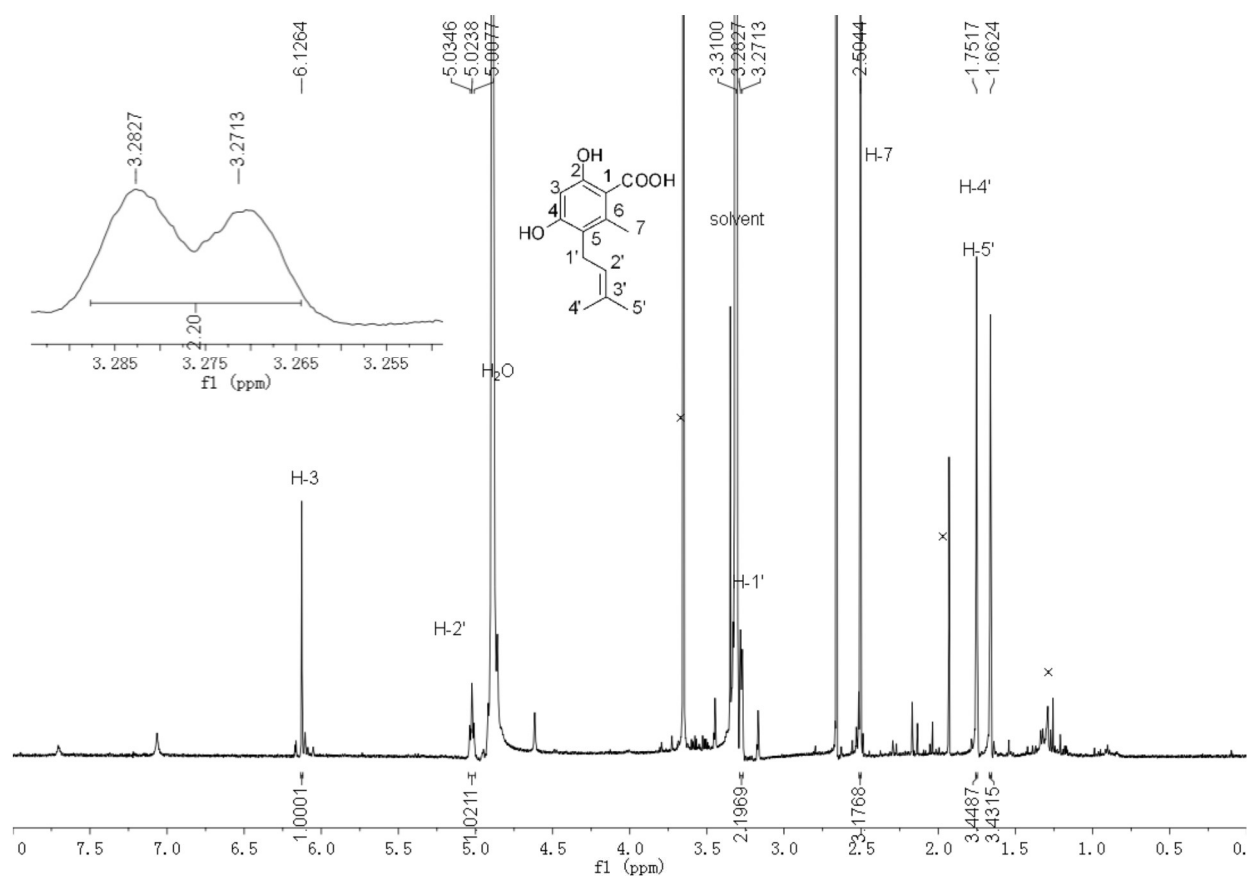
Figure S9: ¹H NMR spectrum of 6b in methanol-D₄ (500 MHz)
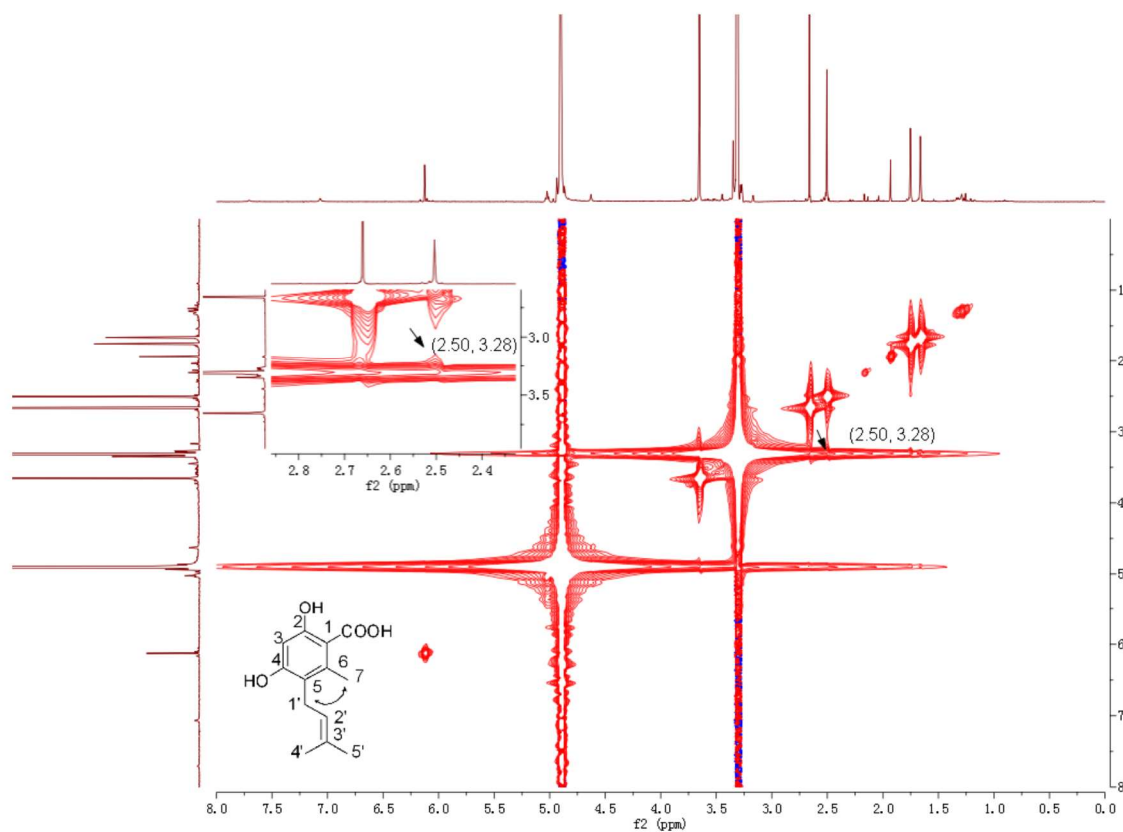
Figure S10: NOESY spectrum of 6b in methanol-D₄ (500 MHz)

11

55
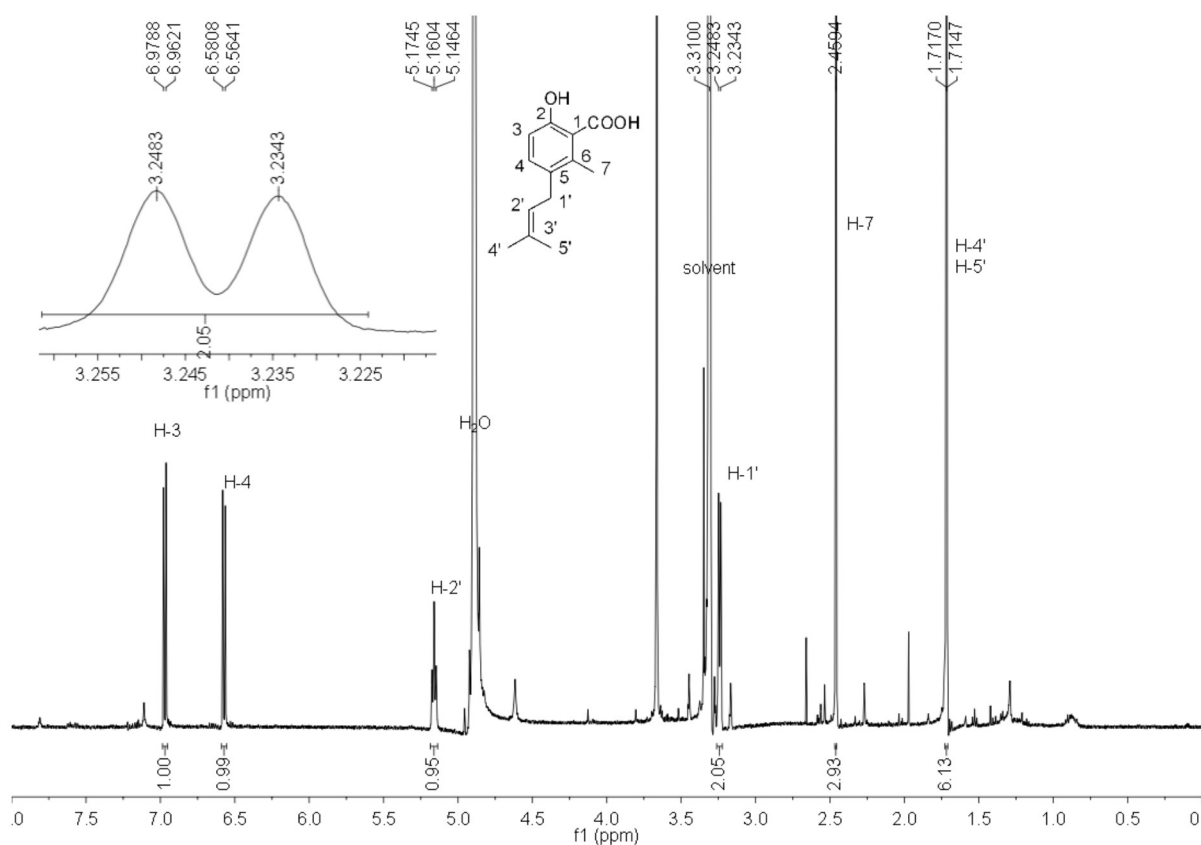
Figure S11: ¹H NMR spectrum of 7b in methanol-D₄ (500 MHz)

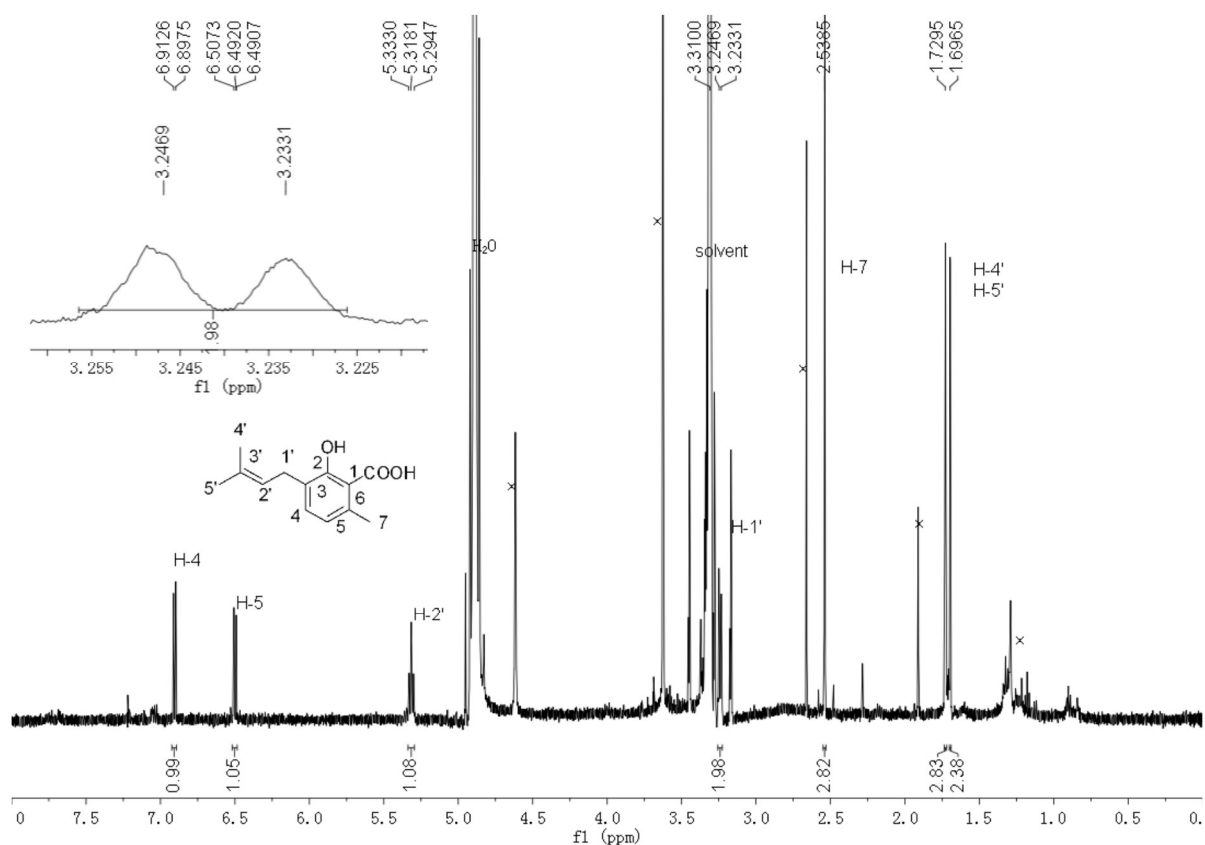**Figure S12: NOESY spectrum of 7b in methanol-D₄ (500 MHz)**

12

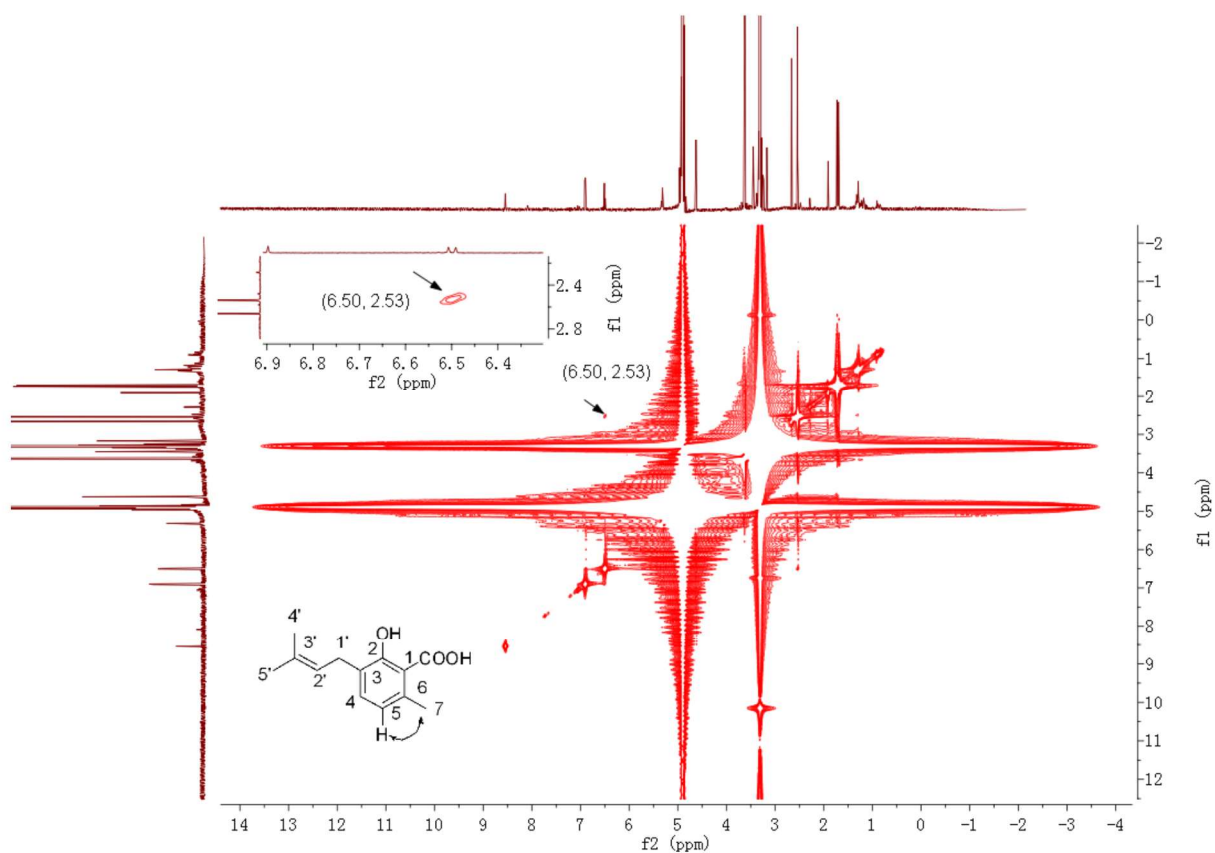**Figure S13: ¹H NMR spectrum of 7c in methanol-D₄ (500 MHz)**

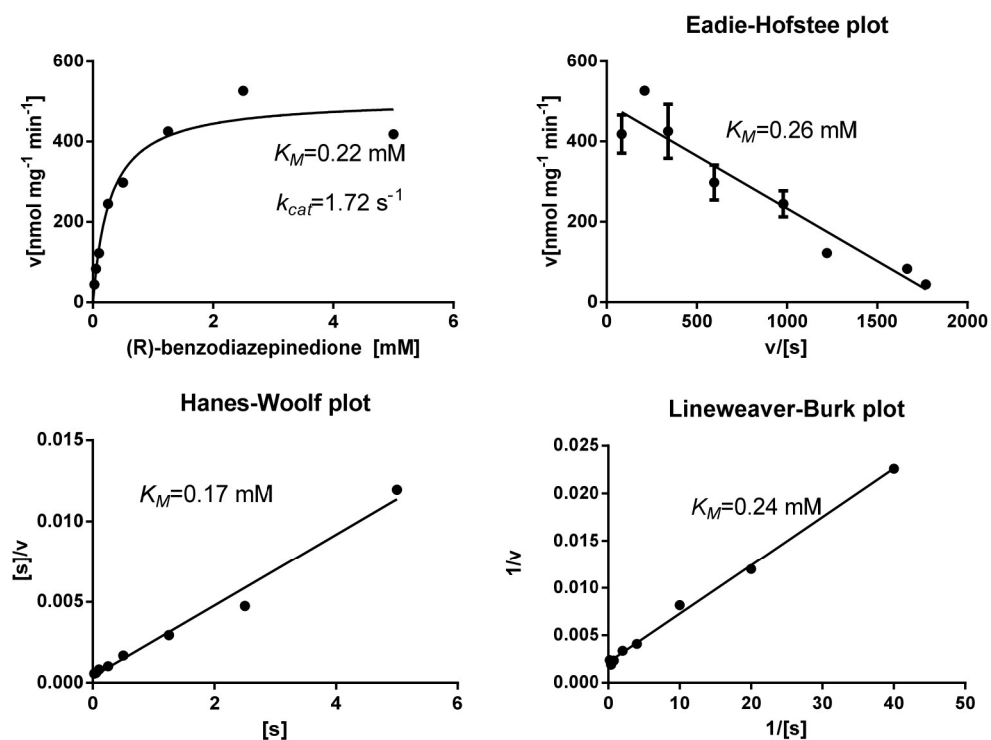**Figure S14: NOESY spectrum of 7c in methanol-D₄ (500 MHz)**

13

Figure S15: Dependence of the product formation of the AnaPT reaction on the presence of (R)-benzodiazepinedione
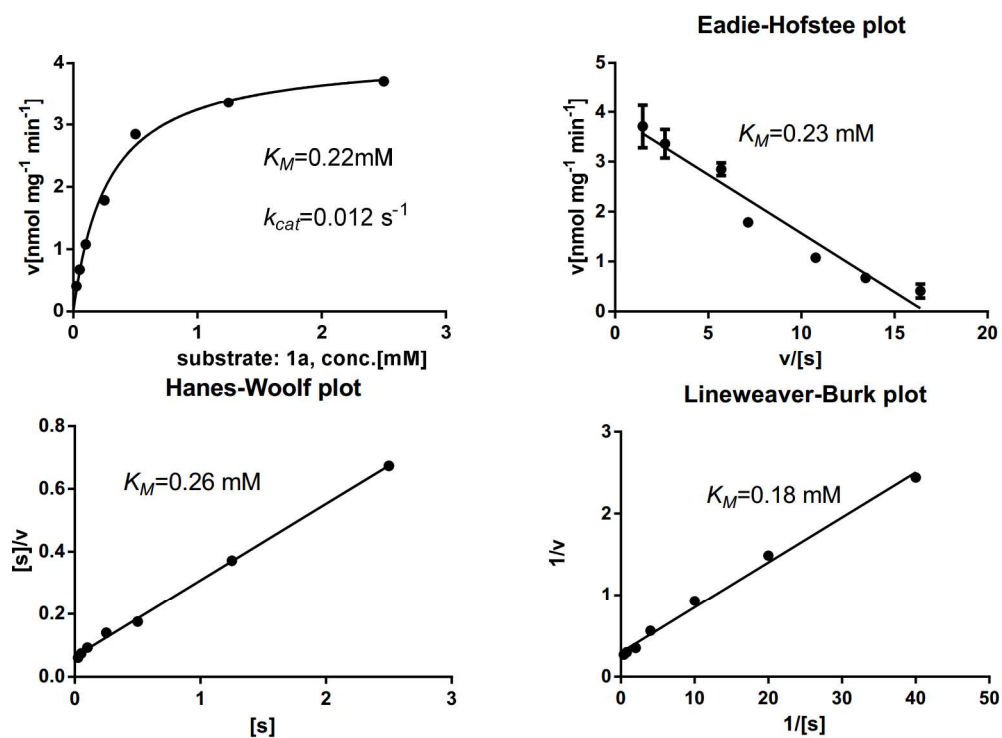

Figure S16: Dependence of the product formation of the AnaPT reaction on the presence of 1a
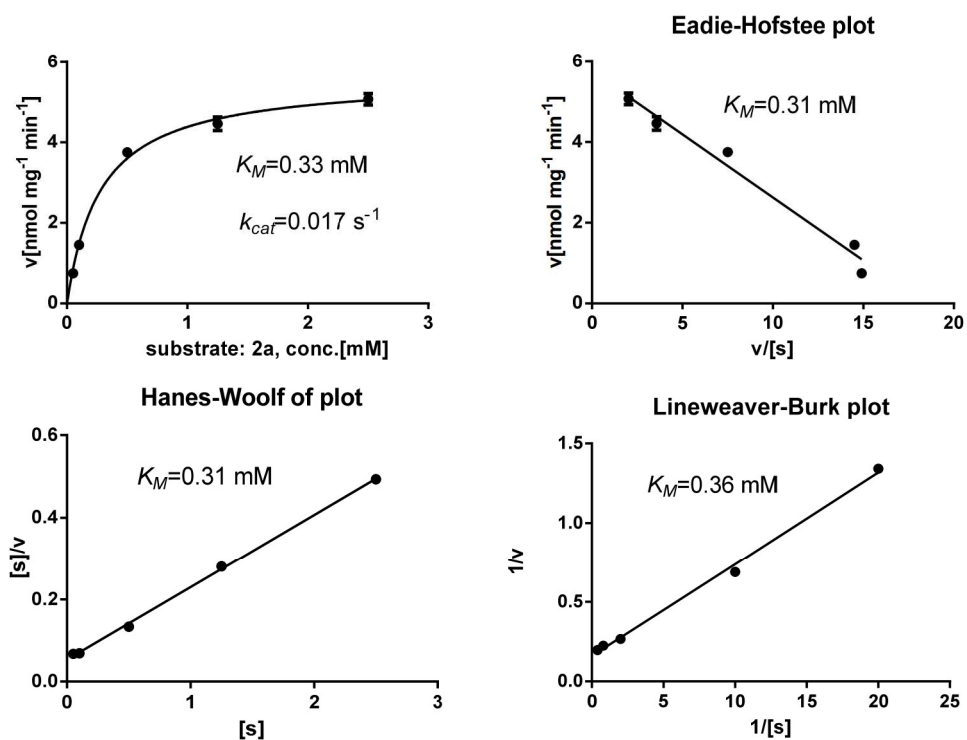
Figure S17: Dependence of the product formation of the AnaPT reaction on the presence of 2a

Figure S18: Dependence of the product formation of the AnaPT reaction on the presence of 3a

Figure S19: Dependence of the product formation of the AnaPT reaction on the presence of 4a
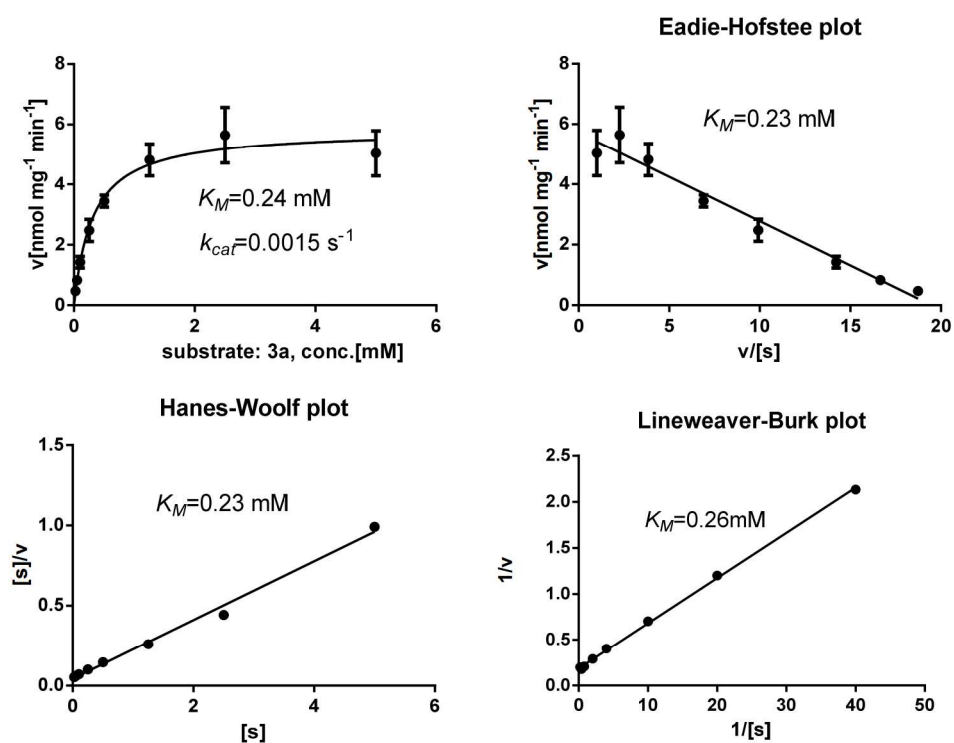

Figure S20: Dependence of the product formation of the AnaPT reaction on the presence of 5a
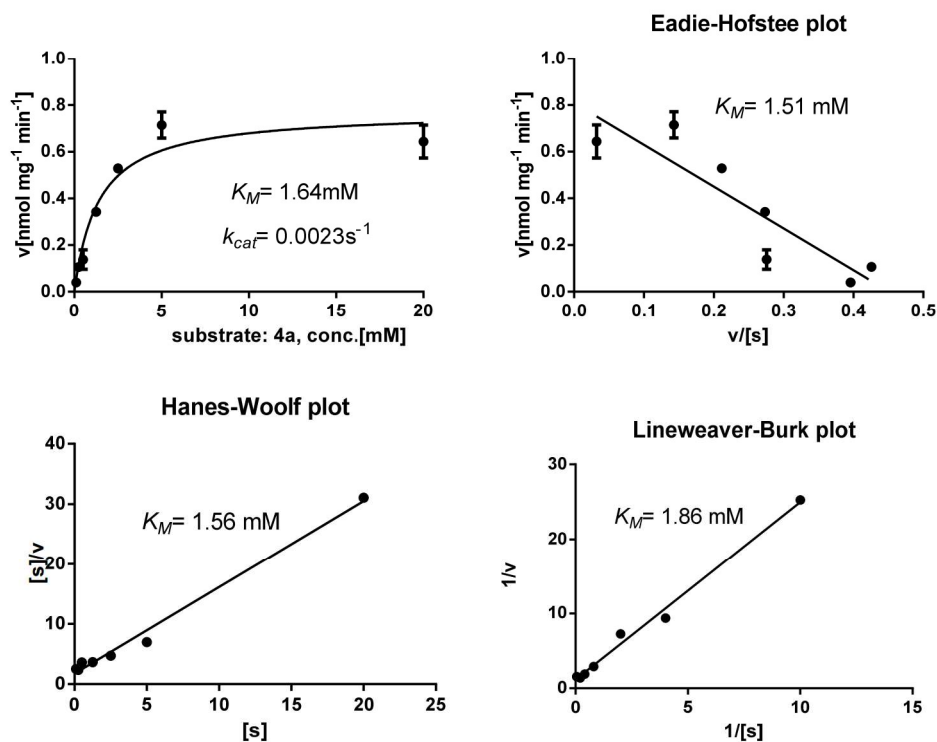
Figure S21: Dependence of the product formation of the AnaPT reaction on the presence of 6a
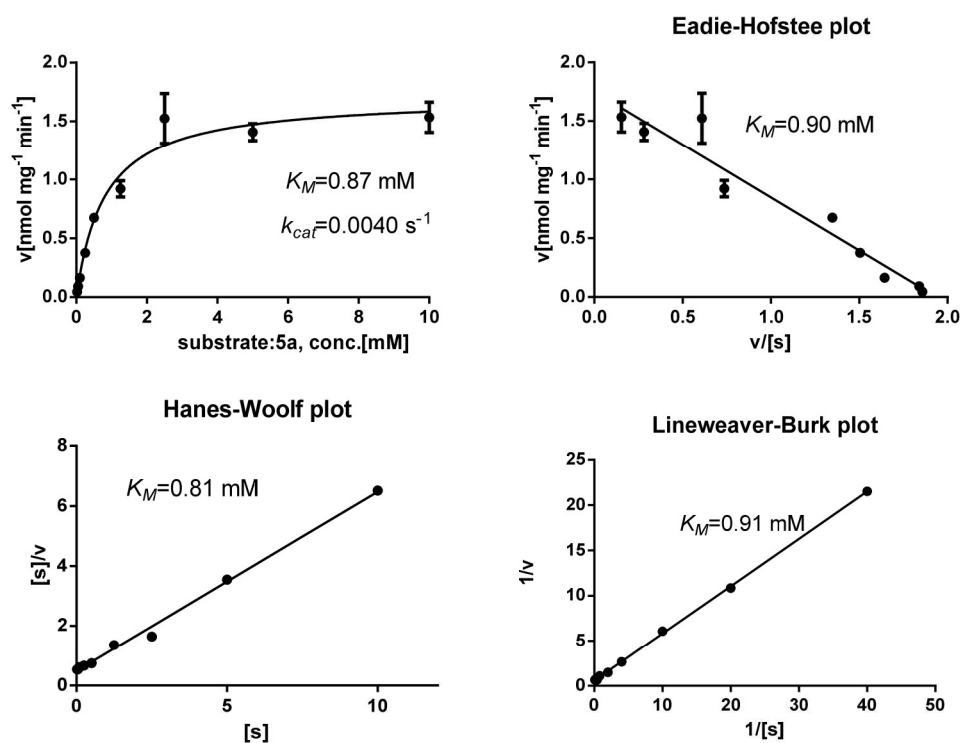

Figure S22: Dependence of the product formation of the AnaPT reaction on the presence of 7a

17

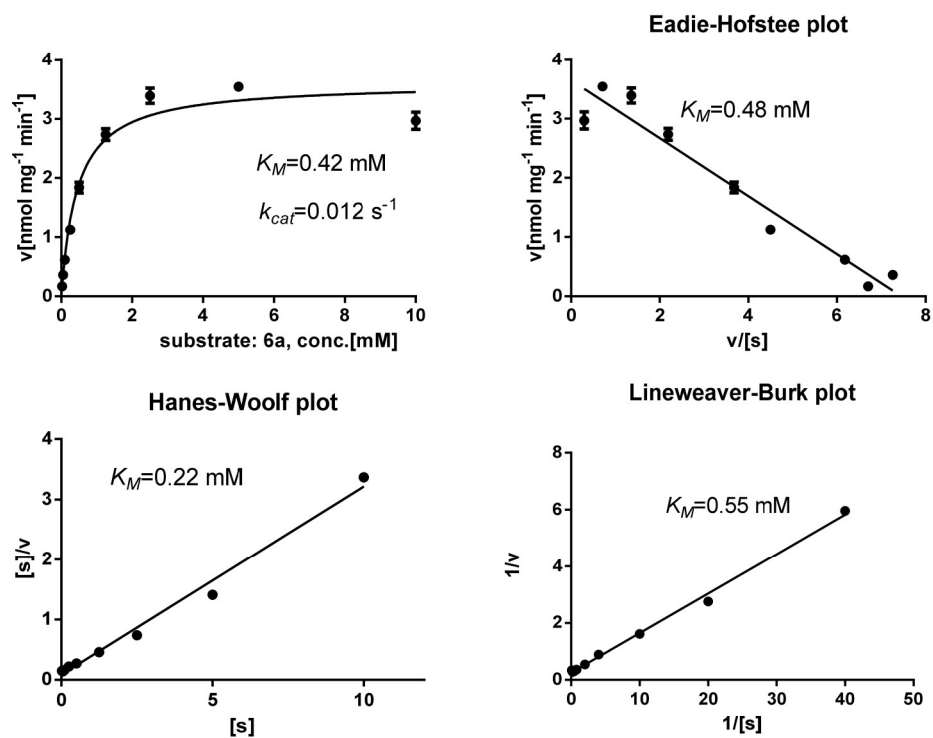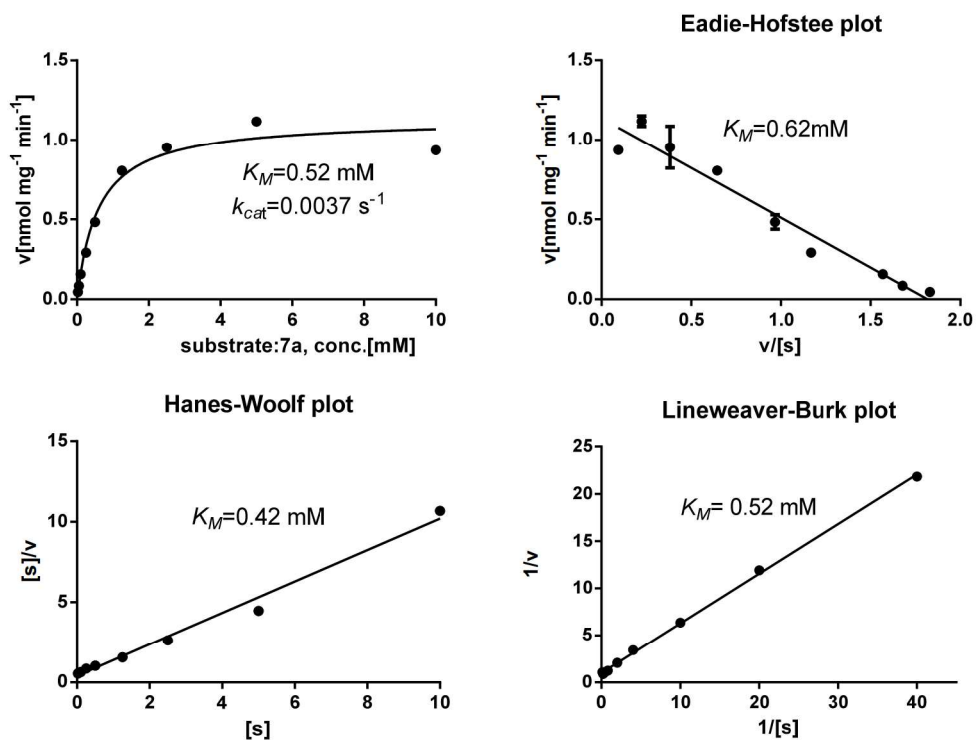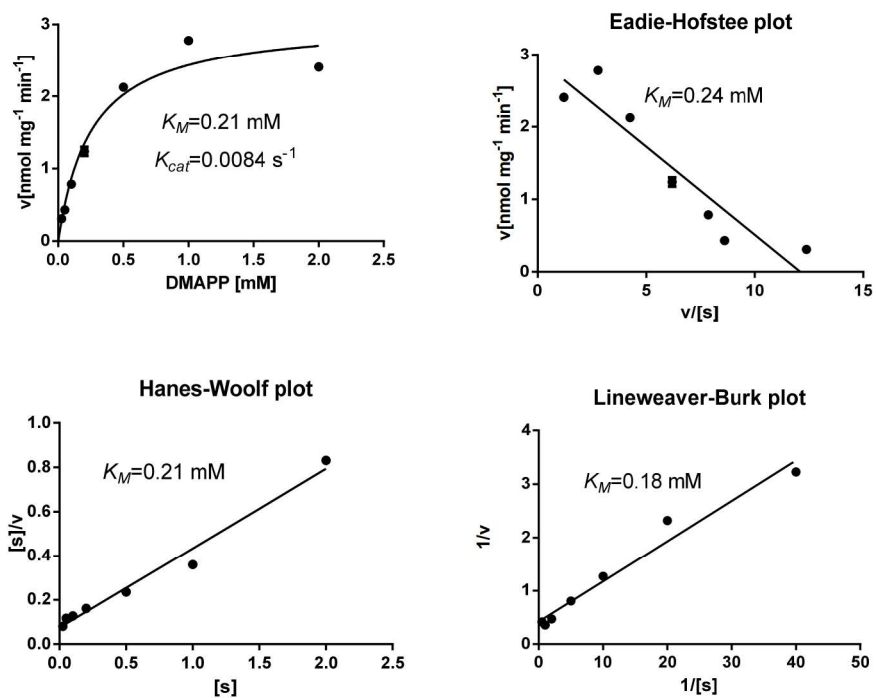**Figure S23: Dependence of the product formation of the AnaPT reaction on the presence of DMAPP with 1a as aromatic substrate**
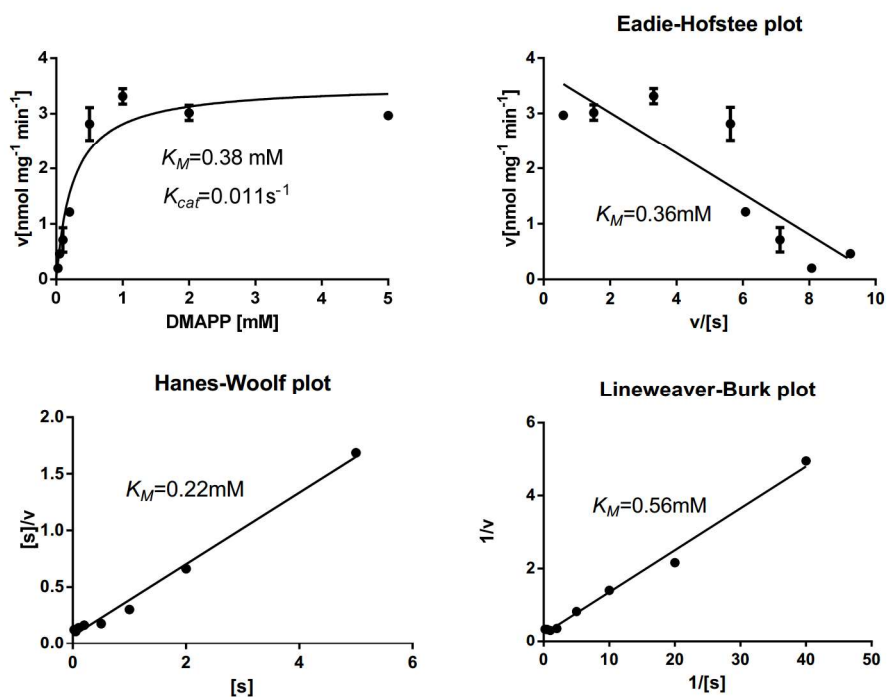

Figure S24: Dependence of the product formation of the AnaPT reaction on the presence of DMAPP with 2a as aromatic substrate

References and Notes

[1]   Mundt, K.; Li, S.-M., *Microbiology* **2013**, *159*, 2169-2179.

[2]   Yin, W.-B.; Yu, X.; Xie, X.-L.; Li, S.-M., *Org. Biomol. Chem.* **2010**, *8*, 2430-2438.

[3]   Yin, W.-B.; Grundmann, A.; Cheng, J.; Li, S.-M., *J. Biol. Chem.* **2009,** *284*, 100-109.

[4]   Yin, W.-B.; Ruan, H.-L.; Westrich, L.; Grundmann, A.; Li, S.-M., *Chembiochem* **2007,** *8*, 1154-1161.

[5]   Grundmann, A.; Li, S.-M., *Microbiology* **2005,** *151*, 2199-2207.

[6]   Yin, S.; Yu, X.; Wang, Q.; Liu, X. Q.; Li, S.-M., *Appl. Microbiol. Biotechnol.* **2013,** *97*, 1649-1660.

[7]   Zou, H.-X.; Xie, X.-L.; Linne, U.; Zheng, X.-D.; Li, S.-M., *Org. Biomol. Chem.* **2010,** *8*, 3037-3044.

[8]   Winkelblech, J.; Li, S.-M., *Chembiochem.* **2014,** *15*, 1030-1039.

[9]   Kremer, A.; Westrich, L.; Li, S.-M., *Microbiology* **2007,** *153*, 3409-3416.

[10] Yu, X.; Liu, Y.; Xie, X.; Zheng, X.-D.; Li, S.-M., *J. Biol. Chem.* **2012,** *287*, 1371-1380.

[11] Unsöld, I. A.; Li, S.-M., *Microbiology* **2005,** *151*, 1499-1505.

[12] Zou, H.-X.; Xie, X.; Zheng, X.-D.; Li, S.-M., *Appl. Microbiol. Biotechnol.* **2011,** *89*, 1443-1451.

[13] Fan, A.; Chen, H.; Wu, R.; Xu, H.; Li, S.-M., *Appl. Microbiol. Biotechnol.* **2014,** *98*, 10119-10129.

19

4.2. *Gem*-diprenylation of acylphloroglucinols by a fungal prenyltransferase of the dimethylallyltryptophan synthase superfamily
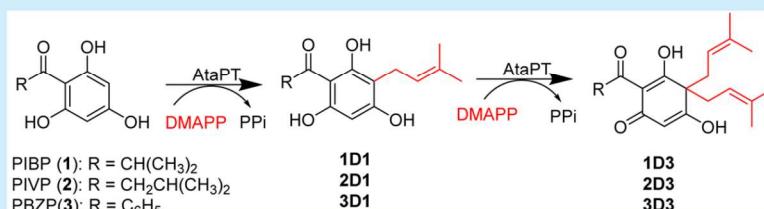
gem-Diprenylation of Acylphloroglucinols by a Fungal Prenyltransferase of the Dimethylallyltryptophan Synthase Superfamily

Kang Zhou,[†] Carsten Wunsch,[†] Jungui Dai,[‡] and Shu-Ming Li*,[†]

[†]Institut für Pharmazeutische Biologie und Biotechnologie, Philipps-Universität Marburg, Robert-Koch-Strasse 4, 35037 Marburg, Germany

[‡]State Key Laboratory of Bioactive Substance and Function of Natural Medicines, Institute of Materia Medica, Chinese Academy of Medical Sciences and Peking Union Medical College, Xian Nong Tan Street, Beijing 100050, China

S *Supporting Information*

PIBP (**1**): R = CH(CH$_3$)$_2$ **1D1**   **1D3**
PIVP (**2**): R = CH$_2$CH(CH$_3$)$_2$ **2D1**   **2D3**
PBZP(**3**): R = C$_6$H$_5$ **3D1**   **3D3**

ABSTRACT: *Aspergillus terreus* aromatic prenyltransferase (AtaPT) catalyzes predominantly *C*-monoprenylation of acylphloroglucinols in the presence of different prenyl diphosphates. With dimethylallyl diphosphate (DMAPP) as prenyl donor, *gem*-diprenylated products 1D3, 2D3, and 3D3 were also detected. High conversion of 1D1 to 1D3, 2D1 to 2D3, and 3D1 to 3D3 was demonstrated by incubation with AtaPT and DMAPP. The first example of *gem*-diprenylation by a member of the dimethylallyltryptophan synthase superfamily is provided.

Prenylated acylphloroglucinols (APs) are characteristic constituents of several plant families. Compounds of this class have fascinating chemical structures and intriguing biological and pharmacological activities.[1−5] Main structural features of prenylated APs are highly oxygenated and densely decorated with prenyl such as dimethylallyl and geranyl moieties. Polyprenylated APs like α- and β-bitter acids (Figure 1) from *Humulus lupulus* (Cannabinaceae), commonly known

α- bitter acids
cohumulone (R = CH(CH$_3$)$_2$)
humulone (R = CH$_2$CH(CH$_3$)$_2$)

β–bitter acids
colupulone (R = CH(CH$_3$)$_2$)
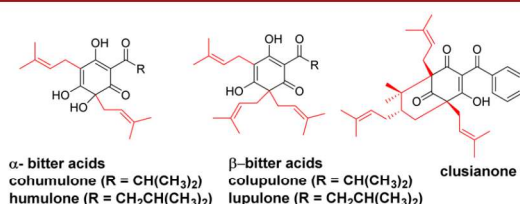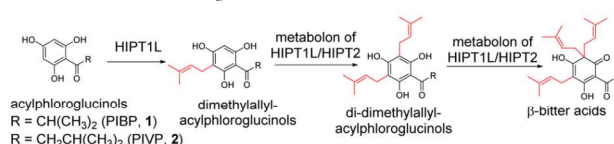lupulone (R = CH$_2$CH(CH$_3$)$_2$)

clusianone

**Figure 1.** Examples of polyprenylated APs from plants.

as hops, are considered as multipotent bioactive compounds including their sedative effects.[4] Clusianone (Figure 1) and its 7-epimer from different plants such as *Garcinia brasiliensis* and *Clusia torresii*, both from the family Clusiaceae, exhibit anti-HIV and antitumor activities.[6−9] An exceptional structure feature of polyprenylated APs is the *gem*-diprenylation at *C*-atoms.

Biogenetically, cohumulone and colupulone are prenylated phlorisobutyrophenone (PIBP, **1**, Scheme 1), while humulone and lupulone prenylated phlorisovalerophenone (PIVP, **2**,

Scheme 1. Prenylation Steps in the Biosynthesis of β-Bitter Acids in *Humulus lupulus*

acylphloroglucinols
R = CH(CH$_3$)$_2$ (PIBP, **1**)
R = CH$_2$CH(CH$_3$)$_2$ (PIVP, **2**)

HIPT1L

dimethylallyl-acylphloroglucinols

metabolon of HIPT1L/HIPT2

di-dimethylallyl-acylphloroglucinols

metabolon of HIPT1L/HIPT2

β-bitter acids

Scheme 1). Clusianone carries the skeleton of phlorbenzophenone (PBZP, **3**, Scheme 2). The AP cores of these compounds are tetraketides and formed by condensation of three malonyl-CoA molecules with different start units, i.e., isobutyryl-CoA in the case of **1**, isovaleryl-CoA in the case of **2**, and benzoyl-CoA in the case of **3**. The responsible polyketide synthases have been characterized.[10−12] In comparison, little is known about the enzymes for the multiple prenylation steps. Only the prenyltransferases involved in the biosynthesis of bitter acids in *H. lupulus* have been reported.[12,13] Tsurumaru et al.[13] reported the overproduction of the membrane-bound prenyltransferase HIPT-1 from *H. lupulus* and its biochemical characterization. It was found that this enzyme catalyzed the prenylation of **2** in the presence of DMAPP and also accepted **1** as prenylation acceptor. Recently, Li et al.[12] identified two membrane-bound prenyltransferases HIPT1L and HIPT2 from *H. lupulus*.

Scheme 2. Prenylations of 1−3 by AtaPT in the Presence of DMAPP, GPP, and FPP
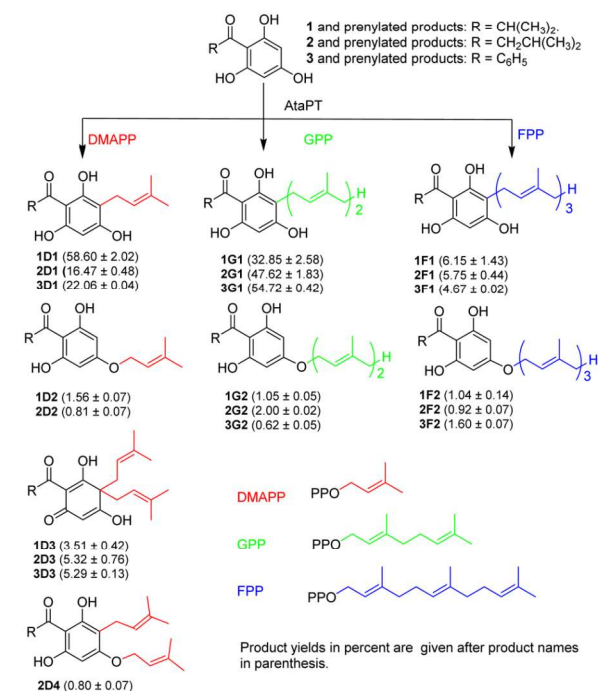
Coexpression of different genes in *Saccharomyces cerevisiae* revealed that HIPT1L and HIPT2 catalyzed three sequential prenylation steps in the ß-bitter acid pathway. HIPT1L was confirmed to be an orthologue of HIPT1 identified by Tsurumaru et al.[13] Interestingly, HIPT2 was only active when it was co-expressed with HIPT1L. This led to the hypothesis that HIPT1L and HIPT2 form a metabolon as the catalytic unit.[12]

In recent years, significant progress has been achieved for the members of the dimethylallyltryptophan synthase (DMATS) superfamily, mainly from ascomycetous fungi.[14] These soluble enzymes use predominantly tryptophan and other indole derivatives as prenyl acceptors but also accept a broad spectrum of aromatic compounds as substrates.[14] Diprenylation of indole derivatives by one DMATS enzyme was observed in several cases.[15−17] However, a *gem*-diprenylation has not been reported for such enzymes or for other soluble prenyltransferases. The sole example of *gem*-diprenylation of an aromatic substrate was described for the metabolon of HIPT1L and HIPT2 mentioned above.[12]

In a previous study,[18] we demonstrated the prenylation of APs 1−3 by the soluble fungal prenyltransferase AnaPT from *Neosartorya fischeri*, which catalyzed the prenylation of (*R*)-benzodiazepinedinone, a cyclic dipeptide of tryptophan, and anthranilic acid.[19] The observed activities of AnaPT toward these substrates are much higher than that of a microsomal fraction containing the overproduced prenyltransferase HIPT1.[13] However, only monoprenylated derivatives were obtained in the presence of DMAPP, and the conversion yields of 1−3 with GPP as prenyl donor were very low.[18]

Very recently, a soluble prenyltransferase AtaPT from *Aspergillus terreus* strain A8-4 was demonstrated to carry an unprecedented promiscuity toward diverse aromatic acceptors and prenyl donors including DMAPP, geranyl diphosphate (GPP), and farnesyl diphosphate (FPP). AtaPT shares high

sequence identity with the hypothetical protein EAU34068 encoded by ATEG_04999 from *A. terreus* NIH2624 and differs at only three residues. Among the tested aromatic substrates, AtaPT also consumed 3 in the presence of DMAPP, GPP, and FPP, although no noteworthy sequence homology exits between AtaPT and HIPT1L or HIPT2. These reactions were not studied in detail.[20]

In this study, we investigate the behavior of AtaPT toward the three APs 1−3, which serve as precursors of most polyprenylated APs,[1−3,5] in the presence of DMAPP, GPP, and FPP. We hope to increase the structure diversity of prenylated APs by high conversion yields with GPP and FPP as well as by multiple prenylations, especially *gem*-diprenylations.

The coding sequence of AtaPT orthologue from *A. terreus* DSM 1958 was amplified by PCR and cloned into the expression vector pQE-70, resulting in the expression construct pCaW7 (see the Supporting Information for details). Sequence analysis revealed that differences at only four residues were found between AtaPT and its orthologue from DSM 1958. S230, T290, A292, and N373 in AtaPT were replaced by A230, K290, E292, and S373 in that of strain DSM 1958, respectively. Because these residues are not located in the active sites,[20] it can be expected that the orthologue from DSM 1958 will fulfill the function of AtaPT, and we therefore use hereafter the name AtaPT also for this enzyme. Gene expression in *E. coli* and purification of the soluble protein resulted in a predominant band on SDS-PAGE with a migration above the 45 kDa size marker, corresponding well to the calculated mass of 48.7 kDa for AtaPT-His$_6$. The protein yield was calculated to be 29 mg of purified protein per liter of culture (see the SI for details).

To compare the activities of AnaPT mentioned above and AtaPT toward 1−3, incubations on a 100 μL scale, containing 20 μg of protein, DMAPP, GPP, or FPP, were carried out at 37 °C for 2 h. HPLC analysis revealed that 1−3 were much better converted by AtaPT than by AnaPT in all enzyme assays. Total conversion yields of 63.67 ± 2.43, 23.4 ± 1.26, and 27.35 ± 0.25% were calculated for 1, 2, and 3 with AtaPT and DMAPP, respectively. These values are significantly higher than those of AnaPT, with conversion yields of 3.64 ± 0.77, 4.33 ± 0.52, and 7.66 ± 0.49%, respectively (Scheme 2; see the SI for details). The poor acceptance of GPP by AnaPT was confirmed in this study, and product formation was only detected in the reaction mixtures of 1 and 3 with GPP. In contrast, GPP served as a very good prenyl donor for the AtaPT reactions, with product yields of 32.85 ± 2.58, 47.62 ± 1.83, and 54.72 ± 0.42% for 1, 2, and 3, respectively (Scheme 2; see the SI for details). FPP was accepted by AtaPT with conversion yields of 7.19 ± 1.57, 6.66 ± 0.51, and 6.27 ± 0.09% for 1, 2, and 3, respectively (Scheme 2; see the SI for details).

Only one product each was detected in the AnaPT reactions of 1−3 with DMAPP as well as those of 1 and 2 with GPP. These products were identified as predominant ones in the AtaPT reactions. Isolation and structure elucidation by NMR and MS analyses (see the SI for details) proved the main products of the AtaPT reactions to be monoprenylated derivatives; that is 1D1−3D1 with DMAPP, being consistent with the AnaPT products,[18] 1G1−3G1 with GPP, and 1F1−3F1 with FPP (Scheme 2, see the SI for details).

Additional product peaks with longer retention times were also detected in the reaction mixtures of AtaPT with 1−3 in the presence of all three prenyl donors (see the SI for details). The intensities of these peaks are clearly increased in the incubation mixtures with 50 μg of protein at 37 °C for 2 h, which were

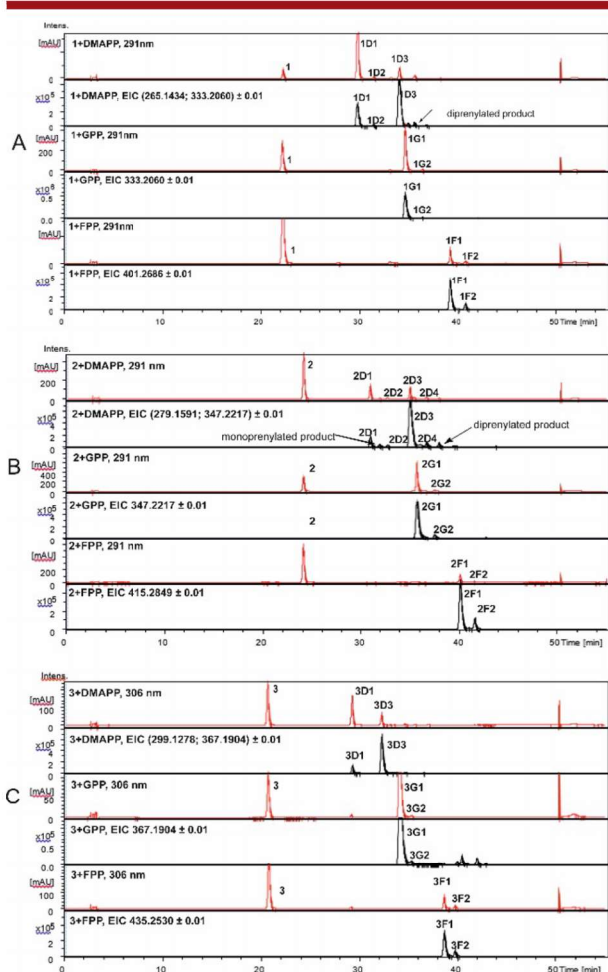detected by LC−MS analysis (Figure 2). In the incubation mixtures of **1**−**3** with GPP and FPP, two monoprenylated

Figure 2. LC−MS analysis of the reaction mixtures of DMAPP, GPP, or FPP with **1** (A), **2** (B), and **3** (C) after incubation with 50 μg of AtaPT per 100 μL at 37 °C for 2 h. Red lines are UV absorptions, and black lines are extracted positive-ion chromatograms (EIC).

derivatives each were detected. In addition to the *C*-prenylated **1G1**−**3G1** and **1F1**−**3F1**, one *O*-prenylated derivative each, **1G2**, **2G2**, **3G2**, **1F2**, **2F2**, or **3F2** ,was identified by NMR and MS analyses as a minor product after isolation and structure elucidation (Scheme 2 and Figure 2; see the SI for details).

In the incubation mixtures of **1** with DMAPP, two mono- and two diprenylated derivatives were detected. In comparison, three mono- and three diprenylated derivatives were found in the reaction mixture of **2** with DMAPP and one mono- and one diprenylated products of **3** with DMAPP. Isolation and structure elucidation proved the presence of *O*-prenylated **1D2** and **2D2** in the reaction mixtures of **1** and **2**, respectively. Interestingly, *gem*-diprenylated derivatives **1D3**, **2D3**, and **3D3** were identified in the reaction mixtures of **1**, **2**, and **3**, respectively (Figure 2 and Scheme 2; see the SI for details).

These results proved the ability of AtaPT for a *gem*-dipenylation of acylphloroglucinols and encouraged us to investigate the conversion of the monoprenylated **1D1**, **2D1**, and **3D1** by AtaPT. **1D1**, **2D1**, and **3D1** were then incubated in the presence of DMAPP with 50 μg of AtaPT at 37 °C for 2 h.

LC−MS analysis revealed clear conversion by detection of the *gem*-diprenylated derivatives **1D3**, **2D3**, and **3D3** as predominant products, with product yields of 4.88 ± 0.15, 57.18 ± 1.07, and 33.31 ± 0.23%, respectively (Figure 3). Better
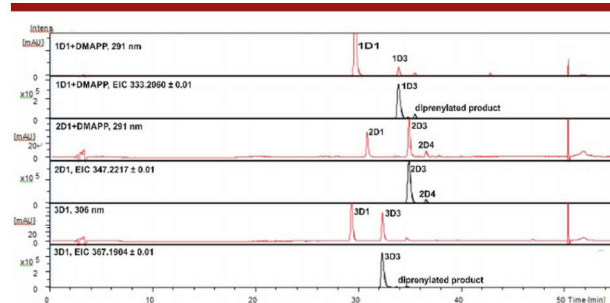

Figure 3. LC−MS analysis of AtaPT reactions (50 μg per 100 μL, 37 °C for 2 h) with DMAPP and **1D1**, **2D1**, or **3D1**. Red lines are UV absorptions, and black lines are extracted positive-ion chromatograms (EIC).

conversion of **2D1** and **3D1** than **1D1** confirmed the higher product yields of **2D3** and **3D3** in the incubation mixtures of **2** and **3** than **1D3** in that of **1** (Figure 2). A minor diprenylated product each with larger retention times and product yields of 1.99 ± 0.07, 8.24 ± 0.87, and 4.16 ± 0.20%, respectively, was also detected. The second product **2D4** from the incubation mixture of **2D1** was proven to be a *C*- and *O*-diprenylated derivative, which was also isolated and identified from the incubation mixture of **2** with DMAPP (Figures 2 and 3 and Schemes 2 and 3; see the SI for details). The second

Scheme 3. Reactions of Monoprenylated Derivatives with AtaPT
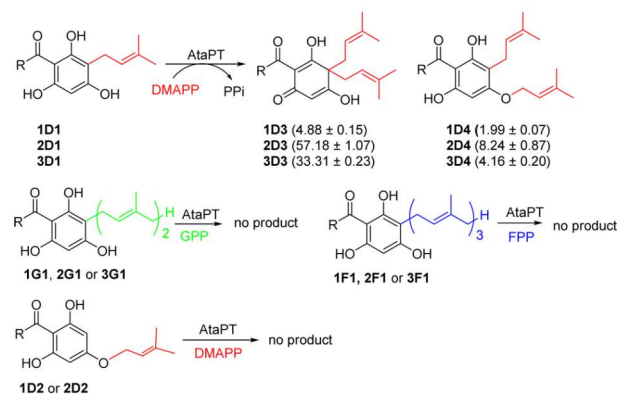
diprenylated derivative of the reaction mixtures with **1D1** and **3D1** could not be isolated and identified. However, on the basis of their retention times and UV spectra together with LC−MS data, it can be speculated that these compounds are also *C*- and *O*-diprenylated derivatives.

These results provide evidence for successive diprenylations of **1**, **2**, and **3** by AtaPT, which was also confirmed by time dependence of the product formation in the incubation mixtures of **2** and **3** with DMAPP. The formation of **2D3** and **3D3** increased continuously, while **2D1** and **3D1** reached their maxima in short time and decreased after that (see the SI for details). No product formation was detected in the incubation mixtures of **1D1**, **2D1**, and **3D1** with AnaPT and DMAPP under the same conditions (data not shown).

As mentioned above, no diprenylated product was detected in the incubation mixtures of AtaPT with **1**–**3** and GPP or FPP (Figure 2 and Scheme 2). This was confirmed by incubation of their *C*-monoprenylated derivatives. Product formation was not observed for the reaction mixtures of **1G1**, **2G1**, and **3G1** with AtaPT in the presence of GPP or those of **1F1**, **2F1**, and **3F1** with FPP (Scheme 3). Incubation of **1D1**, **2D1**, and **3D1** with AtaPT and GPP or FPP did not result in product formation. A previous study showed that AtaPT also catalyzed *C*-diprenylations of several aromatic acceptors in the presence of GPP and FPP, although no *gem*-prenylated products were detected.[20] No formation of diprenylated **1**–**3** with these donors resulted from their orientations in the reaction cavity. No product formation was detected by LC–MS analysis after incubation of **1D2** and **2D2** with 50 μg of AtaPT and DMAPP at 37 °C for 2 h (Scheme 3), excluding the possible formation of *C*- and *O*-diprenylated derivatives from *O*-monoprenylated products.

To obtain more insights into the catalytic efficiency of the tetrameric AtaPT, kinetic parameters including Michaelis–Menten constants (K_M) and turnover numbers (k_{cat}), were determined at pH 7.5 for **1**, **2**, and **3** in the presence of DMAPP, GPP, and FPP as well as DMAPP with **1** and GPP with **3** (see the SI for details). The catalytic efficiency of AtaPT toward **1** is 32-fold of that of AnaPT in the presence of DMAPP. compound **1** was better consumed by AtaPT in the presence of DMAPP and FPP than **2** and **3**. Compound **3** was most efficiently consumed in the presence of GPP. The determined k_{cat}/K_M values for **1**–**3** are in the range of 170–300 s^{-1} M^{-1} in the presence of GPP and between 17 and 37 s^{-1} M^{-1} in the presence of FPP. With **1** as acceptor, a 95-fold k_{cat}/K_M value of that of AnaPT was determined for DMAPP with AtaPT (see Table S8 for details).

In conclusion, we have provided in this study the first example of *gem*-diprenylation of APs by a member of the DMATS superfamily, proving their unprecedented application potential. AtaPT could be an interesting candidate for production of polyprenylated APs like β-bitter acids by synthetic biology.

ASSOCIATED CONTENT

ⓢ Supporting Information

The Supporting Information is available free of charge on the ACS Publications website at DOI: 10.1021/acs.or-glett.6b03594.

> Experimental procedures, detailed NMR data, HR-ESI-MS data, determination of kinetic parameters, as well as NMR spectra (PDF)

AUTHOR INFORMATION

Corresponding Author
*E-mail: shuming.li@staff.uni-marburg.de.

ORCID ⓞ
Shu-Ming Li: 0000-0003-4583-2655

Notes
The authors declare no competing financial interest.

■ REFERENCES
(1) Ciochina, R.; Grossman, R. B. *Chem. Rev.* **2006**, *106*, 3963.
(2) Richard, J. A.; Pouwer, R. H.; Chen, D. Y. *Angew. Chem., Int. Ed.* **2012**, *51*, 4536.
(3) Wu, S.-B.; Long, C.; Kennelly, E. J. *Nat. Prod. Rep.* **2014**, *31*, 1158.
(4) Van Cleemput, M.; Cattoor, K.; De Bosscher, K.; Haegeman, G.; De Keukeleire, D.; Heyerick, A. *J. Nat. Prod.* **2009**, *72*, 1220.
(5) Kobayashi, J.; Tanaka, N. *Heterocycles* **2015**, *90*, 23.
(6) Garnsey, M. R.; Matous, J. A.; Kwiek, J. J.; Coltart, D. M. *Bioorg. Med. Chem. Lett.* **2011**, *21*, 2406.
(7) Sales, L.; Pezuk, J. A.; Borges, K. S.; Brassesco, M. S.; Scrideli, C. A.; Tone, L. G.; dos Santos, M. H.; Ionta, M.; de Oliveira, J. C. *BMC Complementary Altern. Med.* **2015**, *15*, 393.
(8) Piccinelli, A. L.; Cuesta-Rubio, O.; Chica, M. B.; Mahmood, N.; Pagano, B.; Pavone, M.; Barone, V.; Rastrelli, L. *Tetrahedron* **2005**, *61*, 8206.
(9) Nagalingam, S. V.; Wai-Ling, K.; Teng-Jin, K. *Planta Med. Lett.* **2016**, *3*, e10–e13.
(10) Beerhues, L.; Liu, B. *Phytochemistry* **2009**, *70*, 1719.
(11) Okada, Y.; Ito, K. *Biosci., Biotechnol., Biochem.* **2001**, *65*, 150.
(12) Li, H.; Ban, Z.; Qin, H.; Ma, L.; King, A. J.; Wang, G. *Plant Physiol.* **2015**, *167*, 650.
(13) Tsurumaru, Y.; Sasaki, K.; Miyawaki, T.; Uto, Y.; Momma, T.; Umemoto, N.; Momose, M.; Yazaki, K. *Biochem. Biophys. Res. Commun.* **2012**, *417*, 393.
(14) Winkelblech, J.; Fan, A.; Li, S.-M. *Appl. Microbiol. Biotechnol.* **2015**, *99*, 7379.
(15) Fan, A.; Li, S.-M. *Adv. Synth. Catal.* **2013**, *355*, 2659.
(16) Liu, C.; Noike, M.; Minami, A.; Oikawa, H.; Dairi, T. *Biosci., Biotechnol., Biochem.* **2014**, *78*, 448.
(17) Winkelblech, J.; Li, S.-M. *ChemBioChem* **2014**, *15*, 1030.
(18) Zhou, K.; Ludwig, L.; Li, S.-M. *J. Nat. Prod.* **2015**, *78*, 929.
(19) Yin, W.-B.; Grundmann, A.; Cheng, J.; Li, S.-M. *J. Biol. Chem.* **2009**, *284*, 100.
(20) Chen, R.; Gao, B.; Liu, X.; Ruan, F.; Zhang, Y.; Lou, J.; Feng, K.; Wunsch, C.; Li, S.-M.; Dai, J.; Sun, F. *Nat. Chem. Biol.* **2016**, DOI: 10.1038/nchembio.2263.

Supporting Information

Gem-diprenylation of acylphloroglucinols by a fungal prenyltransferase of the dimethylallyltryptophan synthase superfamily

Kang Zhou,[†] Carsten Wunsch, [†] Jungui Dai, [‡] and Shu-Ming Li [*†]

[†]*Pharmazeutische Biologie und Biotechnologie, Philipps-Universität Marburg, Robert-Koch-Str. 4, 35037, Marburg, Germany*

[‡]*State Key Laboratory of Bioactive Substance and Function of Natural Medicines, Institute of Materia Medica, Chinese Academy of Medical Sciences and Peking Union Medical College, Xian Nong Tan Street, Beijing 100050, China*

* Fax:, 49-6421-2825365; Tel:, 49-6421-2822461

Shu-Ming Li: shuming.li@staff.uni-marburg.de

I. Experimental Section

Chemicals

DMAPP, GPP, and FPP were synthesized according to the method described for GPP reported previously.[1] Phlorisobutyrophenone (PIBP, **1**), phlorisovalerophenone (PIVP, **2**), and phlorbenzophenone (PBZP, **3**) were synthesized according to protocols described previously.[2]

Cultivation of *Aspergillus terreus* for DNA isolation

A. terreus DSM 1958 was purchased from German Collection of Microorganisms and Cell Cultures (DSMZ) and cultivated in 300 mL cylindrical flasks containing 100 mL YME medium (yeast extract: 4.0 g L^{-1}, glucose monohydrate: 4.0 g L^{-1}, and malt extract: 10.0 g L^{-1}) at 30 °C for 5 days in darkness for DNA isolation.

DNA propagation in *E. coli* and DNA isolation from fungi

Standard procedures for DNA isolation and manipulation in *E. coli* were performed as described.[3] To isolate genomic DNA from *A. terreus*, the mycelia of a 5 day-old culture were collected and washed with phosphate-buffered saline consisting of 137 mM NaCl, 2.7 mM KCl, 1 mM Na_2HPO_4, and 0.18 mM KH_2PO_4, pH 7.3. Genomic DNA was isolated according to a method described previously.[4]

Amplification of sequence coding forAtaPT (accession number KP893683) orthologue from *A. terreus* DSM 1958

The ATEG_04999 orthologue is composed of two exons of 1148 and 127 bp, interrupted by an intron of 48 bp. The two exons were amplified separately by PCR in a first round and then combined in a second round by using the PCR products from the first round as templates and primers. The High Fidelity PCR kit (Roche) was used for this purpose. Two primers CaW_04999-1 (5′-AA*G*CATGCTCCCCCCATCAGACAGC-3′) and CaW_04999-3 (5′-<u>TTCTTGGTTTGCGAGATATCCACATTGGGA</u>AAATTTCGCCTTGAGTTCATC-3′) were used for amplification of the first exon and CaW_04999-2 (5′-<u>GATGAACTCAAGGCGAAAT</u>TTCCCAATGTGGATATCTCGCAAACCAAGAA-3′) and CaW_04999-4 (5′-CC*GG*ATC*C*CACACGTGCGACATTTC-3′) for the second exon. Bold letters in CaW_04999-1 and CaW_04999-4 represent mutations inserted into the original genome sequence in order to create the restriction sites SphI and BamHI for cloning in pQE-70. The underlined letters in CaW_04999-2 and CaW_04999-3 indicate overlapping sequences for fusion.

Gene cloning, overproduction and purification of AtaPT

The generated PCR fragment consisting of the coding region was cloned in pGEM-T Easy and sequenced. After confirming the sequence, the insert was released by restriction with SphI/BamHI and recloned in pQE-70 vector, resulted in the construct pCaW7 for expression in *E. coli*.

For AtaPT overproduction with pCaW7, *E.coli* M15 [pREP] cells were cultivated as described previously.[5] Protein purification was carried out according to the procedure described by Yin et al.[5] The purity of the obtained protein was proven on SDS-PAGE (Figure S1).

Enzyme assays

The enzyme assays (100 µL) contained 1 mM of acylphloroglucinols **1**, **2**, or **3**, 5 mM of $CaCl_2$, 2 mM of DMAPP, GPP or FPP, 0.2–5.0 % of glycerol, 5 % of DMSO, and 20 µg or 50 µg of purified recombinant protein in 50 mM of Tris-HCl, pH 7.5. The reaction mixtures were incubated at 37 °C for 2 h and terminated by addition of 100 µL methanol. The proteins were removed by centrifugation at 13,000 rpm for 20 min. The supernatants were analyzed on HPLC described below. For analysis on LC-MS, the reaction mixtures were extracted four times with double volumes of ethyl acetate. The organic phases were combined and evaporated under reduced pressure to afford the residues, which were dissolved in 100 µL methanol and analyzed on LC-MS.

Assays for isolation of the enzyme products were carried out in large scales (20–30 mL) containing 1 mM of acylphloroglucinols, 2 mM of DMAPP, GPP or FPP, 5 mM of $CaCl_2$, 0.2–5.0 % of glycerol, 5 % of DMSO, 10–20 mg of recombinant protein in 50 mM of Tris-HCl, pH 7.5. After incubation at 37 °C for 16 h, the reaction mixtures were extracted four times with double volumes of ethyl acetate. The organic phases were combined and evaporated. The residues were dissolved in 0.5–1.0 mL of methanol and purified on a preparative HPLC column.

Assays for determination of the kinetic parameters of acceptors (100 µL) contained 5 mM of $CaCl_2$, 0.2–5.0 % of glycerol, 5% of DMSO, 2 mM of DMAPP, GPP or FPP, **1**, **2**, and **3** at final concentrations of up to 5.0 mM and different amounts of proteins in 50 mM of Tris-HCl, pH 7.5 (Table S8). For determination of the kinetic parameters of the prenyl donors DMAPP and GPP, **1** or **3** at a final concentration of 1 mM, DMAPP of up to 1.0 mM and GPP of up to 4.0 mM were used. Higher DMAPP and GPP concentrations led to inhibition of the AtaPT reactions. The used protein amounts are given in Table S8. The reaction mixtures were incubated within the linear range of the product formation for different times (Table S8 and Figures S32-42) and terminated with 100 µL methanol. Proteins were removed by centrifugation at 13,000 rpm for 20 min and the supernatants were analyzed on HPLC.

Ion dependence of the AtaPT reaction

To determine the ion dependency of AtaPT, incubations with different cations, including Mn^{2+}, Mg^{2+}, Ca^{2+}, Ni^{2+}, Fe^{2+}, Zn^{2+}, Co^{2+}, Cu^{2+}, Na^+, and K^+ at 5 mM, were carried out in the presence of **1** and DMAPP. The 100 μL reaction mixtures contained 50 μg of AtaPT-His$_6$, 2 mM of DMAPP, 1 mM of **1** and were incubated at 37 °C for 2 h. Incubations with EDTA and without additives were used as controls. As shown in Figure S2, different ions had various contributions to the catalytic activity. In comparison to the assay without additives, addition of EDTA did not influence the enzyme activity. Ca^{2+} and Mg^{2+} enhanced the enzyme activity slightly. Ca^{2+} was therefore used in all enzyme assays in this study.

Analysis of enzyme products by HPLC, LC-MS, and NMR

Agilent HPLC series 1200 (Böblingen, Germany) alone and with a micrOTOF-Q III spectrometer with an ESI source (Bruker, Bremen, Germany) were used for analysis of the enzyme products. Analysis of the enzyme products on HPLC without the spectrometer was performed on an Agilent Eclipse XDB-C$_{18}$ column (4.6 × 150mm, 5 μm) with a linear gradient of 10–100 % acetonitrile in water in 40 min and a flow rate at 0.5 mL/min. The column was then washed with acetonitrile for 5 min and equilibrated with 5 % acetonitrile in water for 5 min. The HPLC chromatograms of incubation mixtures of **1**, **2**, and **3** with AtaPT or AnaPT in the presence of DMAPP, GPP or FPP are shown as Figures S3-S5.

Analysis of the enzyme products on LC-MS was carried out on a CS Multospher 120 RP 18 column (2 × 250mm, 5 μm) and a linear gradient of 5–100 % acetonitrile in water, both containing 0.1% formic acid, in 40 min and a flow rate at 0.25 mL/min. The column was then washed with 100 % acetonitrile containing 0.1% formic acid for 5 min and equilibrated with 5 %, acetonitrile in water for 5 min. The parameters of the spectrometer were set as following: electrospray positive ion mode for ionization, capillary voltage with 4.5kV, collision energy with 8.0eV.The LC-MS chromatograms of the incubation mixtures of **1**, **2**, and **3** with AtaPT in the presence of DMAPP, GPP or FPP are provided as Figures 2–3 in the main text. HR-ESI-MS data are given in Table S1.

The enzyme products were isolated on HPLC with an Agilent Eclipse XDB-C18 column (9.4× 250 mm, 5 μm) with a linear gradient of 30–100 % acetonitrile in water in 30 min and a flow rate at 2.0 mL/min. After each run, the column was equilibrated with 10 % acetonitrile in water for 10 min.

^{1}H NMR spectra were recorded at room temperature on an ECA- 400 or an ECX-500 spectrometer (JEOL, Tokyo, Japan). Chemical shifts were referenced to the solvent signal at 2.05 ppm for acetone-D$_6$ and 7.26 ppm for CHCl$_3$. All spectra were processed with MestReNova 5.2.2 (Metrelab Research,

Santiago de Compostella, Spain). NMR spectra and data of the prenylated products are provided as Figures S6-S29 and Tables S2-S7, respectively.

Structure elucidation

Inspection of the ^{1}HNMR spectra of the isolated products indicated the regular attachment of the prenyl moieties, i.e. *via* their C-1, to three different kinds of atoms, which can be clearly distinguished by the chemical shifts of H′-1 of the prenyl chains (d, 2H, $-CH_2-$). The signals of this proton of *O*-prenylated derivatives are strongly downfield shifted to the range of 4.5-4.7 ppm.[6] Chemical shifts between 3.2–3.4 ppm are characteristic for H′-1 of the prenyl moieties attached to an aromatic *C*-atom.[2] The signals at about 2.5 ppm are those attached to sp³ *C*-atoms.

By comparison of NMR data in the literature, the monoprenylated derivatives **1D1**,[2] **2D1**,[2] **3D1**,[2] **1D2**,[7] **1G1**,[8] **2G1**,[8] **3G1**,[9] **1G2**,[10] **3G2**,[7] **1F1**,[11,9] and **3F1**[9] were identified unequivocally. As reported previously, the *gem*-diprenylated derivative **1D3** exists as a mixtures of four tautomeric forms in CDCl₃[12]. The ^{1}H NMR spectrum of **1D3** in CDCl₃ obtained in this study corresponded very well to that in the literature.[12] Existence of tautomeric forms in CDCl₃ was also observed for **2D3** and **3D3** (data not shown). Using acetone-D₆ as solvent, the tautomers of **1D3**, **2D3**, and **3D3** illustrated in Scheme 2 are predominant structures. The NMR data of **2D3** and **3D3** are consistent very well with those reported previously.[13,14]

The structures of **2D2**, **2D4**, **2G2**, **2F1**, **1F2**, **2F2**, and **3F2** have not been reported prior to this study. The *O*-monoprenylated products **2D2**, **2G2**, **1F2**, **2F2**, and **3F2** carry their prenyl moieties at the *para*-position of the acyl residues, which are proven by the identical resonance of H-3 and H-5. The structure of **2F1** was elucidated by comparison with those of **1F1**. Only one singlet for an aromatic proton at δ5.89 ppm was found in the ^{1}H NMR spectrum of **2D4**. The signals of the two dimethylallyl moieties correspond well to those in **2D1** and **2D2**, respectively, indicating *C*- and *O*-prenylation. In addition, the [M+H]⁺ ion of this product is 136 Da larger than that of **2**, confirming the diprenylation of **2**. Conversion of **2D1** to **2D3** and **2D4** by AtaPT provided additional evidence for the structure of **2D4**.

Time dependence of the formation of 2D1 and 2D3 in the reaction mixture of 2 as well as 3D1 and 3D3 in the reaction mixture of 3

To determine the relationship of **2D1** and **2D3** in the reaction mixtures (100 μL) of **2** with AtaPT, time dependence of their formation was determined with 0.5 mM of **2** and 50 μg of AtaPT in the presence of 2 mM of DMAPP. As shown in Figure S30, formation of **2D1** reached its maximal after incubation for 30 min and decreased slowly during further incubations. After incubation for 480 min,

only 12.8% of the maximal value was detected for **2D1**. In contrast, the formation of **2D3** increased continuously during incubation up to 480 min.

In analogy to **2**, **3** was also incubated with AtaPT and DMAPP for different times. As shown in Figure S31, similar results were obtained for the formation of **3D1** and **3D3**. The changes are somewhat slowly than those in the incubation of **2**. The product yield of 3**D1** reached its maximal at 60 min and decreased after 180 min. The formation of **3D3** increased continuously during the whole incubation process. These results confirmed that **2D3** and **3D3** are formed from **2** and **3** *via* **2D1** and **3D1**, respectively.

II. References

(1) Woodside, A. B.; Huang, Z.; Poulter, C. D. *Org. Synth.* **1988**, *66*, 211.
(2) Zhou, K.; Ludwig, L.; Li, S.-M. *J. Nat. Prod.* **2015**, *78*, 929.
(3) Sambrook, J.; Russell, D. W. *Molecular cloning: a laboratory manual;* 3rd ed.; Cold Spring Harbor Laboratory Press, Cold Spring Harbor: New York, 2001.
(4) Yu, X.; Li, S.-M. *Methods Enzymol.* **2012**, *516*, 259.
(5) Yin, W.-B.; Grundmann, A.; Cheng, J.; Li, S.-M. *J. Biol. Chem.* **2009**, *284*, 100.
(6) Zou, H.-X.; Xie, X.; Zheng, X.-D.; Li, S.-M. *Appl. Microbiol. Biotechnol.* **2011**, *89*, 1443.
(7) Bohlmann, F.; Suwita, A. *Phytochemistry* **1978**, *17*, 1929.
(8) Rios, M. Y.; Delgado, G. *Phytochemistry* **1992**, *31*, 3491.
(9) Wang, X.; Lee, Y. R. *Tetrahedron* **2011**, *67*, 9179.
(10) Bohlmann, F.; Mahanta, P. K. *Phytochemistry* **1979**, *18*, 348.
(11) Yu, Q.; Ravn, R. R.; Jacob, M. R.; Khan, S. I.; Agarwal, A. K.; Yu, B. Y.; Li, X. C. *J. Nat. Prod.* **2016**, *79*, 2195.
(12) George, J.-H.; Hesse, M.-D.; Baldwin, E.; dlington, R.-M. *Org. Lett.* **2010**, *12*, 3532.
(13) Mizobuchi, S.; Sato, Y. *Agricultural and Biological Chemistry* **1985**, *49*, 399.
(14) Cann, M. R.; Davis, A. M.; Shannon, P. V. R. *J. Chem. Soc. , Perkin Trans. 1* **1984**, 1413.

III. Table of HR-ESI-MS data

Table S1. HR-ESI-MS data of enzyme products

Product	Chemical formula	HR-ESI-MS data		
		Calculated [M+H]$^+$	Measured [M+H]$^+$	Deviation [ppm]
1D1	$C_{15}H_{21}O_4$	265.1434	265.1428	2.3
1D2	$C_{15}H_{21}O_4$	265.1434	265.1414	7.5
1D3	$C_{20}H_{29}O_4$	333.2060	333.2057	0.9
1D4	$C_{20}H_{29}O_4$	333.2060	333.2052	2.4
2D1	$C_{16}H_{23}O_4$	279.1591	279.1587	1.4
2D2	$C_{16}H_{23}O_4$	279.1591	279.1577	5.0
2D3	$C_{21}H_{31}O_4$	347.2217	347.2217	0.1
2D4	$C_{21}H_{31}O_4$	347.2217	347.2213	1.2
3D1	$C_{18}H_{19}O_4$	299.1278	299.1270	2.7
3D3	$C_{23}H_{27}O_4$	367.1904	367.1902	0.5
3D4	$C_{23}H_{27}O_4$	367.1904	367.1885	5.2
1G1	$C_{20}H_{29}O_4$	333.2060	333.2047	3.9
1G2	$C_{20}H_{29}O_4$	333.2060	333.2063	-0.9
2G1	$C_{21}H_{31}O_4$	347.2217	347.2220	-0.9
2G2	$C_{21}H_{31}O_4$	347.2217	347.2204	3.7
3G1	$C_{23}H_{27}O_4$	367.1904	367.1926	-6.0
3G2	$C_{23}H_{27}O_4$	367.1904	367.1900	1.1
1F1	$C_{25}H_{37}O_4$	401.2686	401.2669	4.2
1F2	$C_{25}H_{37}O_4$	401.2686	401.2680	1.5
2F1	$C_{26}H_{39}O_4$	415.2843	415.2849	-1.4
2F2	$C_{26}H_{39}O_4$	415.2843	415.2840	0.7
3F1	$C_{28}H_{35}O_4$	435.2530	435.2503	6.2
3F2	$C_{28}H_{35}O_4$	435.2530	435.2527	0.7

IV. Tables of NMR data

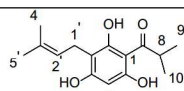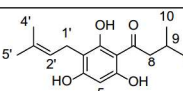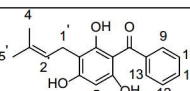**Table S2**. ^{1}H-NMR data of the enzyme products **1D1**, **2D1**, **3D1**, **1D2**, and **2D2**, 500 MHz.

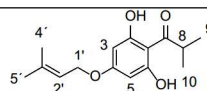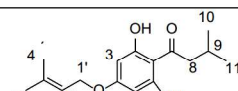| Comp	1D1	2D1	3D1	1D2		2D2	
Solvent	acetone-D$_6$	acetone-D$_6$	acetone-D$_6$	acetone-D$_6$	CDCl$_3$	acetone-D$_6$	CDCl$_3$
Pos.	δ_H, J in Hz	δ_H,(J in Hz	δ_H, J in Hz	δ_H, J in Hz	δ_H, J in Hz	δ_H, J in Hz	δ_H, J in Hz
3	/	/	/	6.00, s	5.93, s	5.99, s	5.92, s
5	6.06, s	6.07, s	6.04, s	6.00, s	5.93, s	5.99, s	5.92, s
6	/	/	/	/	/	/	/
8	3.98, sept, 6.7	2.94, d, 6.7	/	3.98, sept, 6.8	3.85, sept, 6.8	2.96, d, 6.7	2.93, d, 6.7
9	1.13, d, 6.7	2.24, m	7.60, dt, 7.2, 1.3	1.13, d, 6.8	1.17, d, 6.8	2.24, m	2.25, m
10	1.13, d, 6.7	0.95, d, 6.7	7.43, br t, 7.2	1.13, d, 6.8	1.17, d, 6.8	0.95, d, 6.7	0.97, d, 6.7
11	/	0.95, d, 6.7	7.48, tt, 7.2, 1.3	/	/	0.95, d, 6.7	0.97, d, 6.7
12	/	/	7.43, br t, 7.2	/	/	/	/
13	/	/	7.60, dt, 7.2, 1.3	/	/	/	/
1′	3.23, d, 7.2	3.23, d, 7.2	3.29, d, 7.2	4.56, d, 6.7	4.49, d, 6.9	4.55, d, 6.7	4.49, d, 6.8
2′	5.22, tsept, 7.2, 1.4	5.22, tsept, 7.2, 1.4	5.27, tsept, 7.2, 1.4	5.42, tsept, 6.7, 1.5	5.44, br t, 6.9	5.42, br t, 6.7	5.42, br t, 6.8
4′	1.62, s	1.62, s	1.65, s	1.74, s	1.73, s	1.74, s	1.73, s
5′	1.73, s	1.73, s	1.76, s	1.77, s	1.79, s	1.77, s	1.79, s
OH	14.12, s	14.09, s	12.21, s	11.84, s	/	11.83, s	/
OH	9.48, s	9.54, s	9.19, s	/	/	/	/
OH	9.06, s	9.12, s	8.93, s	/	/	/	/

S8

76

Table S3. ^{1}H-NMR data of the enzyme products **1D3**, **2D3**, **3D3**, and **2D4**, 500 MHz

Comp					
	1D3	**2D3**	**3D3**	**2D4**	
Solvent	acetone-D_6	acetone-D_6	acetone-D_6	acetone-D_6	$CDCl_3$
Pos.	δ_H, J in Hz	δ_H, J in Hz	δ_H, J in Hz	δ_H, J in Hz	δ_H, J in Hz
5	5.58, s	5.60, s	5.73, s	6.11, s	5.89, s
8	4.00, sept, 6.8	2.80 [a]	/	2.80 [a]	2.87, d, 6.7
9	1.03, d, 6.8	2.04, m	7.44, br t, 7.4	2.04, m,	2.17, m
10	1.03, d, 6.8	0.94, d, 6.7	7.37, br t, 7.4	0.94, d, 6.7	0.94, d, 6.7
11	/	0.94, d, 6.7	7.46, br t, 7.4	0.94, d, 6.7	0.94, d, 6.7
12	/	/	7.37, br t, 7.4	/	/
13	/	/	7.44, br t, 7.4	/	/
1′	2.51, dd, 13.5, 7.5 2.65, dd, 13.5, 7.5	2.53, dd, 13.2, 7.5 2.65, dd, 13.2, 7.5	2.55, dd, 13.6, 7.2 2.62, dd, 13.6, 7.2	4.57, d, 7.1	4.50, d, 7.1
2′	4.87, tsept, 7.5, 1.5	4.88, br t, 7.5	5.00, br t, 7.2	5.56, br t, 7.1	5.51, br t, 7.1
4′	1.52, s	1.54, s	1.65, s	1.74, s	1.74, s
5′	1.55, s	1.57, s	1.76, s	1.80, s	1.80, s
1″	2.51, dd, 13.5, 7.5 2.65, dd, 13.5, 7.5	2.53, dd, 13.2, 7.5 2.65, dd, 13.2, 7.5	2.55, dd, 13.6, 7.2 2.62, dd, 13.6, 7.2	3.25, d, 7.2	3.37, d, 7.0
2″	4.87, tsept, 7.5, 1.5	4.88, br t, 7.5	5.00, br t, 7.2	5.22, br t, 7.2	5.27, br t, 7.0
4″	1.52, s	1.54, s	1.60, s	1.62, s	1.62, s
5″	1.55, s	1.57, s	1.62, s	1.74, s	1.74, s
OH	/	/	/	14.4, s	14.6, s

[a] overlapping with signals of water

S9

77

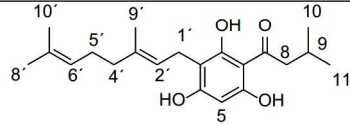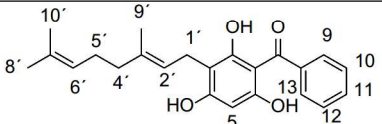**Table S4.** ^{1}H-NMR data of the enzyme products **1G1**, **2G1**, and **3G1** in CDCl$_3$, 400 MHz
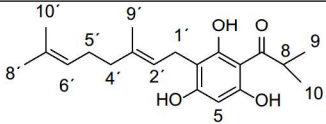
Comp	**1G1**	**2G1**	**3G1**
Pos.	δ_H, J in Hz	δ_H, J in Hz	δ_H, J in Hz
5	5.83, s	5.82, s	5.94, s
8	3.86, sept, 6.8	2.93, d, 6.7	/
9	1.17, d, 6.8	2.25, m	7.65, dt, 7.2, 1.2
10	1.17, d, 6.8	0.97, d, 6.7	7.52, br t, 7.2
11	/	0.97, d, 6.7	7.59, tt, 7.2, 1.2
12	/	/	7.52, br t, 7.2
13	/	/	7.65, dt, 7.2, 1.2
1′	3.38, d, 7.1	3.37, d, 7.1	3.38, d, 7.1
2′	5.25, br t, 7.1	5.25, br t, 7.1	5.27, br t, 7.1
4′	2.10, m	2.11, m	2.08, m
5′	2.10, m	2.11, m	2.08, m
6′	5.05, br t, 7.0	5.04, br t, 7.1	5.04, br t 7.1
8′	1.81, s	1.81, s	1.80, s
9′	1.67, s	1.68, s	1.66, s
10′	1.59, s	1.60, s	1.59, s

S10

Table S5. ^{1}H-NMR data of the enzyme products **1G2**, **2G2**, and **3G2** in CDCl₃, 500 MHz
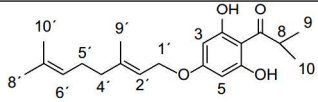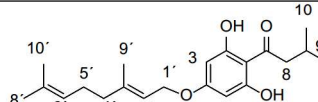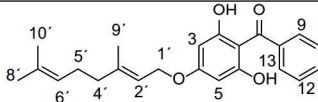
Comp	1G2	2G2	3G2
Pos.	δ_H, J in Hz	δ_H, J in Hz	δ_H, J in Hz
3	5.93, s	5.92, s	6.04, s
5	5.93, s	5.92, s	6.04, s
8	3.85, sept, 6.8	2.92, d, 6.7	/
9	1.17, d, 6.8	2.24, m	7.65, dt, 7.1, 1.4
10	1.17, d, 6.8	0.97, d, 6.7	7.54, br t, 7.1
11	/	0.97, d, 6.7	7.59, tt, 7.1, 1.4
12	/	/	7.54, br t, 7.1
13	/	/	7.65, dt, 7.1, 1.4
1´	4.52, d, 6.9	4.52, d, 6.9	4.56, d, 7.1
2´	5.43, br t, 6.9	5.43, br t, 6.9	5.46, br t, 7.1
4´	2.09, m	2.10, m	2.10, m
5´	2.09, m	2.10, m	2.10, m
6´	5.08, br t, 6.8	5.08, br t, 6.8	5.09, br t, 7.1
8´	1.72, s	1.72, s	1.74, s
9´	1.68, s	1.68, s	1.68, s
10´	1.60, s	1.60, s	1.61, s

S11

Table S6. ^{1}H-NMR data of the enzyme products **1F1**, **2F1**, and **3F1** in acetone-D6, 500 MHz
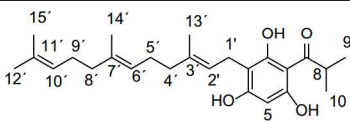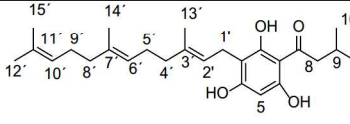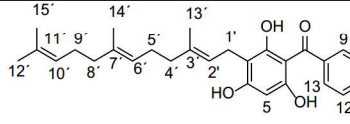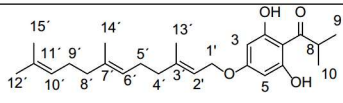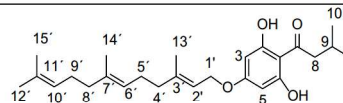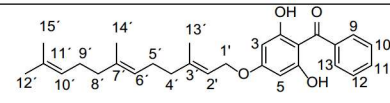
Comp	**1F1**	**2F1**	**3F1**
Pos.	δ_H, J in Hz	δ_H, J in Hz	δ_H, J in Hz
5	6.06, s	6.05, s	6.04, s
8	3.98, sept, 6.8	2.94, d, 6.7	/
9	1.13, d, 6.8	2.24, m	7.59, dt, 7.2, 1.4
10	1.13, d, 6.8	0.95, d, 6.7	7.40, br t, 7.2
11	/	0.95, d, 6.7	7.47, tt, 7.4, 1.4
12	/	/	7.40, br t, 7.2
13	/	/	7.59, dt, 7.2, 1.4
1′	3.25, d, 7.2	3.25, d, 7.2	3.31, d, 7.2
2′	5.25, br t, 7.2	5.25, br t, 7.2	5.30, br t, 7.2
4′	2.08, m	2.08, m	2.09, m
5′	2.08, m	2.08, m	2.09, m
6′	5.10, br t, 7.1	5.10, br t, 7.2	5.12, br t, 7.2
8′	1.93, m	1.97, m	1.97, m
9′	1.93, m	1.97, m	1.97, m
10′	5.07, br t, 7.1	5.07, br t, 7.2	5.08, br t, 7.2
12′	1.76, s	1.76, s	1.78, s
13′	1.64, s	1.64, s	1.64, s
14′	1.57, s	1.56, s	1.57, s
15′	1.57, s	1.56, s	1.57, s

S12

80

Table S7. ^{1}H-NMR data of the enzyme products **1F2**, **2F2**, and **3F2** in acetone-D$_6$, 500 MHz

Comp	**1F2**	**2F2**	**3F2**
Pos.	δ_H, J in Hz	δ_H, J in Hz	δ_H, J in Hz
3	5.97, s	5.99, s	6.04, s
5	5.97, s	5.99, s	6.04, s
8	3.95, sept, 6.8	2.96, d, 6.7	/
9	1.11, d, 6.8	2.24, m	7.63, dt, 7.4, 1.4
10	1.11, d, 6.8	0.95, d, 6.7	7.42, br t, 7.4
11	/	0.95, d, 6.7	7.50, tt, 7.4, 1.4
12	/	/	7.42, br t, 7.4
13	/	/	7.63, dt, 7.4, 1.4
1′	4.57, d, 6.5	4.59, d, 6.6	4.63, d, 6.5
2′	5.41, br t, 6.5	5.43, br t, 6.6	5.46, br t, 6.5
4′	2.09, m	2.13, m	2.14, m
5′	2.09, m	2.13, m	2.14, m
6′	5.11, br t, 6.7	5.14, br t, 7.0	5.15, br t, 6.7
8′	1.94, m	1.97, s	1.98, m
9′	1.94, m	1.97, s	1.98, m
10′	5.06, br t, 6.9	5.09, br t, 7.0	5.10, br t, 6.9
12′	1.73, s	1.76, s	1.78, s
13′	1.62, s	1.65, s	1.65, s
14′	1.58, s	1.61, s	1.62, s
15′	1.55, s	1.58, s	1.58, s

S13

V. Table of kinetic parameters

Table S8. Kinetic parameters of AtaPT toward **1**, **2**, **3**, DMAPP, and GPP

Prenyl donor	Prenyl acceptor	AtaPT Protein amount and incubation time	K_M [mM]	k_{cat} [s^{-1}]	k_{cat}/K_M [s^{-1}M^{-1}]	AnaPT[a] k_{cat}/K_M [s^{-1}M^{-1}]
		Kinetic parameters of acceptors				
DMAPP	1	15μg, 20min	0.16 ± 0.006	0.284 ± 0.002	1775.0	54.5
	2	15μg , 90min	1.10 ± 0.035	0.103 ± 0.002	96.5	51.5
	3	15μg , 90min	0.58 ± 0.064	0.106 ± 0.005	182.8	62.5
GPP	1	15μg , 45min	1.27 ± 0.14	0.227 ± 0.001	178.7	/
	2	15μg, 30min	0.75 ± 0.008	0.197 ± 0.05	262.7	/
	3	15μg , 30min	0.47 ± 0.013	0.137 ± 0.0002	291.5	/
FPP	1	50μg, 90min	0.38 ± 0.027	0.014 ± 0.0003	36.8	/
	2	50μg, 90min	0.42 ± 0.04	0.012 ± 0.0007	28.6	/
	3	50μg , 90min	0.70 ± 0.12	0.012 ± 0.0007	17.1	/
		Kinetic parameters of donors				
DMAPP	1	15μg, 20min	0.071 ± 0.0007	0.270 ± 0.0016	3816.9	40.0
GPP	3	15μg, 30min	0.46 ± 0.003	0.126 ± 0.0004	273.9	/

[a] Data adopted from Zhou, K.; Ludwig, L.; Li, S.-M. *J. Nat. Prod.* **2015**, *78*, 929

VI. Figure of SDS-PAGE
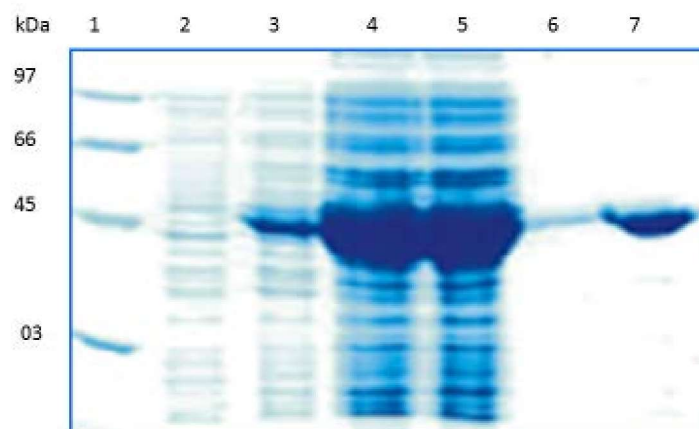
Figure S1. Monitoring of overproduction and purification of AtaPT. The proteins were separated on a 12 % polyacrylamide gel and stained with Coomassie brilliant blue R-250.

Lanes: 1, protein marker; 2, soluble fraction before induction; 3, soluble fraction after induction with 0.5 mM Isopropyl-β-D-thiogalactopyranoside at 37 °C for 6 h; 4, soluble protein fraction after centrifugation; 5, flow fraction; 6, washing fraction; 7, elution fraction.

VII. Graphical representation of the ion dependence of the AtaPT reaction
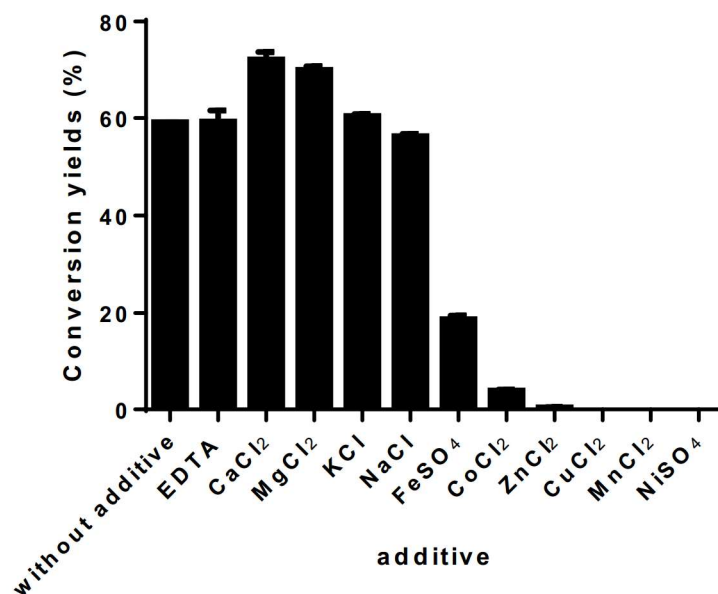
Figure S2. Dependence of the AtaPT reaction on the presence of ions. The reaction mixtures contained (100 µL) 50 µg of AtaPT-His$_6$, 5 mM of additives, 2 mM of DMAPP, 1 mM of **1** and were incubated at 37 °C for 2 h.

VIII. Figures for HPLC analysis of enzyme activities
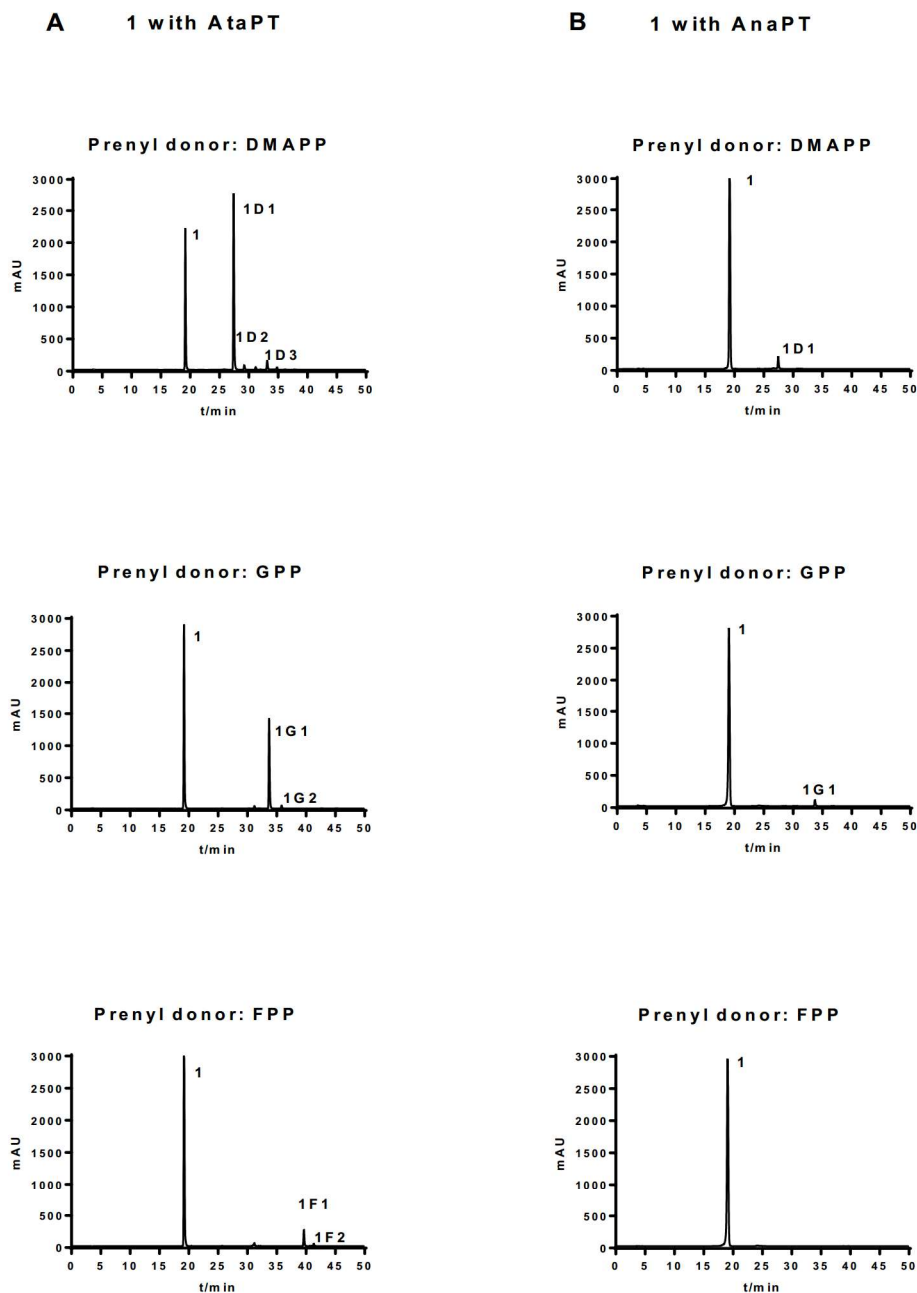
Figure S3. HPLC analysis of the reaction mixtures of **1** with AtaPT and AnaPT. The enzyme assays (100 μL) contained 1 mM of **1**, 5 mM of $CaCl_2$, 2 mM of DMAPP, GPP or FPP, 1.0−6.0% of glycerol (v/v), 5% of DMSO, (v/v), and 20 μg of the purified recombinant protein in 50 mM Tris-HCl, pH 7.5. The reaction mixtures were incubated at 37 °C for 2 h and detected with a diode assay detector. The absorption at 291 nm was used for illustration of the reaction with **1**.
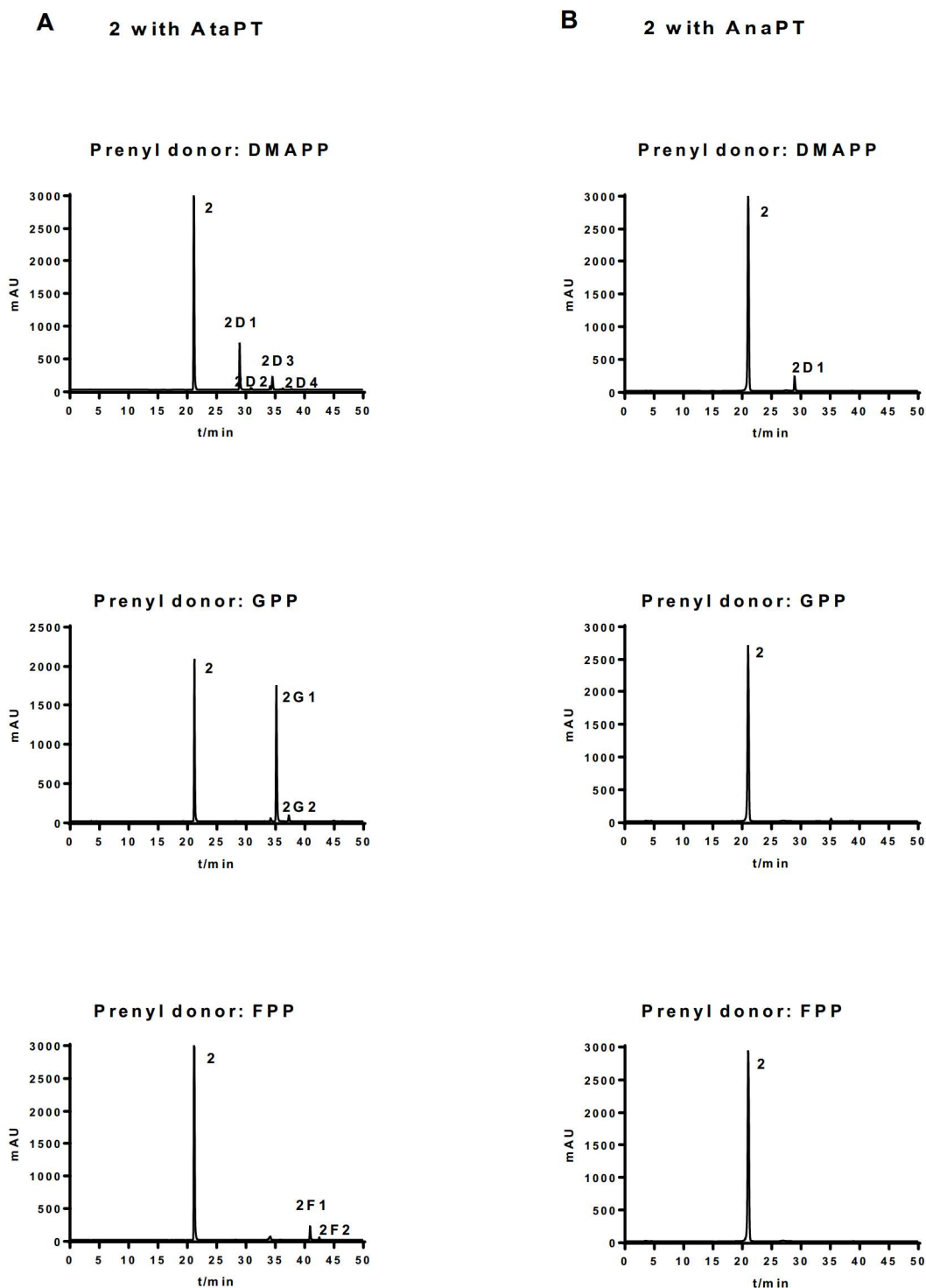
**Figure S4**. HPLC analysis of the reaction mixtures of **2** with AtaPT and AnaPT.

The enzyme assays (100 μL) contained 1 mM of **2**, 5 mM of $CaCl_2$, 2 mM of DMAPP, GPP or FPP, 1.0−6.0% of glycerol (v/v), 5% of DMSO (v/v), and 20 μg of the purified recombinant protein in 50 mM Tris-HCl, pH 7.5. The reaction mixtures were incubated at 37 °C for 2 h and detected with a diode assay detector. The absorption at 291 nm was used for illustration of the reaction with **2**.

A **3 with AtaPT**
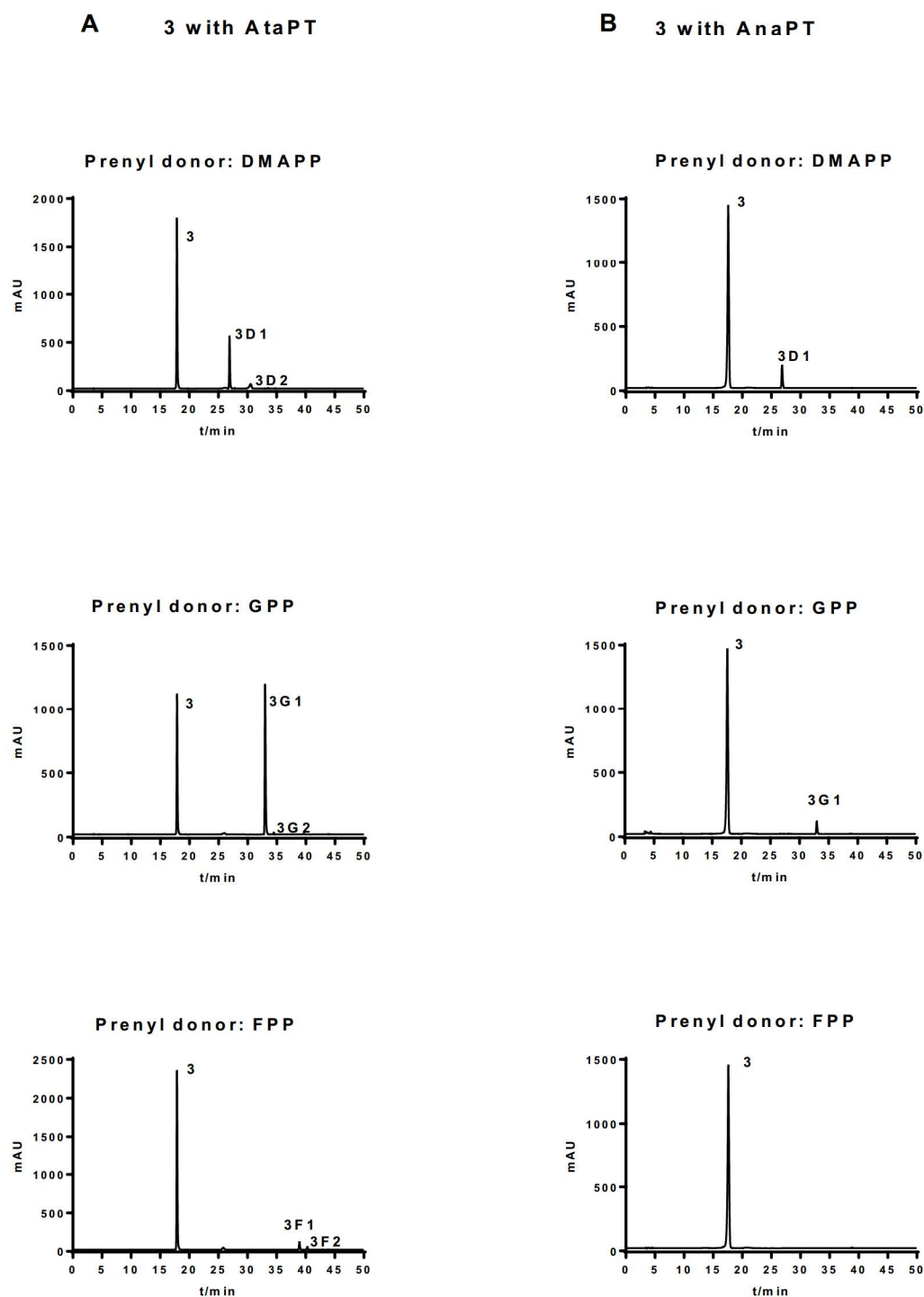
B **3 with AnaPT**

Figure S5. HPLC analysis of the reaction mixtures of **3** with AtaPT and AnaPT. T

The enzyme assays (100 μL) contained 1 mM of **3**, 5 mM of $CaCl_2$, 2 mM of DMAPP, GPP or FPP, 1.0−6.0% of glycerol (v/v), 5% of DMSO (v/v), and 20 μg of the purified recombinant protein in 50 mM Tris-HCl, pH 7.5. The reaction mixtures were incubated at 37 °C for 2 h and detected with a diode assay detector. The absorption at 306 nm was used for illustration of the reaction with **3**.
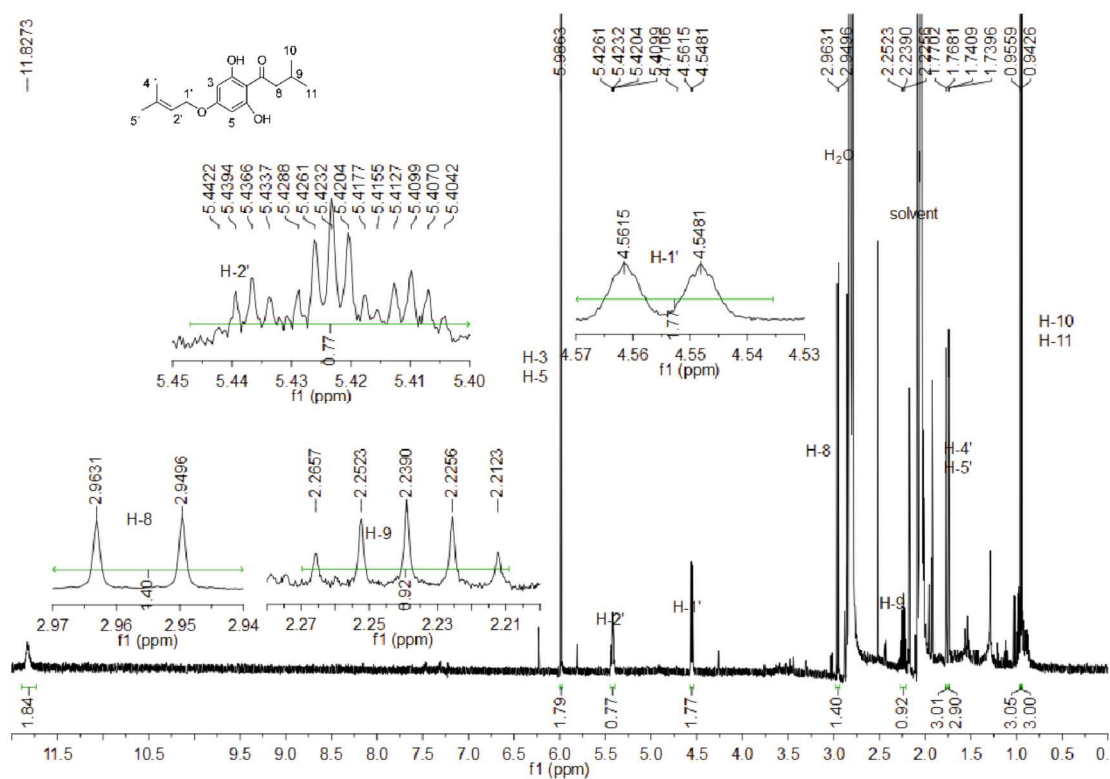
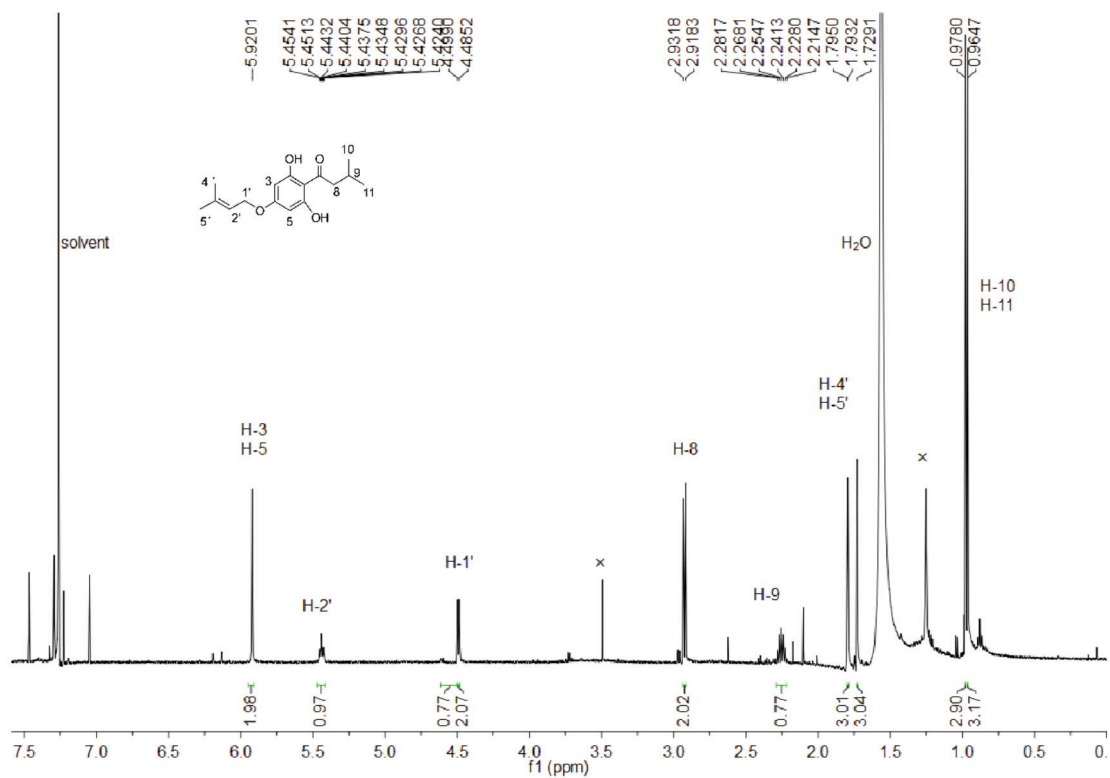# IX. Figures of NMR spectrum
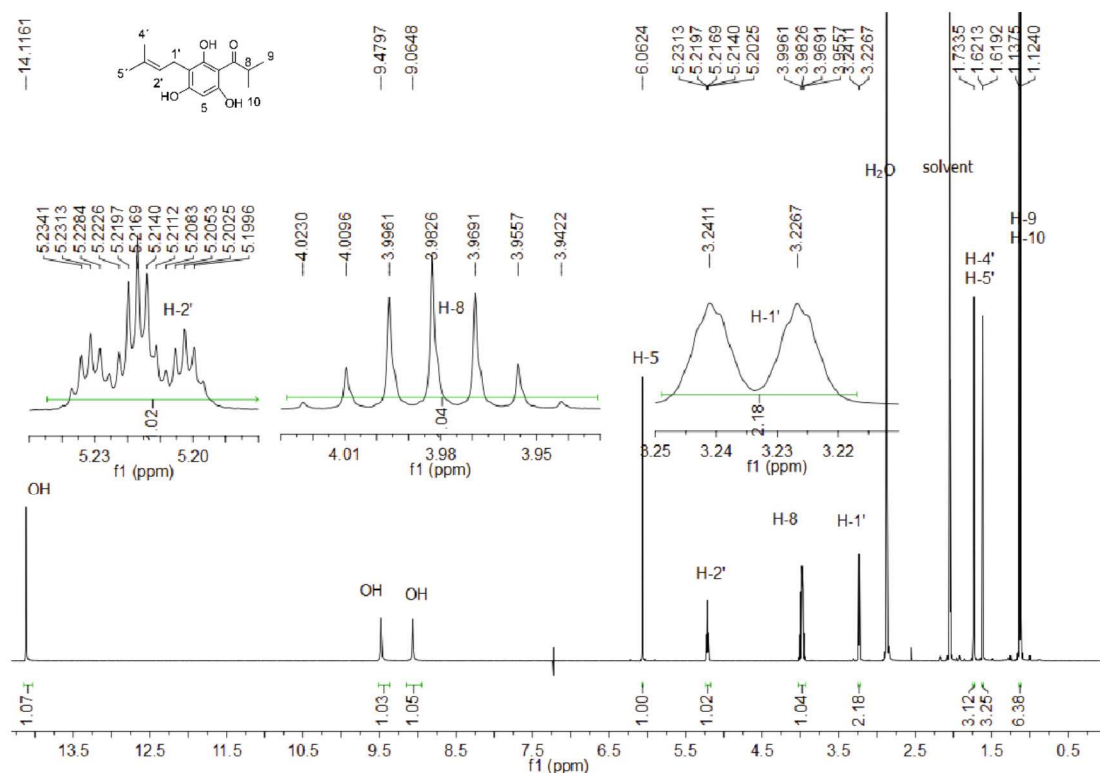
Figure S6. ^{1}H-NMR spectrum of **1D1** in acetone-D$_6$, 500 MHz.
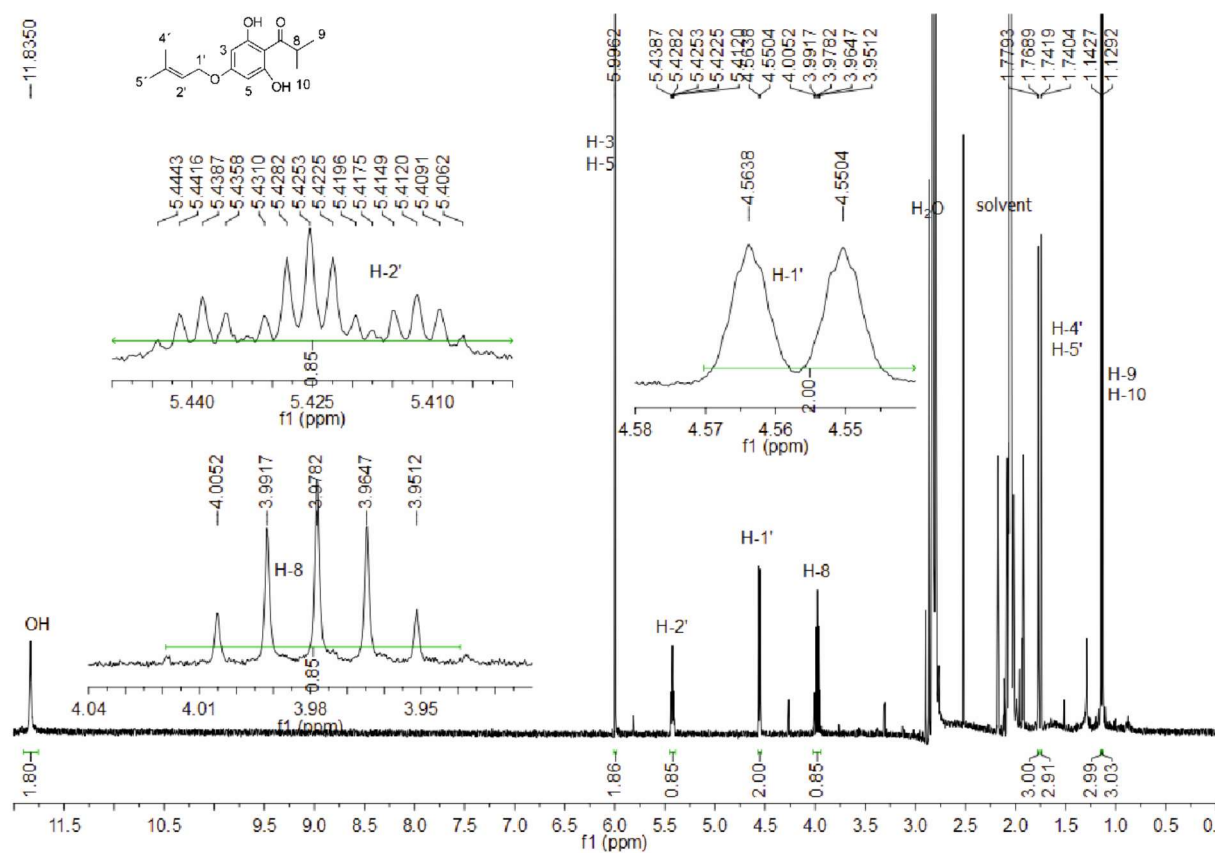
Figure S7. ^{1}H-NMR spectrum of **1D2** in acetone-D$_6$, 500 MHz.
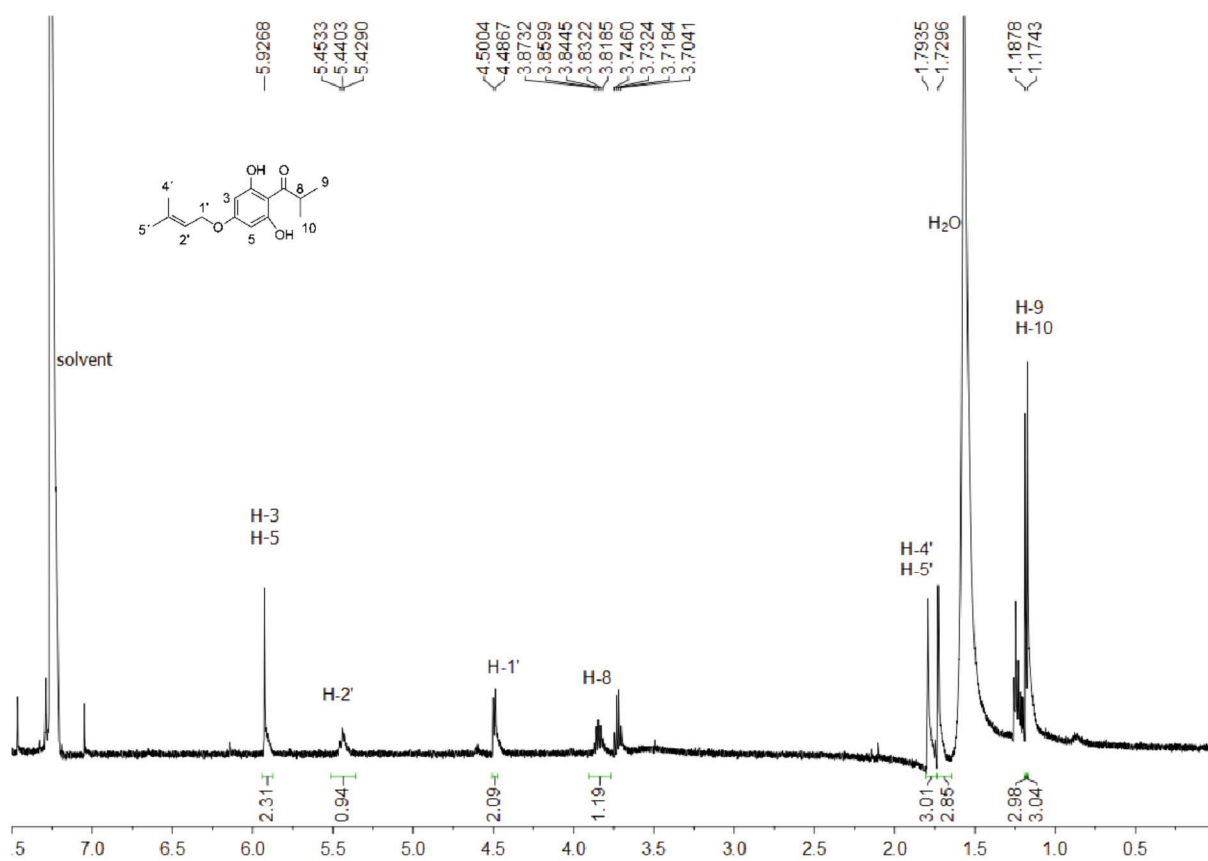
Figure S8. ^{1}H-NMR spectrum of **1D2** in CDCl$_3$, 500 MHz.
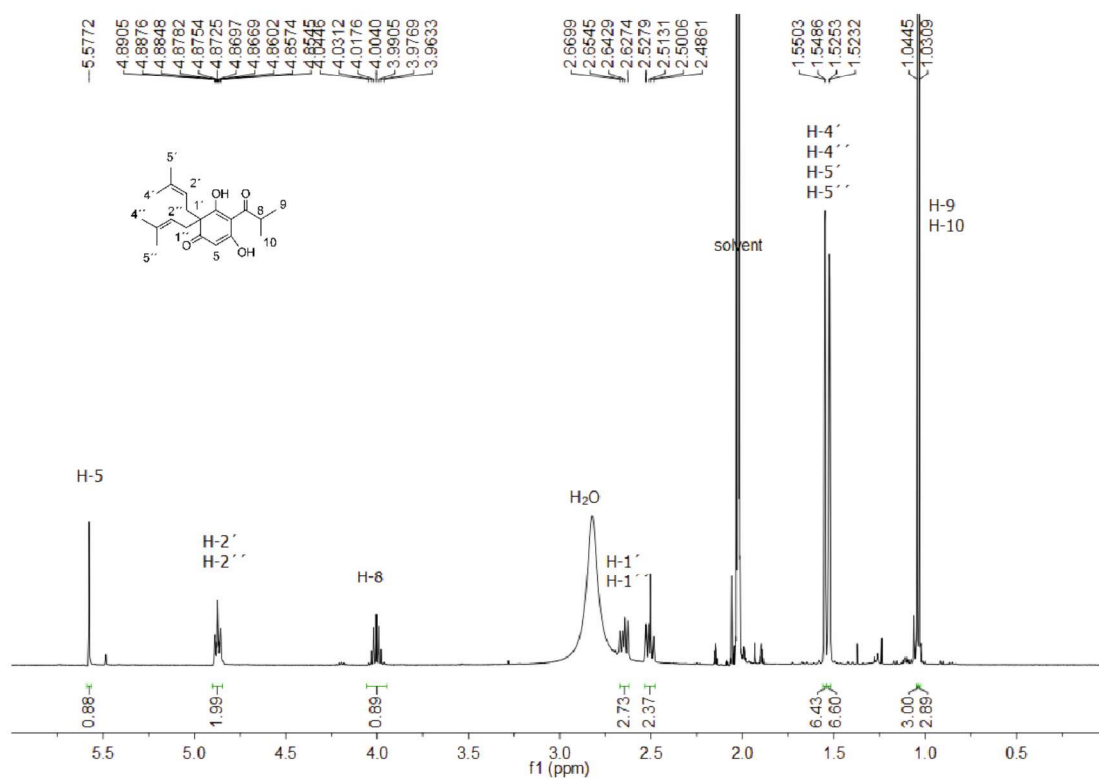
Figure S9. ^{1}H-NMR spectrum of **1D3** in acetone-D$_6$, 500 MHz.
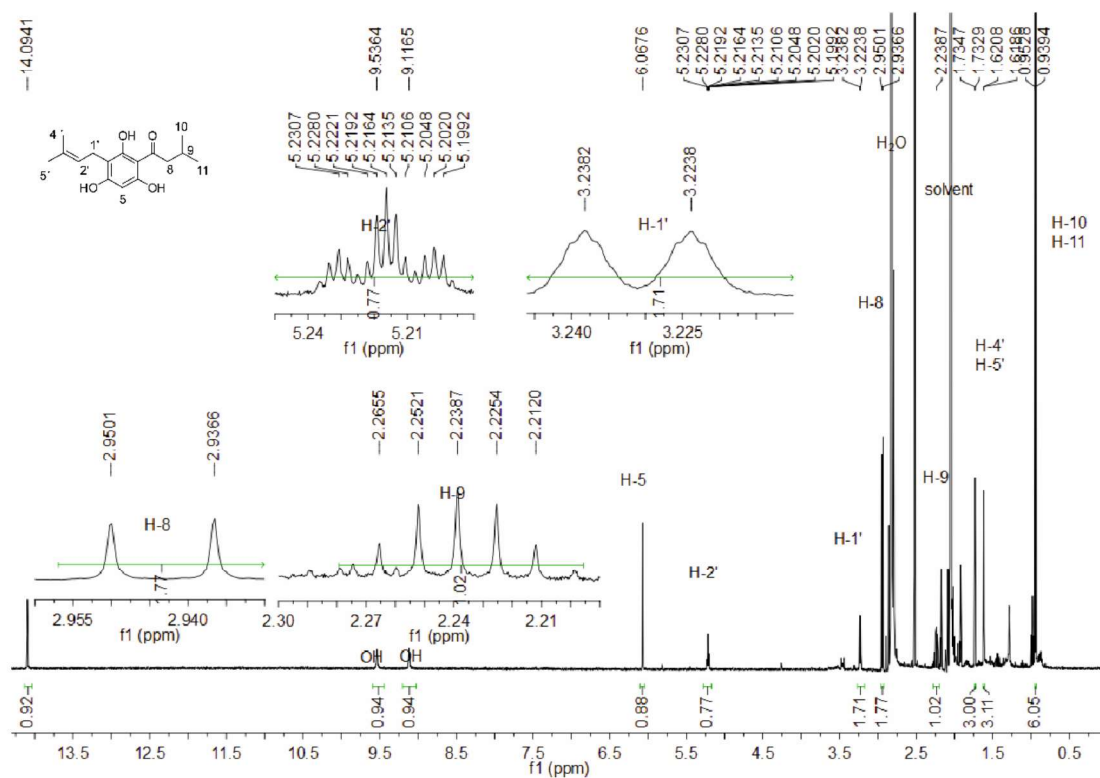
Figure S10. ^{1}H-NMR spectrum of **2D1** in acetone-D$_6$, 500 MHz.

Figure S11. ^{1}H-NMR spectrum of **2D2** in acetone-D$_6$, 500 MHz.

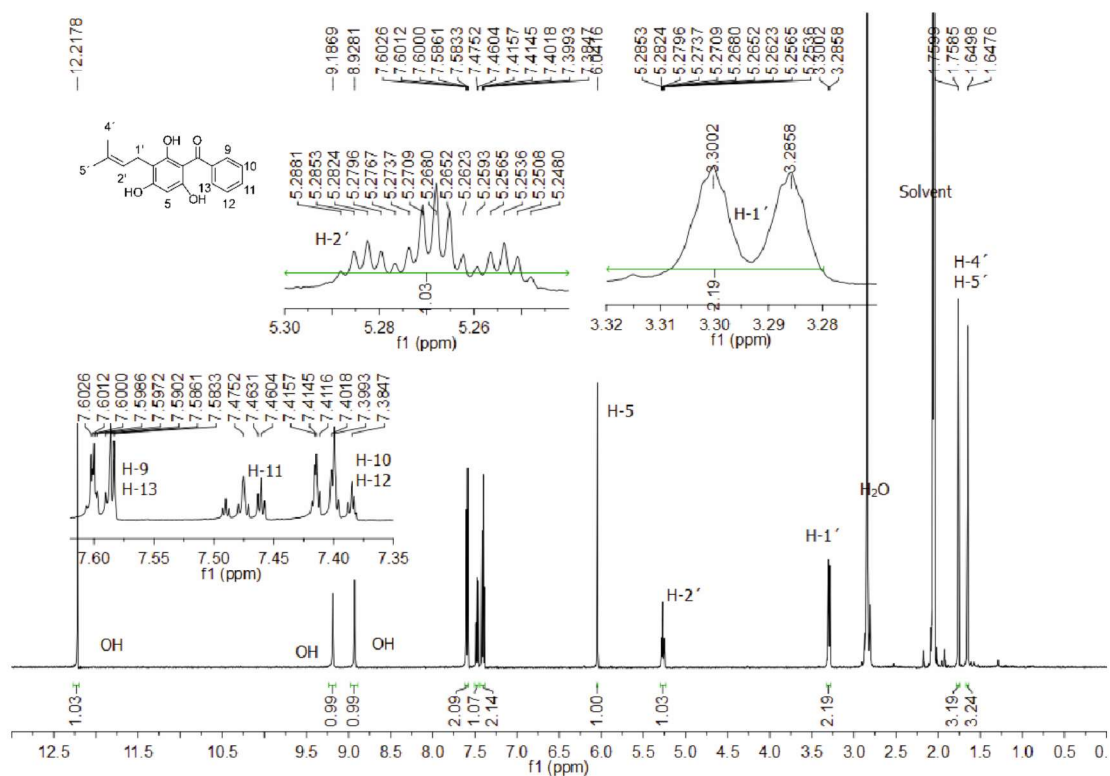**Figure S12**. ^{1}H-NMR spectrum of **2D2** in CDCl$_3$, 500 MHz.

Figure S13. ^{1}H-NMR spectrum of **2D3** in acetone-D$_6$, 500 MHz.

S23
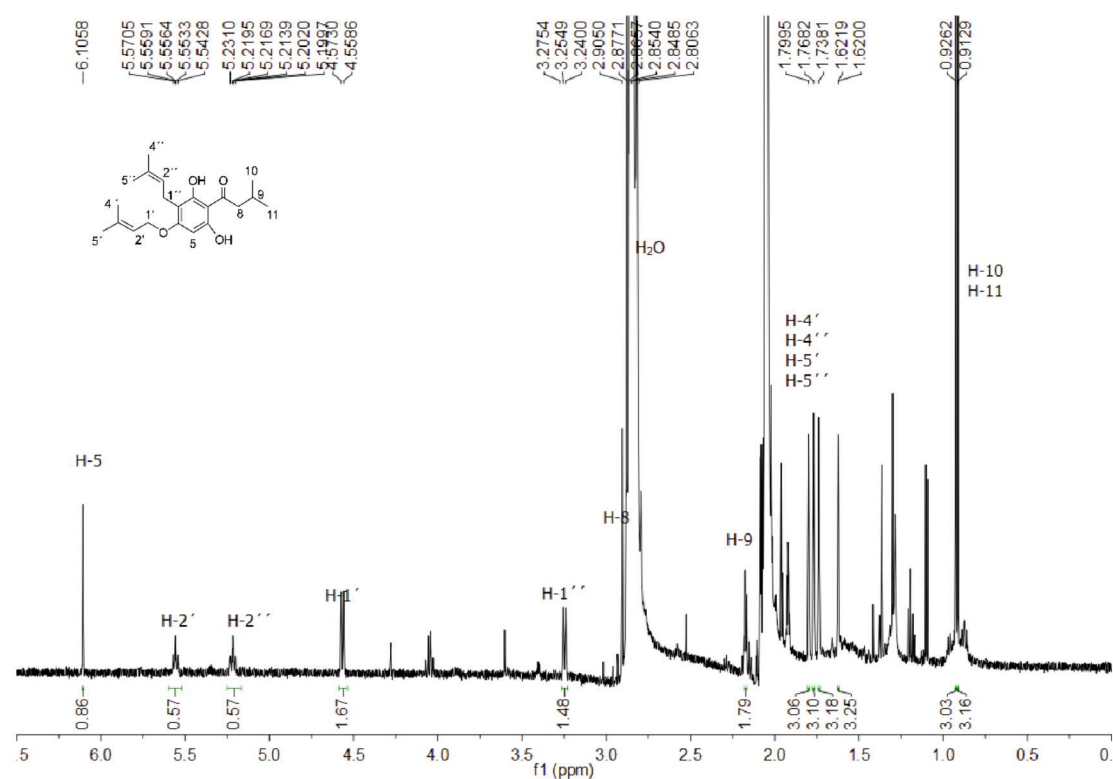
Figure S14. ^{1}H-NMR spectrum of **2D4** in acetone-D$_6$, 500 MHz.
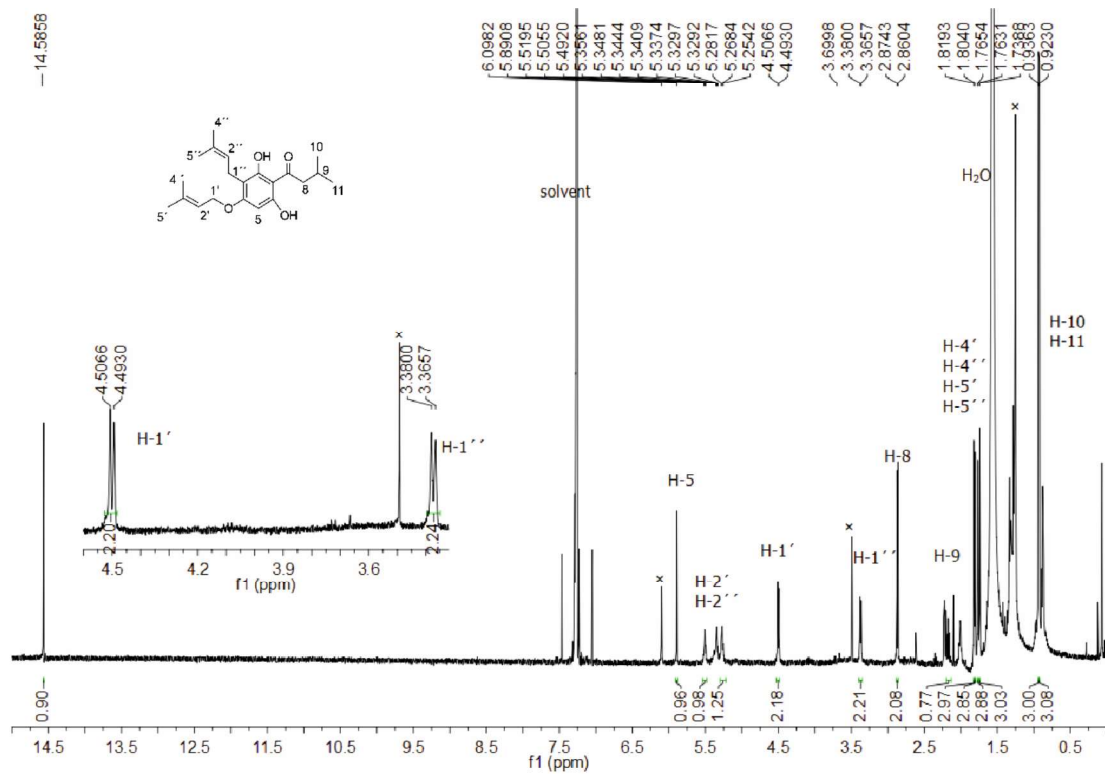
Figure S15. ^{1}H-NMR spectrum of **2D4** in CDCl$_3$, 500 MHz.

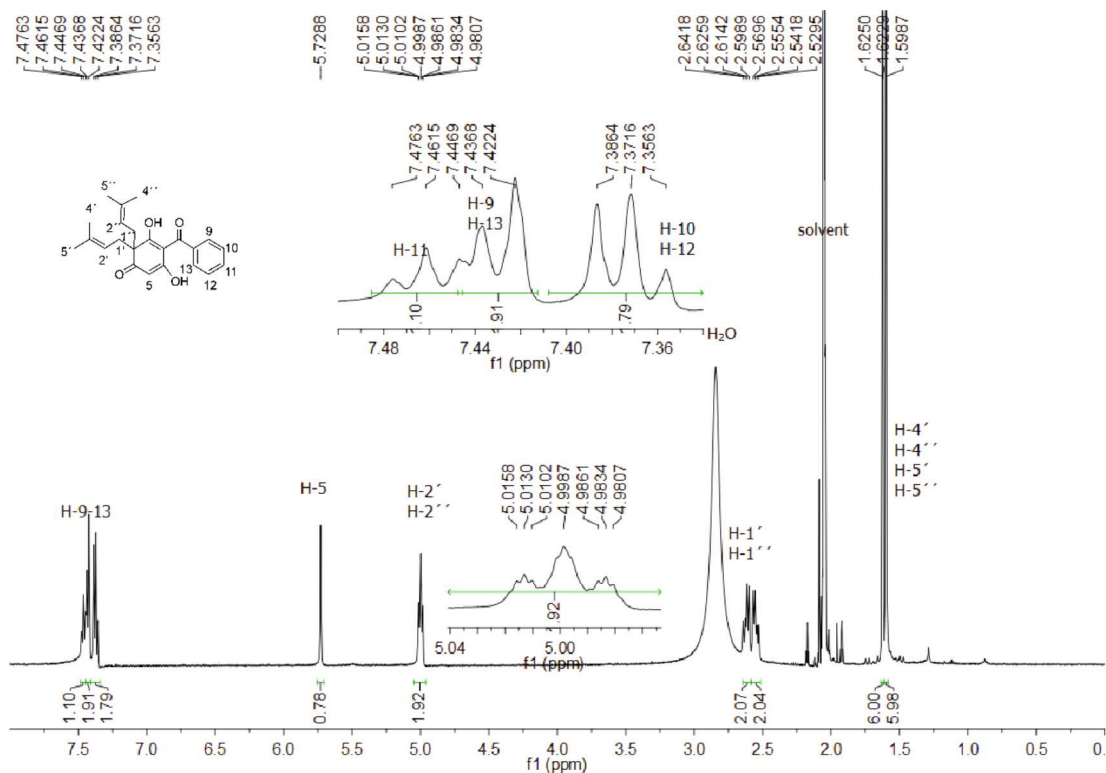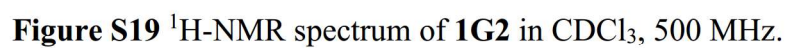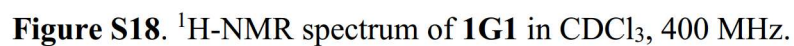**Figure S16.** ^{1}H-NMR spectrum of **3D1** in acetone-D6, 500 MHz.

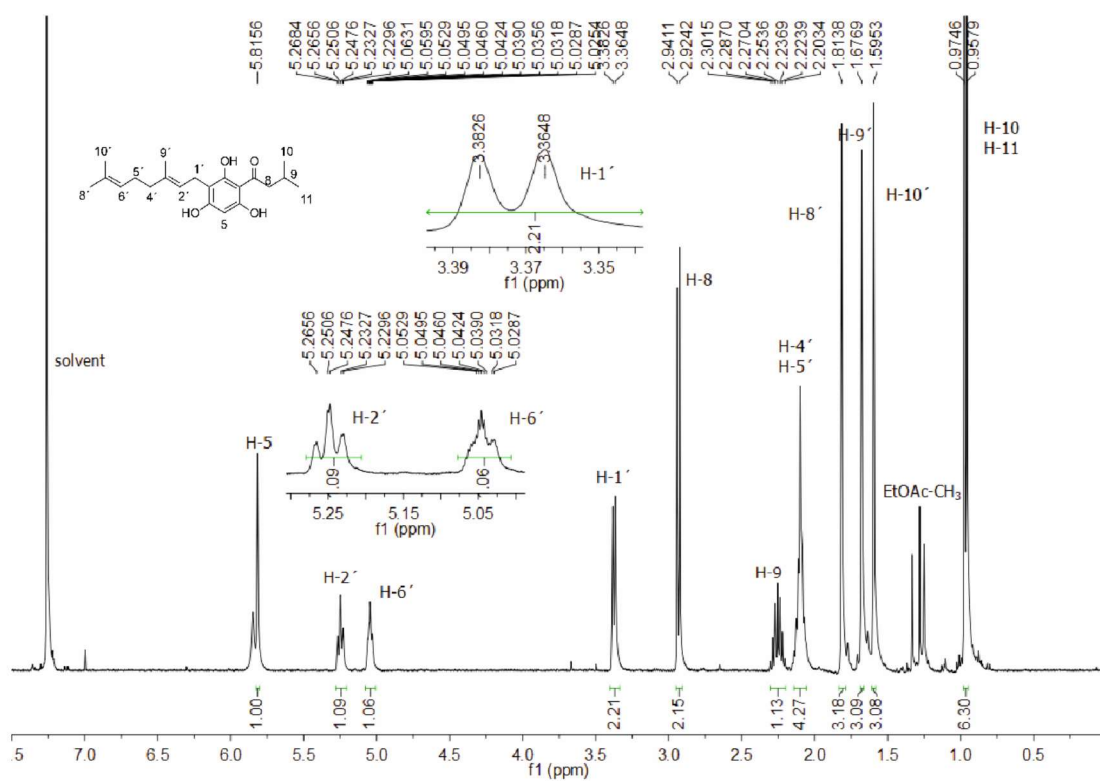**Figure S17**. ^{1}H-NMR spectrum of **3D3** in acetone-D6, 500 MHz.

Figure S18. ^{1}H-NMR spectrum of **1G1** in CDCl$_3$, 400 MHz.

Figure S19 ^{1}H-NMR spectrum of **1G2** in CDCl$_3$, 500 MHz.

Figure S20. ^{1}H-NMR spectrum of **2G1** in CDCl$_3$, 400 MHz.
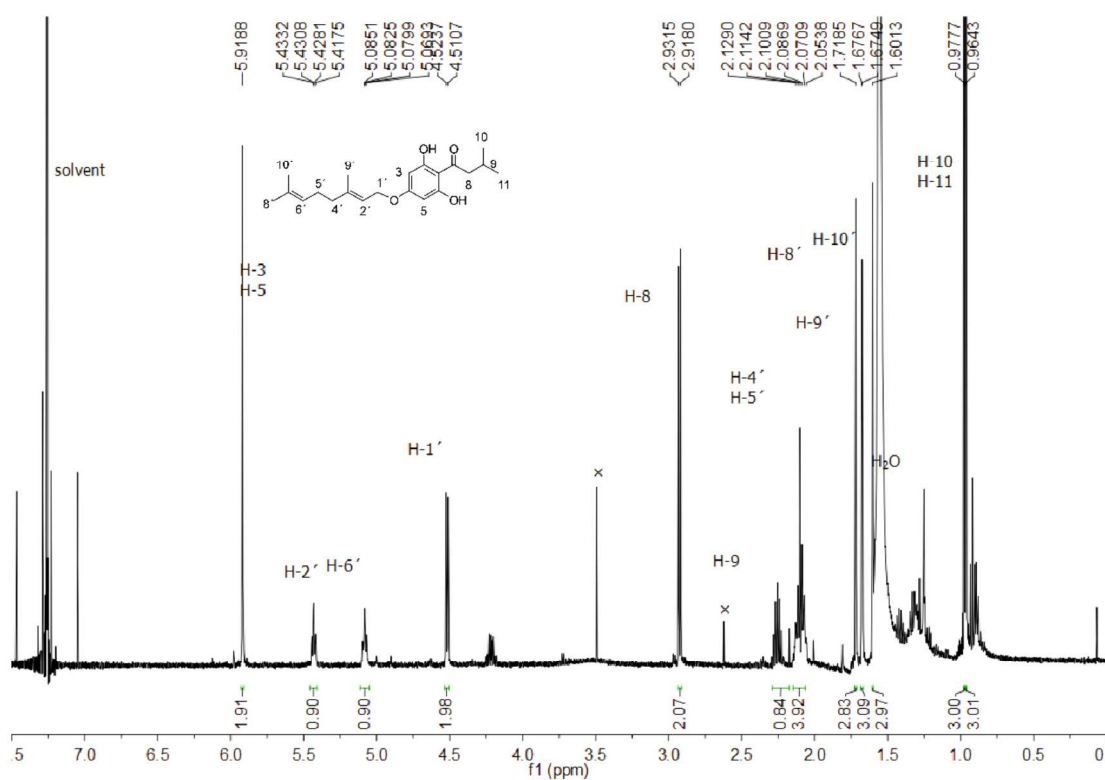

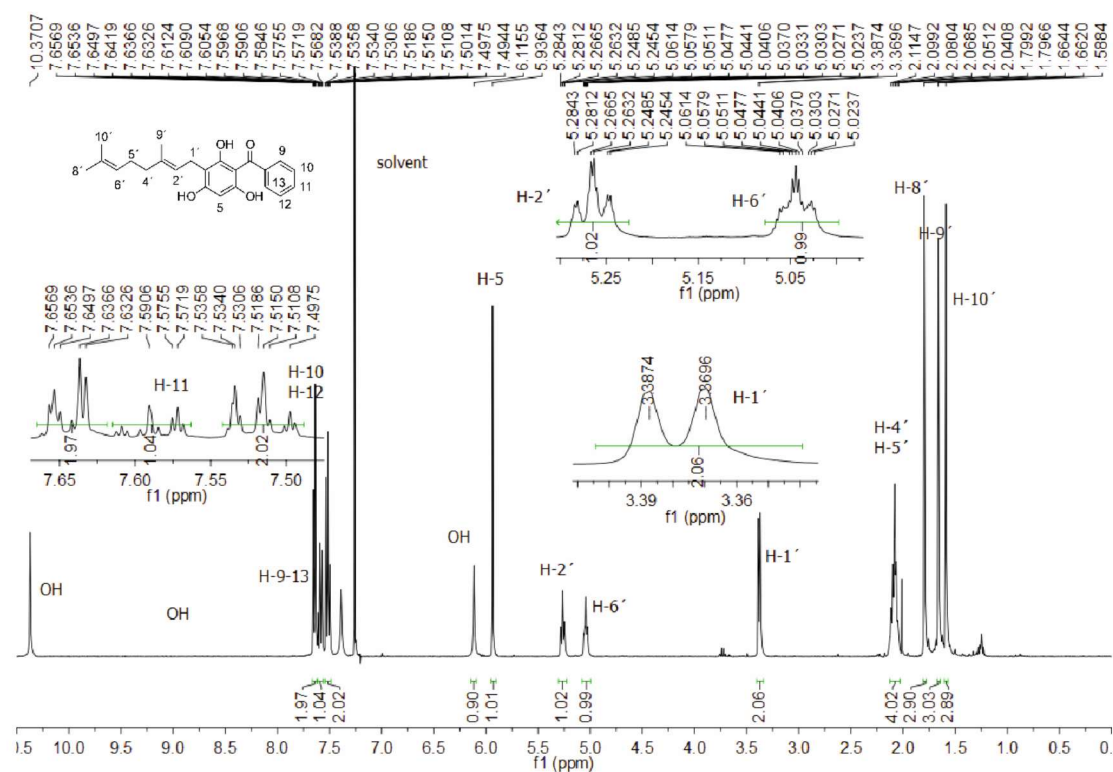**Figure S21**. ^{1}H-NMR spectrum of **2G2** in CDCl$_3$, 500 MHz.

Figure S22. ^{1}H-NMR spectrum of **3G1** in CDCl$_3$, 400 MHz.
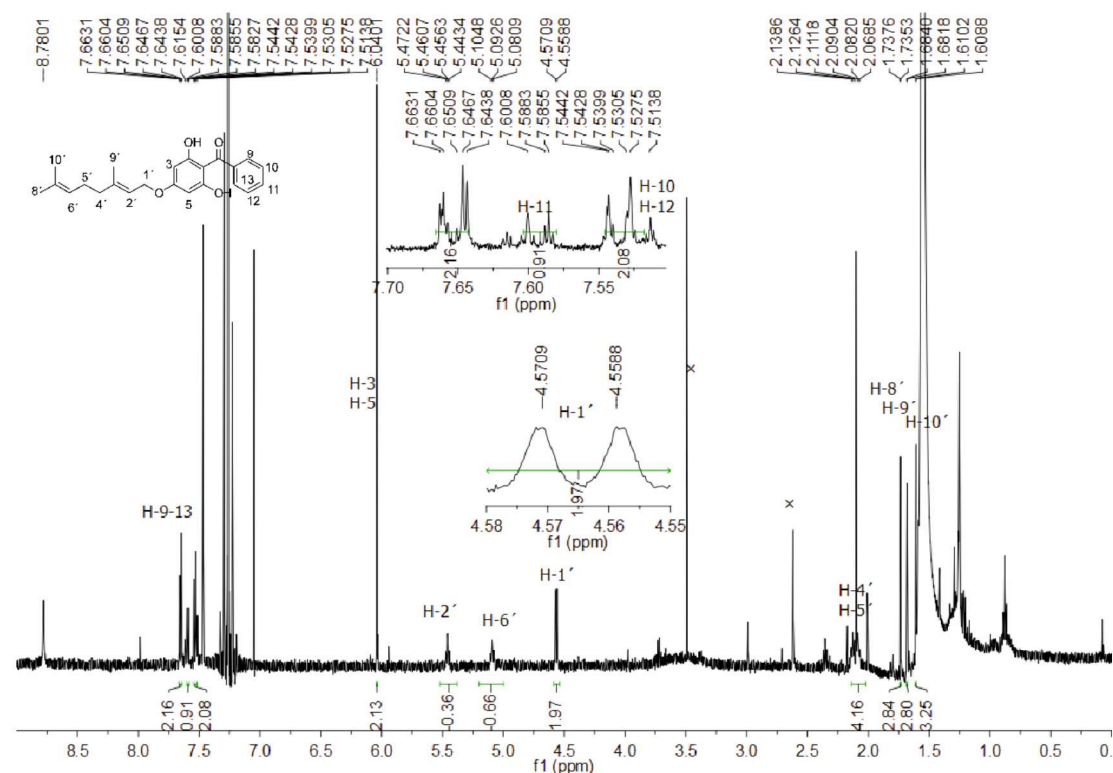

Figure S23. ^{1}H-NMR spectrum of **3G2** in CDCl$_3$, 500 MHz.

Figure S24. ^{1}H-NMR spectrum of **1F1** in acetone-D$_6$, 500 MHz.

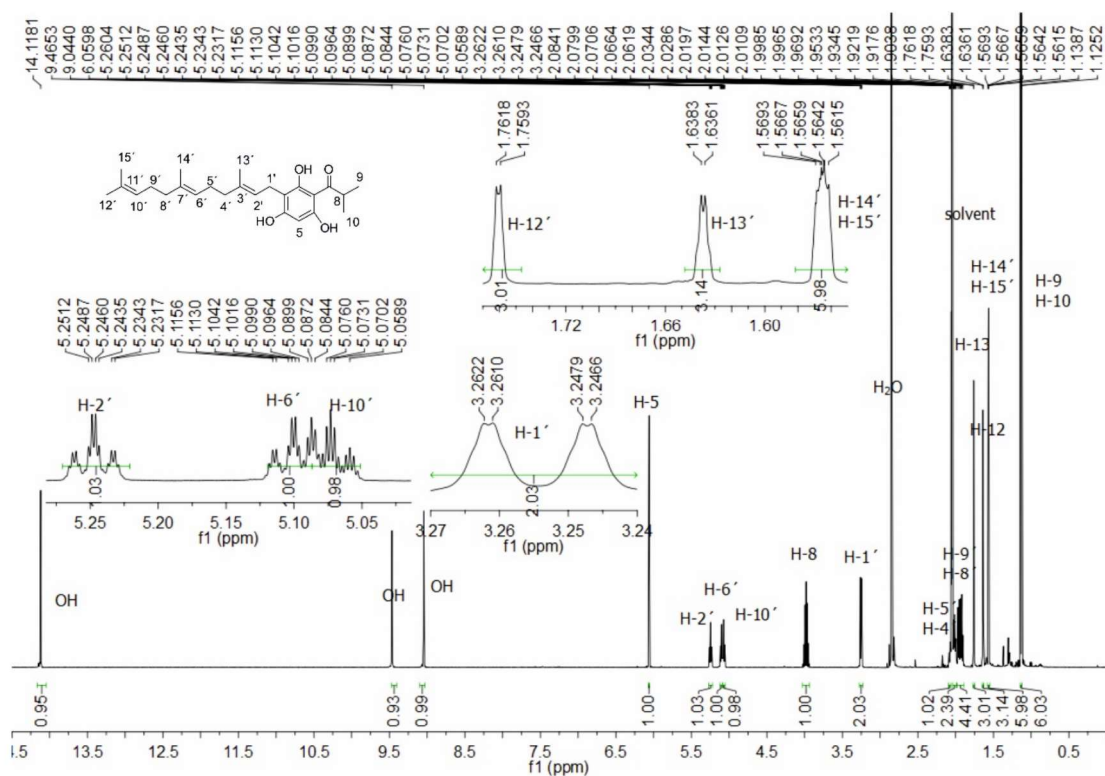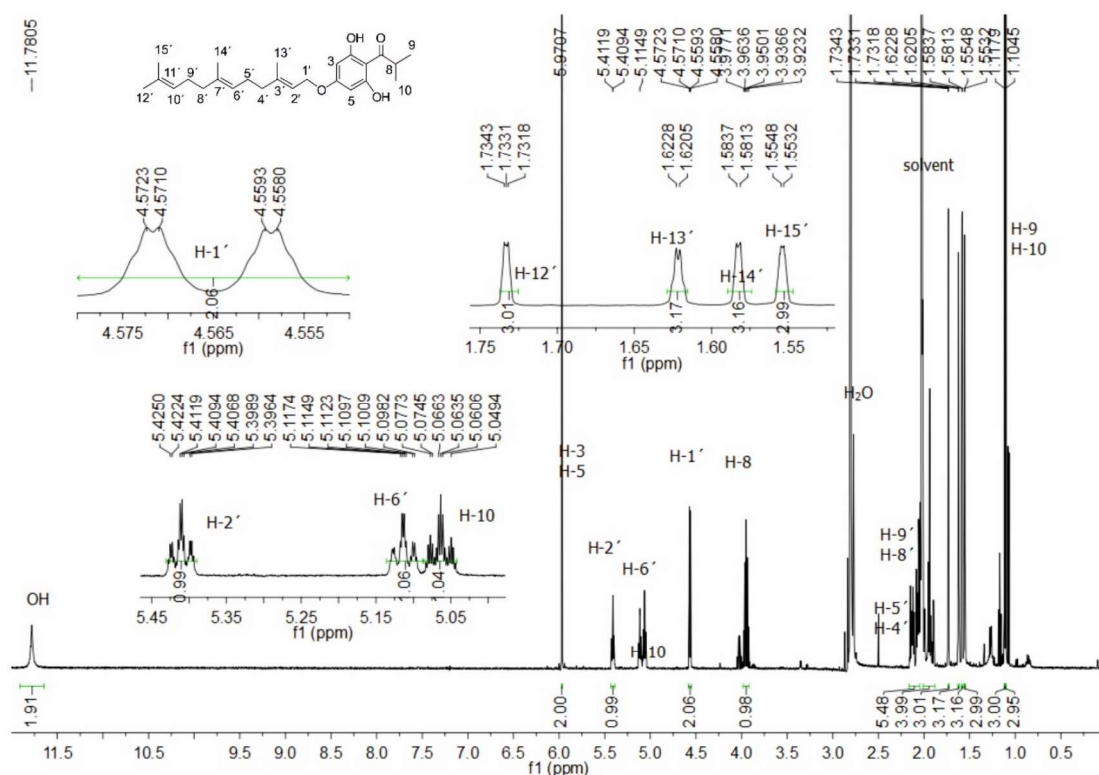**Figure S25**. ^{1}H-NMR spectrum of **1F2** in acetone-D$_6$, 500 MHz.

Figure S26. ^{1}H-NMR spectrum of **2F1** in acetone-D$_6$, 500 MHz.
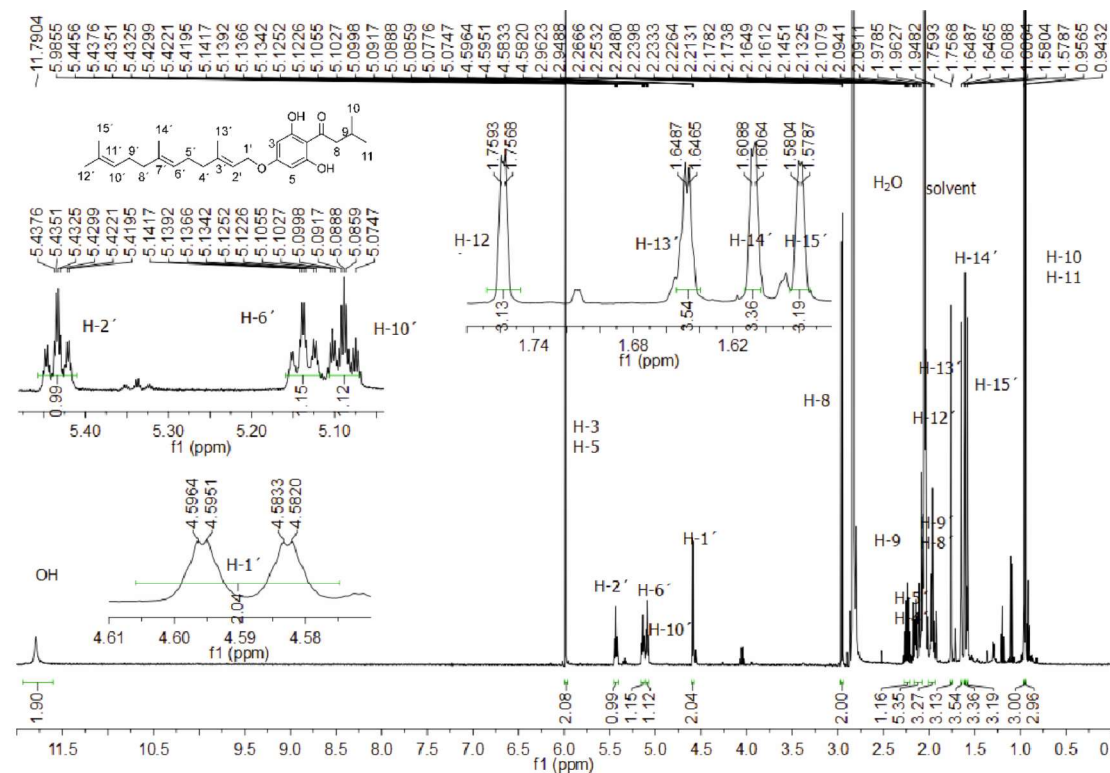
Figure S27. ^{1}H-NMR spectrum of **2F2** in acetone-D$_6$, 500 MHz.
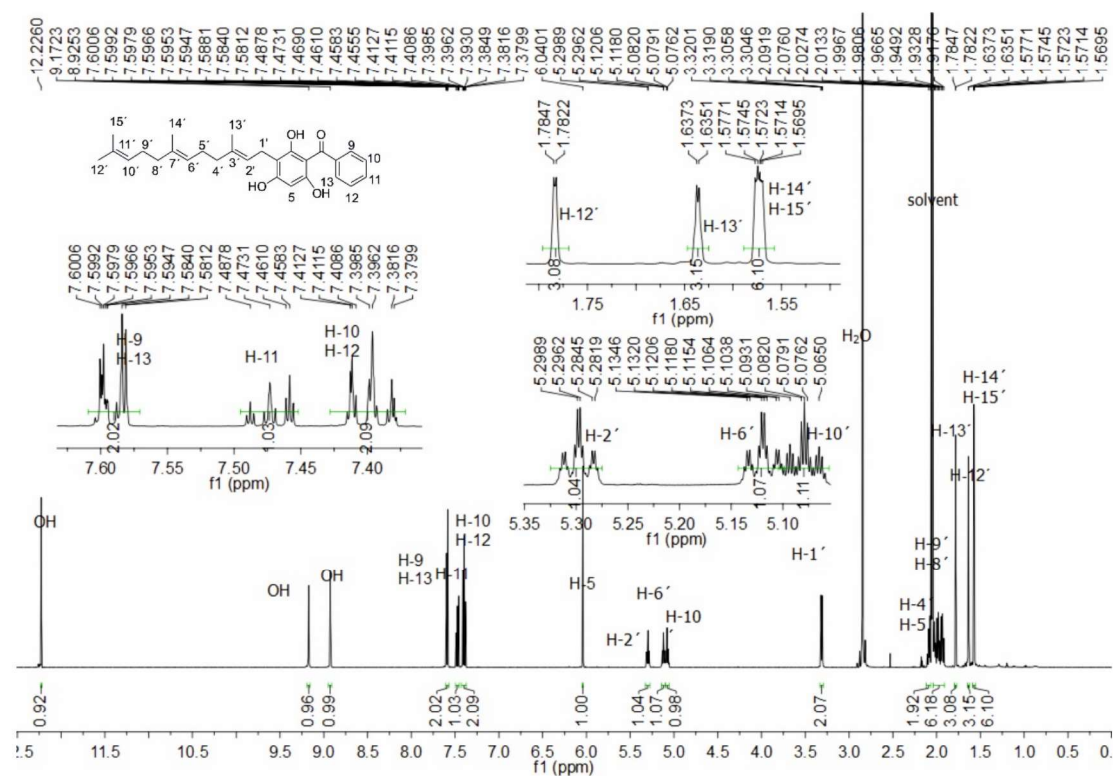
Figure S28. ^{1}H-NMR spectrum of **3F1** in acetone-D6, 500 MHz.

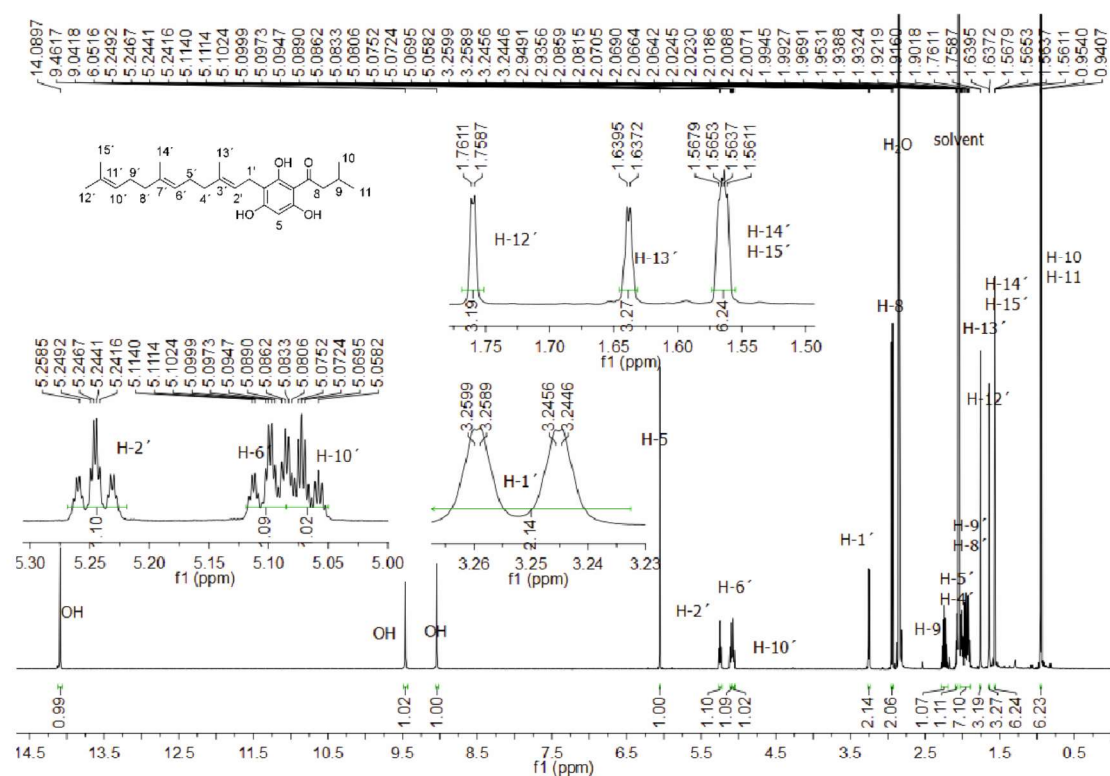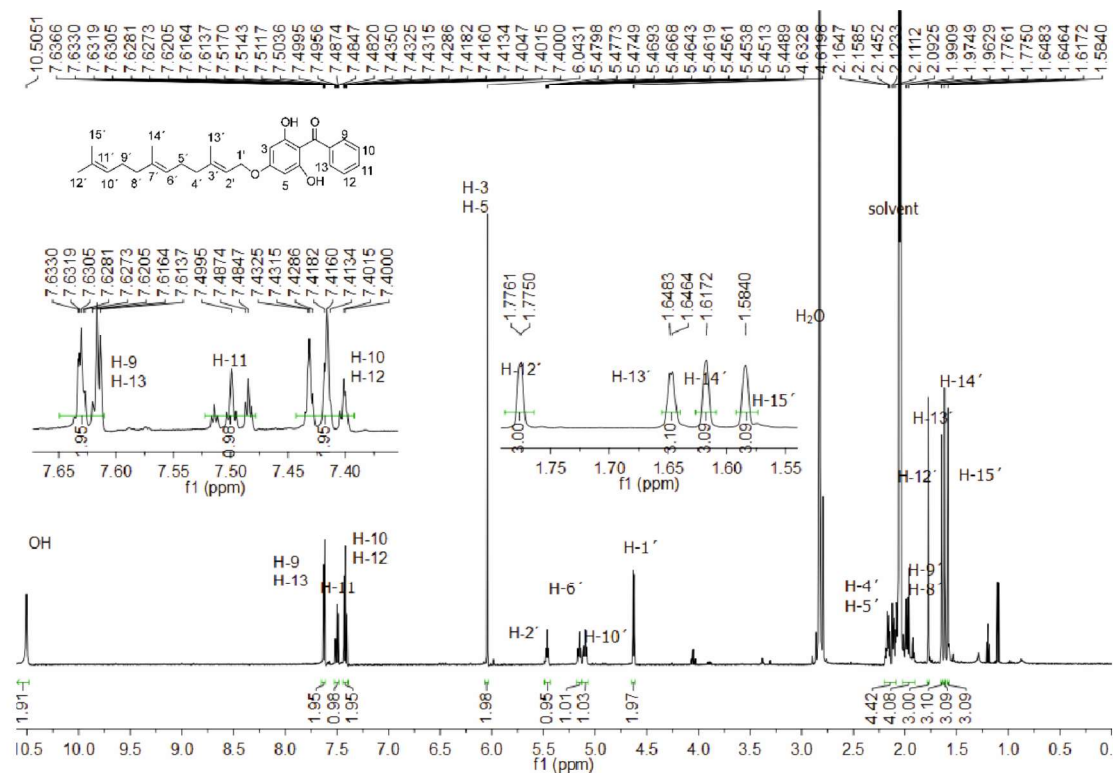**Figure S29.** ^{1}H-NMR spectrum of **3F2** in acetone-D6, 500 MHz.

X. Dependence of product formation of AtaPT reactions on incubation time.
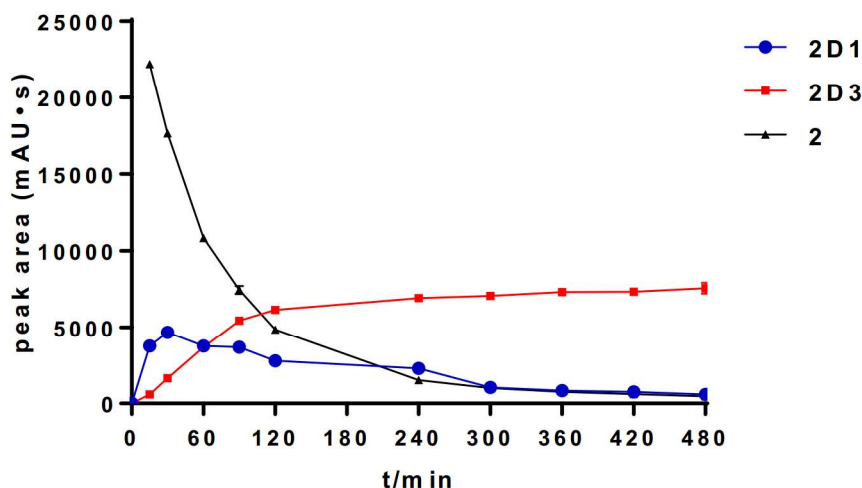
Figure S30. Time dependence of the product formation of AtaPT reaction with **2** and DMAPP.

The enzyme assays (100 μL) contained 0.5 mM of **2**, 5 mM of $CaCl_2$, 2 mM of DMAPP, 1.2% of glycerol, 5% of DMSO, and 50 μg of the purified recombinant protein in 50 mM Tris-HCl, pH 7.5.
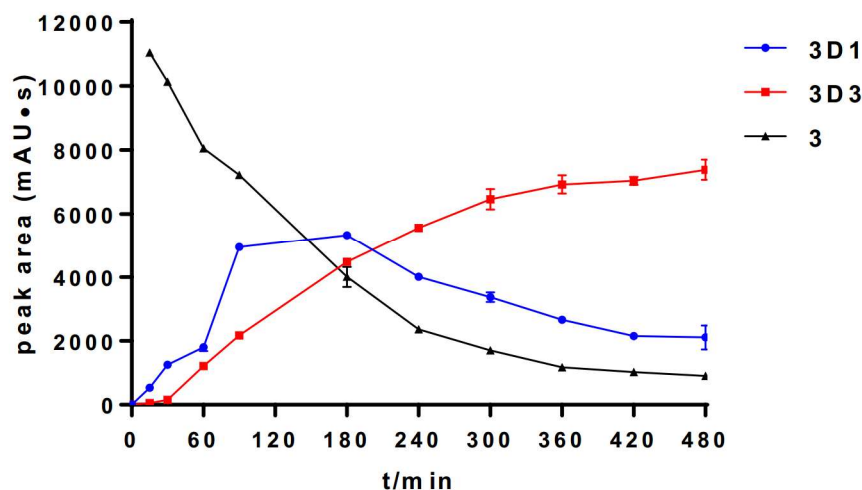
Figure S31. Time dependence of the product formation of AtaPT reaction with **3** and DMAPP.

The enzyme assays (100 μL) contained 0.5 mM of **3**, 5 mM of $CaCl_2$, 2 mM of DMAPP, 1.2% of glycerol, 5% of DMSO, and 50 μg of the purified recombinant protein in 50 mM Tris-HCl, pH 7.5.

XI. Figures of kinetic parameters
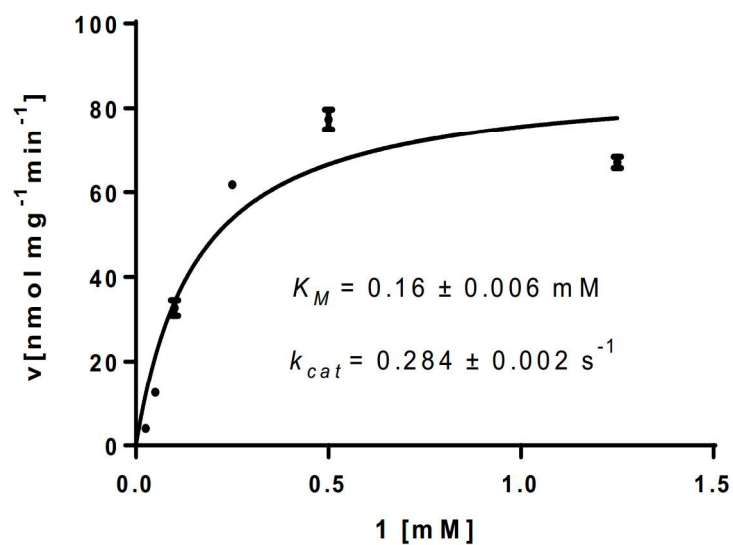
Figure S32. Determination of the kinetic parameters of the AtaPT reaction toward **1** in the presence of DMAPP.
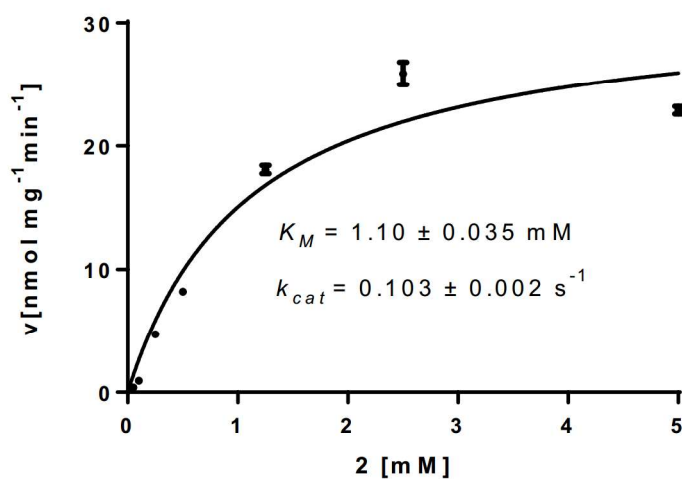
Figure S33. Determination of the kinetic parameters of the AtaPT reaction toward **2** in the presence of DMAPP.

Figure S34. Determination of the kinetic parameters of the AtaPT reaction toward **3** in the presence of DMAPP.

Figure S35. Determination of the kinetic parameters of the AtaPT reaction toward **1** in the presence of GPP.

Figure S36. Determination of the kinetic parameters of the AtaPT reaction toward **2** in the presence of GPP.

Figure S37. Determination of the kinetic parameters of the AtaPT reaction toward **3** in the presence of GPP.

S35

Figure S38. Determination of the kinetic parameters of the AtaPT reaction toward **1** in the presence of FPP.

Figure S39. Determination of the kinetic parameters of the AtaPT reaction toward **2** in the presence of FPP.

Figure S40. Determination of the kinetic parameters of the AtaPT reaction toward **3** in the presence of FPP.

Figure S41. Determination of the kinetic parameters of the AtaPT reaction toward DMAPP with **1** as prenyl acceptor.
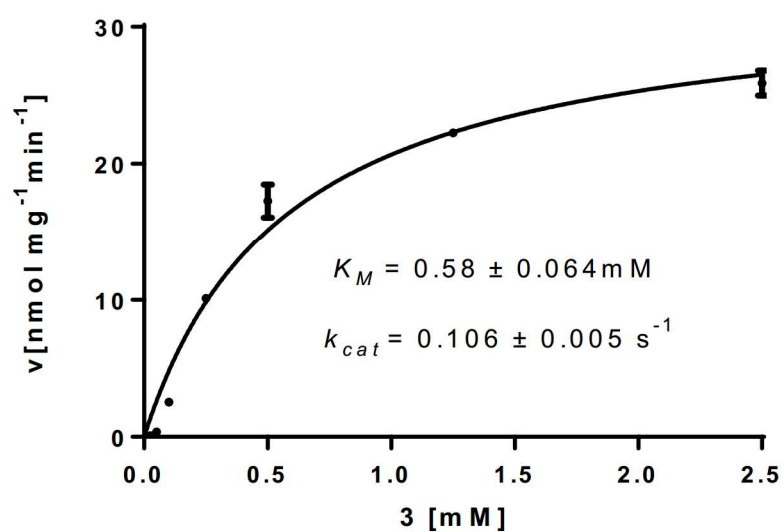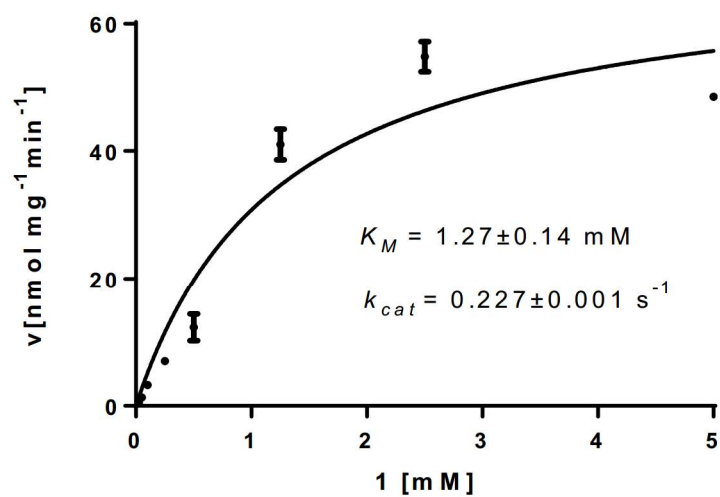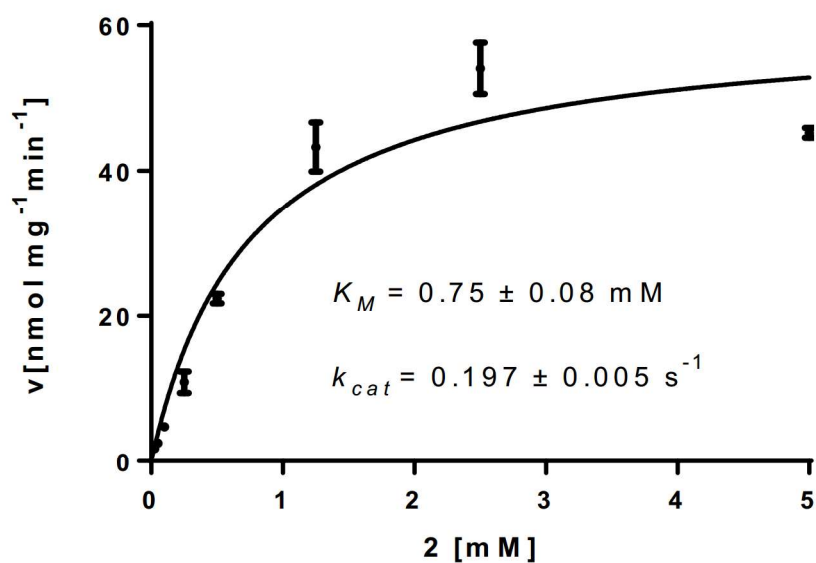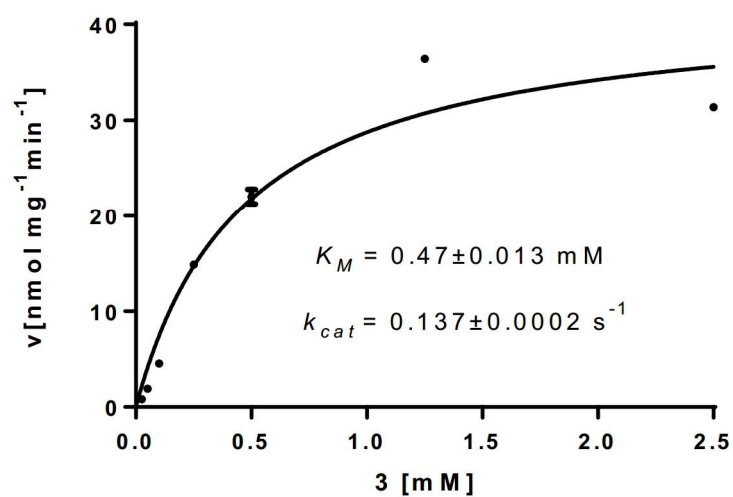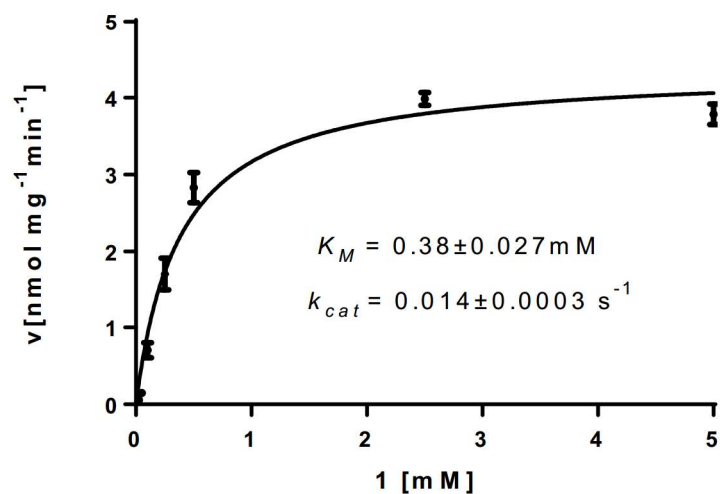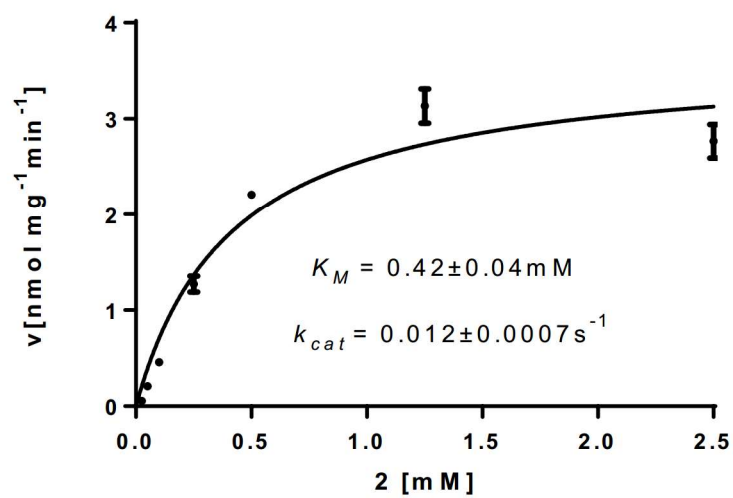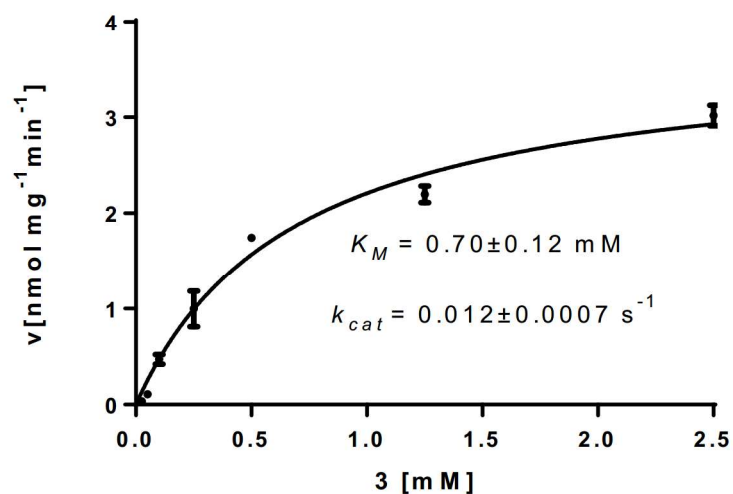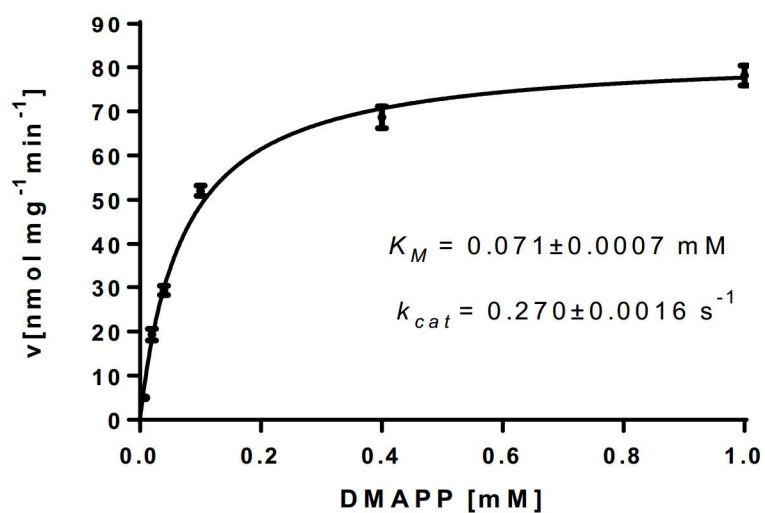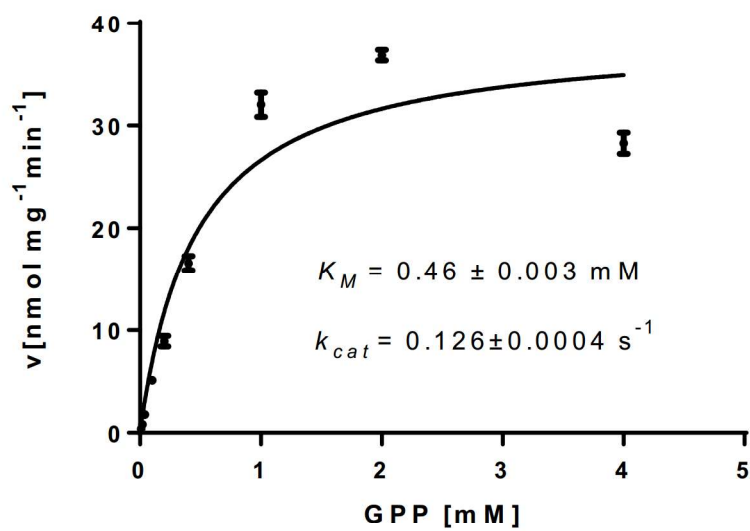
Figure S42. Determination of the kinetic parameters of the AtaPT reaction toward GPP with **3** as prenyl acceptor.

4.3. Complementary flavonoid prenylations by fungal indole prenyltransferases

# Complementary Flavonoid Prenylations by Fungal Indole Prenyltransferases

Kang Zhou,[†] Xia Yu,[†,‡] Xiulan Xie,[§] and Shu-Ming Li*,[†]

[†]Institut für Pharmazeutische Biologie und Biotechnologie, Philipps-Universität Marburg, Marburg 35037, Germany
[§]Fachbereich Chemie, Philipps-Universität Marburg, Marburg 35032, Germany

Ⓢ *Supporting Information*

ABSTRACT: Flavonoids are found mainly in plants and exhibit diverse biological and pharmacological activities, which can often be enhanced by prenylations. In plants, such reactions are catalyzed by membrane-bound prenyltransferases. In this study, the prenylation of nine flavonoids from different classes by a soluble fungal prenyltransferase (AnaPT) involved in the biosynthesis of the prenylated indole alkaloid acetylaszonalenin is demonstrated. The behavior of AnaPT toward flavonoids regarding substrate acceptance and prenylation positions clearly differs from that of the indole prenyltransferase 7-DMATS. The two enzymes are therefore complementary in flavonoid prenylations.
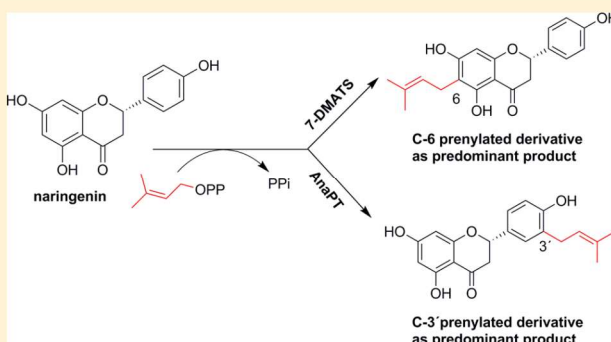
Flavonoids are valuable natural products widely distributed in the plant kingdom. On the basis of their structures, they are categorized into dihydrochalcones, chalcones, flavanones, dihydroflavonols, flavones, flavonols, isoflavones, isoflavonols, pterocarpans, coumestans, aurones, neoflavonoids, and anthocyanidins.[1,2] Flavonoids have been shown to have a wide range of biological and pharmacological activities in in vitro studies, including anti-inflammatory, antibacterial, antiviral, antiallergic, cytotoxic, and antitumor activities.[3] They are also considered potential candidates for the treatment of neurodegenerative and vasodilatory diseases.[2] Prenylations at the two benzene rings often increase the lipophilicity of the backbone compounds, leading to enhancement of their affinity to cell membranes and of their interaction with target proteins.[4−6] Owing to the impressive biological activities and their diverse chemical structures, prenylated flavonoids have been studied by scientists from different research disciplines including natural product chemistry,[7] plant physiology,[8] and chemical syntheses.[9,10]

In plants, the prenyl moieties are transferred from prenyl diphosphates onto the flavonoid skeleton by membrane-bound prenyltransferases.[11,12] For example, SfN8DT-1/SfPFT, SfG6DT, and SfiLDT from *Sophora flavescens* catalyze prenylations of flavanones, isoflavonoids, and chalcones, respectively.[11,13,14] SfN8DT-1, the first identified flavonoid-specific prenyltransferase, was shown to be responsible for the prenylation of a few select flavanones at C-8.[14] SfFPT displayed a high catalytic efficiency for different types of flavonoids with high regiospecificity at C-8.[13] SfG6DT was found to specifically prenylate the isoflavone genistein at C-6,[11] while SfiLDT functions as a chalcone-specific prenyltransferase.[11] LaPT1 from *Lupinus albus* acts as an isoflavonoid-specific B-ring prenyltransferase,[15] while G4DT from *Glycine max* is specific

for pterocarpans.[16] Recently, two isoliquiritigenin 3,3-dimethyl-lallyltransferases MaIDT and CtIDT have been identified in *Morus alba* and *Cudrania tricuspidata*, respectively.[17] With the exception of a few members, these enzymes usually showed high substrate specificities and accepted only their natural substrates or just a few substances with similar structures.

In addition to membrane-bound prenyltransferases from plants, soluble prenyltransferases from bacteria such as NphB and SCO7190 also accept flavonoids as substrates.[18,19] NphB from a *Streptomyces* sp. is a hydroxynaphthalene geranyltransferase.[18] Its homologue SCO7190 from *Streptomyces coelicolor* used dimethylallyl diphosphate (DMAPP) as a prenyl donor and also catalyzes the prenylation of naringenin at C-6.[19] We have demonstrated that the recombinant indole prenyltransferase 7-DMATS from the fungus *Aspergillus fumigatus* accepted chalcones, isoflavonoids, and flavanones much better than flavones and flavonols and mainly catalyzed prenylation at C-6.[20] These results encouraged us to find more prenyltransferases with different substrate specificities and prenylation positions on the flavonoid skeleton, in order to utilize these enzymes for the production of prenylated flavonoids. Preliminary results from the previous study[20] indicated that AnaPT, which catalyzes the C-3 prenylation of (*R*)-benzodiazepindinone in the biosynthesis of acetylaszonalenin[21] and uses diverse aromatic substances for prenylation,[22−25] could be a good candidate.

2229

RESULTS AND DISCUSSION

Twenty-one flavonoids were initially incubated with 75 μg of the recombinant AnaPT in the presence of DMAPP at 37 °C for 16 h. HPLC analysis revealed that naringenin (**1a**), 7-hydroxyflavanone (**2a**), eriodictyol (**3a**), hesperetin (**4a**), silibinin (**5a**), phloretin (**6a**), apigenin (**7a**), genistein (**8a**), and biochanin A (**9a**) were readily accepted by AnaPT under these conditions. Compounds **1a**–**3a** and **5a**–**9a** were incubated with 75 μg of AnaPT at 37 °C for different times (Figure S1, Supporting Information). With the exception of the preferred flavonoid **1a**, product formation was found to be nearly linear for up to 2 h for other substrates. With **1a** as substrate and 40 μg of protein, the AnaPT reaction was found to be linear for up to 2 h (Figure S2, Supporting Information). For better comparison of their acceptance, **1a**–**9a** were incubated with 40 μg of AnaPT at 37 °C for 2 h (Table 1,

Table 1. Product Yields of 1a–9a Catalyzed by 7-DMATS and AnaPT[a]

substrate	product yield (%) 7-DMATS	AnaPT
1a	26.9 ± 0.3	48.2 ± 1.0
2a	1.2 ± 0.0	3.2 ± 0.2
3a	36.0 ± 0.4	4.4 ± 0.3
4a	15.9 ± 2.7	1.5 ± 0.0
5a	0.2 ± 0.2	3.2 ± 0.1
6a	23.1 ± 0.5	12.0 ± 0.3
7a	0.9 ± 0.0	3.3 ± 0.2
8a	6.7 ± 0.2	4.8 ± 0.3
9a	4.5 ± 0.2	7.1 ± 0.0

[a]The enzyme assays (100 μL) contained one of the flavonoids **1a**–**9a** (1 mM), CaCl$_2$ (10 mM), DMAPP (2 mM), glycerol (1.0–6.0% v/v), DMSO (5% v/v), Tris-HCl (50 mM, pH 7.5), and the purified recombinant proteins (40 μg). The reaction mixtures were incubated at 37 °C for 2 h.

Figure S3, Supporting Information). Under these conditions, **1a** was accepted as the best substrate with a product yield of 48.2%, which was calculated by comparison of peak areas in the HPLC chromatogram and intensities of signals in the ^{1}H NMR spectrum of the reaction mixture. Compounds **1a**–**9a** were subsequently incubated with 40 μg of 7-DMATS at 37 °C for 2 h. Under these conditions, product formation with its best substrate **3a**[20] was found to be linear (Figure S2, Supporting Information). HPLC analysis confirmed **3a** as the best substrate, with a product yield of 36.0%, followed by **1a** and **6a**, with product yields of 26.9% and 23.1%, respectively.

To enhance product formation, compounds **1a**–**9a** were incubated with 40 μg of AnaPT or 7-DMATS at 37 °C for 16 h (Figure 1). Under these conditions, product yields of more than 10% were calculated for seven AnaPT reactions (**1a**–**3a**, **5a**, **6a**, **8a**, and **9a**), with **1a** as the best substrate (58.6%) and six 7-DMATS reactions (**1a**, **3a**, **4a**, **6a**, **8a**, and **9a**) with **3a**, **4a**, and **6a** as the best substrates (56.0–77.8%). It is obvious that the flavanones **1a**, **3a**, and **4a**, chalcone **6a**, and isoflavones **8a** and **9a** were better substrates for one or both of the two enzymes than other subgroups. AnaPT accepted **1a**, **2a**, **5a**, **7a**, and **9a** much better than 7-DMATS, while **3a**, **4a**, **6a**, and **8a** were better substrates for 7-DMATS. Interestingly, silibinin (**5a**, also termed silybin), a hepatoprotective dihydroflavonol lignoid from the medicinal plant *Silybum marianum*,[26] was accepted by AnaPT with a product yield of 11.3%. Flavones

were poor substrates for both enzymes. The product yield of the preferred flavone apigenin (**7a**) was determined for AnaPT at 6.7%.
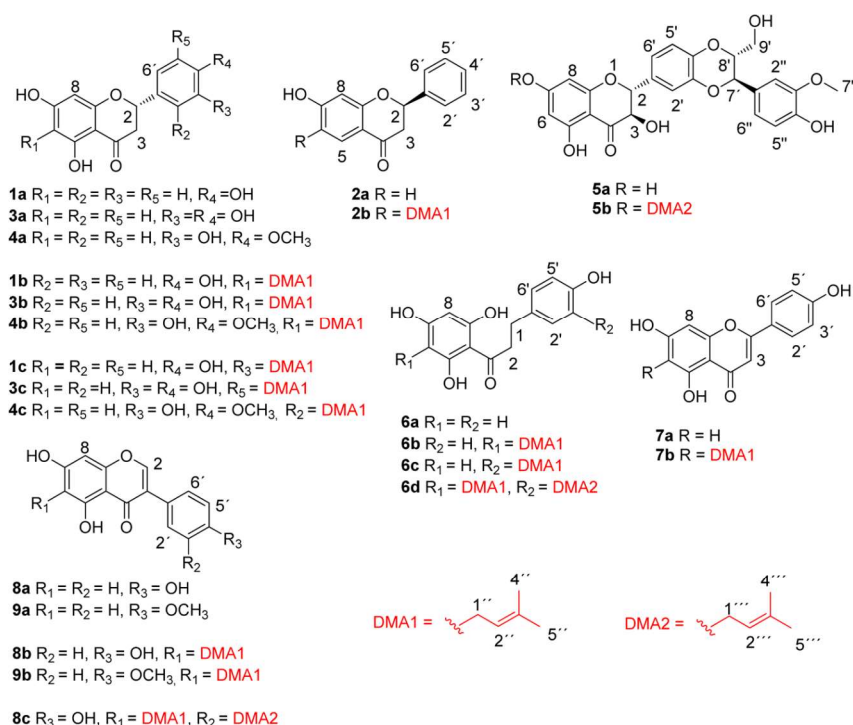
Inspection of the HPLC chromatograms revealed that more than one product peaks were detected in a number of reaction mixtures. Interestingly, the major products of several AnaPT and 7-DMATS reactions differed from each other. For example, the dominant product **1b** in the 7-DMATS reaction with **1a** (product yield 29.6%) was detected only as a minor product, with a yield of 4.4% in its reaction mixture with AnaPT. Instead, product **1c**, with a yield of 54.2%, was found as the main product. Eriodictyol (**3a**) was much better accepted by 7-DMATS, and several products including **3b**, **3c**, and **3d** with comparable yields were observed. In contrast, **3c**, with a product yield of 16.4%, was detected as the main product of the AnaPT reaction (Figure 1). Phloretin (**6a**) was converted by 7-DMATS to one predominate product, **6b**, while a number of products including **6b**, **6c**, and **6d** were detected in its reaction mixture with AnaPT. These results indicate different prenyl transfer reactions catalyzed by these two enzymes.

Previously, we demonstrated that AnaPT also used geranyl diphosphate (GPP) as prenyl donor for prenylation of cyclic dipeptides.[23] Therefore, **1a**–**9a** were incubated with AnaPT in the presence of GPP. HPLC analysis revealed that these compounds were also accepted by AnaPT in the presence of GPP. However, for a given aromatic substrate, the activity was much lower than that with DMAPP. After incubation with 40 μg of AnaPT for 16 h, the highest product yield of 5.9% was found for **6a** (Figure S4, Supporting Information). Under the same conditions, 7-DMATS also used GPP as prenyl donor for its reaction with **1a**–**9a**, but with lower product yields than with AnaPT. The highest product yield of approximately 1% was found for **1a** with 7-DMATS after incubation at 37 °C for 16 h (data not shown).

For structure elucidation, 12 enzyme products **1b**, **1c**, **2b**, **3c**, **5b**, **6b**, **6c**, **6d**, **7b**, **8b**, **8c**, and **9b** were isolated via preparative HPLC from incubation mixtures of **1a**–**3a** and **5a**–**9a** with AnaPT and DMAPP, respectively. Compounds **8b** and **8c** were also isolated from the incubation mixture of **8a** with 7-DMATS and DMAPP. The isolated products were subjected to NMR and HREIMS analyses. With the exception of **6d** and **8c**, the M$^+$ ions of the isolated products are 68 Da larger than the respective substrates, proving the monoprenylation of these compounds. The M$^+$ ions of **6d** and **8c** are 136 Da larger than those of **6a** and **8a**, respectively, corresponding to those of diprenylated derivatives. This conclusion was also confirmed by their molecular formula deduced from HREIMS analysis. The signals at δ_H 3.24–3.55 (d, 2H, −CH$_2$−), 5.18–5.36 (tsept or m, 1H, −C=CH), 1.62–1.71 (d or s, 3H, −C=C−CH$_3$), and 1.67–1.78 (d or s, 3H, −C=C−CH$_3$) in the ^{1}H NMR spectra of the isolated products indicated the presence of dimethylallyl moieties in their structures (Tables 2 and 3, Experimental Section, and Figures S5–S8 and S12–S18, Supporting Information). The resonance of the methylene group in the range 3.24–3.55 ppm proved the attachment of the dimethylallyl moieties to aromatic carbon atoms.[22] Compounds **1b**,[27] **1c**,[20] **2b**,[28] **3c**,[20] **6b**,[20] **7b**,[29] **8b**,[20] **8c**,[30] and **9b**[20] were identified as known compounds by comparison of their ^{1}H NMR data with reported data. These compounds are 6- (**1b**, **2b**, **6b**, **7b**, **8b**, and **9b**) or 3′-prenylated (**1c** and **3c**) or 6,3′-diprenylated derivatives (**8c**).

The ^{1}H NMR spectrum of **5b** (Figure S9, Supporting Information) was similar to that of its substrate, silybin,[31] and

Chart 1

1a $R_1 = R_2 = R_3 = R_5 = H$, $R_4 = OH$
3a $R_1 = R_2 = R_5 = H$, $R_3 = R_4 = OH$
4a $R_1 = R_2 = R_5 = H$, $R_3 = OH$, $R_4 = OCH_3$

2a $R = H$
2b $R = DMA1$

5a $R = H$
5b $R = DMA2$

1b $R_2 = R_3 = R_5 = H$, $R_4 = OH$, $R_1 = DMA1$
3b $R_2 = R_5 = H$, $R_3 = R_4 = OH$, $R_1 = DMA1$
4b $R_2 = R_5 = H$, $R_3 = OH$, $R_4 = OCH_3$, $R_1 = DMA1$

1c $R_1 = R_2 = R_5 = H$, $R_4 = OH$, $R_3 = DMA1$
3c $R_1 = R_2 = H$, $R_3 = R_4 = OH$, $R_5 = DMA1$
4c $R_1 = R_5 = H$, $R_3 = OH$, $R_4 = OCH_3$, $R_2 = DMA1$

6a $R_1 = R_2 = H$
6b $R_2 = H$, $R_1 = DMA1$
6c $R_1 = H$, $R_2 = DMA1$
6d $R_1 = DMA1$, $R_2 = DMA2$

7a $R = H$
7b $R = DMA1$

8a $R_1 = R_2 = H$, $R_3 = OH$
9a $R_1 = R_2 = H$, $R_3 = OCH_3$

8b $R_2 = H$, $R_3 = OH$, $R_1 = DMA1$
9b $R_2 = H$, $R_3 = OCH_3$, $R_1 = DMA1$

8c $R_3 = OH$, $R_1 = DMA1$, $R_2 = DMA2$

$DMA1 =$

$DMA2 =$

showed additional signals for a dimethylallyl moiety (δ_H 4.63, 2H, d, $J = 8.0$ Hz, H-1‴; 5.45, 1H, m, H-2‴; 1.77, 3H, s, H-5‴; and 1.74, 3H, s, H-4‴) (Table 2). The chemical shift of H-1‴ at 4.63 ppm indicated that the prenylation has taken place at an oxygen atom. This conclusion was supported by the same number and coupling pattern of the aromatic protons in the spectra of **5b** and its substrate. To prove the prenylation position in **5b**, HSQC and HMBC spectra (Figures S10 and S11, Supporting Information) were also taken into consideration. As shown in Figure S11 (Supporting Information), correlations of H-1‴ with C-7, C-2‴, and C-3‴ were evident, proving the prenylation of the 7-hydroxy group (Table 2).

Comparing the ^{1}H NMR spectra of **6c** (Figure S13, Supporting Information) and **6d** (Figure S14, Supporting Information) with that of **6a** revealed the disappearance of the AA′BB′ systems for B-ring protons in **6c** and **6d**. Instead, an ABX system was observed in their spectra. This indicates the prenylation of both substances at C-3′. Signals of two prenyl moieties (δ_H 3.24, 2H, d, $J = 7.3$ Hz; 5.22, 1H, tsept, $J = 7.3$, 0.9 Hz; 1,74, 3H, d, $J = 0.7$ Hz; 1.62, 3H, d, $J = 1.1$ Hz, and δ_H 3.28, 2H, d, $J = 7.3$ Hz; 5.32, 1H, tsept, $J = 7.3$, 1.1 Hz; 1.70, 3H, d, $J = 1.1$ Hz; 1.68, 3H, d, $J = 1.3$ Hz) were observed in the ^{1}H NMR spectrum of **6d**. Comparing the spectrum of **6d** with that of **6b** revealed the disappearance of the signal for H-6 in both cases. These results proved that **6c** is a 3′-monoprenylated derivative and **6d** bears the two prenyl moieties at C-6 and C-3′ (Table 3). A literature search indicated that the structures of **5b**, **6c**, and **6d** have not been reported prior to this work.

In summary, AnaPT displayed in several cases different behaviors regarding prenylation position from those of 7-DMATS reported previously.[20] For **1a**, **3a**, and **6a**, 7-DMATS is preferred for C-6 prenylation, and 6-prenylated derivatives **1b**, **3b**, and **6b** were detected as predominant or one of the

main products. In contrast, 3′-prenylation was observed as the main reactions in the assays of these compounds with AnaPT.

Kinetic parameters including Michaelis−Menten constants (K_M) and turnover numbers (k_{cat}) were determined at the pH optimum of the AnaPT reactions (pH 7.5) in a Tris-HCl buffer system by Hanes−Woolf, Eadie−Hofstee, and Lineweaver−Burk plots. The data obtained for (R)-benzodiazepinedinone, **1a−3a**, and **5a−9a** were compared (Figures S19−S26, Supporting Information). As shown in Table 4, **1a**, **3a**, and **5a** were found to have comparable affinities to (R)-benzodiazepinedione toward AnaPT, with K_M values of 0.26, 0.29, and 0.18 mM, respectively, while **2a** and **6a** showed lower affinity to AnaPT. The K_M values of **7a** and **9a** at 0.11 mM are even lower than that of (R)-benzodiazepinedione. As reported previously,[20] 7-DMATS displayed affinity to **6a** and **8a** similar to its natural substrate L-tryptophan. The turnover numbers of AnaPT with **1a−3a** and **5a−9a** in the range 0.001−0.05 s^{-1} are much smaller than that with (R)-benzodiazepinedione, at 1.72 s^{-1}. It is evident that catalytic efficiency of AnaPT toward flavonoids should be improved in the future by suitable approaches such as mutagenesis experiments.

In conclusion, AnaPT used in this study was identified in the ascomycetous fungus *Neosartorya fischeri* and proved to be responsible for the 3-prenylation of (R)-benzodiazepindinone in the biosynthesis of acetylaszonalenin.[21] This enzyme was demonstrated to exhibit significant substrate and catalytic promiscuity in vitro. It has an unprecedented ability to recognize diverse aromatic substrates such as tryptophan-containing cyclic dipeptides, hydroxynaphthalenes, and acyl-phloroglucinols and catalyzes Friedel−Crafts alkylations.[22,24,25,32] In addition to its prenyl donor DMAPP, AnaPT also accepted GPP and unnatural alkyl donors as substrates.[23,33]
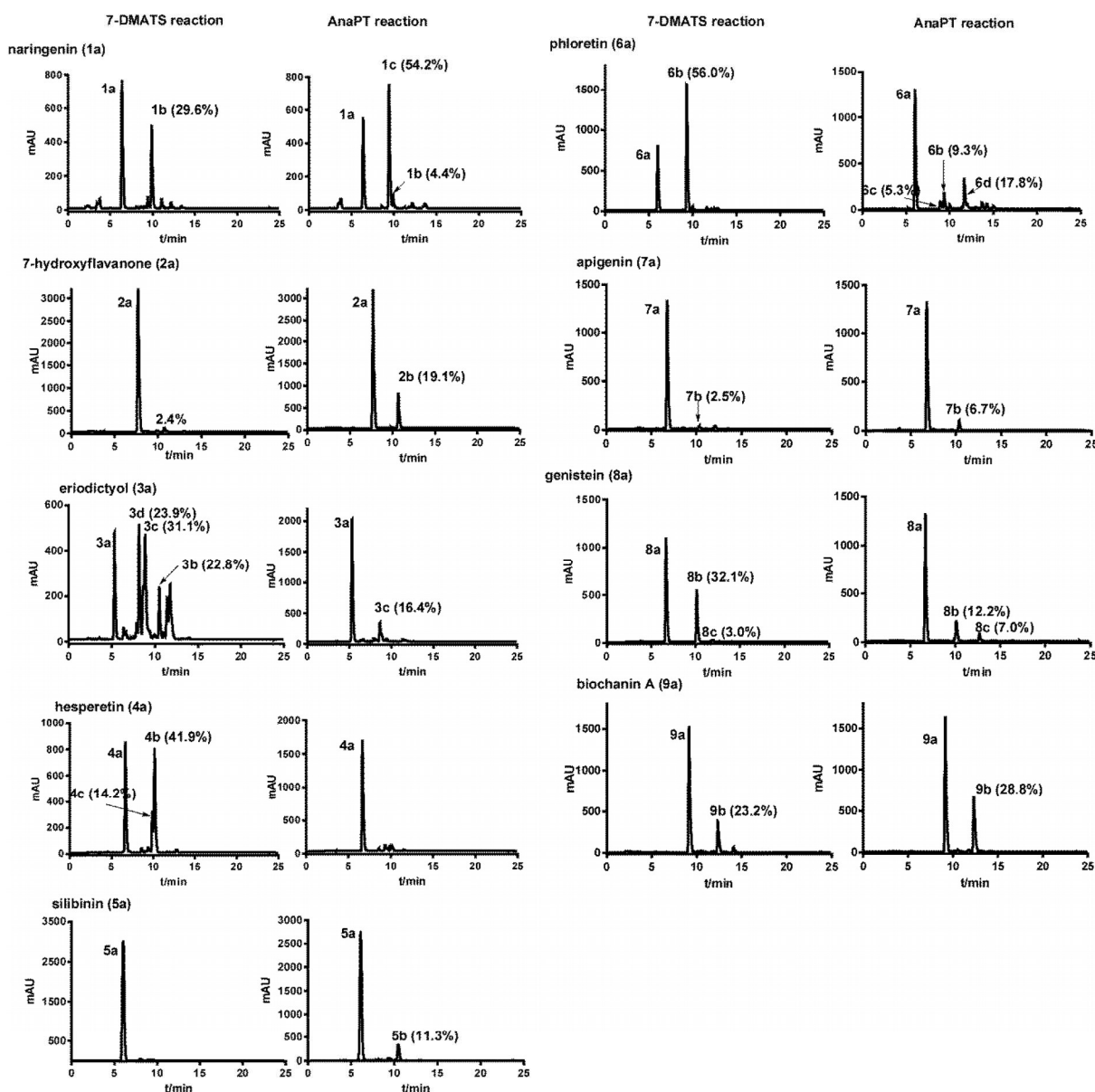
Figure 1. HPLC analysis of the reaction mixtures of 7-DMATS and AnaPT. The enzyme assays (100 μL) contained one of the flavonoids **1a**–**9a** (1 mM), CaCl$_2$ (10 mM), DMAPP (2 mM), glycerol (1.0–6.0% v/v), DMSO (5% v/v), Tris-HCl (50 mM, pH 7.5), and the purified recombinant proteins (40 μg). The reaction mixtures were incubated at 37 °C for 16 h and detected on a diode assay detector. The absorption at 277 nm was used for illustration of the reaction with **2a** and 296 nm for other substrates.

In this study, we demonstrated prenylations of different flavonoids such as flavanones and isoflavones by AnaPT at C-6 of the A ring or C-3′ of the B ring, which expands significantly its potential for modification of small molecules. More importantly, AnaPT and 7-DMATS displayed different substrate preferences and prenylation positions, so that these two fungal indole prenyltransferases could be used complementarily for prenylation of flavonoids. Prenylations of the flavonoid skeleton contribute significantly to structural diversity and biological activity of natural products and are usually crucial in the biosynthesis of these compounds. Therefore, the soluble indole prenyltransferases AnaPT and 7-DMATS could also be used for production of prenylated flavonoids in microorganisms by synthetic biological approaches.

■ EXPERIMENTAL SECTION

General Experimental Procedures. Flavonoids and solvents used in this study were purchased from Alfa Aesar (Karlsruhe, Germany), Acros Organics (Geel, Belgium), Carl Roth (Karlsruhe, Germany), Sigma-Aldrich (Steinheim, Germany), and TCI (Zwyndrecht, Belgium). The triammonium salts of DMAPP and GPP were synthesized according to the method described for GPP by Woodside and co-workers.[34] NMR spectra were recorded at room temperature on a JEOL ECA-400 or -500 or a Bruker Avance 600 MHz spectrometer and processed with MestReNova 5.2.2. Chemical shifts were referenced to the signal of acetone-d_6 at 2.05 ppm. The enzyme products were also analyzed by EIMS on an Auto SPEC (Micromass Co. UK Ltd.).

Overproduction and Purification of AnaPT and 7-DMATS as Well as Enzyme Assay. Overproduction and purification of AnaPT and 7-DMATS were carried out as described previously.[21,35] The

Table 2. NMR Spectroscopic Data (600 Hz, Acetone-d_6) for 5b

pos	δ_C, type	δ_H, mult (J in Hz)	HMBC	pos	δ_C, type	δ_H, mult (J in Hz)	HMBC
2	83.5, CH	5.13, d (13.8)	C-3, C-4, C-9, C-1′, C-2′, C-6′	1″	128.1, C		
3	72.5, CH	4.38, d (13.8)		2″	111.0, CH	7.14, d (2.1)	C-1″, C-3″, C-6″
4	198.1, C			3″	147.7, C		
5	165.2, C			4″	147.4, C		
6	94.5, CH	6.06, d (3.3)	C-5, C-7, C-8, C-10	5″	114.8, CH	6.88, d (8.4)	C-1″, C-2″, C-4″, C-6″
7	168.4, C			6″	120.6, CH	6.98, d (8.0, 2.1)	C-7′, C-1″, C-2″, C-4″, C-5″
8	95.5, CH	6.09, d (3.3)	C-6, C-7,C-9, C-10	7″	55.5, CH₃	3.87, s	C-3″
9	162.2, C			1‴	65.3, CH₂	4.63, d (8.0)	C-7, C-2‴, C-3‴
10	101.1, C			2‴	119.0, CH	5.45, m	C-4‴, C-5‴
1′	130.2, C			3‴	138.2, C		
2′	116.5, CH	7.14, d (2.1)	C-2, C-6′, C-7′	4‴	17.3, CH₃	1.74, s	C-2‴, C-3‴, C-5‴
3′	143.9, C			5‴	24.8, CH₃	1.77, s	C-2‴, C-3‴, C-4‴
4′	144.2, C						
5′	116.4, CH	6.98, d (8.4)	C-1′, C-3′, C-6′, C-8′				
6′	121.0, CH	7.10 dd, (8.4, 2.1)	C-2, C-2′, C-3′, C-4′				
7′	76.5, CH	5.00, d (8.0)	C-8′, C-9′, C-1″, C-2″, C-6″				
8′	78.7, CH	4.16, m					
9′	60.9, CH₂	3.52, dd (14.5, 4.9)	C-7′, C-8′				
		3.75, dd (14.5, 2.6)					

Table 3. ^{1}H NMR Spectroscopic Data (500 Hz, Acetone-d_6) for 6c and 6d

	6c	6d
pos	δ_H, mult (J in Hz)	δ_H, mult (J in Hz)
1	2.84, t (7.7)	2.87, t (7.7)
2	3.29, t (7.7)	3.32, t (7.7)
6	5.90, s	
8	5.90, s	6.07, s
2′	6.96, d (2.2)	6.99, d (2.1)
5′	6.70, d (8.1)	6.72, d (8.2)
6′	6.88, dd (8.1, 2.2)	6.90, dd (8.2, 2.1)
1″	3.26, d (7.2)	3.24, d (7.3)
2″	5.30, tsept (7.2, 1.1)	5.22, tsept (7.3, 0.9)
4″	1.66, d (1.3)	1.62, d (1.1)
5″	1.68, d (1.1)	1.74, d (0.7)
1‴		3.28, d (7.3)
2‴		5.32, tsept (7.3, 1.1)
4‴		1.68, d (1.3)
5‴		1.70, d (1.1)

enzyme assay mixtures (100 μL) contained **1a–9a** (1 mM), CaCl₂ (10 mM), DMAPP or GPP (2 mM), glycerol (1.0–6.0% v/v), DMSO (5% v/v), Tris-HCl (50 mM, pH 7.5), and purified recombinant protein

(40 μg). The reaction mixtures were incubated at 37 °C for different times and terminated by addition of 100 μL of MeOH. The proteins were removed by centrifugation at 13 000 rpm for 20 min. Assays for isolation of the enzyme products were carried out in large scales (10–15 mL) containing aromatic substrates (1 mM), DMAPP (2 mM), CaCl₂ (10 mM), glycerol (1.0–6.0% v/v), DMSO (5% v/v), Tris-HCl (50 mM, pH 7.5), and 7.5 mg of recombinant protein per 10 mL assay. After incubation for 16 h at 37 °C, the reaction mixtures of **1a–3a** and **5a–9a** were extracted three or four times with double the volume of EtOAc. The organic phases were combined and evaporated. The residues were dissolved in acetone-d_6 for recording ^{1}H NMR spectra. After measurement, the NMR samples were evaporated, dissolved in MeOH (0.5–1.0 mL), and purified by HPLC. Assays for determination of kinetic parameters (100 μL) contained CaCl₂ (10 mM), glycerol (1.0–6.0% v/v), DMSO (5% v/v), Tris-HCl (50 mM, pH 7.5), DMAPP (2 mM), (R)-benzodiazepinedinone, **1a–3a**, or **5a–9a** at final concentrations of up to 5.0 mM and different amounts of AnaPT, i.e., 1 μg for (R)-benzodiazepinedinone, 40 μg for **1a**, or 75 μg for **2a**, **3a**, and **5a–9a**. To keep product formation in the linear region (Figures S1 and S2, Supporting Information), the reaction mixtures were incubated for different times: 15 min for **1a**, 60 min for (R)-benzodiazepinedione, 120 min for **3a** and **9a**, 180 min for **2a**, **5a**, and **6a**, or 240 min for **7a** and **8a**. The reactions were terminated with 100 μL of MeOH. Protein was removed by centrifugation at 13 000 rpm for 20 min.

Table 4. Kinetic Parameters of AnaPT and 7-DMATS Reactions

	AnaPT			7-DMATS[a]		
substrate	K_M [mM]	k_{cat} [s^{-1}]	k_{cat}/K_M [s^{-1} M^{-1}]	K_M [mM]	k_{cat} [s^{-1}]	k_{cat}/K_M [s^{-1} M^{-1}]
L-tryptophan				0.14	0.23	1643
(R)-benzodiazepinedione	0.22	1.72	7818			
naringenin (**1a**)	0.26	0.042	161.5	0.99	0.023	23
7-hydroxyflavanone (**2a**)	0.48	0.0042	8.8			
eriodictyol (**3a**)	0.29	0.0039	13.4	1.26	0.39	312
hesperetin (**4a**)				1.10	0.026	24
silibinin (**5a**)	0.18	0.0017	9.4			
phloretin (**6a**)	0.81	0.0025	3.1	0.13	0.036	286
apigenin (**7a**)	0.11	0.0018	16.4			
genistein (**8a**)	0.51	0.0042	8.2	0.16	0.027	171
biochanin A (**9a**)	0.11	0.011	100.0	0.07	0.019	261

Analysis of Enzyme Products by HPLC, NMR, and MS. An Agilent HPLC series 1200 was used for analysis and isolation of the enzyme products. A Multosper 120 RP-18 column (250 × 4 mm, 5 um C+S Chromatographic Service, Langerwehe, Germany) was used for analysis at a flow rate of 1 mL/min, and a Multosper 120 RP18 column (250 × 10 mm, 5 μm) for isolation at a flow rate of 2.5 mL/min. H_2O (solvent A) and MeCN (solvent B), both containing 0.5% TFA, were used as solvents. A linear gradient of 40−100% (v/v) solvent B in 15 min was used for analysis of the enzymatic products. The column was then washed with 100% solvent B for 5 min and equilibrated with 40% solvent B for another 5 min. Detection was carried out using a photodiode array detector. Solvents for isolation of the enzyme products were H_2O (solvent C) and MeCN (solvent D) without acid. The enzyme products were isolated with a linear gradient of 50−100% D in C in 25 min. After each run, the column was equilibrated with 50% solvent D for 10 min. HPLC analysis of the (R)-benzodiazepinedione reaction was carried out as described previously.[21]

Compound 1b: t_R = 10.02 min; UV (extracted from PDA) (MeCN/H_2O) λ_{max} 230, 288 nm; MS m/z 340.1293 (calculated for $C_{20}H_{20}O_5$, 340.1311); ^1H NMR (500 Hz, acetone-d_6) δ 7.39 (2H, d, J = 8.7 Hz, H-2′/H-6′), 6.89 (2H, d, J = 8.7 Hz, H-3′/H-5′), 6.03 (1H, s, H-8), 5.43 (1H, dd, J = 12.9, 3.0 Hz, H-2), 5.23 (1H, tsept, J = 7.3, 1.5 Hz, H-2″), 3.17 (1H, dd, J = 17.1, 12.9 Hz, H-3), 3.24 (2H, d, J = 7.3 Hz, H-1″), 2.72 (1H, dd, J = 17.1, 3.0 Hz, H-3), 1.75 (3H, d, J = 0.8 Hz, H-5″), 1.64 (3H, d, J = 1.1 Hz, H-4″).

Compound 1c: t_R = 9.52 min; UV (extracted from PDA) (MeCN/H_2O) λ_{max} 230, 296 nm; MS m/z 340.1309 (calculated for $C_{20}H_{20}O_5$, 340.1311); ^1H NMR (500 Hz, acetone-d_6) δ 7.29 (1H, d, J = 2.2 Hz, H-2′), 7.21 (1H, dd, J = 8.3, 2.2 Hz, H-6′), 6.89 (1H, d, J = 8.3 Hz, H-5′), 5.95 (1H, d, J = 2.2 Hz, H-6), 5.94 (1H, d, J = 2.2 Hz, H-8), 5.43 (1H, dd, J = 12.9, 3.0 Hz, H-2), 5.35 (1H, tsept, J = 7.4, 1.5 Hz, H-2″), 3.34 (2H, d, J = 7.4 Hz, H-1″), 3.18 (1H, dd, J = 17.1, 12.9 Hz, H-3), 2.71 (1H, dd, J = 17.1, 3.0 Hz, H-3), 1.71 (3H, d, J = 0.7 Hz, H-5″), 1.70 (3H, d, J = 1.4 Hz, H-4″).

Compound 2b: t_R = 12.43 min; UV (extracted from PDA) (MeCN/H_2O) λ_{max} 240, 277, 320 nm; MS m/z 308.1389 (calculated for $C_{20}H_{20}O_3$, 308.1412); ^1H NMR (500 Hz, acetone-d_6) δ 7.59 (1H, s, H-5), 7.57 (2H, br d, J = 8.2 Hz, H-2′/H-6′), 7.44 (2H, t, J = 8.2 Hz, H-3′/H-5′), 7.38 (1H, tt, J = 8.2, 1.4 Hz, H-4′), 6.49 (1H, s, H-8), 5.54 (1H, dd, J = 13.0, 3.0 Hz, H-2), 5.33 (1H, tsept, J = 7.4, 1.5 Hz, H-2″), 3.28 (2H, d, J = 7.4 Hz, H-1″), 3.01 (1H, dd, J = 16.7, 13.0 Hz, H-3), 2.72 (1H, dd, J = 16.7, 3.0 Hz, H-3), 1.73 (3H, d, J = 0.9 Hz, H-5″), 1.71 (3H, d, J = 1.4 Hz, H-4″).

Compound 3c: t_R = 8.99 min; UV (extracted from PDA) (MeCN/H_2O) λ_{max} 230, 290 nm; MS m/z 356.1234 (calculated for $C_{20}H_{20}O_6$, 356.1260); ^1H NMR (500 Hz, acetone-d_6) δ 6.90 (1H, d, J = 2.0 Hz, H-2′), 6.80 (1H, d, J = 2.0 Hz, H-6′), 5.95 (1H, d, J = 1.2 Hz, H-6), 5.94 (1H, d, J = 1.2 Hz, H-8), 5.37 (1H, dd, J = 12.9, 3.0 Hz, H-2), 5.35 (1H, tsept, J = 7.3, 1.5 Hz, H-2″), 3.35 (2H, d, J = 7.3 Hz, H-1″), 3.12 (1H, dd, J = 17.1, 12.9 Hz, H-3), 2.70 (1H, dd, J = 17.1, 3.0 Hz, H-3), 1.71 (3H, d, J = 0.6 Hz, H-5″), 1.70 (3H, d, J = 1.1 Hz, H-4″).

Compound 5b: t_R = 11.08 min; UV (extracted from PDA) (MeCN/H_2O) λ_{max} 230, 290 nm; MS m/z 550.1839 (calculated for $C_{30}H_{30}O_{10}$, 550.1900); ^1H NMR (500 Hz, acetone-d_6) Table 1.

Compound 6b: t_R = 9.09 min; UV (extracted from PDA) (MeCN/H_2O) λ_{max} 230, 290 nm; MS m/z 342.1438 (calculated for $C_{20}H_{22}O_5$, 342.1467); ^1H NMR (500 Hz, acetone-d_6) δ 7.09 (2H, d, J = 8.5 Hz, H-2′/H-6′), 6.74 (2H, d, J = 8.5 Hz, H-3′/H-5′), 6.07 (1H, s, H-8), 3.24 (2H, d, J = 7.2 Hz, H-1″), 5.22 (1H, tsept, J = 7.2, 1.1 Hz, H-2″), 3.33 (2H, t, J = 7.7 Hz, H-2), 2.88 (2H, t, J = 7.7 Hz, H-1), 1.74 (3H, d, J = 0.7 Hz, H-5″), 1.62 (3H, d, J = 1.1 Hz, H-4″).

Compound 6c: t_R = 8.70 min; UV (extracted from PDA) (MeCN/H_2O) λ_{max} 230, 285 nm; MS m/z 342.1505 (calculated for $C_{20}H_{22}O_5$, 342.1467); ^1H NMR (500 Hz, acetone-d_6) Table 2.

Compound 6d: t_R = 11.59 min; UV (extracted from PDA) (MeCN/H_2O) λ_{max} 230, 290 nm; MS m/z 410.2071 (calculated for $C_{25}H_{30}O_5$, 410.2093); ^1H NMR (500 Hz, acetone-d_6) Table 2.

Compound 7b: t_R = 11.55 min; UV (extracted from PDA) (MeCN/H_2O) λ_{max} 220, 277, 330 nm; MS m/z 338.1149 (calculated

for $C_{20}H_{18}O_5$, 338.1154); ^1H NMR (500 Hz, acetone-d_6) δ 7.93 (2H, d, J = 9.0 Hz, H-2′/H-6′), 7.02 (2H, d, J = 9.0 Hz, H-3′/H-5′), 6.62 (1H, s, H-3), 6.64 (1H, s, H-8), 5.27 (1H, tsept, J = 7.3, 1.4 Hz, H-2″), 3.35 (2H, d, J = 7.3 Hz, H-1″), 1.78 (3H, d, J = 1.0 Hz, H-5″), 1.65 (3H, d, J = 1.1 Hz, H-4″).

Compound 8b: t_R = 10.52 min; UV (extracted from PDA) (MeCN/H_2O) λ_{max} 215, 265 nm; MS m/z 338.1175 (calculated for $C_{20}H_{18}O_5$, 338.1154); ^1H NMR (500 Hz, acetone-d_6) δ 8.15 (1H, s, H-2), 7.45 (2H, d, J = 6.5 Hz, H-2′/H-6′), 6.90 (2H, d, J = 8.7 Hz, H-3′/H-5′), 6.51 (1H, s, H-8), 5.27 (1H, tsept, J = 7.2, 1.2 Hz, H-2″), 3.36 (2H, d, J = 7.2 Hz, H-1″), 1.78 (3H, d, J = 0.7 Hz, H-5″), 1.65 (3H, d, J = 1.2 Hz, H-4″).

Compound 8c: t_R = 12.73 min; UV (extracted from PDA) (MeCN/H_2O) λ_{max} 215, 266 nm; MS m/z 406.1768 (calculated for $C_{25}H_{26}O_5$, 406.1780); ^1H NMR (500 Hz, acetone-d_6) δ 8.10 (1H, s, H-2), 7.32 (1H, d, J = 2.3 Hz, H-2′), 7.25 (1H, d, J = 8.3, 2.3 Hz, H-6′), 6.88 (1H, d, J = 8.3 Hz, H-2′), 6.50 (1H, s, H-8), 5.36 (1H, m, H-2‴), 5.26 (1H, m, H-2″), 3.35 (2H, d, J = 7.5 Hz, H-1‴), 3.33 (2H, d, J = 6.0 Hz, H-1″), 1.76 (3H, d, J = 0.8 Hz, H-4‴), 1.71 (3H, d, J = 1.2 Hz, H-5″), 1.70 (3H, d, J = 1.2 Hz, H-5‴), 1.63 (3H, d, J = 1.1 Hz, H-4″).

Compound 9b: t_R = 13.55 min; UV (extracted from PDA) (MeCN/H_2O) λ_{max} 215, 265 nm; MS m/z 352.1310 (calculated for $C_{21}H_{20}O_5$, 352.1311); ^1H NMR (500 Hz, acetone-d_6) δ 8.18 (1H, s, H-2), 7.54 (2H, d, J = 8.8 Hz, H-2′/H-6′), 7.00 (2H, d, J = 8.8 Hz, H-3′/H-5′), 6.51 (1H, s, H-8), 5.27 (1H, tsept, J = 7.2, 1.5 Hz, H-2″), 3.84 (3H, s, OCH₃), 3.36 (2H, d, J = 7.2 Hz, H-1″), 1.78 (3H, d, J = 0.6 Hz, H-5″), 1.65 (3H, d, J = 1.1 Hz, H-4″).

■ ASSOCIATED CONTENT

Ⓢ Supporting Information

The Supporting Information is available free of charge on the ACS Publications website at DOI: 10.1021/acs.jnat-prod.5b00422.

NMR spectra; HPLC chromatograms of enzyme assays with GPP; kinetic parameters (PDF)

■ AUTHOR INFORMATION

Corresponding Author

*E-mail: shuming.li@staff.uni-marburg.de. Tel/Fax: +49-6421-28-22461/25365.

Present Address

‡Department of Chemical and Biomolecular Engineering, University of California, Los Angeles, 420 Westwood Plaza, Los Angeles, California 90095, United States.

Notes

The authors declare no competing financial interest.

■ REFERENCES

(1) Marais, J. P. J.; Deavours, B.; Dixon, R. A.; Ferreira, D. In *The Science of Flavonoids*; Grotewold, E., Ed.; Springer Science + Business Media, Inc: New York, 2006; Chapter 1, pp 1−46.

(2) Sandhar, H. K.; Kumar, B.; Prasher, S.; Tiwari, P.; Salhan, M.; Sharma, P. *Int. Pharm. Sci.* **2011**, 1, 25−41.

(3) Agrawal, A. D. *Int. J. Pharm. Sci. Nanotechnol.* **2011**, 4, 1394−1398.

(4) Botta, B.; Vitali, A.; Menendez, P.; Misiti, D.; Delle, M. G. *Curr. Med. Chem.* **2005**, 12, 717−739.

113

(5) Chen, X.; Mukwaya, E.; Wong, M. S.; Zhang, Y. *Pharm. Biol.* **2014**, *52*, 655−660.

(6) Wesolowska, O.; Gasiorowska, J.; Petrus, J.; Czarnik-Matusewicz, B.; Michalak, K. *Biochim. Biophys. Acta, Biomembr.* **2014**, *1838*, 173−184.

(7) Hanáková, Z.; Hošek, J.; Babula, P.; Dall'Acqua, S.; Václavík, J.; Šmejkal, K. *J. Nat. Prod.* **2015**, *78*, 850−863.

(8) Lukaseder, B.; Vajrodaya, S.; Hehenberger, T.; Seger, C.; Nagl, M.; Lutz-Kutschera, G.; Robien, W.; Greger, H.; Hofer, O. *Phytochemistry* **2009**, *70*, 1030−1037.

(9) Tischer, S.; Metz, P. *Adv. Synth. Catal.* **2007**, *349*, 147−151.

(10) Hossain, M. M.; Kawamura, Y.; Yamashita, K.; Tsukayama, M. *Tetrahedron* **2006**, *62*, 8625−8635.

(11) Sasaki, K.; Tsurumaru, Y.; Yamamoto, H.; Yazaki, K. *J. Biol. Chem.* **2011**, *286*, 24125−24134.

(12) Yazaki, K.; Sasaki, K.; Tsurumaru, Y. *Phytochemistry* **2009**, *70*, 1739−1745.

(13) Chen, R.; Liu, X.; Zou, J.; Yin, Y.; Ou, C.; Li, J.; Wang, R.; Xie, D.; Zhang, P.; Dai, J. *Adv. Synth. Catal.* **2013**, *355*, 1817−1828.

(14) Sasaki, K.; Mito, K.; Ohara, K.; Yamamoto, H.; Yazaki, K. *Plant Physiol.* **2008**, *146*, 1075−1084.

(15) Shen, G.; Huhman, D.; Lei, Z.; Snyder, J.; Sumner, L. W.; Dixon, R. A. *Plant Physiol.* **2012**, *159*, 70−80.

(16) Akashi, T.; Sasaki, K.; Aoki, T.; Ayabe, S.; Yazaki, K. *Plant Physiol.* **2008**, *149*, 683−693.

(17) Wang, R.; Chen, R.; Li, J.; Liu, X.; Xie, K.; Chen, D.; Yin, Y.; Tao, X.; Xie, D.; Zou, J.; Yang, L.; Dai, J. *J. Biol. Chem.* **2014**, *289*, 35815−35825.

(18) Ozaki, T.; Mishima, S.; Nishiyama, M.; Kuzuyama, T. *J. Antibiot.* **2009**, *62*, 385−392.

(19) Kumano, T.; Richard, S. B.; Noel, J. P.; Nishiyama, M.; Kuzuyama, T. *Bioorg. Med. Chem.* **2008**, *16*, 8117−8126.

(20) Yu, X.; Li, S.-M. *ChemBioChem* **2011**, *12*, 2280−2283.

(21) Yin, W.-B.; Grundmann, A.; Cheng, J.; Li, S.-M. *J. Biol. Chem.* **2009**, *284*, 100−109.

(22) Yu, X.; Xie, X.; Li, S.-M. *Appl. Microbiol. Biotechnol.* **2011**, *92*, 737−748.

(23) Pockrandt, D.; Li, S.-M. *ChemBioChem* **2013**, *14*, 2023−2028.

(24) Yin, W.-B.; Xie, X.-L.; Matuschek, M.; Li, S.-M. *Org. Biomol. Chem.* **2010**, *8*, 1133−1141.

(25) Yin, W.-B.; Cheng, J.; Li, S.-M. *Org. Biomol. Chem.* **2009**, *7*, 2202−2207.

(26) Biedermann, D.; Vavrikova, E.; Cvak, L.; Kren, V. *Nat. Prod. Rep.* **2014**, *31*, 1138−1157.

(27) Adib, A. M.; Ahmad, F.; Idris, M. S. *J. Chem. Sci.* **2008**, *120*, 469−473.

(28) Alam, S.; Islam, A.; Das, N. C. *J. Bangladesh Acad. Sci.* **2004**, *28*, 117−120.

(29) Delle Monache, G.; Scurria, R.; Vitali, A.; Botta, B.; Monacelli, B.; Pasqua, G.; Palocci, C.; Cernia, E. *Phytochemistry* **1994**, *37*, 893−898.

(30) Pistelli, L.; Spera, K.; Flamini, G.; Mele, S.; Morelli, I. *Phytochemistry* **1996**, *42*, 1455−1458.

(31) Lee, D. Y. W.; Liu, Y. *J. Nat. Prod.* **2003**, *66*, 1171−1174.

(32) Zhou, K.; Ludwig, L.; Li, S.-M. *J. Nat. Prod.* **2015**, *78*, 929−933.

(33) Liebhold, M.; Xie, X.; Li, S.-M. *Org. Lett.* **2013**, *15*, 3062−3065.

(34) Woodside, A. B.; Huang, Z.; Poulter, C. D. *Org. Synth.* **1988**, *66*, 211−215.

(35) Kremer, A.; Westrich, L.; Li, S.-M. *Microbiology* **2007**, *153*, 3409−3416.

114

Supporting Information
for
Complementary Flavonoid Prenylations by Fungal Indole Prenyltransferases

Kang Zhou, [†] Xia Yu, [†,‡] Xiulan Xie, [§] and Shu-Ming Li [†] *

[†] Institut für Pharmazeutische Biologie und Biotechnologie, Philipps-Universität Marburg, Marburg 35037, Germany

[‡] Present address: Department of Chemical and Biomolecular Engineering, University of California, Los Angeles, 420 Westwood Plaza, Los Angeles, 90095, USA

[§] Fachbereich Chemie, Philipps-Universität Marburg, Marburg 35032, Germany

*Tel: + (49)6421-2822461; Fax +(49)6421-2825365. E-Mail: shuming.li@staff.uni-marburg.de

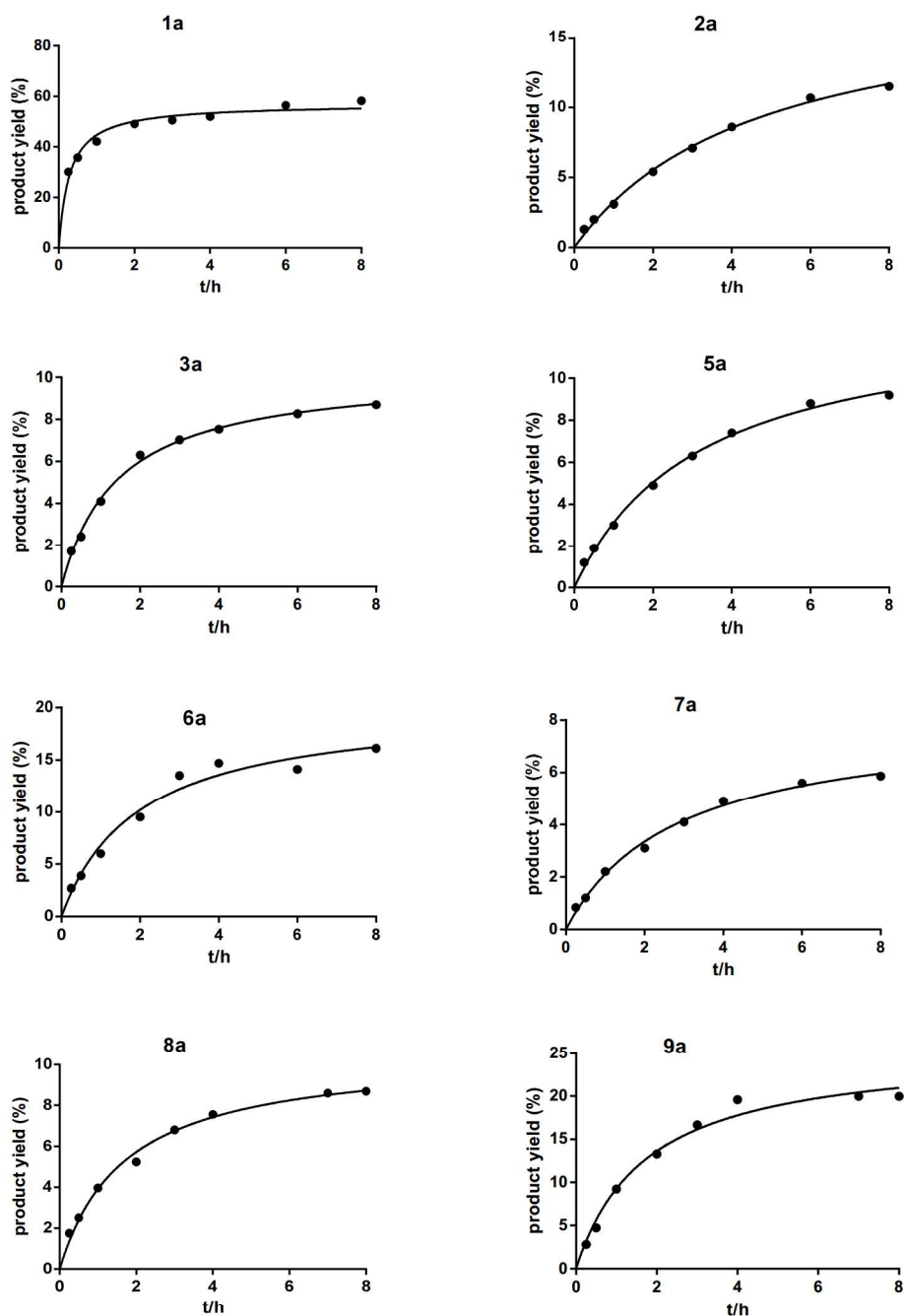# List of Supporting Information

Figure S1: Dependence of the product formation of 1a–3a and 5a–9a on incubation times in the presence of DMAPP.

The enzyme assays (100 μL) contained one of eight flavonoids (1 mM), Tris-HCl (50 mM, pH 7.5), CaCl$_2$ (10 mM), DMAPP (2 mM), glycerol (1.0–6.0 % v/v), DMSO (5 % v/v), and the purified recombinant AnaPT (75 μg).
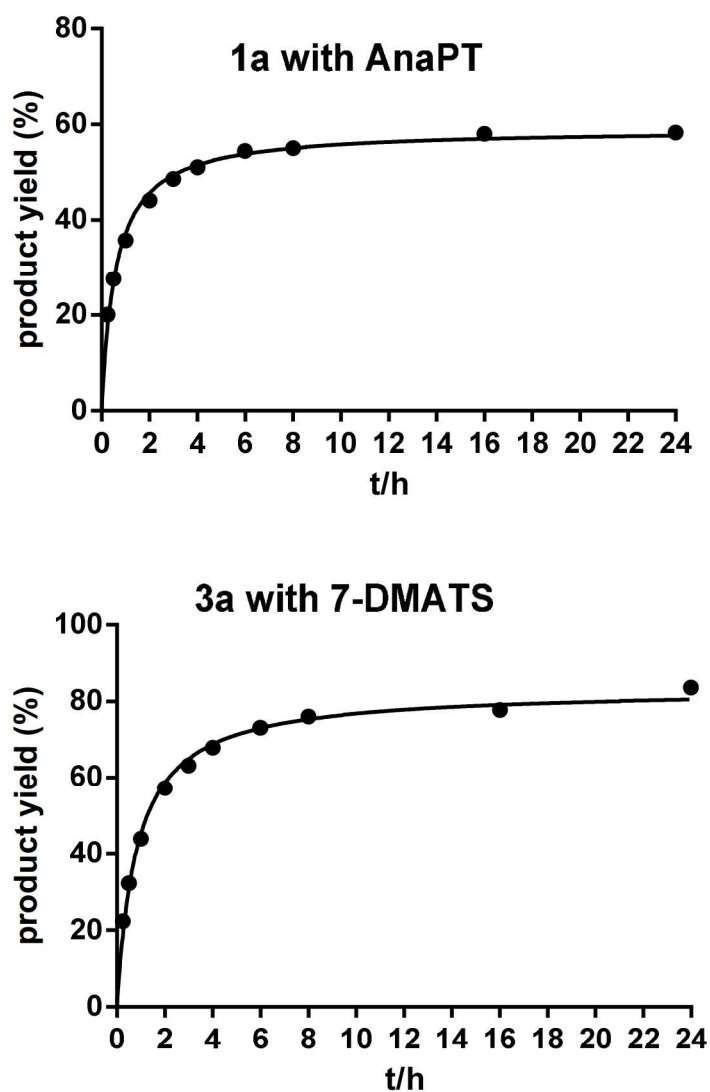
3

117

Figure S2: Dependence of the product formation of 1a and 3a on incubation times in the presence of DMAPP.

The enzyme assays (100 μL) contained **1a** or **3a** (1 mM), Tris-HCl (50 mM, pH 7.5), CaCl$_2$ (10 mM), DMAPP (2 mM), glycerol (1.0–6.0 % v/v), DMSO (5 % v/v), and the purified recombinant AnaPT or 7-DMATS (40 μg).

4
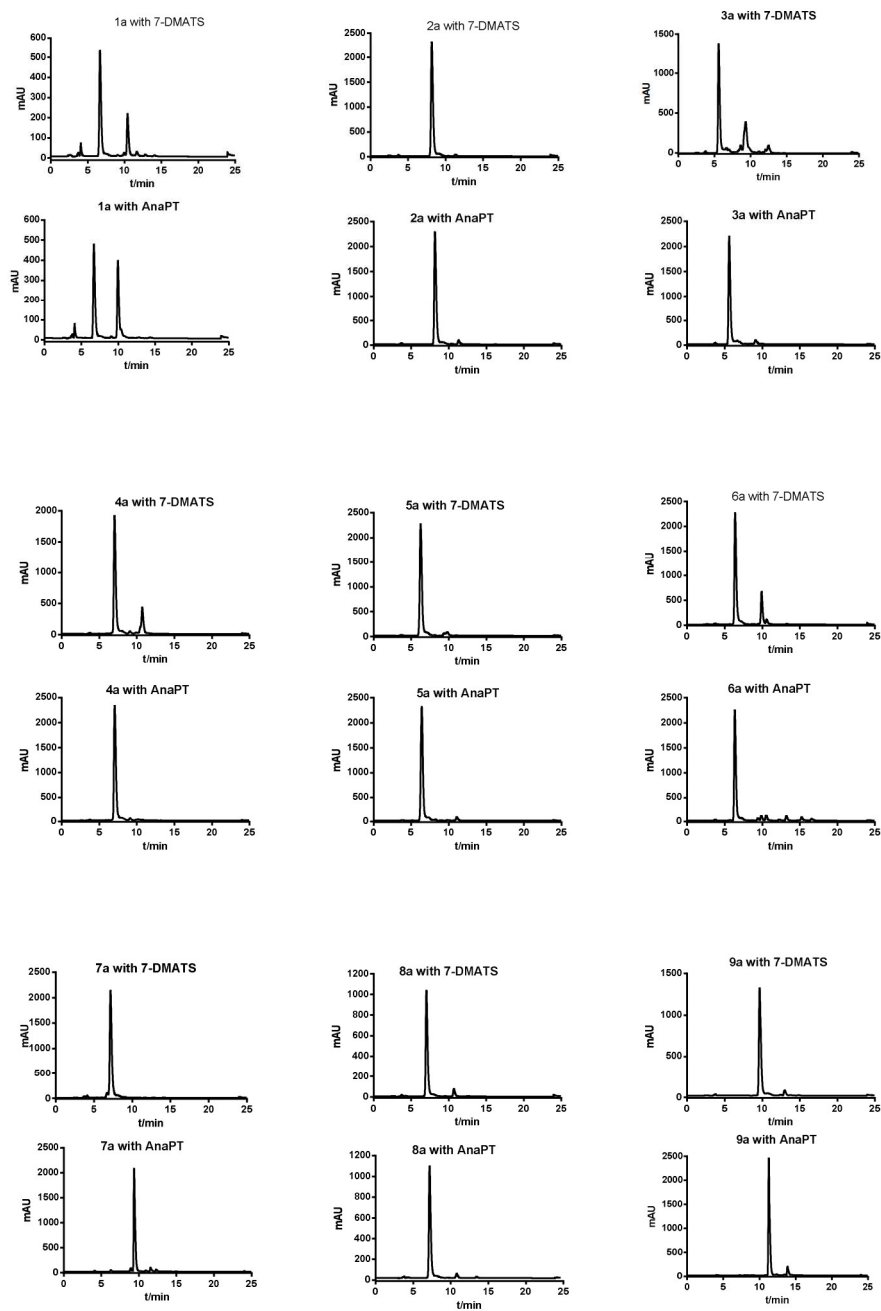
Figure S3 HPLC analysis of reaction mixtures of 7-DMATS and AnaPT.

The enzyme assays (100 μL) contained one of the flavonoids **1a–9a** (1 mM), $CaCl_2$ (10 mM), DMAPP (2 mM), glycerol (1.0–6.0 % v/v), dimethyl sulfoxide (DMSO, 5 % v/v), Tris-HCl (50 mM, pH 7.5) and purified recombinant protein (40 μg). The reaction mixtures are incubated at 37 °C for 2 h. The absorption at 277 nm was used for illustration of the reaction with **2a** and 296 nm for other reactions.

5
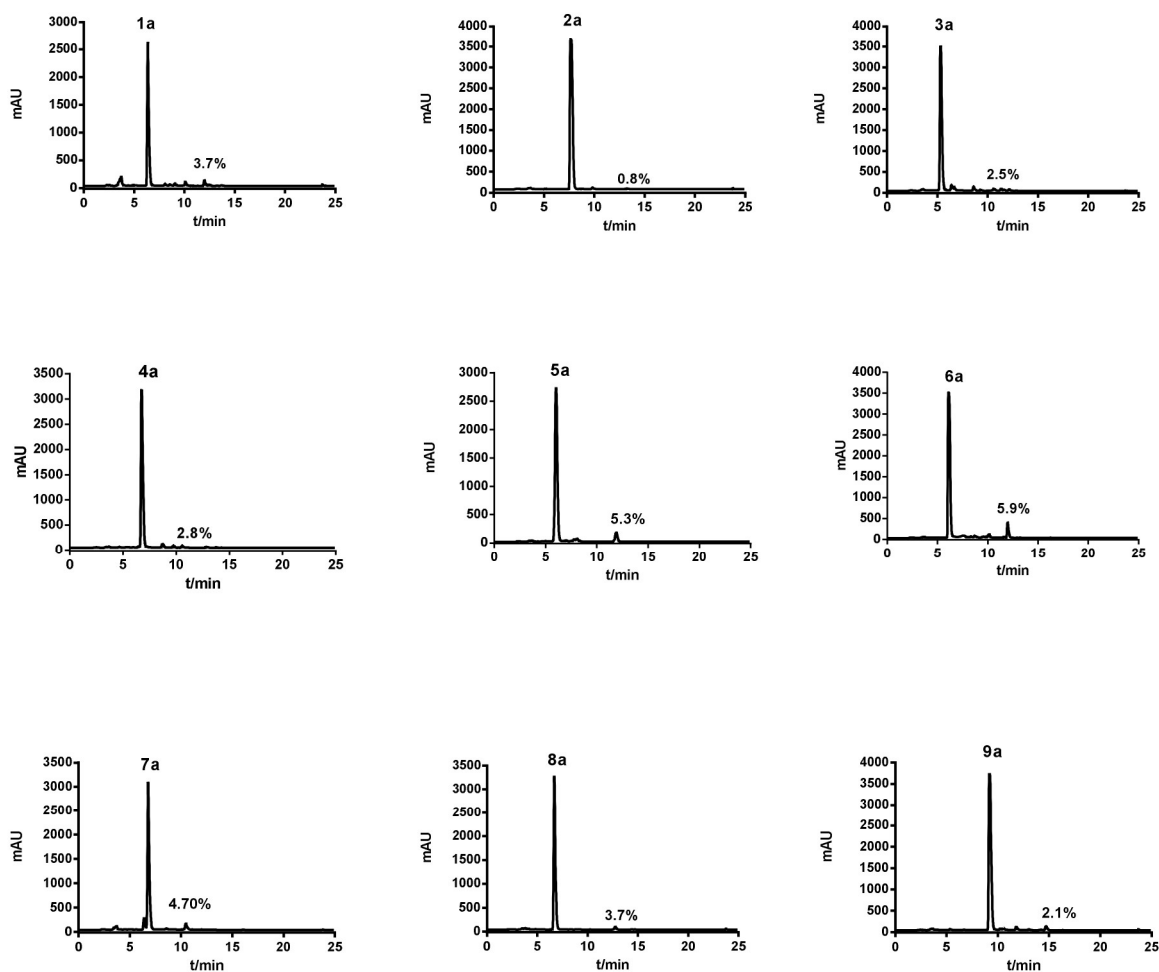
Figure S4: HPLC chromatograms of enzyme assays of AnaPT in the presence of GPP.

The enzyme assays (100 μL) contained one of the flavonoids **1a–9a** (1 mM), CaCl$_2$ (10 mM), GPP (2 mM), glycerol (1.0–6.0 % v/v), DMSO (5 % v/v), Tris-HCl (50 mM, pH 7.5) and purified recombinant protein (75 μg). The reaction mixtures were incubated at 37 ℃ for 16 h. The wavelength for illustration of product formation was 277 nm (**2a**) or 296 nm (**1a**, **3a–9a**)

6
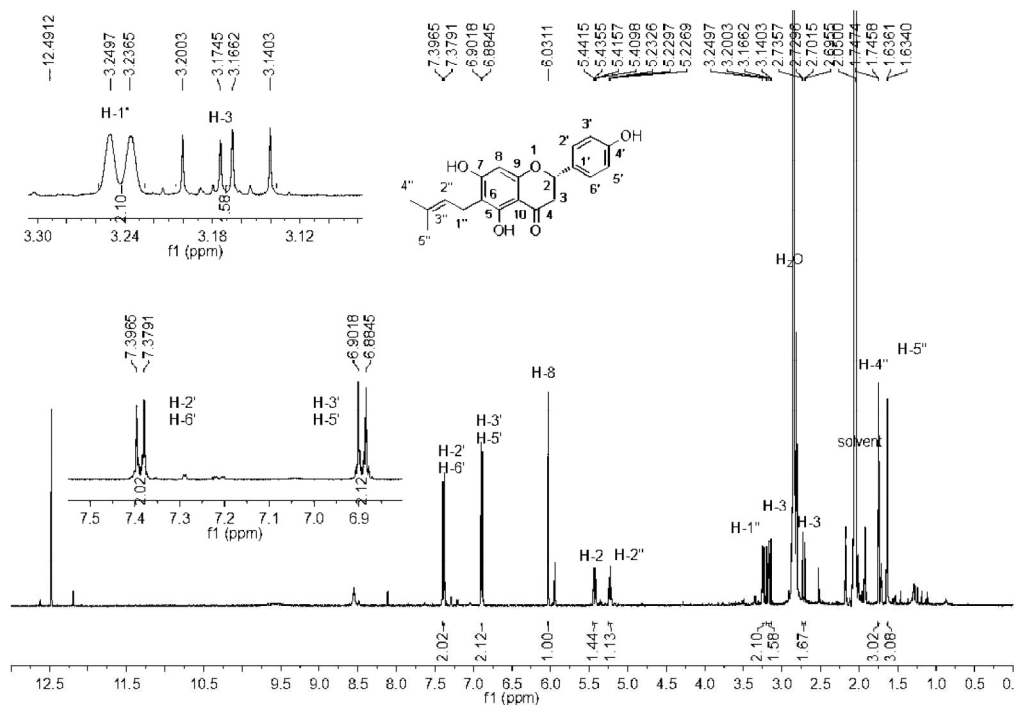
Figure S5: ^{1}H NMR spectrum of **1b** in acetone-d_6 (500 MHz).
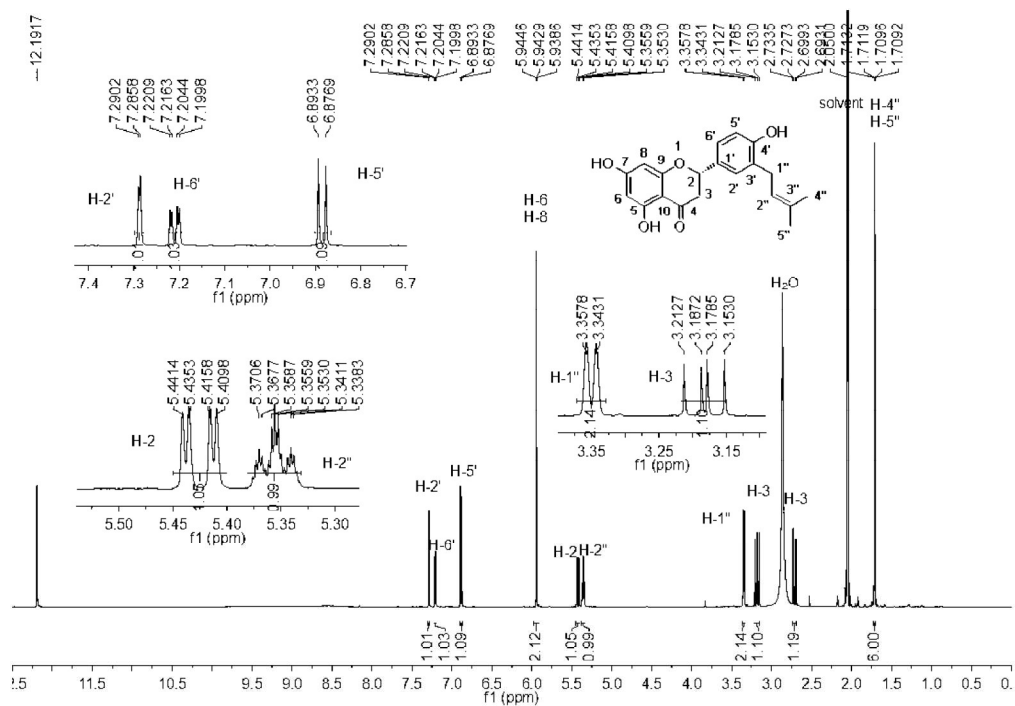
Figure S6: ^{1}H NMR spectrum of **1c** in acetone-d_6 (500 MHz).

7

121

Figure S7: ^{1}H NMR spectrum of 2b in acetone-d_6 (500 MHz).

Figure S8: ^{1}H NMR spectrum of 3c in acetone-d_6 (500 MHz).
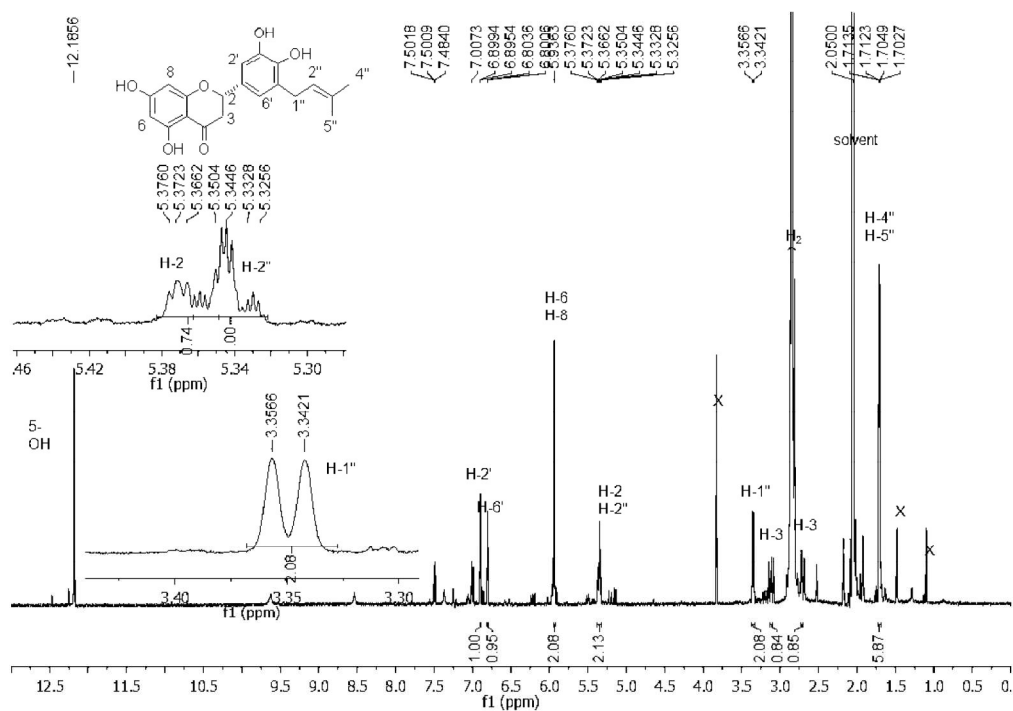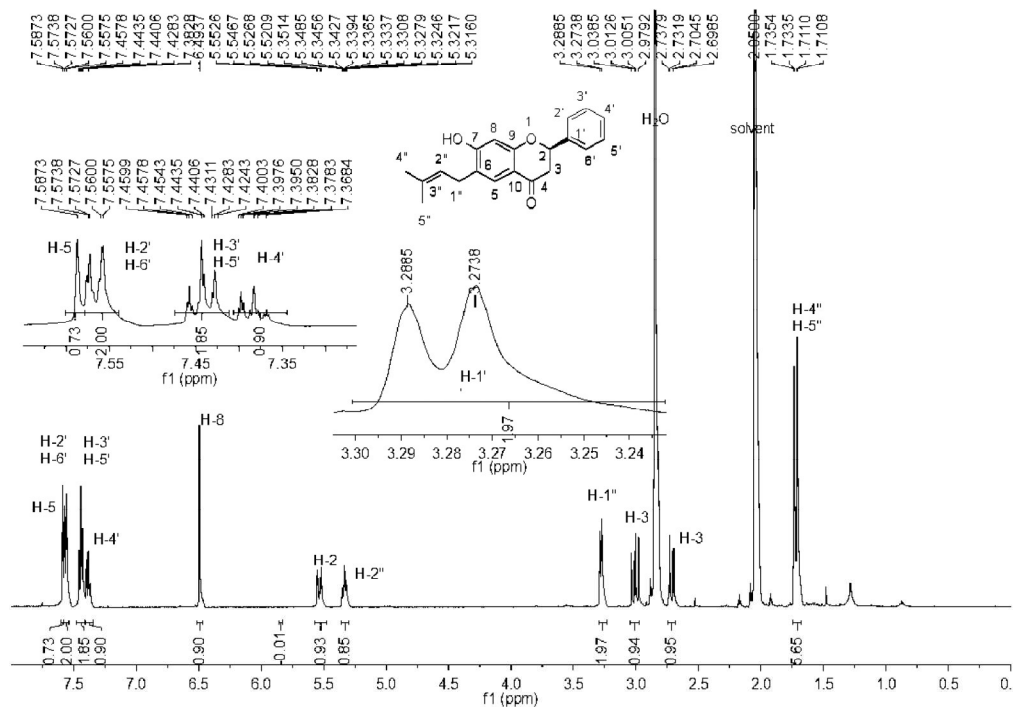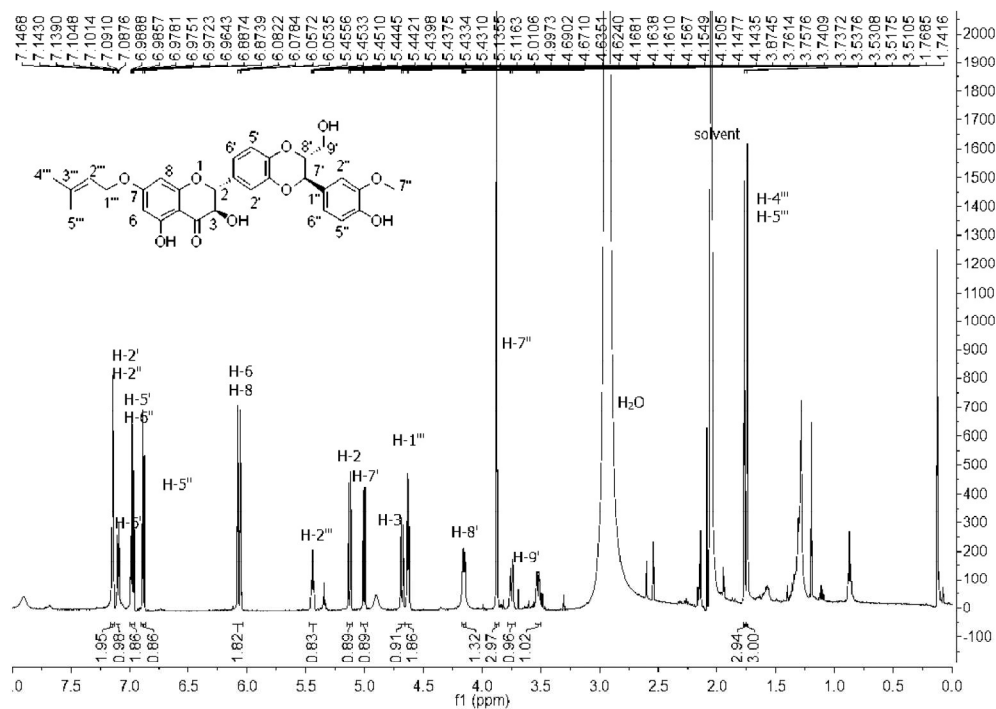
Figure S9: ^1H NMR spectrum of **5b** in acetone-d_6 (600 MHz).
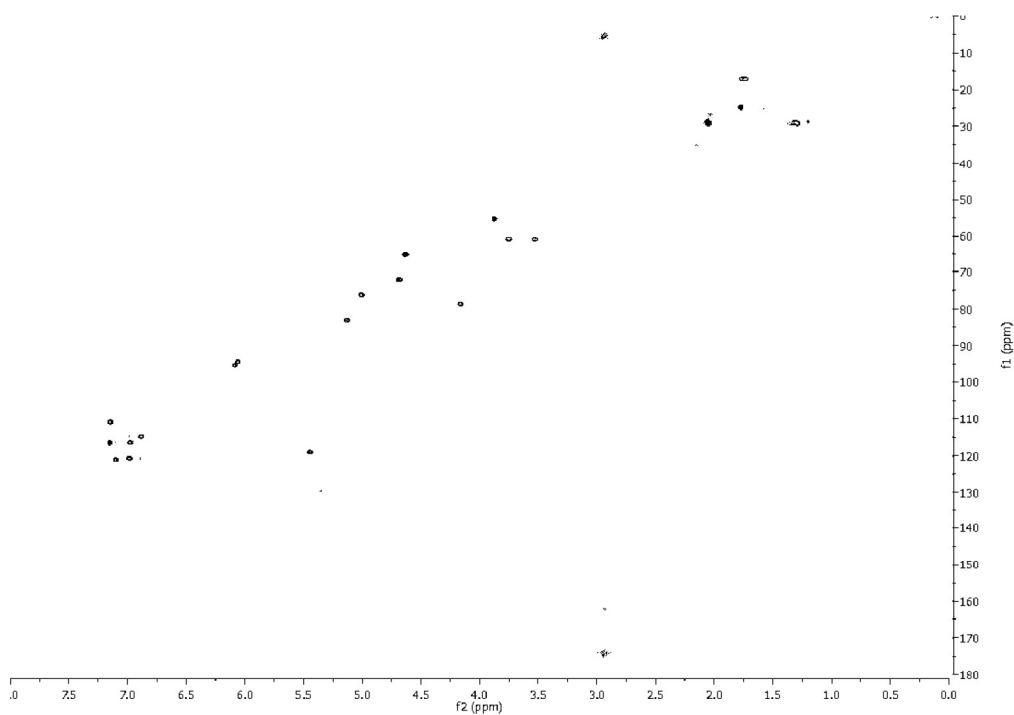
Figure S10: HSQC spectrum of **5b** in acetone-d_6 (600, 150 MHz).

9
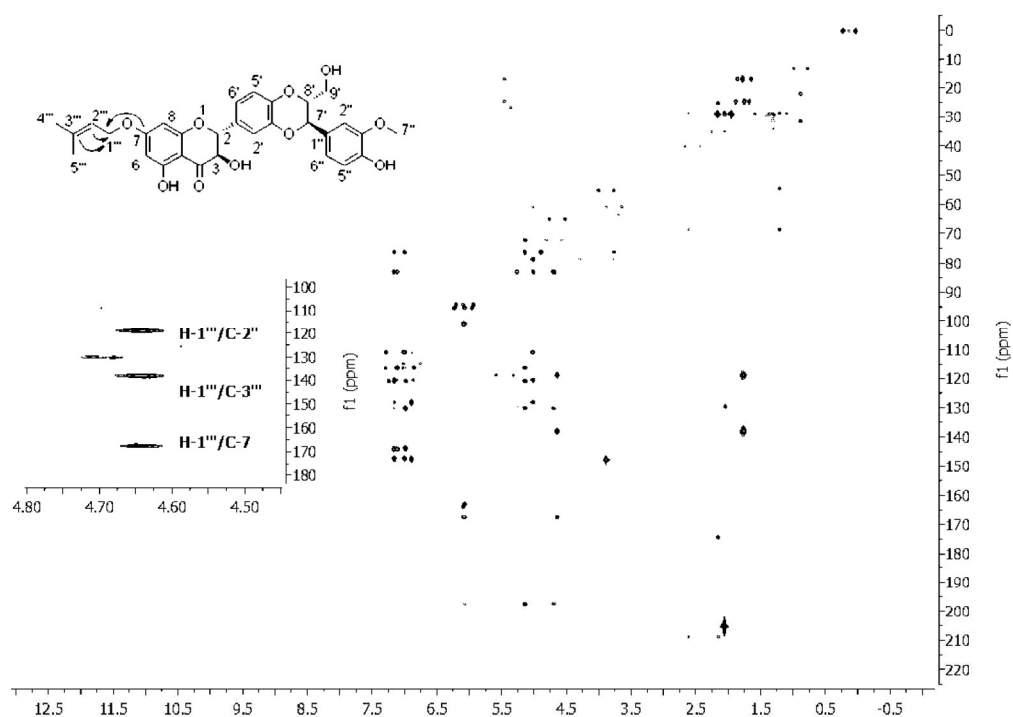
Figure S11: HMBC spectrum of 5b in acetone-d_6 (600, 150 MHz).
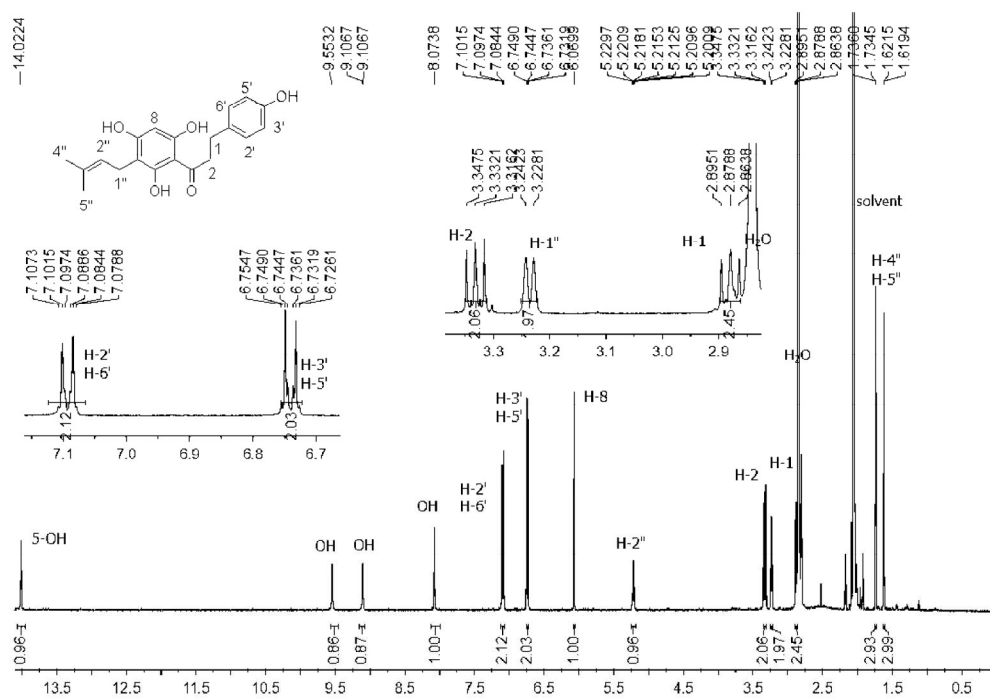
Figure S12: ^{1}H NMR spectrum of 6b in acetone-d_6 (500 MHz).

10
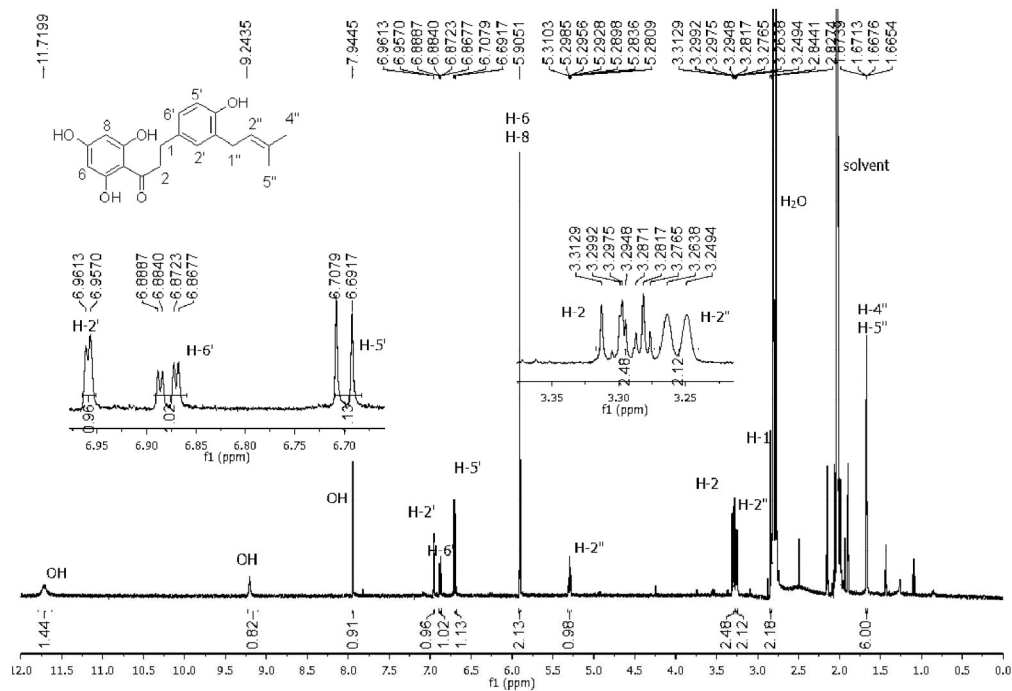
Figure S13: ^{1}H NMR spectrum of 6c in acetone-d_6 (500 MHz).
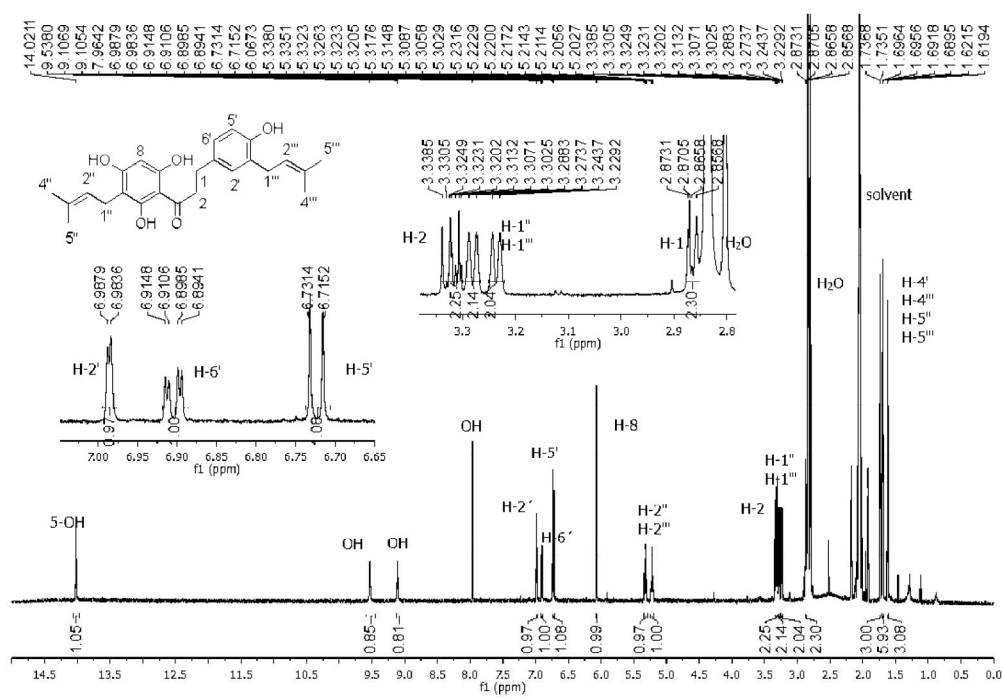
Figure S14: ^{1}H NMR spectrum of 6d in acetone-d_6 (500 MHz).

11
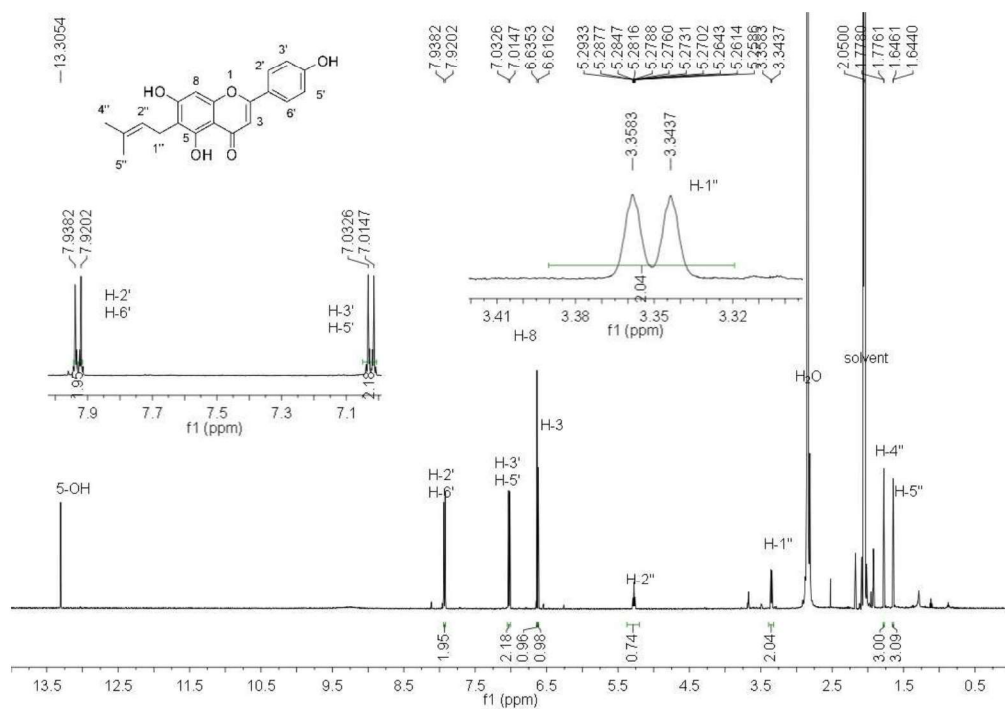
Figure S15: ^{1}H NMR spectrum of 7b in acetone-d_6 (500 MHz).
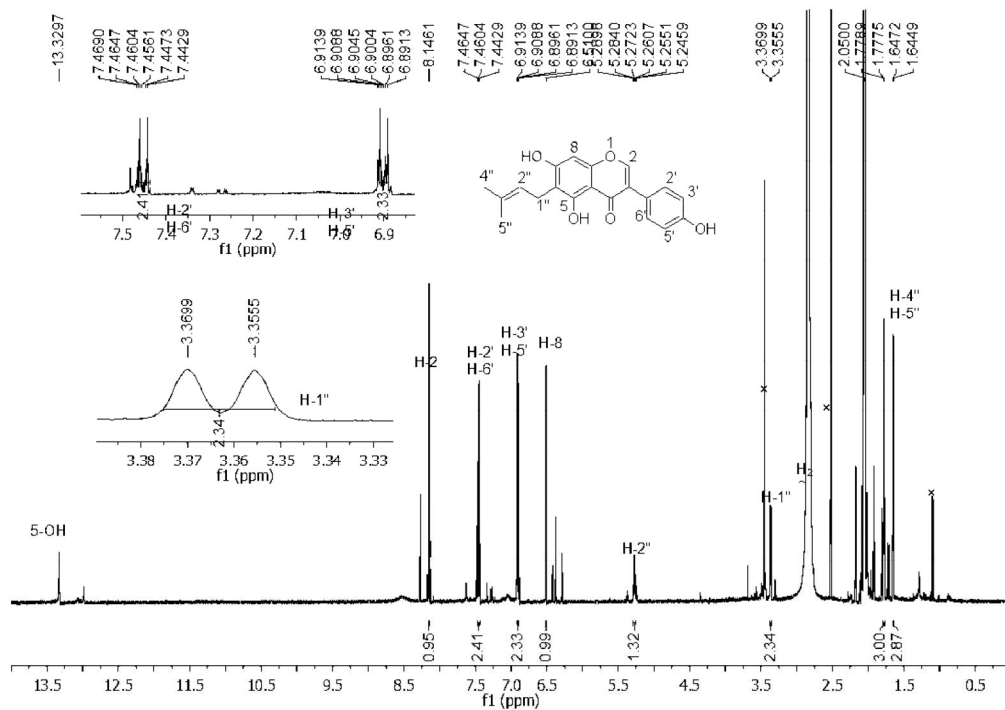
Figure S16: ^{1}H NMR spectrum of 8b in acetone-d_6 (500 MHz).

12
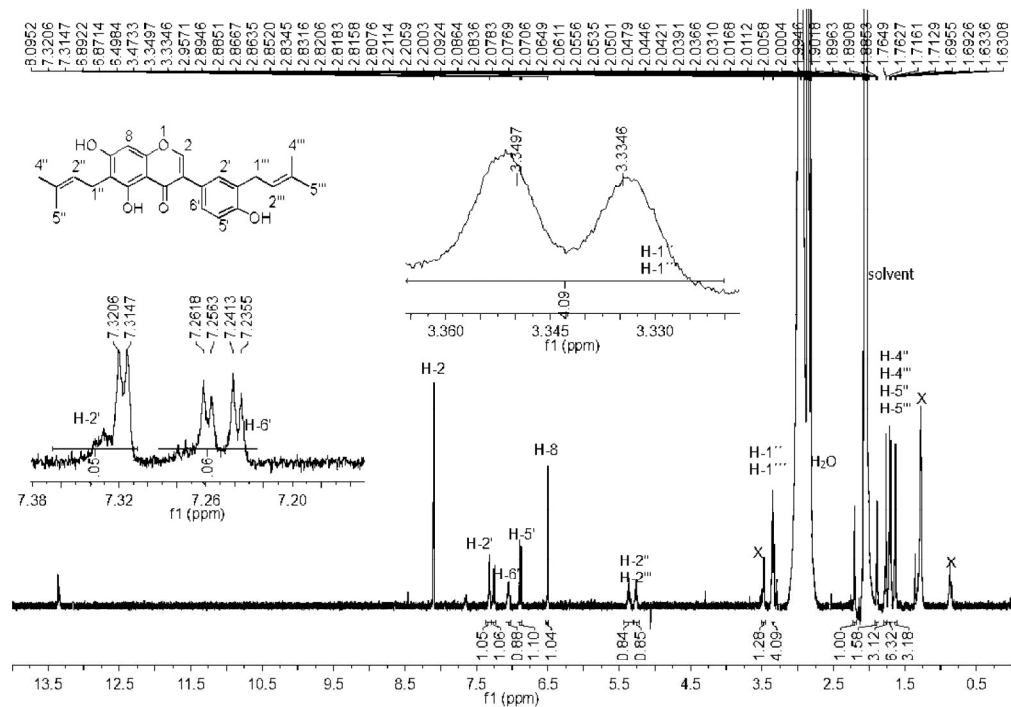
Figure S17: ^{1}H NMR spectrum of **8c** in acetone-d_6 (400 MHz).
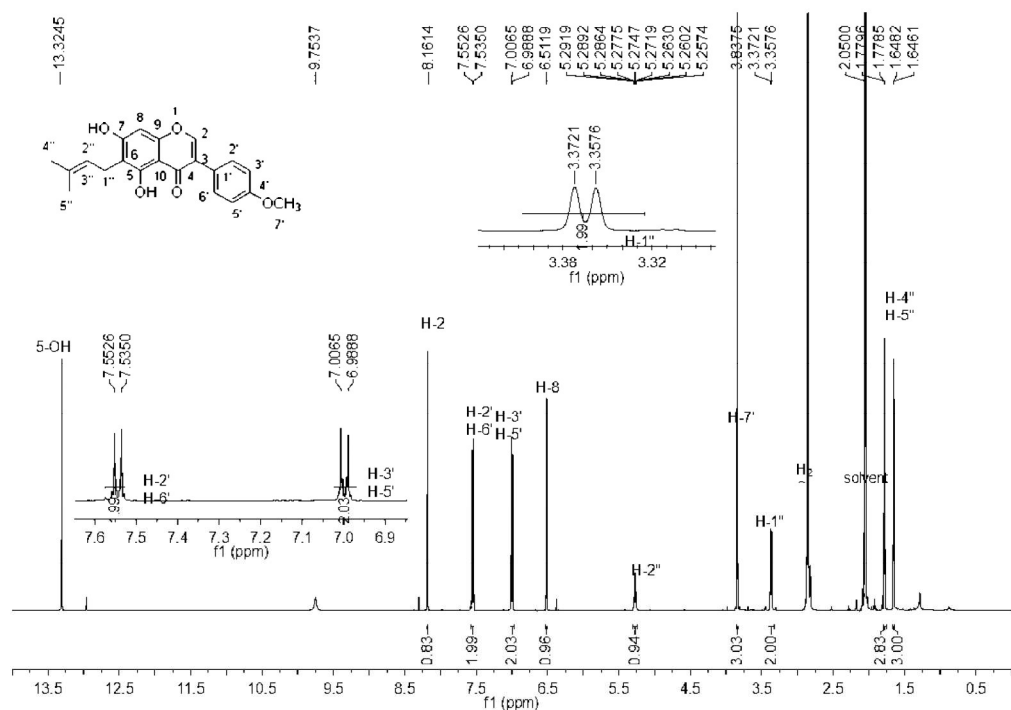
Figure S18: ^{1}H NMR spectrum of **9b** in acetone-d_6 (500 MHz).

13
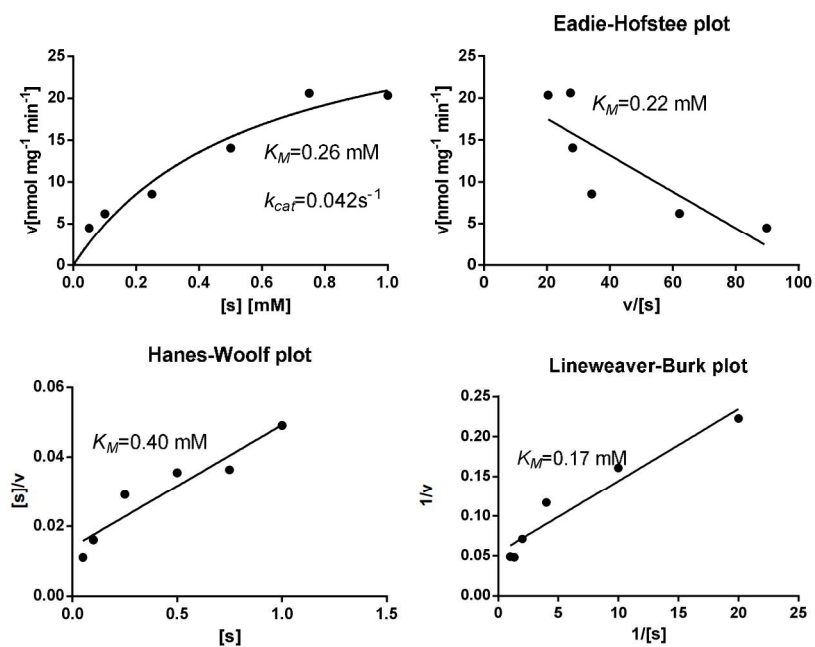
Figure S19: Determination of the kinetic parameters of the AnaPT reaction toward 1a.
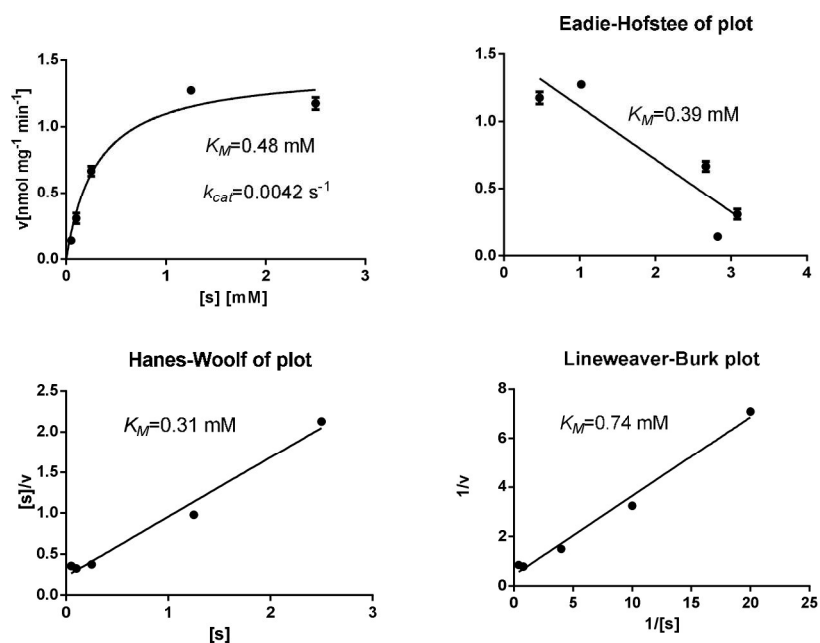
Figure S20: Determination of the kinetic parameters of the AnaPT reaction toward 2a.

14
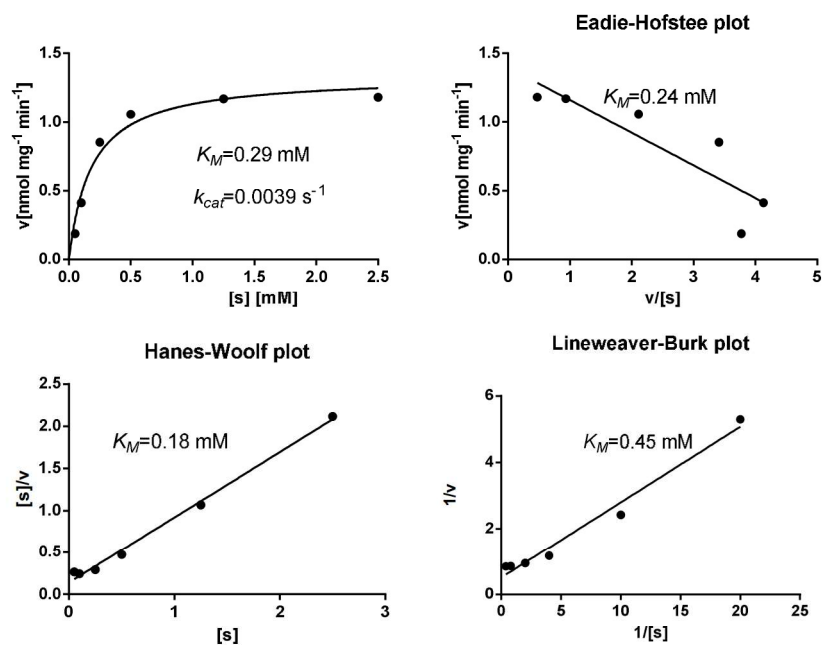
Figure S21: Determination of the kinetic parameters of the AnaPT reaction toward 3a.
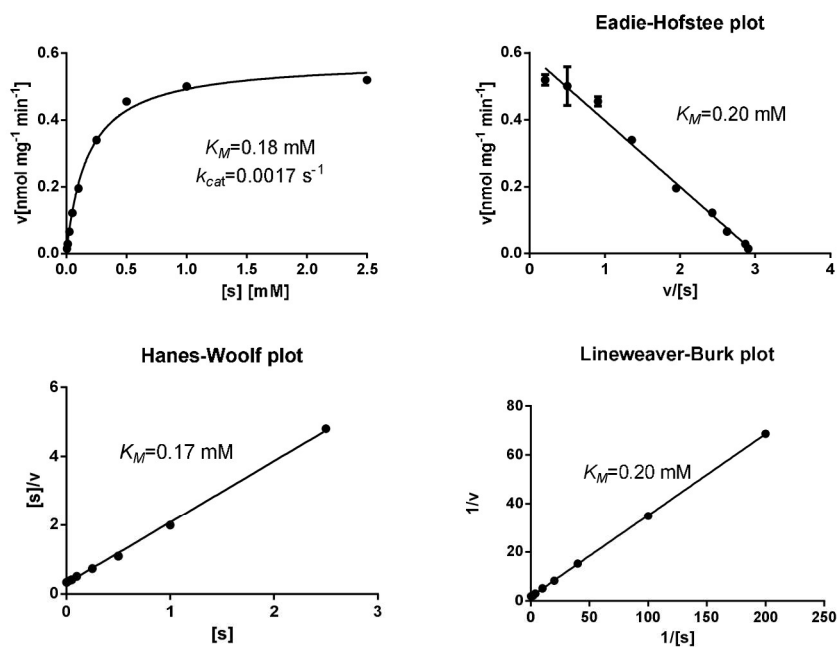
Figure S22: Determination of the kinetic parameters of the AnaPT reaction toward 5a.

15
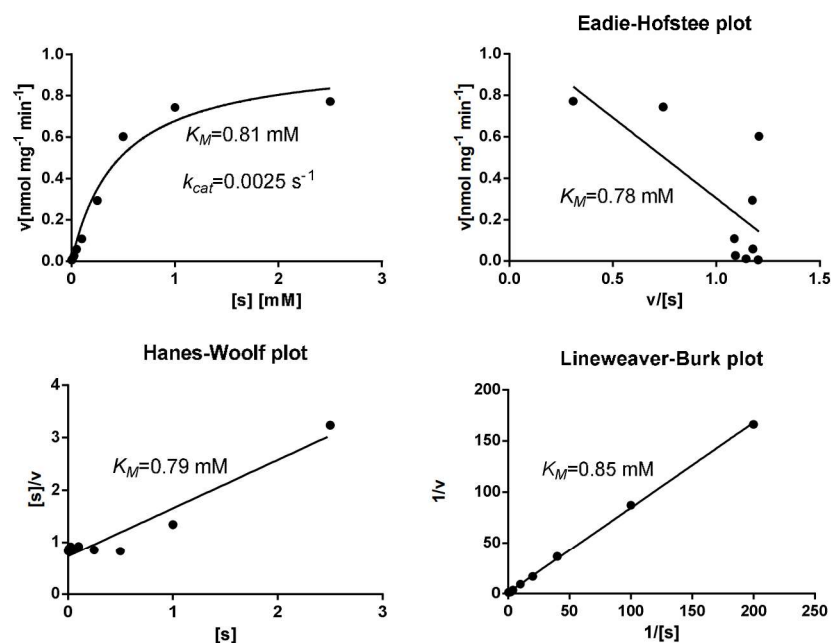
Figure S23: Determination of the kinetic parameters of the AnaPT reaction toward 6a.
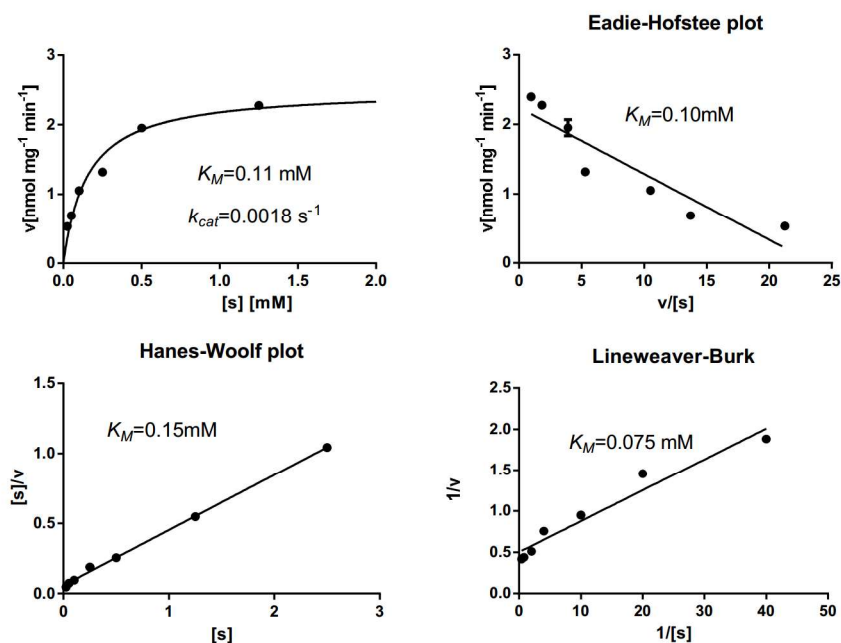
Figure S24: Determination of the kinetic parameters of the AnaPT reaction toward 7a.

16

130
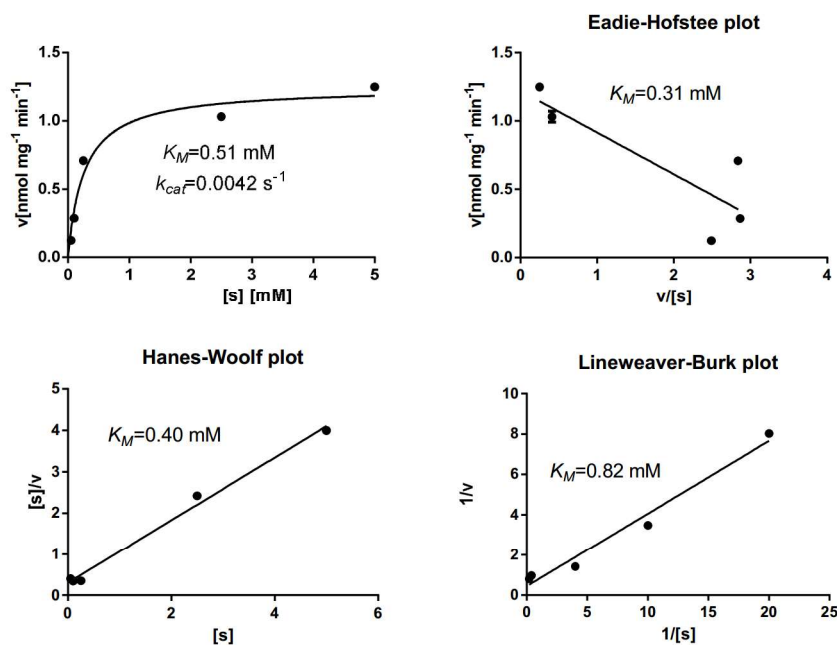
Figure S25: Determination of the kinetic parameters of the AnaPT reaction toward 8a.
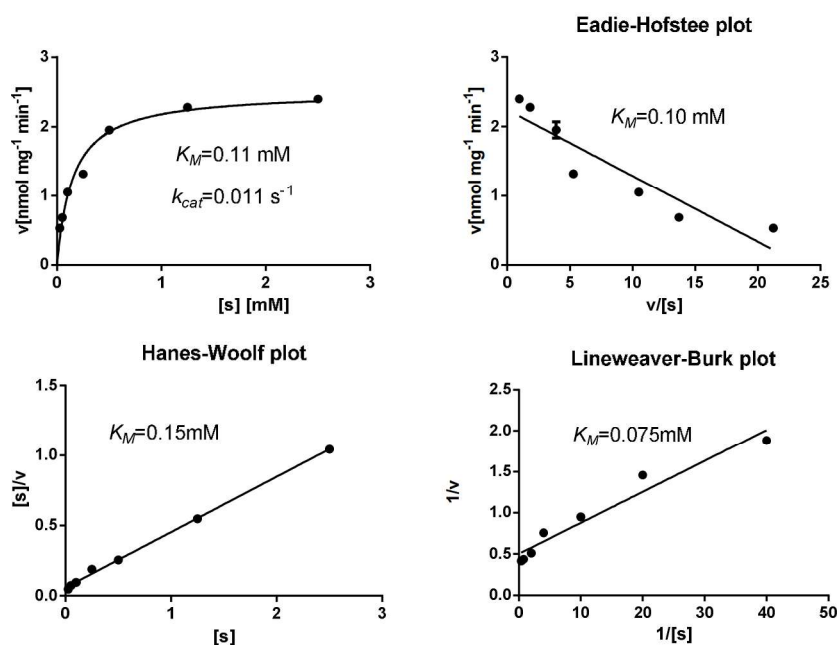
Figure S26: Determination of the kinetic parameters of the AnaPT reaction toward 9a.

17

4.4. Saturation mutagenesis on Tyr205 of the cyclic dipeptide *C2*-prenyltransferase FtmPT1 results in mutants with strongly increased *C3*-prenylating activity

CrossMark

BIOTECHNOLOGICALLY RELEVANT ENZYMES AND PROTEINS

Saturation mutagenesis on Tyr205 of the cyclic dipeptide *C2*-prenyltransferase FtmPT1 results in mutants with strongly increased *C3*-prenylating activity

Kang Zhou[1] · Wei Zhao[2] · Xiao-Qing Liu[2] · Shu-Ming Li[1]

Abstract The fungal indole prenyltransferase FtmPT1 is involved in the biosynthesis of fumitremorgins and catalyzes, in the presence of dimethylallyl diphosphate, a predominant regular prenylation of *cyclo*-L-Trp-L-Pro (brevianamide F) at position C-2 of the indole nucleus. Analysis of the substrate-bound structure of FtmPT1 revealed that brevianamide F forms a hydrogen bond via its carbonyl oxygen in the diketopiperazine moiety with the hydroxyl group of Tyr205 near the center of the prenyltransferase (PT) barrel. In this study, Tyr205 was mutated to 19 other proteinogenic amino acids by one-step site-directed mutagenesis. The obtained mutants were assayed in the presence of dimethylallyl diphosphate with brevianamide F. The enzyme products were isolated on HPLC and their structures were elucidated by NMR and MS analyses. Mutation of Tyr205 to Phe or Met did not change the behavior of FtmPT1 significantly, with regularly *C2*-prenylated brevianamide F as the predominant product. Interestingly, 15 of the obtained mutants also produced regularly *C3*-prenylated brevianamide F, with relative yields between 33 and 110 % of those of the regularly *C2*-prenylated derivatives. Among them, Y205C, Y205L, Y205N, Y205I, and Y205S showed similar brevianamide F consumption. Y205H, Y205Q, Y205V, Y205G, and Y205E showed activities between 47 and 77 % of that of the wild type. These results provide a solid basis for the construction of a brevianamide F regular *C3*-prenyltransferase by site-directed mutagenesis. Assaying stereoisomers of brevianamide F, *cyclo*-D-Trp-D-Pro, *cyclo*-L-Trp-D-Pro, and *cyclo*-D-Trp-L-Pro, with two selected mutants Y205N and Y205L resulted in the formation of reversely *C3*-prenylated derivatives as predominant products, being in sharp contrast to their regularly *C2*- and *C3*-prenylated derivatives with *cyclo*-L-Trp-L-Pro.

Keywords Cyclic dipeptide · Dimethylallyltryptophan synthase · Enzyme catalysis · Friedel–Crafts alkylation · Prenyltransferase · Saturation mutagenesis

✉ Xiao-Qing Liu
liuxq@mail.cnu.edu.cn

✉ Shu-Ming Li
shuming.li@staff.uni-marburg.de

[1] Institut für Pharmazeutische Biologie und Biotechnologie, Philipps-Universität Marburg, 35037 Marburg, Germany

[2] College of Life Sciences, Capital Normal University, No. 105 Xisanhuan Beilu, Beijing 100048, China

Introduction

Prenyl transfer reactions are found ubiquitously in nature and are utilized by living organisms for modifications of both macromolecules like cell membrane components, proteins or tRNAs, and small natural products (Winkelblech et al. 2015). In these reactions, prenyl moieties (nxC_5 units) with different chain lengths are transferred by prenyltransferases from prenyl donors such as dimethylallyl diphosphate (DMAPP, $1x\ C_5$) or geranyl diphosphate (GPP, $2x\ C_5$) to various alphatic or aromatic acceptors. Decoration of small molecule backbone skeletons by prenylation leads often to the generation of biologically active products (Heide 2009; Li 2010; Winkelblech et al. 2015). According to their origins, primary amino acid sequences, biochemical features as well as their structure folding, these enzymes are divided into different subgroups (Winkelblech et al. 2015). The most investigated prenyltransferases in the last decade build the

🖉 Springer

subgroup dimethylallyl tryptophan synthase (DMATS) super-family from microorganisms. DMATS enzymes are soluble proteins, mainly catalyze Friedel–Crafts alkylations by attachment of prenyl moieties to various aromatic acceptors including indole derivatives, and are involved in the biosynthesis of bacterial and fungal secondary metabolites. Until now, more than 40 members of this group have been characterized biochemically (Winkelblech et al. 2015). Twelve of the DMATS enzymes use tryptophan and 14 tryptophan-containing cyclic dipeptides as substrates. Usually, they show significant substrate tolerance toward a large number of aromatic substrates and catalyze regiospecific and stereospecific prenylations on the indole ring. These features make the prenyltransferases useful tools as biocatalysts for production of prenylated products (Fan et al. 2015a). For example, the indole prenyltransferase FtmPT1 from the ascomyceteous fungus *Aspergillus fumigatus* uses DMAPP as prenyl donor and *cyclo*-L-Trp-L-Pro (brevianamide F) as acceptor and catalyzes predominantly a regular *C2*-prenylation (Fig. 1) (Grundmann and Li 2005; Li 2011; Wollinsky et al. 2012). Three fungal indole prenyltransferases, AnaPT, CdpNPT, and CdpC3PT, act as reverse *C3*-prenyltransferases on different cyclic dipeptides, leading to the formation of prenylated pyrrolo[2,3-b]indoles with *anti-cis* or *syn-cis* configuration of the ring systems (Fan et al. 2015a; Schuller et al. 2012; Winkelblech et al. 2015; Yin et al. 2009, 2010; Yu et al. 2013). The indole prenyltransferase ArdB from *Aspergillus fischeri* catalyzes reverse *C3*-prenylation of a tripeptide derivative (Haynes et al. 2013). Regularly *C3*-prenylated cyclic dipeptides and derivatives thereof are rare in nature. Until now, only nocardioazines A and B from *Nocardiopsis* were reported (Raju et al. 2011). Correspondingly, little is known about the responsible prenyltransferases for regular *C3*-prenylation. Recently, a prenyltransferase was identified in the producer of nocardioazines and proven to be responsible for a regular *C3*-prenylation of *cyclo*-L-Trp-L-Trp (Alqahtani et al. 2015). In

comparison to reverse *C3*-prenyltransferases, there is still a deficiency with the availability of regular *C3*-prenyltransferases for application in the chemoenzymatic synthesis or synthetic biology.

Crystal structures of unliganded FtmPT1 from *A. fumigatus* and its ternary complex with brevianamide F and DMSPP, a non-hydrolyzable analogue of DMAPP, were solved in 2010 and used as basis to understand the catalytic mechanism (Jost et al. 2010). As the tryptophan prenyltransferase FgaPT2 (Metzger et al. 2009), FtmPT1 assumes a rare α/β-barrel fold, consisting of ten circularly arranged β-strands surrounded by α-helices, arranged in five structurally similar ααββ repeats. Prenyl transfer reaction is performed in a hydrophobic reaction chamber at the center of the barrel (Jost et al. 2010). Several amino acid residues in FtmPT1 including Gly115 and Tyr205 were proposed to be involved in the binding of brevianamide F. The corresponding residues in FgaPT2 structures are Thr102 and Tyr191 (Jost et al. 2010). Mutation of Gly115 in FtmPT1 redirected the prenylation of brevianamide F from regular *C2*- to reverse *C3*-prenylation (Jost et al. 2010).

The aforementioned FgaPT2 from *A. fumigatus* catalyzes *C4*-prenylation of L-tryptophan (Unsöld and Li 2005), and its structure was solved in 2009 (Metzger et al. 2009). With high protein amount, FgaPT2 was able to catalyze the *C4*-prenylation of five tryptophan-containing cyclic dipeptides (Steffan et al. 2007) and *C3*-prenylation of tyrosine (Fan et al. 2015b). Arg244 was proposed to bind the hydroxylate group of tryptophan (Metzger et al. 2009). Saturation mutagenesis on Arg244 led to identification of 13 mutants, which displayed differentially increased enzyme activities for tryptophan-containing cyclic dipeptides, with up to 76-fold turnover number of that of FgaPT2 (Fan and Li 2016). Lys174 was proposed to abstract one proton from the intermediate cation and to rearomatization for end products (Metzger et al. 2009). FgaPT2_K174F exhibited much higher

Fig. 1 Main reactions catalyzed by FtmPT1 (**a**) and its Tyr205 mutants (**b**)
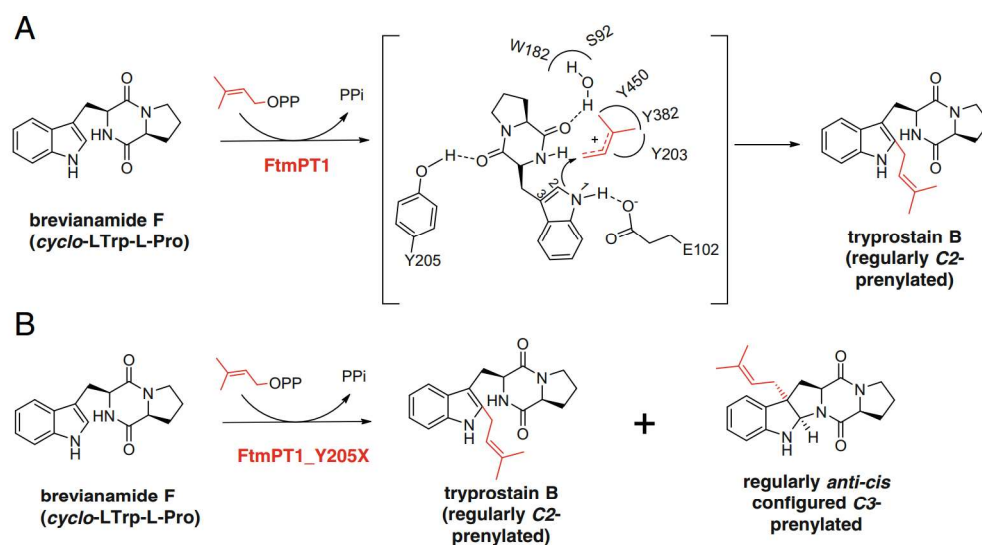
catalytic efficiency toward L-tyrosine than FgaPT2, while its activity toward L-tryptophan was almost abolished (Fan et al. 2015b). These studies demonstrated the potential of site-directed (saturation) mutagenesis on amino acid residues in the active center for creation of new biocatalysts.

Tyr205 in FtmPT1 was proposed in a previous study (Jost et al. 2010) to be involved in the hydrogen bond formation via its hydroxyl group with the keto group of the diketopiperazine moiety in brevianamide F. The corresponding residue Tyr191 and the aforementioned Arg244 in FgaPT2 interact with the carboxyl residue of the tryptophan side chain (Jost et al. 2010). We proposed that the location and orientation of brevianamide F in the reaction chamber can be influenced by replacement of Tyr205 with other amino acids, which could result in the formation of mutants with different enzyme activities.

Materials and methods

Chemicals

DMAPP was synthesized according to the method described for geranyl diphosphate reported previously (Woodside et al. 1988). Synthesis of cyclic dipeptides was described elsewhere (Yu et al. 2013).

Bacterial strains, plasmids, and culture conditions

Escherichia coli XL1-Blue MRF'(Stratagene, Heidelberg, Germany) was used for cloning and expression experiments. pAG12 containing *ftmPT1* in pQE70 was constructed previously (Grundmann and Li 2005) and used as expression vector for FtmPT1 and as DNA template for site-directed mutagenesis experiments. *E. coli* cells harboring plasmids were grown in liquid lysogeny broth (LB) medium and on solid LB medium with 1.5 % (*w/v*) agar at 37 °C. Fifty micrograms carbenicillin per milliliter was used for selection of recombinant *E. coli* strains.

Site-directed mutagenesis

One-step site-directed mutagenesis protocols (Olafsen et al. 2006) with degenerated primers at bps 613–615 were used to generate mutants of FtmPT1 listed in Table 1. The Expand Long Template PCR system (Roche Diagnostics, Mannheim, Germany) was used for plasmids pWZ1–pWZ18, pST3, and pKZ27. pWZ2 was used as template for construction of the double mutant G115T_Y205N. PCR were carried out in 50-μL reactions containing 3.75 U of DNA polymerase mix, 200–600 ng plasmid DNA, 15 pmol of each primer, and 35 pmol dNTPs. Reactions were run for 20 cycles at 94 °C for 40 s, 55–65 °C for 1 min, and 68 °C for 6 min as

well as an additional 7 min at 68 °C (Table S1 in Electronic Supplementary Material). PCR mixtures were digested with *DpnI* and subsequently transformed into *E. coli* XL1-Blue MRF'. The obtained plasmids were isolated and subjected to sequencing to confirm the desired mutations in the respective constructs.

Overproduction and purification of the recombinant proteins

Protein overproduction and purification of FtmPT1 and its Tyr205 mutants were carried out as described previously (Grundmann and Li 2005) and analyzed on SDS-PAGE (Fig. S1 in Electronic Supplementary Material). Protein concentration was estimated by measurement of the absorption at 280 nm on a NanoDrop 2000c UV–vis spectrophotometer and by comparison of their intensities with those of protein markers on SDS-PAGE.

Enzyme assays with purified recombinant proteins

The enzyme assays (100 μL) contained cyclic dipeptide (1 mM), $CaCl_2$ (10 mM), DMAPP (2 mM), glycerol (0.2–5.0 % *v/v*), dimethyl sulfoxide (DMSO, 5 % *v/v*), Tris-HCl (50 mM, pH 7.5), and purified recombinant protein (5 μg). The reaction mixtures were incubated at 37 °C for 2 h and terminated by addition of 100 μL methanol. The proteins were removed by centrifugation at 13,000 rpm for 20 min. The supernatants were analyzed on HPLC described below and the results are given in Table 2. For analysis on LC–MS, the reaction mixtures were extracted twice with double volume of ethyl acetate. The organic phases were combined and evaporated under reduced pressure to afford the residues, which were dissolved in 100 μL methanol and analyzed on LC–MS. Assays for isolation of the enzyme products were carried out in large scales (10–15 mL) containing cyclic dipeptide (1 mM), DMAPP (2 mM), $CaCl_2$ (10 mM), glycerol (0.2–5.0 % *v/v*), DMSO (5 % *v/v*), Tris-HCl (50 mM, pH 7.5), and 3–8 mg recombinant proteins per 10–15 mL incubation mixtures. After incubation for 16 h at 37 °C, the reaction mixtures were extracted four times with double volume of ethyl acetate. The organic phases were combined and evaporated. The residues were dissolved in methanol (0.5–1.0 mL) and purified on a preparative HPLC. Assays for determination of kinetic parameters (100 μL) contained $CaCl_2$ (10 mM), glycerol (0.2–5.0 % *v/v*), DMSO (5 % *v/v*), Tris-HCl (50 mM, pH 7.5), DMAPP (2 mM), **1a–4a** at final concentrations of up to 2.0 mM, and different amounts of proteins (Table 3). The reaction mixtures were incubated within the linear range of the product formation for different times (Table 3) and terminated with 100 μL methanol. Proteins were removed by centrifugation at 13,000 rpm for 20 min, and the supernatants were analyzed on HPLC.

Table 1 Mutated derivatives of FtmPT1 at Tyr205 and respective primers used for site-directed mutagenesis

Sequence(5′–3′)	Bases at 613–615	Mutant	Plasmid	Protein yield (mg/L of culture)
fw GCGTATTTC**NNN**CCGCAGCCCAAATCTGC rev GGGCTGCGG**NNN**GAAATACGCCTTGACCAG	ATA	**FtmPT1_Y205I**	pWZ1	2.6
	AAT	**FtmPT1_Y205N**	pWZ2	5.3
	GCG	**FtmPT1_Y205A**	pWZ3	0.6
	ACA	**FtmPT1_Y205T**	pWZ4	0.2
	GTA	**FtmPT1_Y205V**	pWZ5	0.6
fw GCGTATTTC**CNN**CCGCAGCCCAAATCTGC rev GGGCTGCGG**NNG**GAAATACGCCTTGACCAG	CAG	**FtmPT1_Y205Q**	pWZ6	0.6
	CGG	**FtmPT1_Y205R**	pWZ7	1.5
	CAC	**FtmPT1_Y205H**	pWZ8	3.1
	CCA	**FtmPT1_Y205P**	pWZ9	0.7
	CTC	**FtmPT1_Y205L**	pWZ10	4.3
fw GCGTATTTC**NGN**CCGCAGCCCAAATCTGC rev GGGCTGCGG**NCN**GAAATACGCCTTGACCAG	AGT	**FtmPT1_Y205S**	pWZ11	4.4
	TGG	**FtmPT1_Y205W**	pWZ12	5.8
	GGC	**FtmPT1_Y205G**	pWZ13	0.9
fw GCGTATTTC**RWS**CCGCAGCCCAAATCTGC rev GGGCTGCGG**SWY**GAAATACGCCTTGACCAG	GAC	**FtmPT1_Y205D**	pWZ14	4.6
	GAG	**FtmPT1_Y205E**	pWZ15	5.8
fw GCGTATTTC**TGT**CCGCAGCCCAAATCTGC rev GGGCTGCGG**ACA**GAAATACGCCTTGACCAG	TGT	**FtmPT1_Y205C**	pWZ16	8.7
fw GCGTATTTC**AWG**CCGCAGCCCAAATCTGC rev GGGCTGCGG**CWT**GAAATACGCCTTGACCAG	ATG	**FtmPT1_Y205M**	pWZ17	2.5
	AAG	**FtmPT1_Y205K**	pWZ18	5.0
fw GCGTATTTC**TTC**CCGCAGCCCAAATCTGC rev GGGCTGCGG**GAA**GAAATACGCCTTGACCAG	TTC	**FtmPT1_Y205F**	pST3	3.0
fw GATTCGAATT**AC**GGTTGATCCCGTCACGGC- TGACTCTGGC rev GGGATCAAC**GT**AATTCGAATCAACGC- CCGAGCGACG	ACG[a]	**FtmPT1_G115T_Y205N**	pKZ27	2.8

pAG 12 was used as DNA template for site-directed mutagenesis experiments of the single mutants and pWZ2 as DNA template for preparation of FtmPT1_G115T_Y205N

Analysis of enzyme products by HPLC, LC–MS, and NMR

An Agilent HPLC series 1200 (Böblingen, Germany) was used for analysis and isolation of the enzyme products. Analysis of the enzyme products was performed on an Agilent Eclipse XDB-C$_{18}$ column (150 × 4.6 mm, 5 μm) with a linear gradient of 5–100 % (v/v) methanol (solvent B) in water (solvent A) in 40 min and a flow rate at 0.5 mL/min. The column was then washed with 100 % (v/v) solvent B for 5 min and equilibrated with 5 % (v/v) solvent B for 5 min. The enzyme products were isolated on a Multospher 120 RP18 column (250 × 10 mm, 5 μm, C+S Chromatographie Service, Langerwehe, Germany) with a linear gradient of 10–50 % B in A in 30 min and a flow rate at 2.5 mL/min. After each run, the column was equilibrated with 10 % solvent B for 10 min. The HPLC chromatograms of the incubation mixtures of **1a** with FtmPT1 and its Tyr205 mutants are illustrated in Fig. S2 in Electronic Supplementary Material.
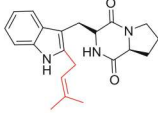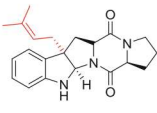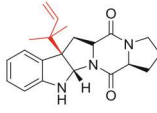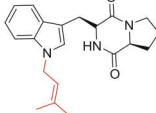
MS spectra were obtained with a micrOTOF-Q III spectrometer (Bruker, Bremen, Germany) with an ESI source. The spectrometer was equipped with an Agilent 1260 HPLC system. The LC–MS chromatograms of incubation mixtures of **1a**–**4a** with Y205N are provided in Figs. S3–S6 in Electronic Supplementary Material. ^{1}H NMR spectra were recorded at room temperature on an ECX-400 or 500 spectrometer (JEOL, Tokyo, Japan). Chemical shifts were referenced to the solvent signal at 7.26 ppm for CHCl$_3$. All spectra were processed with MestReNov. 5.2.2 (Metrelab Research, Santiago de Compostela, Spain).

Compound **1c** t_R = 35.4 min; UV (extracted from PDA) (MeOH/H$_2$O) λmax 243, 296 nm; MS: m/z 352.2038 ([M+ H]$^+$, calculated for C$_{21}$H$_{26}$N$_3$O$_2$: 352.2020). ^{1}H NMR (500 Hz, CDCl$_3$) δ_H 7.10 (dd, 1H, J = 7.4 and 1.4 Hz, H-4), 7.09 (t, 1H, J = 7.4 Hz, H-6), 6.78 (t, 1H, J = 7.4 Hz, H-5), 6.61 (dd, 1H, J = 7.4 and 0.8 Hz, H-7), 5.24 (s, 1H, H-2), 5.17 (br t, 1H, J = 7.5 Hz, H-2'), 4.06 (m, 2H, H-11 and H-14), 3.53 (m, 2H, H-17), 2.64 (dd, 1H, J = 13.0 and 6.4 Hz, H-10), 2.36 (m, 3H, H-1'and H-10), 2.30 (m, 1H, H-19), 2.13 (m, 1H, H-18), 2.04 (m, 1H, H-18), 1.89 (m, 1H, H-19), 1.70 (s, 3H, H-4'), 1.52 (s, 3H, H-5'). These data correspond well to those in literature (Caballero et al. 2003).

Compound **2d** t_R = 34.7 min; UV (extracted from PDA) (MeOH/H$_2$O) λmax 240, 296 nm; MS: m/z 352.2009 ([M+

Table 2 Substrate consumption and product yields (%) of brevianamide F prenylation catalyzed by FtmPT1 and its mutants

WT/mutant	Substrate consumption	C2-regularly prenylated (1b)	C3-regularly prenylated (1c)	Relative yield 1c/1b	C3-reversely prenylated (1d)	N1-regularly prenylated (1e)
FtmPT1 (WT)	98.3 ± 0.1	96.2 ± 0.2	N.D.	–	N.D.	2.1 ± 0.2
FtmPT1_Y205F	97.0 ± 0.1	90.6 ± 0.3	3.5 ± 0.2	0.04 %	N.D.	2.9 ± 0.1
FtmPT1_Y205C	96.2 ± 0.1	66.1 ± 0.7	26.1 ± 0.6	39.5 %	N.D.	4.0 ± 0.1
FtmPT1_Y205L	95.9 ± 0.2	56.4 ± 0.1	31.8 ± 0.1	56.4 %	N.D.	7.7 ± 0.1
FtmPT1_Y205M	95.8 ± 0.1	84.5 ± 0.4	8.3 ± 0.2	9.8 %	N.D.	2.8 ± 0.1
FtmPT1_Y205N	94.4 ± 0.1	51.6 ± 0.1	35.6 ± 0.2	70.0 %	2.8±0.1	4.4 ± 0.1
FtmPT1_Y205I	93.8 ± 0.2	64.0 ± 0.7	25.3 ± 0.6	39.5 %	N.D.	4.5 ± 0.2
FtmPT1_Y205S	93.3 ± 0.9	57.5 ± 0.9	29.0 ± 0.1	50.4 %	1.8±0.6	5.0 ± 0.1
FtmPT1_Y205H	76.4 ± 0.6	44.5 ± 0.1	27.0 ± 0.3	60.7 %	N.D.	4.9 ± 0.1
FtmPT1_Y205Q	69.1 ± 0.2	49.3 ± 2.2	16.6 ± 1.1	33.7 %	N.D.	3.2 ± 0.2
FtmPT1_Y205V	66.7 ± 1.3	47.3 ± 2.1	15.6 ± 1.3	33.0 %	N.D.	3.8 ± 0.1
FtmPT1_Y205G	49.0 ± 3.2	17.4 ± 1.3	16.0 ± 1.7	92.0 %	12.2±1.1	3.4 ± 0.4
FtmPT1_Y205E	46.9 ± 2.9	25.7 ± 1.9	14.8 ± 0.5	57.6 %	3.0±0.2	3.2 ± 0.2
FtmPT1_Y205W	36.5 ± 2.1	30.0 ± 2.3	N.D.	–	N.D.	6.5 ± 0.6
FtmPT1_Y205A	32.0 ± 2.0	17.5 ± 2.6	12.3 ± 2.7	70.3 %	N.D.	2.2 ± 0.4
FtmPT1_Y205R	28.2 ± 0.4	7.4 ± 0.1	5.7 ± 0.2	77.0 %	13.2±0.1	1.9 ± 0.1
FtmPT1_Y205K	21.1 ± 1.5	8.9 ± 0.5	9.8 ± 0.5	110 %	1.6±0.3	0.8 ± 0.1
FtmPT1_Y205D	20.5 ± 3.3	9.5 ± 1.8	5.3 ± 0.8	55.8 %	3.6±0.7	2.1 ± 0.4
FtmPT1_Y205P	17.9 ± 1.0	12.9 ± 0.8	5.0 ± 0.6	38.7 %	N.D.	N.D.
FtmPT1_Y205T	12.7 ± 0.5	12.7 ± 0.9	N.D.	–	N.D.	N.D.

The data are means of two independent measurements

N.D. not detected

Table 3 Kinetic parameters of FtmPT1, Y205N, and Y205L reactions

Enzymes	Protein amount and incubation time	Substrates	K_M [mM]	k_{cat} [s^{-1}]	k_{cat}/K_M [s^{-1} M^{-1}]
FtmPT1	1.0 μg, 5 min	cyclo-L-Trp-L-Pro (1a)	0.057 ± 0.00021	8.91 ± 0.064	156,316
Y205N	1.0 μg, 45 min	cyclo-L-Trp-L-Pro (1a)	0.11 ± 0.0026	1.36 ± 0.074	12,364
	2.5 μg, 60 min	cyclo-D-Trp-D-Pro (2a)	0.32 ± 0.0010	0.25 ± 0.016	781
	1.0 μg, 5 min	cyclo-L-Trp-D-Pro (3a)	0.62 ± 0.042	0.32 ± 0.011	516
	5.0 μg, 30 min	cyclo-D-Trp-L-Pro (4a)	0.40 ± 0.029	0.21 ± 0.011	525
Y205L	1.0 μg, 30 min	cyclo-L-Trp-L-Pro (1a)	0.19 ± 0.0031	4.26 ± 0.0098	22,421
	2.5 μg, 10 min	cyclo-D-Trp-D-Pro (2a)	0.28 ± 0.0093	1.39 ± 0.10	4964
	2.5 μg, 10 min	cyclo-L-Trp-D-Pro (3a)	0.083 ± 0.014	0.18 ± 0.018	2169
	2.5 μg, 45 min	cyclo-D-Trp-L-Pro (4a)	0.46 ± 0.023	0.41 ± 0.009	891

H]$^+$, calculated for $C_{21}H_{26}N_3O_2$: 352.2020). ^{1}H NMR (400 Hz, CDCl$_3$) δ_H 7.17 (dd, 1H, J = 7.6 and 0.8 Hz, H-4), 7.07 (t, 1H, J = 7.6 Hz, H-6), 6.73 (t, 1H, J = 7.6 Hz, H-5), 6.55 (d, 1H, J = 7.6 Hz, H-7), 5.95 (dd, 1H, J = 16.7 and 10.2 Hz, H-2'), 5.39 (s, 1H, H-2), 5.15 (dd, 1H, J = 10.2 and 1.2 Hz, H-1'), 5.12 (dd, 1H, J = 16.7 and 1.2 Hz, H-1'), 4.16 (t, 1H, J = 8.7, H-11), 4.09 (ddd, 1H, J = 9.0, 7.3, and 1.7 Hz, H-14), 3.43 (m, 2H, H-17), 2.79 (dd, 1H, J = 14.0 and 8.9 Hz, H-10), 2.55 (dd, 1H, J = 14.0 and 8.9 Hz, H-10), 2.32 (m, 1H, H-19), 2.05 (m, 1H, H-19), 1.97 (m, 1H, H-18), 1.87 (m, 1H, H-18), 1.14 (s, 3H, H-4'), 0.99 (s, 3H, H-5'). ^{1}H NMR data correspond well to those in literature (Yu et al. 2013).

Compound **3d** t_R = 34.0 min; UV (extracted from PDA) (MeOH/H$_2$O) λmax 250, 296 nm; MS: m/z 352.2016 ([M+ H]$^+$, calculated for $C_{21}H_{26}N_3O_2$: 352.2020). ^{1}H NMR (400 Hz, CDCl$_3$) δ_H 7.17 (d, 1H, J = 7.5 Hz, H-4), 7.08 (t, 1H, J = 7.6 Hz, H-6), 6.74 (t, 1H, J = 7.6 Hz, H-5), 6.56 (d, 1H, J = 7.6 Hz, H-7), 5.93 (dd, 1H, J = 17.6 and 11.2 Hz, H-2'), 5.70 (s, 1H, H-2), 5.12 (d, 1H, J = 11.2 Hz, H-1'), 5.08 (d, 1H, J = 17.6 Hz, H-1'), 4.02 (ddd, 1H, J = 11.7, 5.7, and 1.8 Hz, H-14), 3.97 (ddd, 1H, J = 12.0, 5.3, and 1.8 Hz, H-11), 3.90 (m, 1H, H-17), 3.29 (m, 1H, H-17), 2.51 (dd, 1H, J = 12.0 and 5.3 Hz, H-10), 2.40 (m, 1H, H-19), 2.31 (t, 1H, J = 12.0 Hz, H-10), 1.97 (m, 1H, H-18), 1.88 (m, 1H, H-18), 1.76 (m, 1H, H-19), 1.12 (m, 3H, H-4'), 1.00 (s, 3H, H-5'). ^{1}H NMR data correspond well to those in literature (Yu et al. 2013).

Compound **4d** t_R = 34.0 min; UV (extracted from PDA) (MeOH/H$_2$O) λmax 250, 296 nm; MS: m/z 352.2013 ([M+ H]$^+$, calculated for $C_{21}H_{26}N_3O_2$: 352.2020). ^{1}H NMR (400 Hz, CDCl$_3$) δ_H 7.17 (d, 1H, J = 7.6 Hz, H-4), 7.08 (t, 1H, J = 7.6 Hz, H-6), 6.74 (t, 1H, J = 7.6 Hz, H-5), 6.56 (d, 1H, J = 7.6 Hz, H-7), 5.92 (dd, 1H, J = 17.7 and 11.2 Hz, H-2'), 5.70 (s, 1H, H-2), 5.12 (d, 1H, J = 11.2 Hz, H-1'), 5.06 (d, 1H, J = 17.7 Hz, H-1'), 4.02 (m, 1H, H-14), 3.96 (m, 1H, H-11), 3.90 (m, 1H, H-17), 3.27 (m, 1H, H-17), 2.51 (dd, 1H, J = 12.0 and 5.4 Hz, H-10), 2.41 (m, 1H, H-19), 2.31 (t, 1H, J = 12.0 Hz, H-10), 1.97 (m, 1H, H-18), 1.89 (m, 1H, H-18), 1.76 (m, 1H, H-19) 1.12 (m, 3H, H-4'), 1.00 (s, 3H, H-5'). ^{1}H NMR data correspond well to those in literature (Yu et al. 2013).

Results

Generation of Tyr205 mutants by saturation mutagenesis with degenerated primers

To generate Tyr205 mutants, saturation mutagenesis experiments were carried out by site-directed mutagenesis using the expression construct pAG12 (Grundmann and Li 2005) as template. Different oligo nucleotides with wobbles at base pairs of 613 to 615 were used as degenerated primer pairs (Table 1). After identification of ten mutants amplified by using primers containing NNN or CNN at these positions,

the remained mutants were obtained with more specific primers (Table 1). Finally, all 19 mutations at Tyr205 were constructed and used for expression.

Overproduction and purification of the obtained mutants

Under the conditions for FtmPT1 overproduction (Grundmann and Li 2005), protein yields between 5.0 and 9 mg/L of culture were obtained for five mutants, Y205N, Y205W, Y205E, Y205C, and Y205K. These values are significantly lower than 20 mg/L culture reported previously for FtmPT1 (Grundmann and Li 2005), for which 10.6 mg/L culture was calculated in this study. Protein yields between 1 and 5 mg/L culture were estimated for nine mutants, Y205I, Y205R, Y205H, Y205L, Y205S, Y205D, Y205M, Y205F, and G115T_Y205N. Protein yields of lower than 1 mg/L culture were found for six other mutants. SDS-PAGE analysis revealed that 12 mutants, Y205N, Y205L, Y205F, Y205I, Y205M, Y205R, Y205S, G115T_Y205N, Y205G, Y205H, Y205Q, and Y205C, were purified to near homogeneity. Predominant bands with expected size were observed for other mutants (Fig. S1 in Electronic Supplementary Material).

Mutation on Tyr205 redirected partially the prenylation position of brevianamide F

Brevianamide F was incubated in the presence of 2 mM DMAPP with 5 μg of purified FtmPT1 or its 19 Tyr205 single mutants at 37 °C for 2 h. Under the HPLC conditions used in this study, the enzyme products were separated very well from each other (Fig. S2 in Electronic Supplementary Material) and the chromatograms were highly reproducible. The results of the 19 mutants can be categorized in different groups. The first group consisting of Y205F and Y205M showed one predominant product peak **1b** at 33.0 min with comparable enzyme activity to FtmPT1. By comparison of retention times, UV, and NMR spectra, this peak was identified as the regularly *C2*-prenylated derivative, i.e., the identical product as FtmPT1 itself. Y205W and Y205T also converted brevianamide F mainly to the regularly *C2*-prenylated product, but with much lower enzyme activities.

In the HPLC chromatograms of 15 other mutants, two or more product peaks were detected. With an exception for the assay with Y205R, the regularly *C2*-prenylated brevianamide F (**1b**) at 33.0 min was still detected as the major product. Interestingly, **1c** at 35.4 min was observed as the second predominant product peak in reaction mixtures of most mutants. This peak was identified as a regularly *anti-cis*-configured *C3*-prenylated brevianamide F by isolation and interpretation of its ^{1}H NMR spectrum (see below for structure elucidation). Relative yields of **1c** to **1b** were determined between 33 and 110 % (Table 2). Five mutants, Y205C, Y205L, Y205N, Y205I, and Y205S, showed similar enzyme activity as the

wild type with substrate consumption of more than 90 % under the tested conditions. The relative product yields of **1c** to **1b** varied from 39 to 70 % in the reaction mixtures of these mutants (Table 2). Five mutants, Y205H, Y205Q, Y205V, Y205G, and Y205E, showed lower enzyme activity with substrate consumption between 46.9 and 76.4 %. The relative product yields of **1c** to **1b** were found between 33 and 92 %. Other mutants like Y205A, Y205R, Y205K, Y205D, and Y205P accepted brevianamide F with significantly reduced activities. In addition to the regularly *C2*-prenylated derivative **1b** and the regularly *C3*-prenylated **1c**, product peaks **1d** at 34.8 min and **1e** at 35.8 min were also detected in the reaction mixtures of most mutants (Fig. S2 in Electronic Supplementary Material). By comparing their retention times and UV and NMR spectra with those of authentic compounds, these two products were identified as reversely *C3*-prenylated and regularly *N1*-prenylated derivatives, respectively. With an exception for those in the reaction mixture of Y205G, **1d** and **1e** were found as minor products with product yields of less than 5 % in most cases. In the case of Y205G, the ratio of **1b:1c:1d:1e** was calculated to be 5.1:4.7:3.6:1.

Structure elucidation of the detected enzyme products

As aforementioned, **1b, 1d,** and **1e** were identified, by comparing their retention times and UV spectra with those of authentic samples, as regularly *C2*-, reversely *C3*-, and regularly *N1*-prenylated derivatives of **1a**, respectively. For structure confirmation of the enzyme products, we carried out large-scale overnight incubations (10–15 mL) of **1a** with five selected mutants, Y205I, Y205C, Y205S, Y205L, and Y205N. The reaction mixtures were extracted with ethyl acetate, and the obtained organic phases were evaporated to dryness and subjected to ^{1}H NMR analysis. As shown in Fig. S7 in Electronic Supplementary Material, the spectra of these mixtures are very similar, indicating the presence of the same or similar products. Due to different product yields and ratios, the signal intensities of these products differed from each other in the mixtures. Comparison with NMR data of known products confirmed the presence of the regularly *C2*-prenylated (**1b**), the reversely *C3*-prenylated (**1d**), and the regularly *N1*-prenylated derivative (**1e**) (Grundmann and Li 2005; Jost et al. 2010; Yin et al. 2007; Yu et al. 2013). LC–MS analysis of the reaction mixture of **1a** with Y205N (Fig. S3 in Electronic Supplementary Material) also confirmed the peaks at 23.0, 23.8, and 24.8 min as monoprenylated derivatives.

To determine the prenylation position in its structure, **1c** was isolated on a preparative HPLC from an incubation mixture of **1a** with Y205N and subjected to NMR analysis. Signals for a regular prenyl moiety were clearly found at 5.17 (t, 1H, H-2'), 2.36 (m, 2H, H-1'), 1.70 (s, 3H, H-4'), and 1.52 (s, 3H, H-5') in the ^{1}H NMR spectrum (Fig. S8 in Electronic Supplementary Material). The appearance of H'-1

of the dimethylallyl moiety and H-2 of the original indole ring with up-field shifted chemical shifts at 2.36 (m, 2H, H-1') and 5.24 (s, 1H, H-2) indicated a *C3*-prenylation in **1c** (Caballero et al. 2003; Wollinsky et al. 2012). Regularly *C3*-prenylated derivatives have been identified as minor products of FtmPT1 reactions with tryptophan-containing cyclic dipeptides including D-Trp-D-Pro (Wollinsky et al. 2012). In these products, the prenyl moieties are on the same side of the C_{10}–C_{11} bond and take a *syn-cis* configuration of the four fused rings. Detailed analysis revealed that the ^{1}H NMR data of **1c** differed clearly from those of the regularly *syn-cis*-configured *C3*-prenylated D-Trp-D-Pro (Wollinsky et al. 2012), which would have an identical spectrum as its enantiomer, i.e., the regularly *syn-cis*-configured *C3*-prenylated L-Trp-L-Pro (brevianamide F). The data of **1c** corresponded very well to those of the chemically synthesized regularly *anti-cis*-configured *C3*-prenylated brevianamide F (Caballero et al. 2003). Therefore, the structure of **1c** can be unequivocally elucidated as illustrated (Fig. 2 and Table 2).

Behaviors of Y205N and Y205L toward *cyclo*-Trp-Pro stereoisomers

In a previous study, we identified several regularly *syn-cis*-configured *C3*-prenylated cyclic dipeptides as side products of the FtmPT1 reactions (Wollinsky et al. 2012). In that study, FtmPT1 converted all the four *cyclo*-Trp-Pro stereoisomers mainly to regularly *C2*-prenylated derivatives. Product yields of 83.0, 29.1, and 79.1 % were calculated for FtmPT1 reactions (5 μg protein at 37 °C for 2 h) with *cyclo*-L-Trp-L-Pro (**1a**), *cyclo*-D-Trp-L-Pro (**2a**), and *cyclo*-L-Trp-D-Pro (**3a**), respectively. In the reaction mixture of D-Trp-D-Pro (**4a**), both regularly *C2*- and *C3*-prenylated derivatives were identified, with product yields of 43.4 and 11.8 %, respectively. These results were also reproduced in this study and are depicted in Fig. 2.

HPLC analysis of the incubation mixtures of Y205N and Y205L with the four stereoisomers of *cyclo*-Trp-Pro revealed different behaviors. As shown in Fig. 2, two main products **1b** and **1c** were detected in the incubation mixtures of Y205N and Y205L with **1a**. Conversion yields of **1c** at 35.6 ± 0.2 and 31.8 ± 0.1 % were obtained for **1a** with Y205N and Y205L, respectively (Table 2). As shown in Fig. 2, Y205N converted *cyclo*-D-Trp-D-Pro (**2a**), *cyclo*-L-Trp-D-Pro (**3a**), and *cyclo*-D-Trp-L-Pro (**4a**) mainly to one dominant peak each (**2d**, **3d**, or **4d**), with product yields of 21.6 ± 1.1, 41.1 ± 1.9, and 32.5 ± 1.1 %, respectively. **2d**, **3d**, and **4d** were isolated from the reaction mixtures of **2a**, **3a**, and **4a** with Y205N and identified as reversely *C3*-prenylated derivatives, by comparison of their ^{1}H NMR data with those of the known compounds (Yu et al. 2013) (Materials and methods; Figs. S3–S6 and S8–S11 in Electronic Supplementary Material). Regularly *C2*-prenylated derivatives **2b–4b** were identified as minor
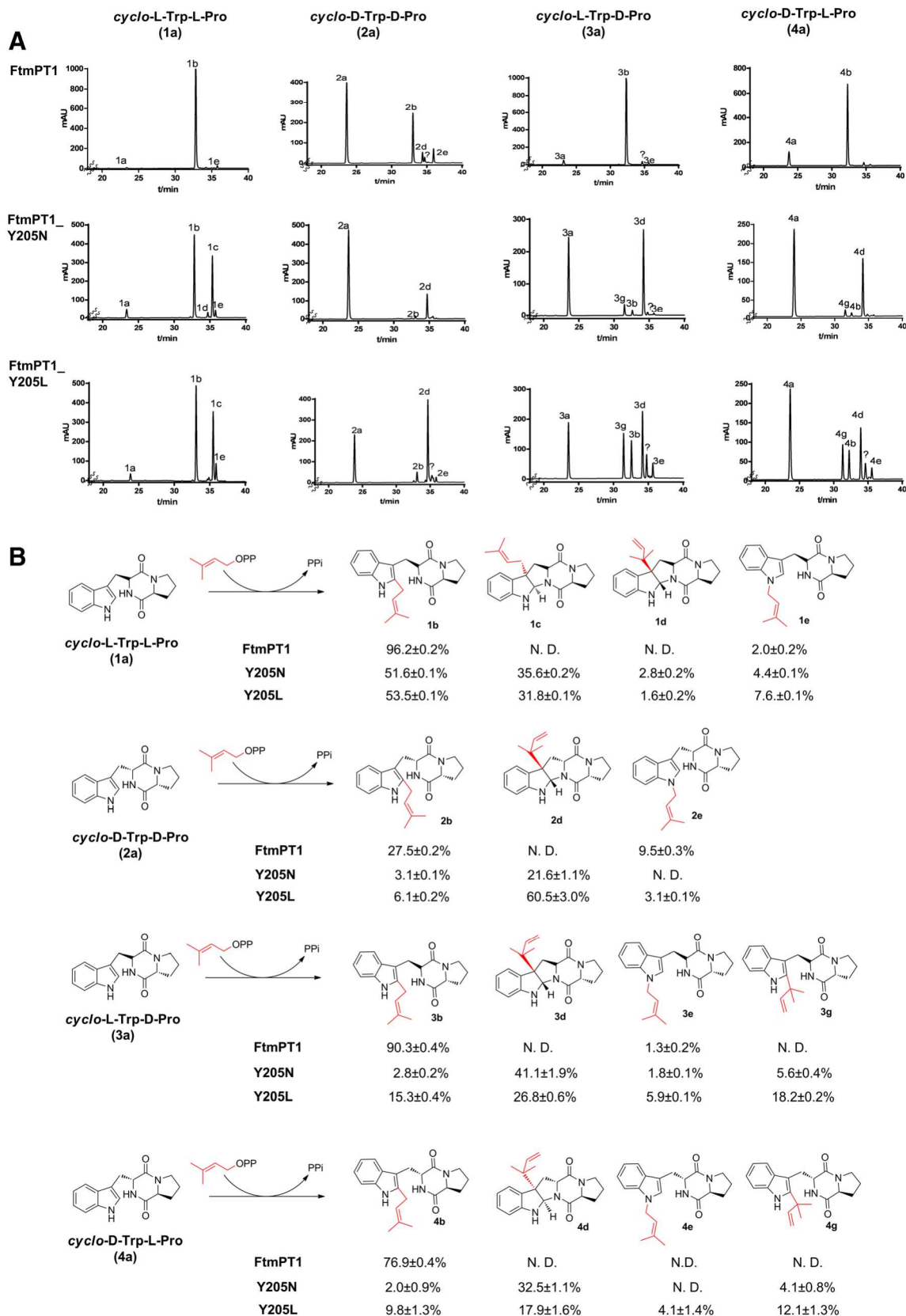
A

| cyclo-L-Trp-L-Pro (1a) | cyclo-D-Trp-D-Pro (2a) | cyclo-L-Trp-D-Pro (3a) | cyclo-D-Trp-L-Pro (4a) |

FtmPT1

FtmPT1_Y205N

FtmPT1_Y205L

B

cyclo-L-Trp-L-Pro (1a)

	1b	1c	1d	1e
FtmPT1	96.2±0.2%	N. D.	N. D.	2.0±0.2%
Y205N	51.6±0.1%	35.6±0.2%	2.8±0.2%	4.4±0.1%
Y205L	53.5±0.1%	31.8±0.1%	1.6±0.2%	7.6.±0.1%

cyclo-D-Trp-D-Pro (2a)

	2b	2d	2e
FtmPT1	27.5±0.2%	N. D.	9.5±0.3%
Y205N	3.1±0.1%	21.6±1.1%	N. D.
Y205L	6.1±0.2%	60.5±3.0%	3.1±0.1%

cyclo-L-Trp-D-Pro (3a)

	3b	3d	3e	3g
FtmPT1	90.3±0.4%	N. D.	1.3±0.2%	N. D.
Y205N	2.8±0.2%	41.1±1.9%	1.8±0.1%	5.6±0.4%
Y205L	15.3±0.4%	26.8±0.6%	5.9±0.1%	18.2±0.2%

cyclo-D-Trp-L-Pro (4a)

	4b	4d	4e	4g
FtmPT1	76.9±0.4%	N. D.	N.D.	N. D.
Y205N	2.0±0.9%	32.5±1.1%	N. D.	4.1±0.8%
Y205L	9.8±1.3%	17.9±1.6%	4.1±1.4%	12.1±1.3%

◀ **Fig. 2** HPLC chromatograms of the incubation mixture of FtmPT1, Y205N, and Y205L with *cyclo*-Trp-Pro isomers (**a**) and reactions catalyzed by the enzymes (**b**)

products of **2a–4a**, respectively (Figs. S4–S6 in Electronic Supplementary Material for LC–MS analysis).

2d was also identified as the predominant product of Y205L with **2a**, with a product yield of 60.5 ± 3.0 %. The two enantiomers **3a** and **4a** were converted by Y205L to two similar complex product mixtures. Detailed inspection of the HPLC chromatograms indicated the presence of **3b** and **3d** as well as **4b** and **4d** with the same retention times as those in the incubation mixtures of **3a** and **4a** with FtmPT1 and/or Y205N. **3g** and **3e** as well as **4g** and **4e** showed the same retention times as those of the reversely *C2*- and regularly *N1*-prenylated derivatives, which were obtained from the incubation mixtures of **3a** with BrePT (Yin et al. 2013) and CdpNPT (Yu et al. 2013), respectively (data not shown). The product yields of 15.3 ± 0.4, 26.8 ± 0.6, 5.9 ± 0.6, and 18.2 ± 0.2 % were calculated for **3b**, **3d**, **3e**, and **3g**, respectively. The product yields of **4b**, **4d**, **4e**, and **4g** were found to be 9.8 ± 1.3, 17.9 ± 1.6, 4.1 ± 1.4, and 12.1 ± 1.3 %, respectively (Fig. 2).

Double mutant at positions Gly115 and Tyr205

In a previous study, we have demonstrated that mutation on Gly115 to threonine led to a change in the prenylation pattern and position, i.e., from regular *C2*-prenylation catalyzed by FtmPT1 to reverse *C3*-prenylation catalyzed by FtmPT1_G115T. We were curious to prove the effect of Y205N and G115T together. Therefore, a plasmid pKZ27 for overproduction of the double mutant FtmPT1_G115T_Y205N was constructed (Table 1). HPLC analysis of the incubation mixture of **1a** with 5 μg enzyme at 37 °C for 2 h revealed a drastic reduction of the enzyme activity (Fig. S12 in Electronic Supplementary Material). A very small product peak with a retention time corresponding to that of **1c** was observed in the chromatogram. This result indicated that both positions could not be altered in the meantime. Similar results were also obtained for G115T_Y205N with **2a**, **3a**, or **4a** (Fig. S12 in Electronic Supplementary Material).

Kinetic parameters of the prenyl transfer reactions of 1a–4a with two of the identified best Tyr205 mutants

To get information on the catalytic efficiency of Y205N and Y205L toward all the *cyclo*-Trp-Pro stereoisomers, kinetic parameters including Michaelis–Menten constants (K_M) and turnover numbers (k_{cat}) were determined at pH 7.5 in a Tris-HCl buffered system by Lineweaver–Burk plot (Figs. S13–S21 in Electronic Supplementary Material). The investigated reactions followed apparently Michaelis–Menten kinetics. Under this condition, a K_M value at 0.057 ± 0.00021 mM was determined for

FtmPT1 with *cyclo*-L-Trp-L-Pro (**1a**), corresponding very well to 0.055 mM published previously (Grundmann and Li 2005). The turnover number k_{cat} at 8.91 ± 0.064 s^{-1} is higher than 5.57 s^{-1} determined in that study. As shown in Table 3, Y205N and Y205L accepted **1a** as the best substrate among the four isomers with approximate two- to three-fold K_M values and 15 to 48 % turnover number of those of FtmPT1. *cyclo*-D-Trp-D-Pro (**2a**) and *cyclo*-L-Trp-D-Pro (**3a**) were accepted better by Y205L than Y205N. *cyclo*-D-Trp-L-Pro (**4a**) was accepted by Y205L slightly better than Y205N. These results are in good agreement with the product yields presented in Fig. 2.

Discussion

Prenyltransferases of the DMATS superfamily are capable of prenylation of a wide range of substrates with different skeletons including indole, tyrosine, xanthone, flavonoid, and naphthalene derivatives. Tryptophan and tryptophan-containing cyclic dipeptides are used as prenylation substrates by a large number of the identified DMATS enzymes (Winkelblech et al. 2015). The until now characterized cyclic dipeptide prenyltransferases from this group catalyzed mainly regular *N1*-prenylation, regular and reverse *C2*-prenylation, reverse *C3*-prenylation, and regular *C7*-prenylation (Winkelblech et al. 2015). Recently, a regular *C3*-prenyltransferase of *cyclo*-L-Trp-L-Trp NozC was identified in *Nocardiopsis* and proven to be involved in the biosynthesis of nocardioazines (Alqahtani et al. 2015). NozC shares practically no sequence similarity with the known DMATS enzymes on the amino acid level. Biochemical properties of this enzyme like substrate specificity have not been reported.

In this study, we identified a key amino acid residue Tyr205 in FtmPT1 for the interaction with its aromatic substrate brevianamide F. Saturation mutagenesis on this position resulted in all 19 possible mutants. HPLC analysis of the incubation mixtures of brevianamide F and DMAPP with the obtained mutants led to identification of at least seven derivatives, Y205F, Y205C, Y205L, Y205M, Y205N, Y205I, and Y205S, which had comparable enzyme activities with the non-mutated FtmPT1 (Table 2). In addition to the regularly *C2*-prenylated derivative **1b**, the regularly *C3*-prenylated brevianamide F **1c** was also clearly identified in the reaction mixtures with Y205C, Y205L, Y205N, Y205I, and Y205S. Several mutants like Y205H, Y205Q, and Y205V showed lower activity than the mutants mentioned above, but also with **1b** and **1c** as main products. This proved that Tyr205 is important for the prenyl transfer reaction but can be replaced by other amino acids. In these cases, the role of Tyr205 would be fulfilled by other amino acids. However, changes at this position could influence the acceptance of **1a** or the orientation of the prenyl transfer reaction. The residues at 205 in the mentioned mutants differ from each other in size, hydrophobicity, and functional group. Tyr205 was

postulated to be involved in the binding of **1a** (Jost et al. 2010) via its hydroxyl group. The binding pockets of these mutants or their binding sites to **1a** should differ from that of FtmPT1 and also from each other. This hypothesis is supported by the fact that several Tyr205 mutants showed much lower activity than FtmPT1 (Table 2 and Fig. S2).

FtmPT1_Y205N, especially FtmPT1_Y205L, differed from the FtmPT1 wild type in behaviors toward the four *cyclo*-Trp-Pro isomers. Regularly *C2*-prenylated derivatives were detected as main products of FtmPT1 reactions with all these isomers. In contrast, the reversely *C3*-prenylated products were found to be the main products of Y205N and Y205L reactions with *cyclo*-D-Trp-D-Pro, *cyclo*-D-Trp-L-Pro, and *cyclo*-L-Trp-D-Pro, while regularly *C2*- and *C3*-prenylated derivatives were identified in their reaction mixtures with *cyclo*-L-Trp-L-Pro (Fig. 2). These results indicate different positions and orientations of the three isomers in the reaction chamber than brevianamide F.

Regularly *C3*-prenylated derivatives have been identified as side products of FtmPT1 reactions with several cyclic dipeptides, especially those with low activities. A minor peak in the reaction mixture of FtmPT1 with **1a**, with a relative yield of 0.8 % of that of *C2*-prenylated, was speculated to be a regularly *C3*-prenylated derivative (Wollinsky et al. 2012). It should be mentioned that the regularly *C3*-prenylated derivatives **1c** identified in that study carrying a *syn-cis* configuration of the ring system. In this study, the regularly *C3*-prenylated derivative has an *anti-cis* configuration. Product yields of **1c** were observed for **1a** with Y205C, Y205L, Y205N, Y205I, Y205S, and Y205H at more than 25 %. The ratios of the *C3*-prenylated **1c** to *C2*-prenylated derivative **1b** were found between 40 and 70 %. Therefore, these mutants can be used for production of regularly C3-prenylated brevianamide F in the chemoenzymatic synthesis and synthetic biology. More specific enzymes for regular *C3*-prenylation should be created in the future, e.g., by mutagenesis of mutants obtained in this study.

References

Alqahtani N, Porwal SK, James ED, Bis DM, Karty JA, Lane AL, Viswanathan R (2015) Synergism between genome sequencing, tandem mass spectrometry and bio-inspired synthesis reveals insights into nocardioazine B biogenesis. Org Biomol Chem 13:7177–7192

Caballero E, Avendãnno C, Menéndez JC (2003) Brief total synthesis of the cell cycle inhibitor tryprostatin B and related preparation of its alanine analogue. J Organomet Chem 68:6944–6951

Fan A, Li S-M (2016) Saturation mutagenesis on Arg244 of the tryptophan C4-prenyltransferase FgaPT2 leads to enhanced catalytic ability and different preferences for tryptophan-containing cyclic dipeptides. Appl Microbiol Biotechnol 100:5389–5399

Fan A, Winkelblech J, Li S-M (2015a) Impacts and perspectives of prenyltransferases of the DMATS superfamily for use in biotechnology. Appl Microbiol Biotechnol 99:7399–7415

Fan A, Zocher G, Stec E, Stehle T, Li S-M (2015b) Site-directed mutagenesis switching a dimethylallyl tryptophan synthase to a specific tyrosine C3-prenylating enzyme. J Biol Chem 290:1364–1373

Grundmann A, Li S-M (2005) Overproduction, purification and characterization of FtmPT1, a brevianamide F prenyltransferase from *Aspergillus fumigatus*. Microbiology 151:2199–2207

Haynes SW, Gao X, Tang Y, Walsh CT (2013) Complexity generation in fungal peptidyl alkaloid biosynthesis: a two-enzyme pathway to the hexacyclic MDR export pump inhibitor ardeemin. ACS Chem Biol 8:741–748

Heide L (2009) Prenyl transfer to aromatic substrates: genetics and enzymology. Curr Opin Chem Biol 13:171–179

Jost M, Zocher G, Tarcz S, Matuschek M, Xie X, Li S-M, Stehle T (2010) Structure-function analysis of an enzymatic prenyl transfer reaction identifies a reaction chamber with modifiable specificity. J Am Chem Soc 132:17849–17858

Li S-M (2010) Prenylated indole derivatives from fungi: structure diversity, biological activities, biosynthesis and chemoenzymatic synthesis. Nat Prod Rep 27:57–78

Li S-M (2011) Genome mining and biosynthesis of fumitremorgin-type alkaloids in ascomycetes. J Anthropol 64:45–49

Metzger U, Schall C, Zocher G, Unsöld I, Stec E, Li S-M, Heide L, Stehle T (2009) The structure of dimethylallyl tryptophan synthase reveals a common architecture of aromatic prenyltransferases in fungi and bacteria. Proc Natl Acad Sci U S A 106:14309–14314

Olafsen T, Kenanove V, Wu AW (2006) Tunable pharmacokinetics: modifying thein vivo half-life of antibodies by directed mutagenesis of the Fc fragment. Nat Protoc 1:2048–2060

Raju R, Piggott AM, Huang XC, Capon RJ (2011) Nocardioazines: a novel bridged diketopiperazine scaffold from a marine-derived bacterium inhibits p-glycoprotein. Org Lett 13:2770–2773

Schuller JM, Zocher G, Liebhold M, Xie X, Stahl M, Li S-M, Stehle T (2012) Structure and catalytic mechanism of a cyclic dipeptide prenyltransferase with broad substrate promiscuity. J Mol Biol 422:87–99

Steffan N, Unsöld IA, Li S-M (2007) Chemoenzymatic synthesis of prenylated indole derivatives by using a 4-dimethylallyltryptophan synthase from *Aspergillus fumigatus*. Chembiochem 8:1298–1307

Unsöld IA, Li S-M (2005) Overproduction, purification and characterization of FgaPT2, a dimethylallyltryptophan synthase from *Aspergillus fumigatus*. Microbiology 151:1499–1505

Winkelblech J, Fan A, Li S-M (2015) Prenyltransferases as key enzymes in primary and secondary metabolism. Appl Microbiol Biotechnol 99:7379–7397

Wollinsky B, Ludwig L, Xie X, Li S-M (2012) Breaking the regioselectivity of indole prenyltransferases: identification of regular C3-prenylated hexahydropyrrolo[2,3-*b*]indoles as side products of the regular C2-prenyltransferase FtmPT1. Org Biomol Chem 10:9262–9270

Woodside AB, Huang Z, Poulter CD (1988) Trisammonium geranyl diphosphate. Org Synth 66:211–215

Yin W-B, Ruan H-L, Westrich L, Grundmann A, Li S-M (2007) CdpNPT, an *N*-prenyltransferase from *Aspergillus fumigatus*: overproduction, purification and biochemical characterisation. Chembiochem 8: 1154–1161

Yin W-B, Grundmann A, Cheng J, Li S-M (2009) Acetylaszonalenin biosynthesis in *Neosartorya fischeri*: identification of the biosynthetic gene cluster by genomic mining and functional proof of the genes by biochemical investigation. J Biol Chem 284:100–109

Yin W-B, Xie X-L, Matuschek M, Li S-M (2010) Reconstruction of pyrrolo[2,3-*b*]indoles carrying an α-configured reverse C3-

dimethylallyl moiety by using recombinant enzymes. Org Biomol Chem 8:1133–1141

Yin S, Yu X, Wang Q, Liu XQ, Li S-M (2013) Identification of a brevianamide F reverse prenyltransferase BrePT from *Aspergillus versicolor* with a broad substrate specificity towards tryptophan-containing cyclic dipeptides. Appl Microbiol Biotechnol 97:1649–1660

Yu X, Zocher G, Xie X, Liebhold M, Schütz S, Stehle T, Li S-M (2013) Catalytic mechanism of stereospecific formation of *cis*-configured prenylated pyrroloindoline diketopiperazines by indole prenyltransferases. Chem Biol 20:1492–1501

143

Applied Microbiology and Biotechnology

Saturation mutagenesis on Tyr205 of the cyclic dipeptide *C2*-prenyltransferase FtmPT1 results in mutants with strongly increased *C3*-prenylating activity

Kang Zhou[1] • Wei Zhao[2] • Xiao-Qing Liu[2*] • Shu-Ming Li[1*]

[1] Institut für Pharmazeutische Biologie und Biotechnologie, Philipps-Universität Marburg, Marburg 35037, Germany

[2] College of Life Sciences, Capital Normal University, No.105 Xisanhuan Beilu, Beijing 100048, China

* Corresponding authors

Shu-Ming Li
Address
Institut für Pharmazeutische Biologie und Biotechnologie, Deutschhausstraße 17a, 35037 Marburg, Germany

E-Mail: shuming.li@staff.uni-marburg.de

Tel: + (49)6421-2822461
Fax: + (49)6421-2825365

Xiao-Qing Liu
Address
College of Life Sciences, Capital Normal University, No.105 Xisanhuan Beilu, Beijing 100048, China

E-Mail: liuxq@mail.cnu.edu.cn

Tel: + (86)010-68902327

Contents

Table S1 PCR conditions for the site-directed mutagenesis

Component	Concentration	Step	Temperature	Time	Cycles
Plasmid DNA	200-600 ng	Initialization denaturation	94 °C	2 min	1
Primer	15 pmol each	Denaturation	94 °C	40 s	
dNTP Mix	35 pmol	Annealing	55–65 °C	1 min	20
10× buffer	1×	Extension	68 °C	6 min	
High Fidelity Polymerase	3.75 U	Final elongation	68 °C	7 min	1
Final volume	50 μL	Final hold	4 °C	∞	1

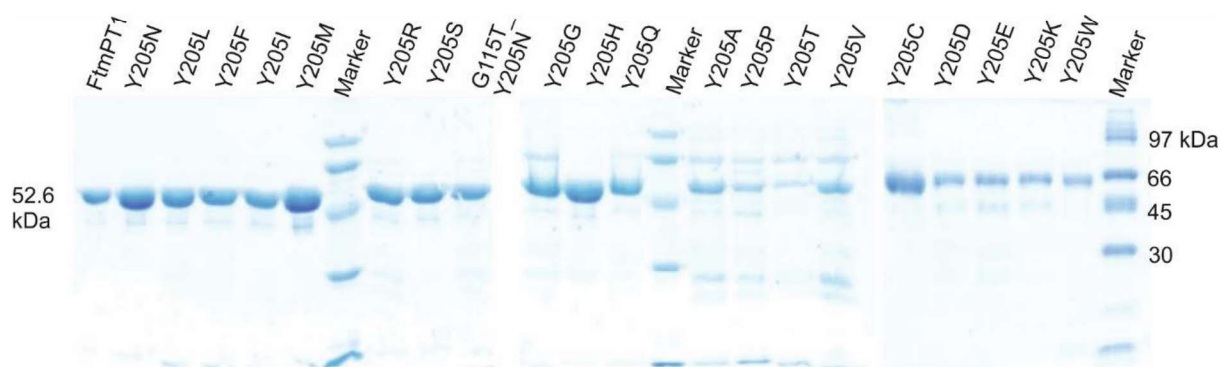**Fig. S1 Analysis of the overproduced and purified FtmPT1 and its mutants on SDS-PAGE**

The proteins were separated on a 12 % polyacrylamide gel and stained with Coomassie brilliant blue R-250. Due to the low protein concentration, 50 µL of Y205G, Y205Q, Y205A, Y205P or Y205V and 100 µL of Y205T were concentrated to near dryness in freezer dryer, dissolved in 10 µL sample buffer and used for SDS-PAGE.
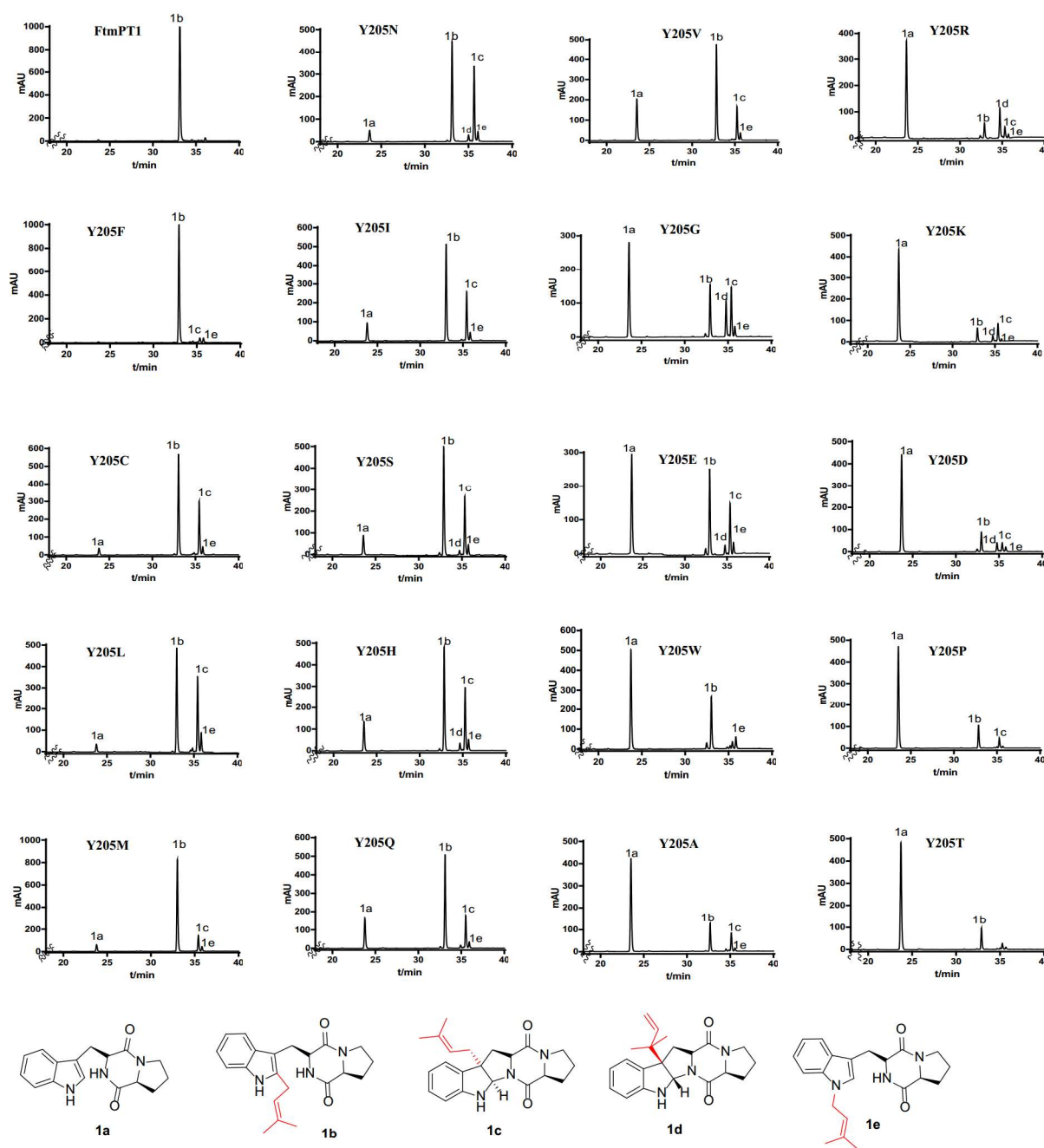
Fig. S2 HPLC chromatograms of incubation mixtures of brevianamide F (1a) with FtmPT1and its Tyr205 mutants

The reaction mixtures (100 μl) containing 5 μg FtmPT1 or one of its mutants, 1 mM brevianamide F, 2 mM DMAPP, 10 mM $CaCl_2$, 0.2 – 5.0 % (v/v) glycerol, 5 % (v/v) DMSO were incubated at 37 °C for 2 h. The substances were detected with a Photo Diode Array detector and illustrated for absorption at 296 nm.
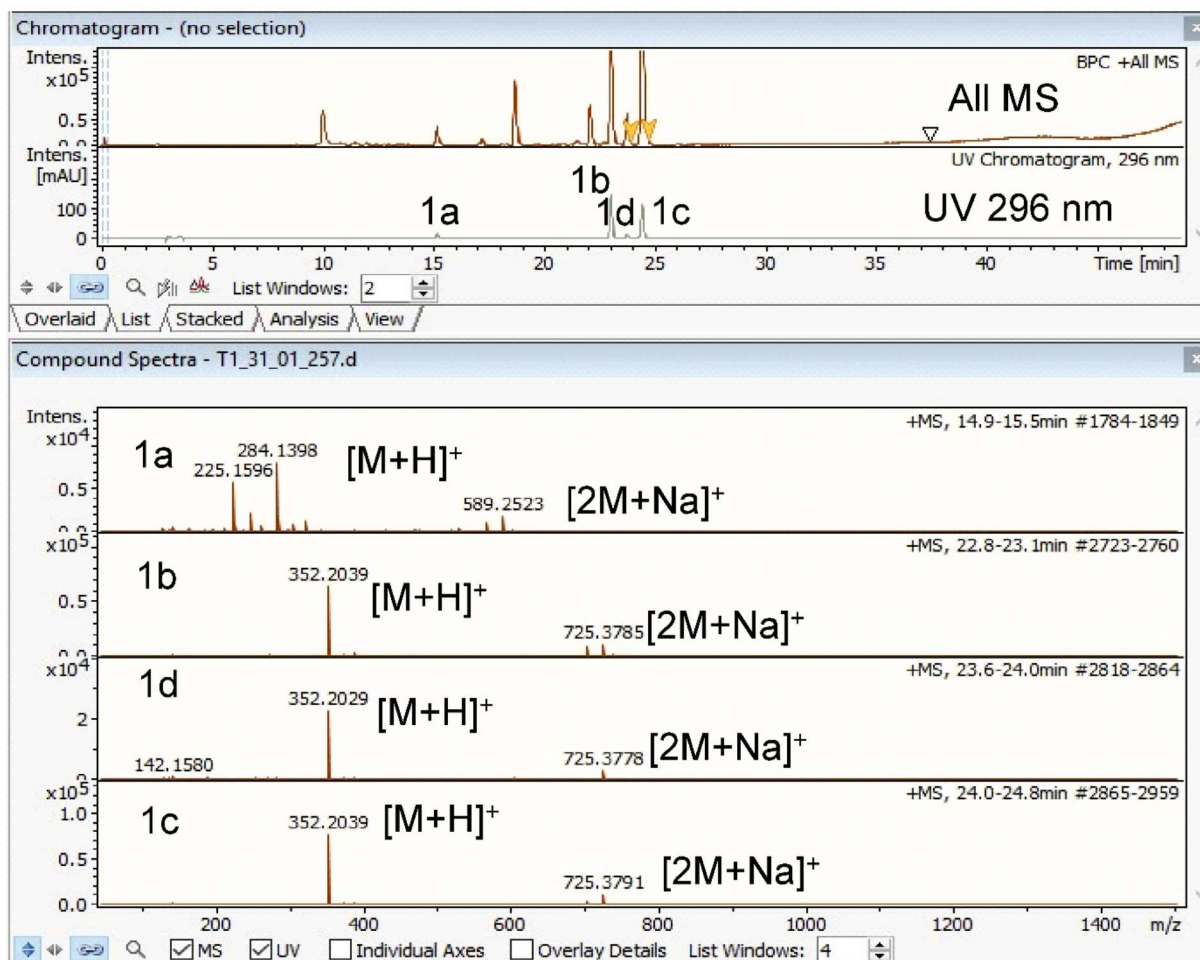
Fig. S3 LC-MS chromatogram of the incubation mixture of 1a with Y205N
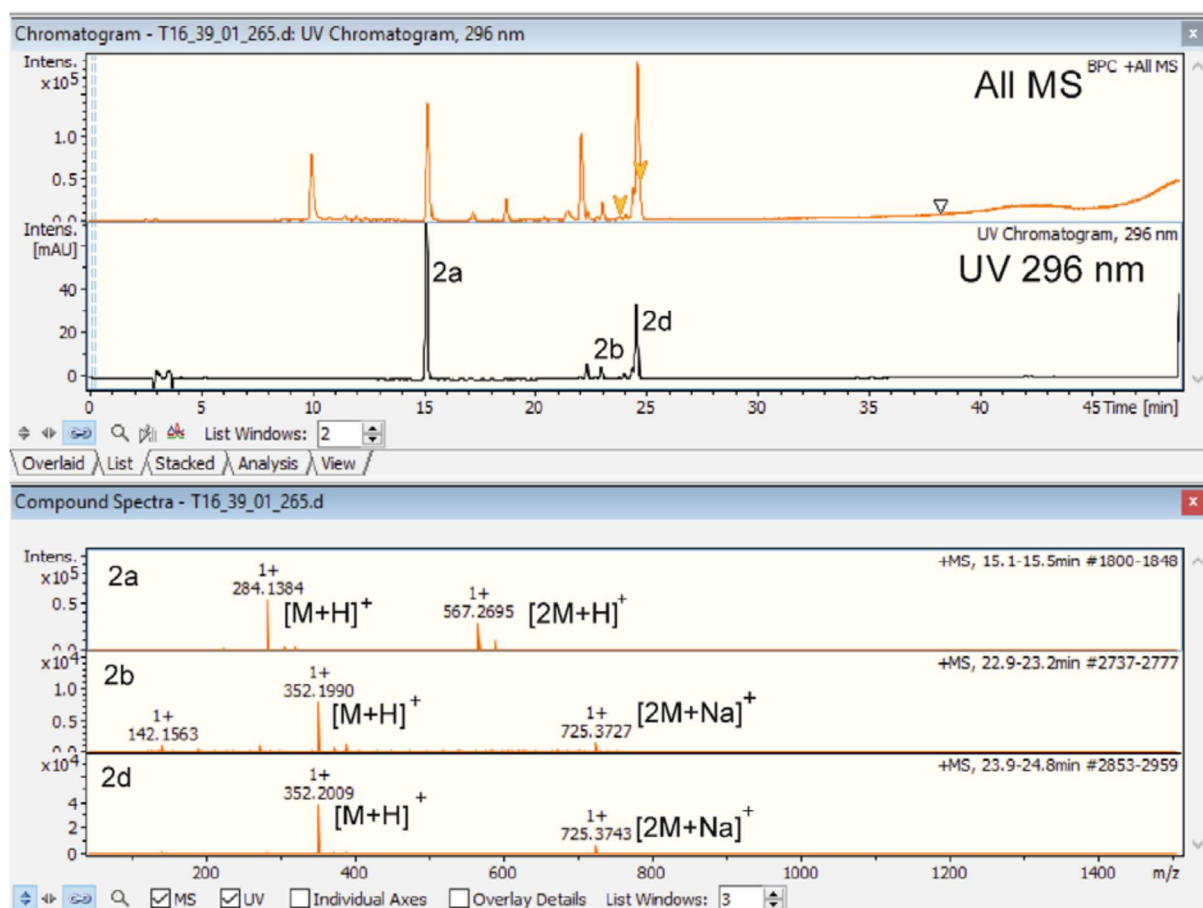
Fig. S4 LC-MS chromatogram of the incubation mixture of 2a with Y205N
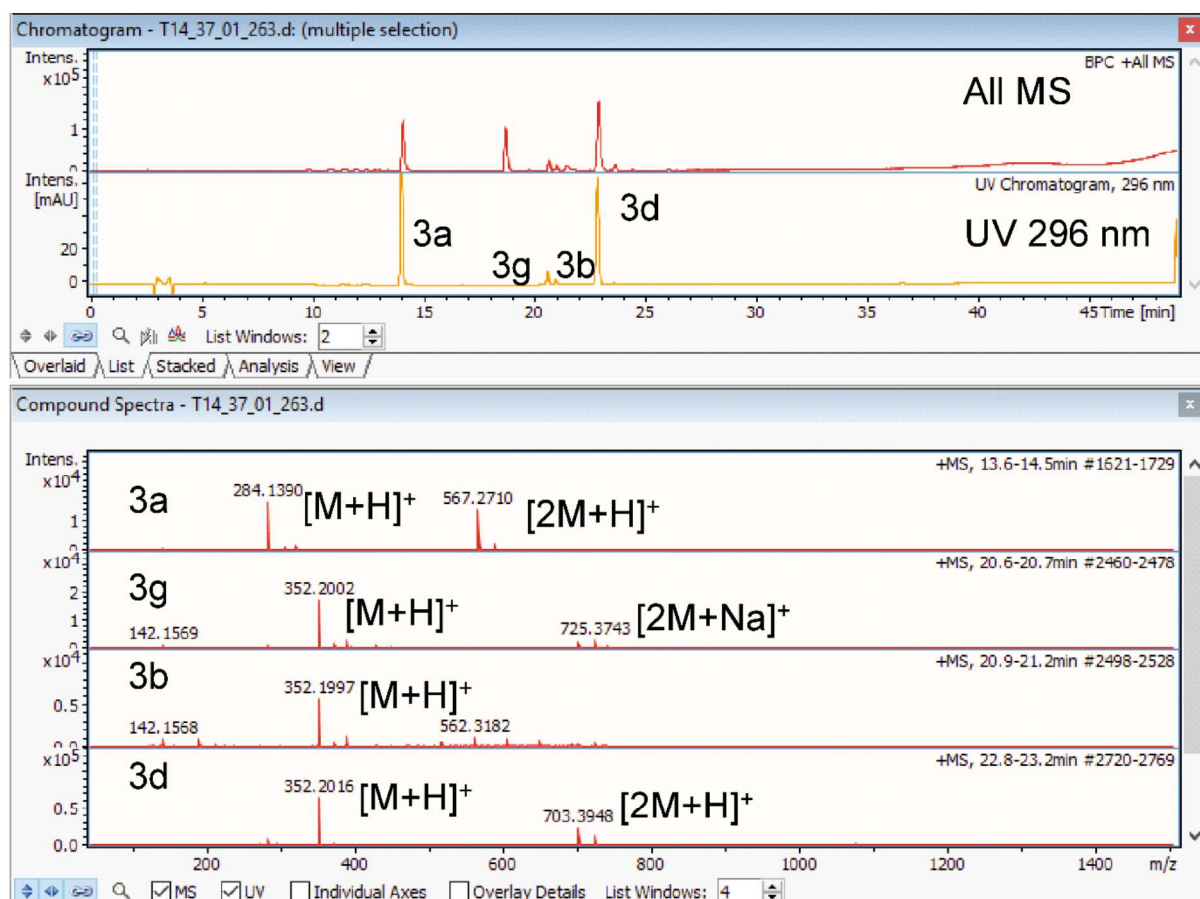
Fig. S5 LC-MS chromatogram of the incubation mixture of 3a with Y205N
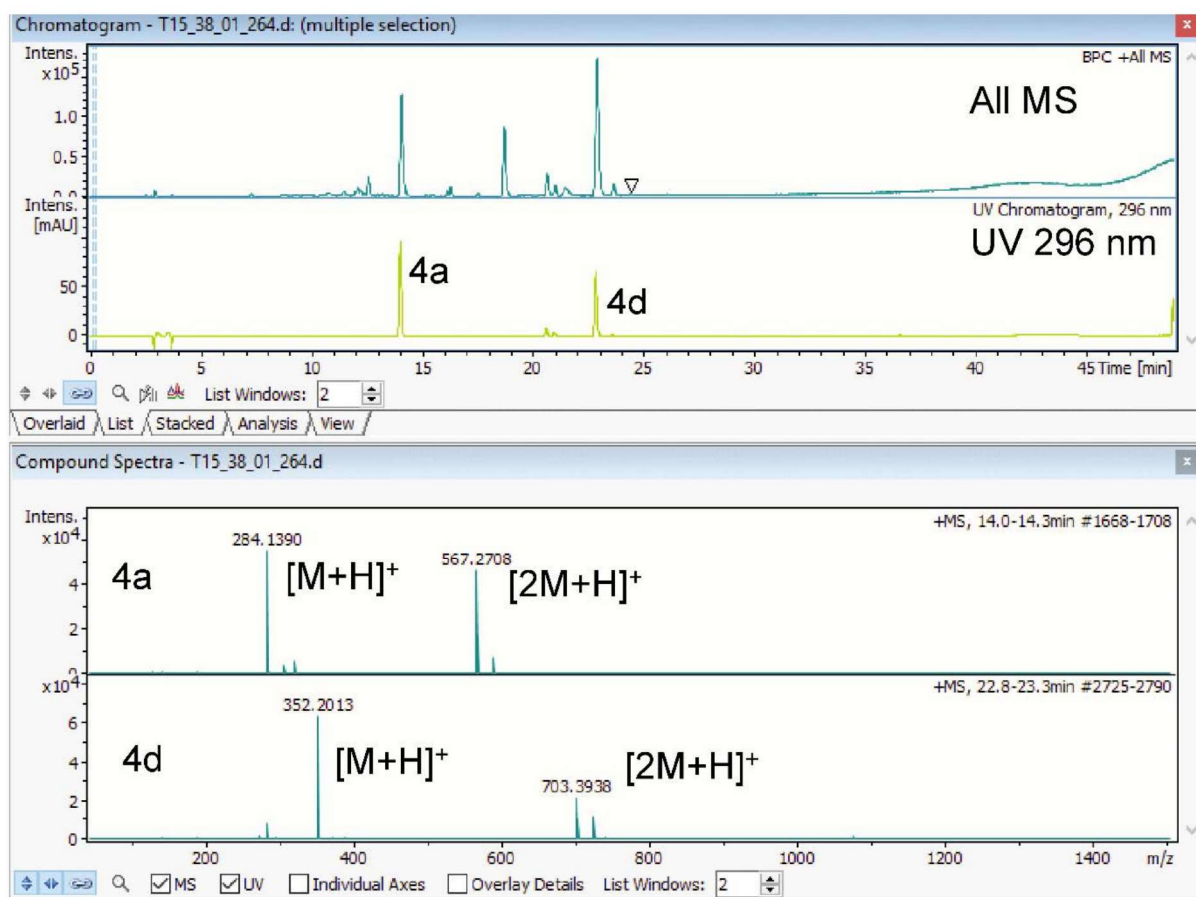
Fig. S6 LC-MS chromatogram of the incubation mixture of 4a with Y205N
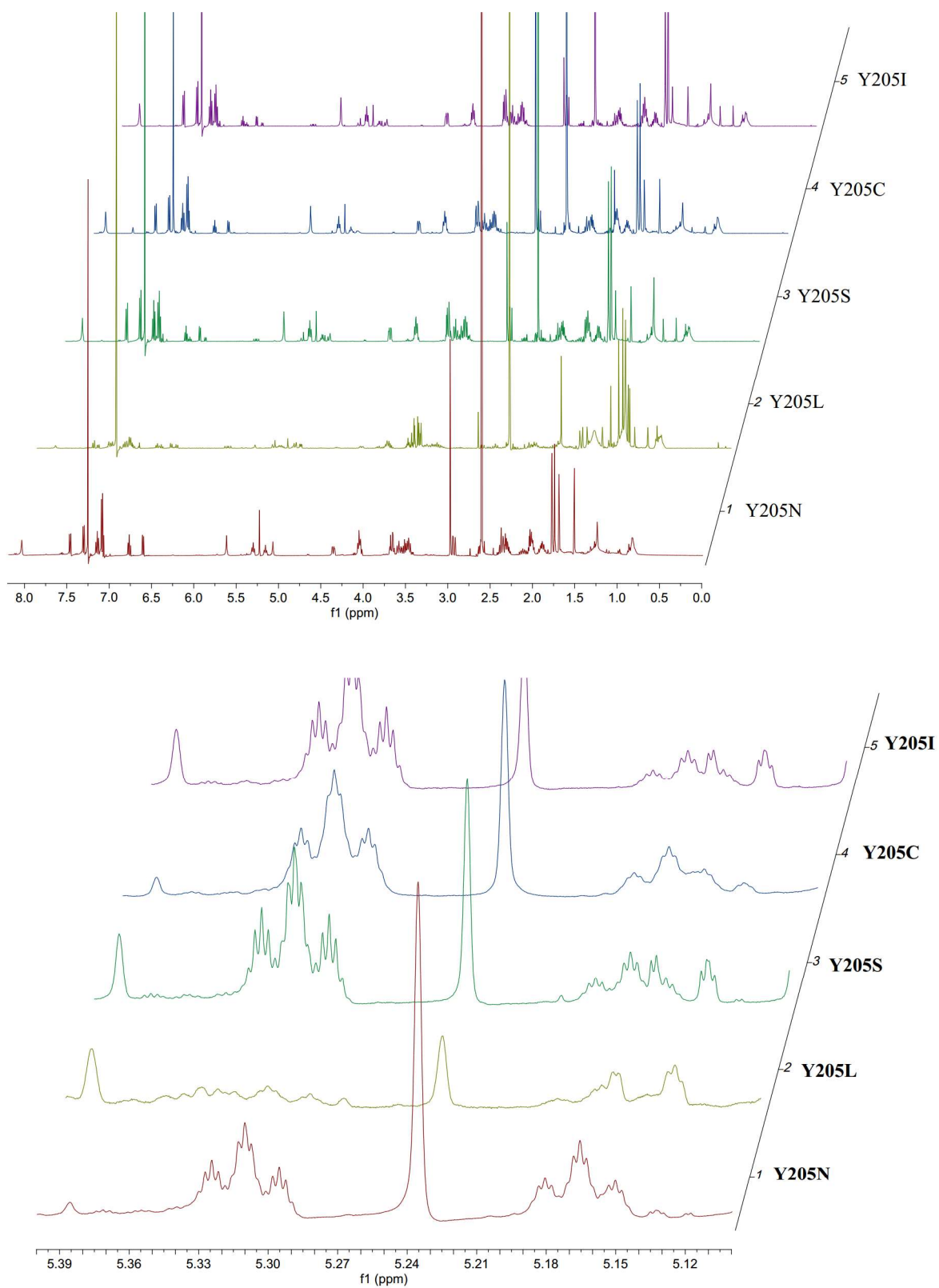
Fig. S7 ¹H NMR spectra of incubation mixtures of 1a with selected mutants in CDCl₃
(400 MHz for the incubation mixture of **1a** with Y205L and 500 MHz for other incubations).
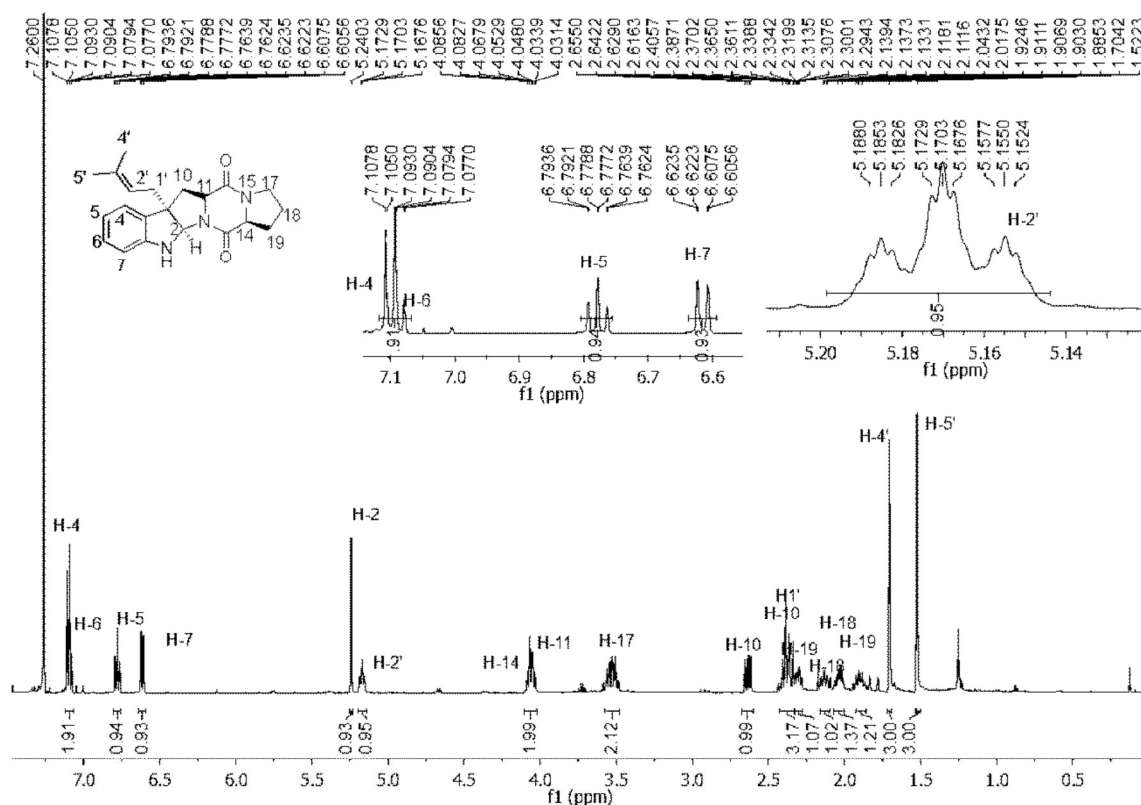
Fig. S8 ^{1}H NMR spectrum of 1c in CDCl$_3$ (500 MHz)
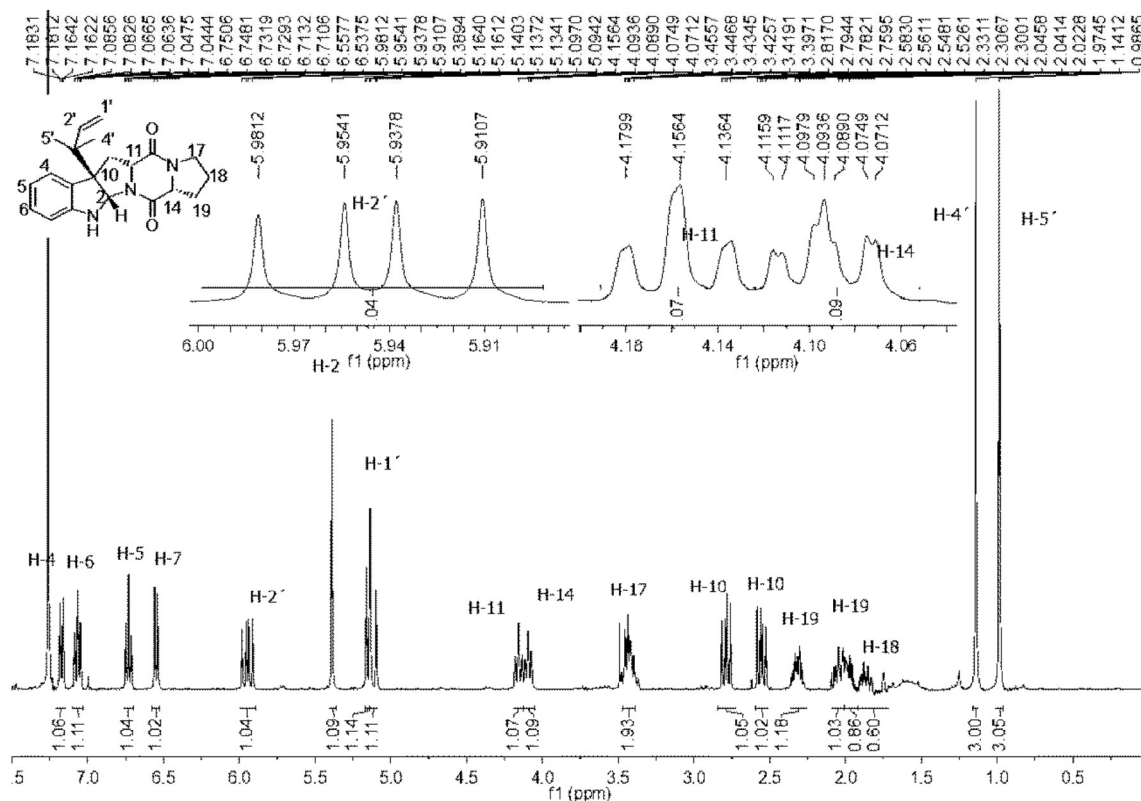
Fig. S9 ^{1}H NMR spectrum of 2d in CDCl$_3$ (400 MHz)
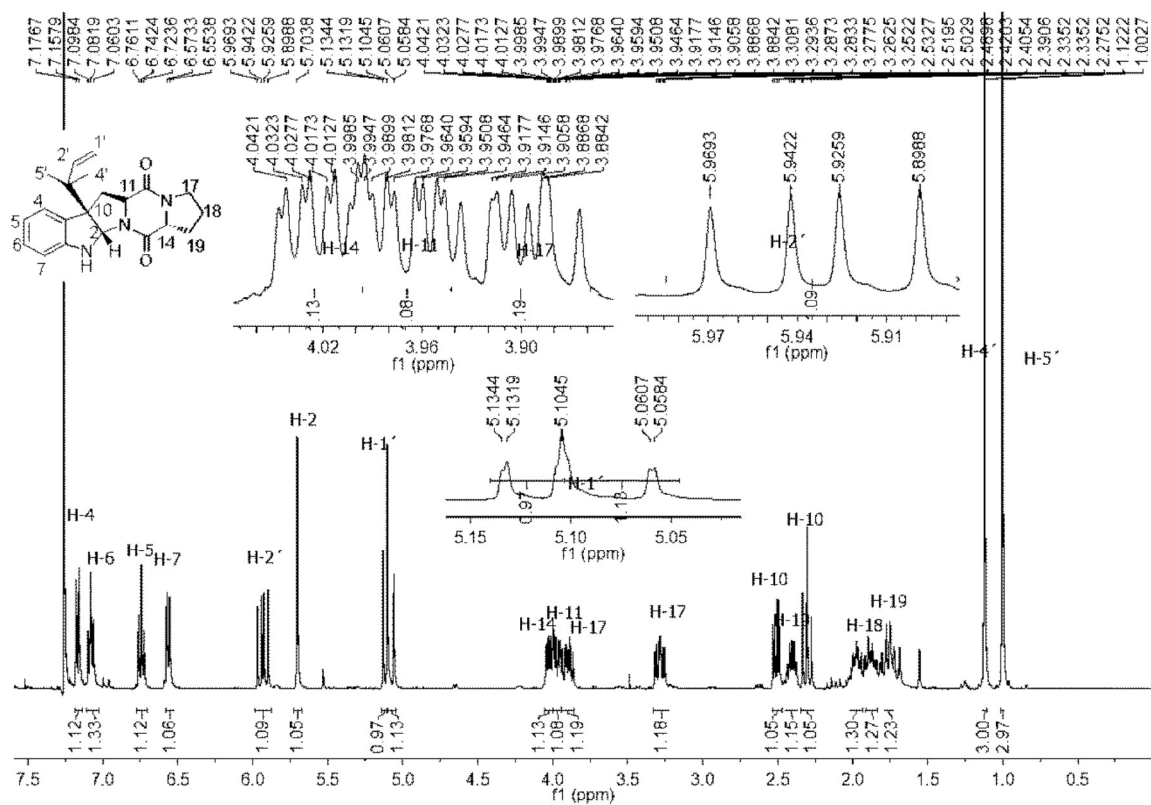
Fig. S10 ¹H NMR spectrum of 3d in CDCl₃ (400 MHz)
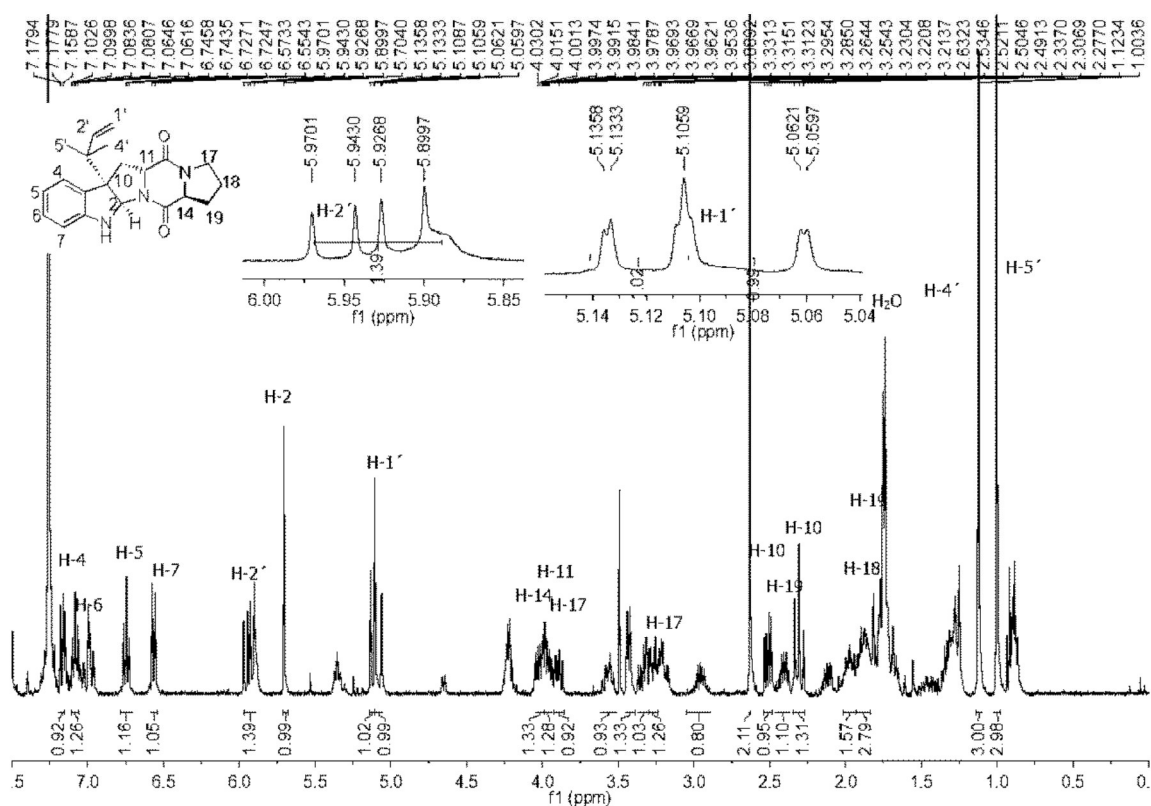
Fig. S11 ¹H NMR spectrum of 4d in CDCl₃ (400 MHz)

12
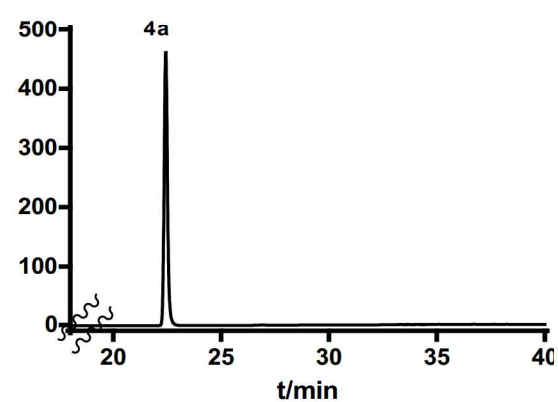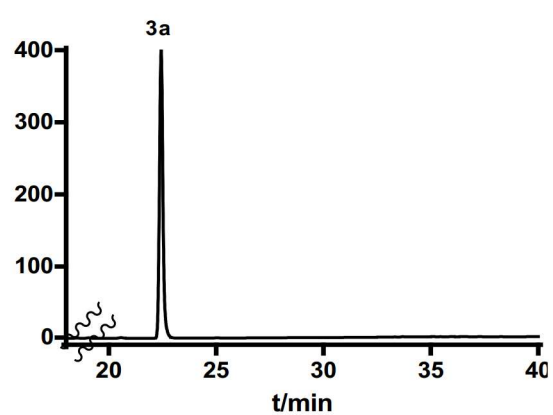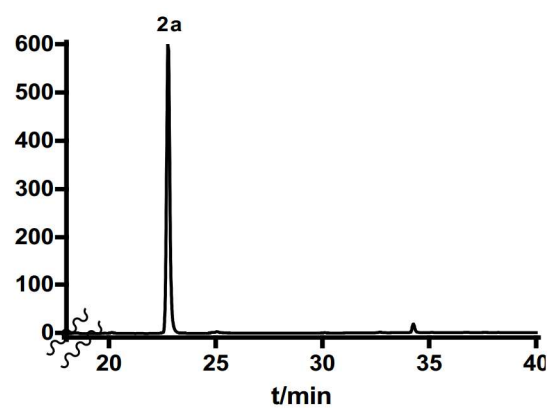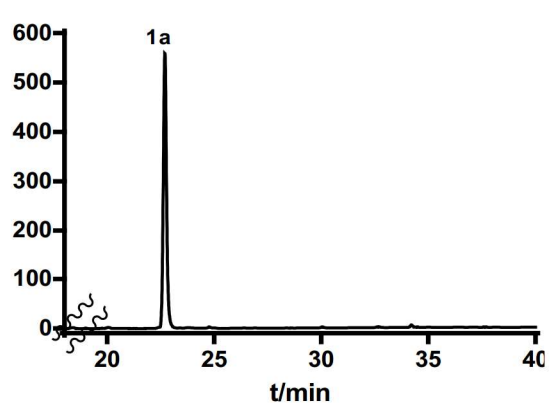
Fig. S12 HPLC chromatograms of the incubation mixtures of FtmPT1_G115T_Y205N with *cyclo*-L-Trp-L-Pro (1a), *cyclo*-D-Trp-D-Pro (2a), *cyclo*-L-Trp-D-Pro (3a), and *cyclo*-D-Trp-L-Pro (4a).

13
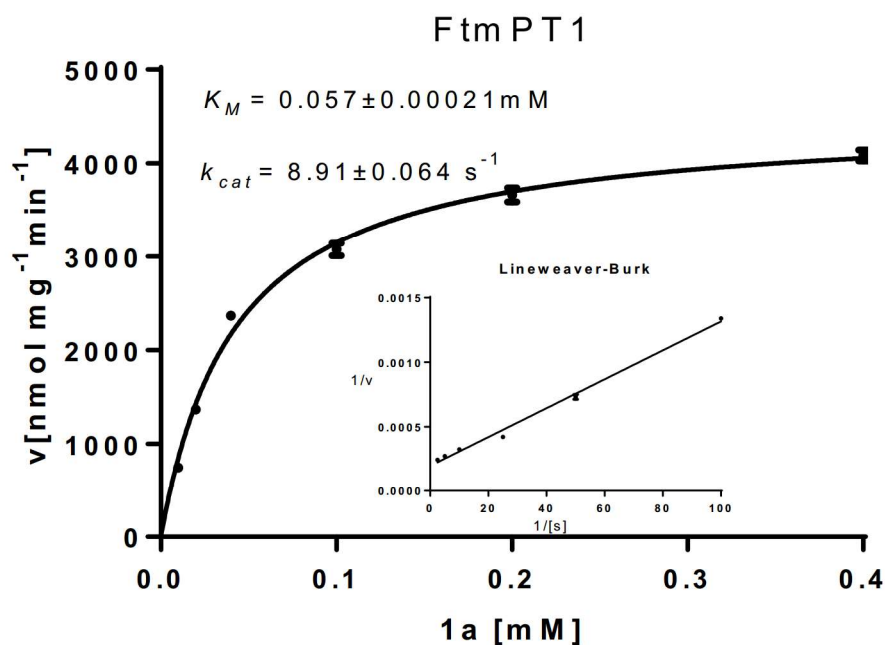
Fig. S13 Determination of the kinetic parameters of the FtmPT1 reaction toward 1a
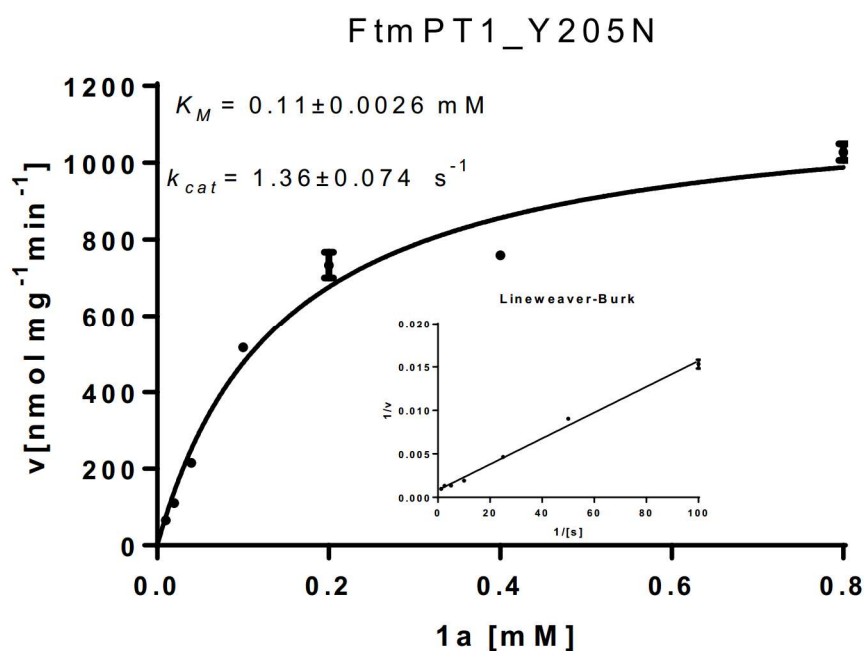
Fig. S14 Determination of the kinetic parameters of the Y205N reaction toward 1a

.

14
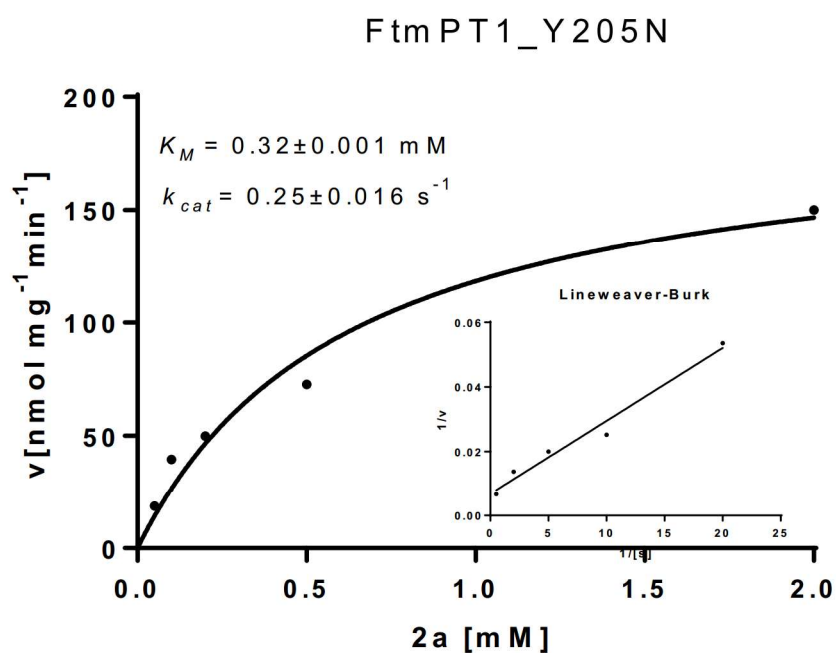
Fig. S15 Determination of the kinetic parameters of the Y205N reaction toward 2a
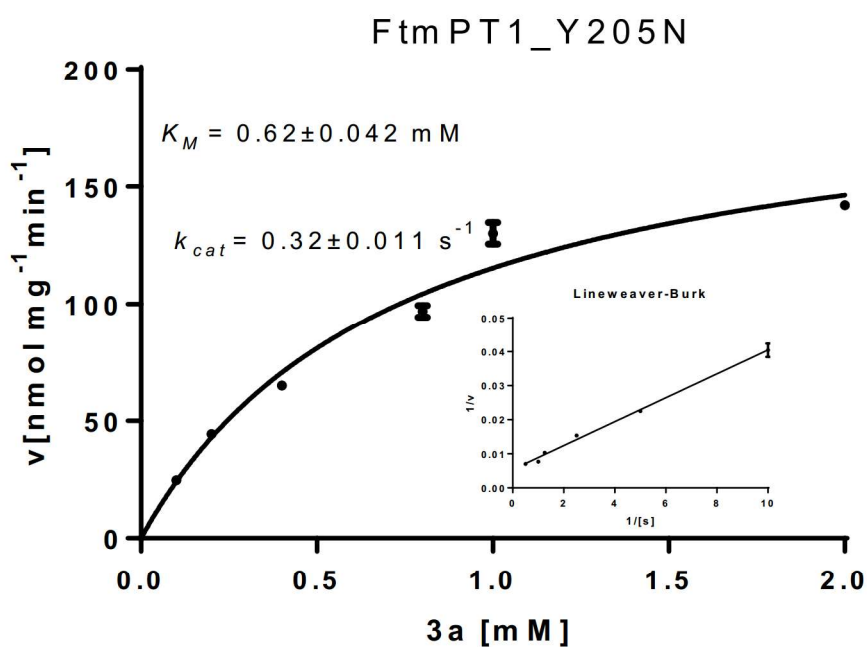
Fig. S16 Determination of the kinetic parameters of the Y205N reaction toward 3a

15
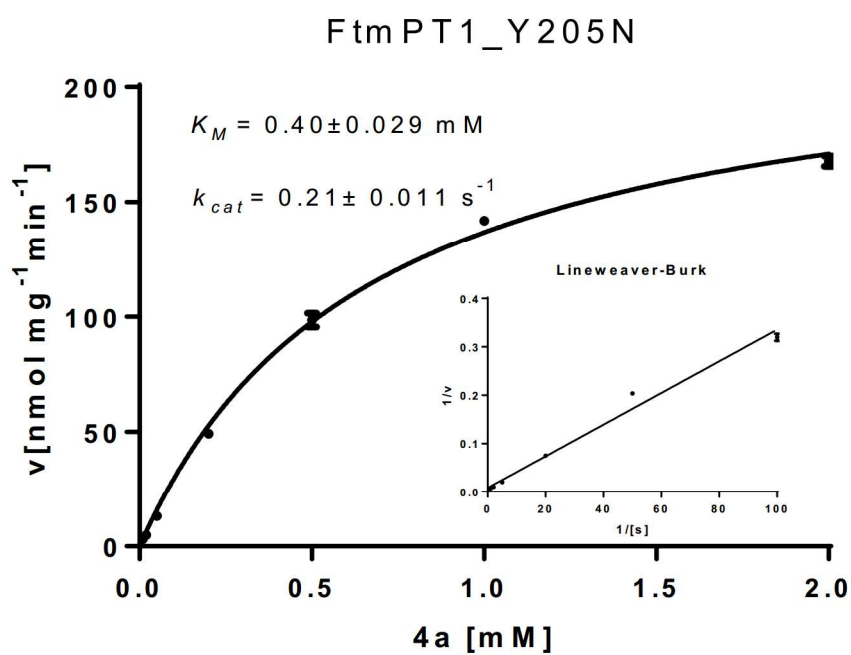
Fig. S17 Determination of the kinetic parameters of the Y205N reaction toward 4a
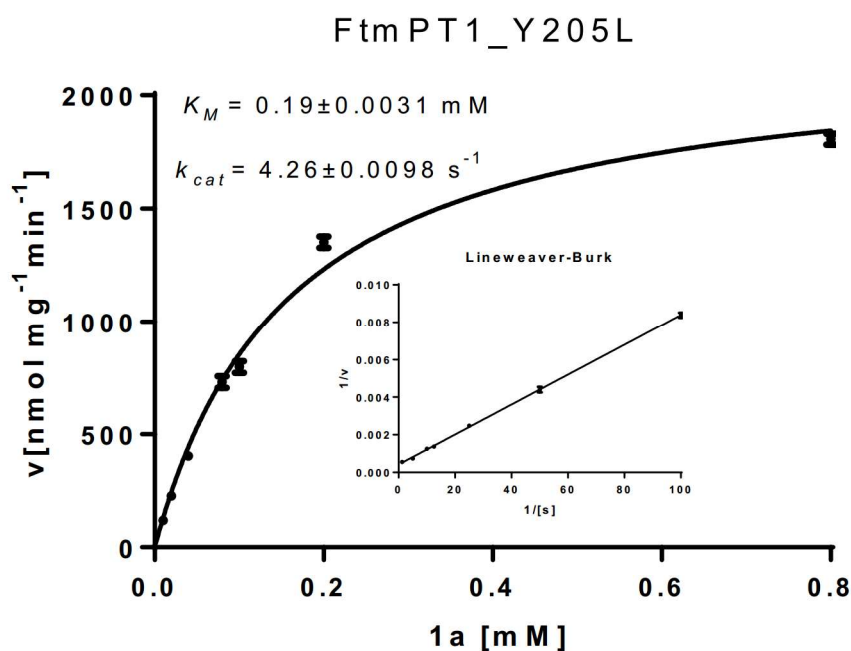
Fig. S18 Determination of the kinetic parameters of the Y205L reaction toward 1a
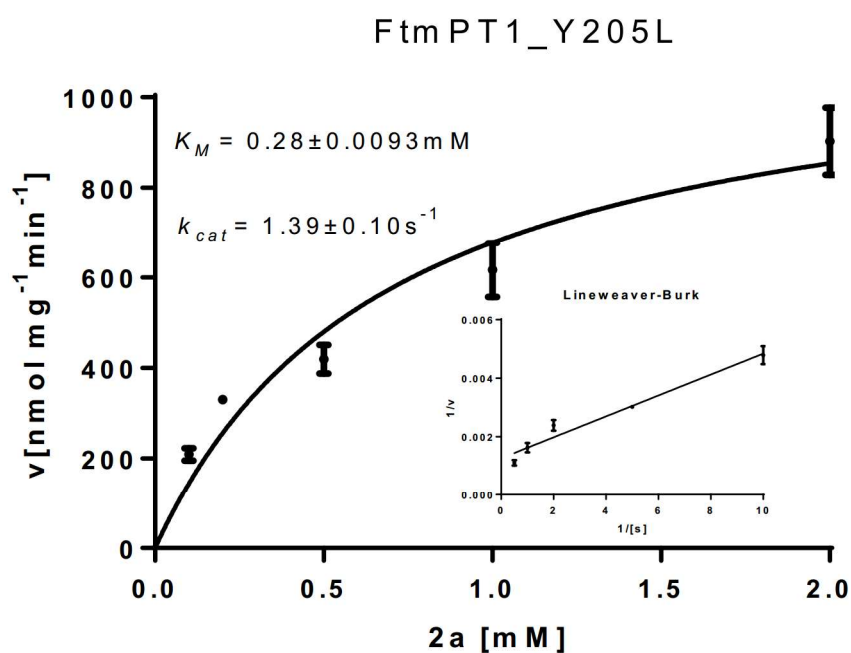
Fig. S19 Determination of the kinetic parameters of the Y205L reaction toward 2a
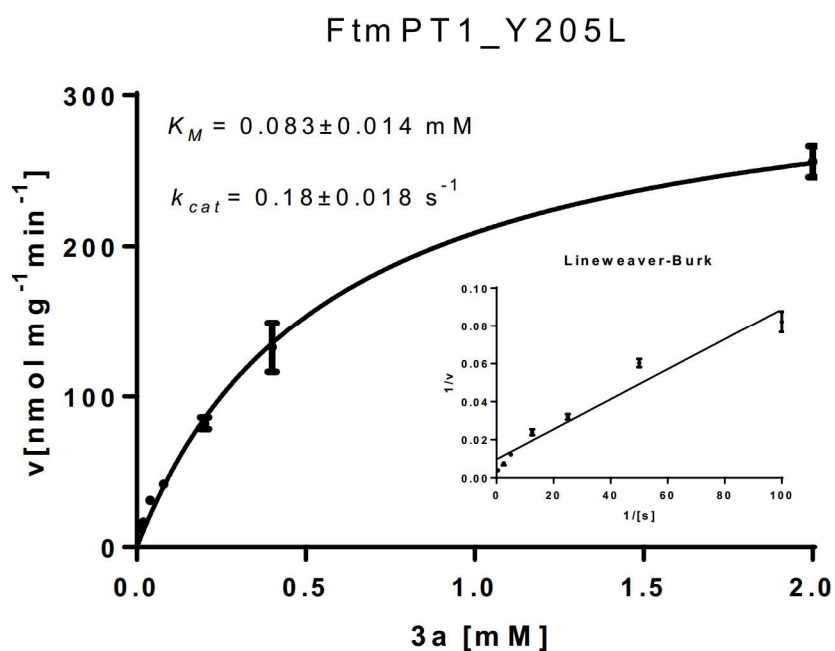
Fig. S20 Determination of the kinetic parameters of the Y205L reaction toward 3a
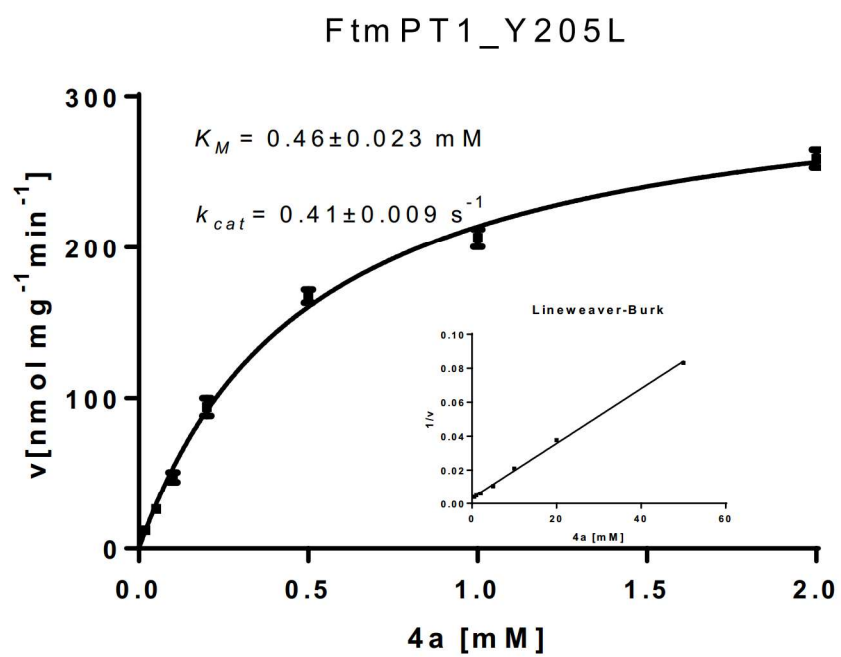
Fig. S21 Determination of the kinetic parameters of theY205L reaction toward 4a

5. Conclusions and future prospects

In this thesis, novel strategies for chemoenzymatic synthesis of prenylated acylphloroglucinols (APs) were developed by using prenyltransferases of the DMATS superfamily and natural prenyl donors, including DMAPP, GPP, and FPP.

Initially, prenyl donors and three APs were synthesized and their reactions with thirteen soluble fungal prenyltransferases were investigated. Nine regular dimethylallyl products were obtained from the reactions with AnaPT. The obtained results proved that AnaPT shows higher activities toward these compounds than other tested enzymes. It could be an interesting candidate as a biocatalyst for prenylation of phloroglucinol analogues. The observed activities of AnaPT toward these substrates are much higher than that of a microsomal fraction containing the overproduced prenyltransferase from the hop plant. However, only monoprenylated derivatives were obtained in the presence of DMAPP and the conversion yields of APs with GPP as prenyl donor were very low.

Recently, a soluble prenyltransferase AtaPT from *A. terreus* was demonstrated to carry an unprecedented promiscuity toward diverse drug-like aromatic acceptors and prenyl donors including DMAPP, GPP, and FPP. The activity of AtaPT toward APs was further investigated in my thesis. Incubation of AtaPT with three APs and three prenyl donors provided further insights into the catalytic properties of AtaPT. Total conversion yields of AtaPT are significantly higher than those of AnaPT. GPP also served as an excellent prenyl donor for the reaction of AtaPT. Twenty-one enzyme products were isolated and their structures were elucidated by NMR and LC-MS analyses. G*em*-diprenylated derivatives were identified in the reaction mixtures of three APs in the presence of DMAPP. These results proved the ability of AtaPT for *gem*-dipenylation of APs. The *C*-monodimethylallyl products were further accepted by AtaPT in the presence of DMAPP and *gem*-diprenylated derivatives as predominant products were observed.

Subsequently, prenylations of different flavonoids like flavanones and isoflavones by AnaPT at C-6 of the A-ring or C-3′of the B-ring were demonstrated. Twelve enzyme products were isolated by preparative HPLC from reaction mixtures of flavonoids with AnaPT and DMAPP. Former study revealed that 7-DMATS accepted chalcones, isoflavonoids, and flavanones much better than flavones and flavonols and mainly catalyzed prenylation at C-6. AnaPT and

7-DMATS display different substrate preferences and prenylation positions, so that these two fungal indole prenyltransferases could be used complementarily for prenylation of flavonoids. Prenylations of the flavonoid skeleton contribute significantly to structural diversity and biological activity of natural products and are usually crucial in the biosynthesis of these compounds.

Furthermore, *C3*-prenylating activity of *cyclo*-Trp-Pro isomers by the *cyclo*-L-Trp-L-Pro *C2*-prenyltransferase FtmPT1 was significantly improved by saturation mutagenesis experiments on Tyr205. In addition to the regularly *C2*-prenylated *cyclo*-L-Trp-L-Pro, the regularly *C3*-prenylated *cyclo*-L-Trp-L-Pro was also identified in the reaction mixtures with mutants in the presence of DMAPP. FtmPT1_Y205N, especially FtmPT1_Y205L, differ from FtmPT1 wildtype in behaviours toward the four *cyclo*-Trp-Pro isomers. Regularly *C2*-prenylated derivatives were detected as main products of FtmPT1 reactions with all these isomers. In contrast, the reversely *C3*-prenylated products were found to be the main products of Y205N and Y205L reactions with *cyclo*-D-Trp-D-Pro, *cyclo*-D-Trp-L-Pro, and *cyclo*-L-Trp-D-Pro. These mutants can be used for production of regularly *C3*-prenylated brevianamide F in the chemoenzymatic synthesis and synthetic biology.

For future prospects, the following works should be performed:

- ➢ Coexpression of AtaPT or AnaPT in engineered yeast strain harboring CCL2/CCL4/VPS genes for production of prenylated APs.
- ➢ Creation of more specific enzymes for regular *C3*-prenylation.
- ➢ Investigation of the acceptance of other cyclic dipeptides catalyzed by FtmPT1 mutants, for example *cyclo*-L-Trp-L-Ala and its isomers.
- ➢ Collection all available data of mutated DMATS enzymes to rational design PTs which could catalyze additional Friedel-Crafts reactions for production of desired products.

6. References

Adam P, Arigoni D, Bacher A, Eisenreich W (2002) Biosynthesis of hyperforin in *Hypericum perforatum*. J Med Chem 45:4786-4793

Agrawal AD (2011) Pharmacological activities of flavonoids: A review. Int J Pharm Sci Nanotech 4:1394-1398

Akashi T, Sasaki K, Aoki T, Ayabe S, Yazaki K (2009) Molecular cloning and characterization of a cDNA for pterocarpan 4-dimethylallyltransferase catalyzing the key prenylation step in the biosynthesis of glyceollin, a soybean phytoalexin. Plant Physiol 149:683-693

Alqahtani N, Porwal SK, James ED, Bis DM, Karty JA, Lane AL, Viswanathan R (2015) Synergism between genome sequencing, tandem mass spectrometry and bio-inspired synthesis reveals insights into nocardioazine B biogenesis. Org Biomol Chem 13:7177-7192

Aussel L, Pierrel F, Loiseau L, Lombard M, Fontecave M, Barras F (2014) Biosynthesis and physiology of coenzyme Q in bacteria. Biochim Biophys Acta 1837:1004-1011

Awakawa T, Zhang L, Wakimoto T, Hoshino S, Mori T, Ito T, Ishikawa J, Tanner ME, Abe I (2014) A methyltransferase initiates terpene cyclization in teleocidin B biosynthesis. J Am Chem Soc 136:9910-9913

Bayse CA, Merz KM (2014) Mechanistic insights into Mg^{2+}-independent prenylation by CloQ from classical molecular mechanics and hybrid quantum mechanics/molecular mechanics molecular dynamics simulations. Biochemistry 53:5034-5041

Biedermann D, Vavrikova E, Cvak L, Kren V (2014) Chemistry of silybin. Nat Prod Rep 31:1138-1157

Bonitz T, Zubeil F, Grond S, Heide L (2013) Unusual *N*-prenylation in diazepinomicin biosynthesis: The farnesylation of a benzodiazepine substrate is catalyzed by a new member of the ABBA prenyltransferase superfamily. PLoS One 8:e85707

Botta B, Menendez P, Zappia G, de Lima RA, Torge R, Monachea GD (2009) Prenylated isoflavonoids: Botanical distribution, structures, biological activities and biotechnological studies. An update (1995-2006). Curr Med Chem 16:3414-3468

Botta B, Monache GD, Menendez P, Boffi A (2005a) Novel prenyltransferase enzymes as a tool for flavonoid prenylation. Trends Pharmacol Sci 26:606-608

Botta B, Vitali A, Menendez P, Misiti D, Delle MG (2005b) Prenylated flavonoids: pharmacology and biotechnology. Curr Med Chem 12:717-739

Chang YW, Yuan CM, Zhang J, Liu S, Cao P, Hua HM, Dai YT, Hao XJ (2016) Speramides A-B, two new prenylated indole alkaloids from the freshwater-derived fungus *Aspergillus ochraceus* KM007. Tetrahedron Lett 57:4952-4955

REFERENCES

Chen J, Morita H, Wakimoto T, Mori T, Noguchi H, Abe I (2012) Prenylation of a nonaromatic carbon of indolylbutenone by a fungal indole prenyltransferase. Org Lett 14:3080-3083

Chen M, Shao CL, Fu XM, Xu RF, Zheng JJ, Zhao DL, She ZG, Wang CY (2013a) Bioactive indole alkaloids and phenyl ether derivatives from a marine-derived *Aspergillus* sp. fungus. J Nat Prod 76:547-553

Chen R, Gao B, Liu X, Ruan F, Zhang Y, Lou J, Feng K, Wunsch C, Li S-M, Dai J, Sun F (2017) Molecular insights into the enzyme promiscuity of an aromatic prenyltransferase. Nat Chem Biol 13:226-234

Chen R, Liu X, Zou J, Yin Y, Ou C, Li J, Wang R, Xie D, Zhang P, Dai J (2013b) Regio- and stereospecific prenylation of flavonoids by *Sophora flavescens* prenyltransferases. Adv Synth Catal 355:1817-1828

Chen X, Mukwaya E, Wong MS, Zhang Y (2014a) A systematic review on biological activities of prenylated flavonoids. Pharm Biol 52:655-660

Cheng W, Li W (2014) Structural insights into ubiquinone biosynthesis in membranes. Science 343:878-881

Chooi YH, Cacho R, Tang Y (2010) Identification of the viridicatumtoxin and griseofulvin gene clusters from *Penicillium aethiopicum*. Chem Biol 17:483-494

Chooi YH, Fang J, Liu H, Filler SG, Wang P, Tang Y (2013) Genome mining of a prenylated and immunosuppressive polyketide from pathogenic fungi. Org Lett 15:780-783

Chooi YH, Wang P, Fang J, Li Y, Wu K, Wang P, Tang Y (2012) Discovery and characterization of a group of fungal polycyclic polyketide prenyltransferases. J Am Chem Soc 134:9428-9437

Chu YS, Niu XM, Wang YL, Guo JP, Pan WZ, Huang XW, Zhang KQ (2010) Isolation of putative biosynthetic intermediates of prenylated indole alkaloids from a thermophilic fungus *Talaromyces thermophilus*. Org Lett 12:4356-4359

Ciochina R, Grossman RB (2006) Polycyclic polyprenylated acylphloroglucinols. Chem Rev 106:3963-3986

Cole RJ, Dorner JW, Springer JP, Cox RH (1981) Indole metabolites from a strain of *Aspergillus flavus*. J Agr Food Chem 29:293-295

Cuesta-Rubio O, Cuesta-Rubio H, Frontana-Uribe BA, Cárdenas J (2001) Nemorosone, the major constituent of floral resins of *Clusia rosea*. Phytochemistry 57:279-283

Dhillon DS, Brown SA (1976) Localization,purification,and characterization of dimethylallylpyrophosphate:umbelliferone dimethylallythransferase from *Ruta graveolens*. Arch Biochem Biophys 177:74-83

Ding Y, Wet JR, Cavalcoli J, Li S, Greshock TJ, Miller KA, Finefield JM, Sunderhaus JD, McAfoos TJ, Tsukamoto S, Williams RM, Sherman DH (2010) Genome-based characterization of two prenylation steps in the assembly of the stephacidin and

notoamide anticancer agents in a marine-derived *Aspergillus* sp. J Am Chem Soc 132:12733-12740

Dixon RA, Steele CL (1999) Flavonoids and isoflavonoids - a gold mine for metabolic engineering. Trends Plant Sci 4:394-400

Edwards DJ, Gerwick WH (2004) Lyngbyatoxin biosynthesis: sequence of biosynthetic gene cluster and identification of a novel aromatic prenyltransferase. J Am Chem Soc 126:11432-11433

El-Seedi HR, El-Barbary MA, El-Ghorab DMH, Bohlin L, Borg-Karlson AK, Göransson U, Verpoorte R (2010) Recent insights into the biosynthesis and biological activities of natural xanthones. Curr Med Chem 17:854-901

Ellestad GA, Mirando P, Kunstmann MP (1973) Structure of the metabolite LL-S490ß from an unidentified *Aspergillus* species. J Org Chem 38:4204-4205

Ellis BE, Brown SA (1974) Isolation of dimethylallylpyrophosphate: umbelliferone dimethylally transferase from *Ruta graveolens*. Can J Biochem 52:734-738

Fan A, Chen H, Wu R, Xu H, Li S-M (2014) A new member of the DMATS superfamily from *Aspergillus niger* catalyzes prenylations of both tyrosine and tryptophan derivatives. Appl Microbiol Biotechnol 98:10119-10129

Fan A, Li S-M (2013) One substrate - seven products with different prenylation positions in one-step reactions: prenyltransferases make it possible. Adv Synth Catal 355:2659-2666

Fan A, Li S-M (2016) Saturation mutagenesis on Arg244 of the tryptophan C4-prenyltransferase FgaPT2 leads to enhanced catalytic ability and different preferences for tryptophan-containing cyclic dipeptides. Appl Microbiol Biotechnol 100:5389-5399

Fan A, Winkelblech J, Li S-M (2015a) Impacts and perspectives of prenyltransferases of the DMATS superfamily for use in biotechnology. Appl Microbiol Biotechnol 99:7399-7415

Fan A, Zocher G, Stec E, Stehle T, Li S-M (2015b) Site-directed mutagenesis switching a dimethylallyl tryptophan synthase to a specific tyrosine *C3*-prenylating enzyme. J Biol Chem 290:1364-1373

Fredenhagen A, Petersen F, Tintelnot-Blomley M, Rosel J, Mett H, Hug P (1997) Semicochliodinol A and B: inhibitors of HIV-1 protease and EGF-R protein tyrosine kinase related to asterriquinones produced by the fungus *Chrysosporium merdarium*. J Antibiot 50:395-401

Gallagher RT, Wilson BJ (1978) Aflatrem, the tremorgenic mycotoxin from *Aspergillus flavus*. Mycopathologia 66:183-185

Garnsey MR, Matous JA, Kwiek JJ, Coltart DM (2011) Asymmetric total synthesis of (+)- and (-)-clusianone and (+)- and (-)-clusianone methyl enol ether via ACC alkylation and evaluation of their anti-HIV activity. Bioorg Med Chem Lett 21:2406-2409

Gebler J C, and Poulter CD (1992) Purification and characterization of dimethylallyl tryptophan synthase from *Claviceps purpurea*. *Arch. Biochem. Biophys.* 296, 308-313.

REFERENCES

George J-H, Hesse M-D, Baldwin E, dlington R-M (2010) Biomimetic synthesis of polycyclic polyprenylated acylphloroglucinol natural products isolated from *Hypericum papuanum*. Org Lett 12:3532-3535

Grienke U, Richter M, Walther E, Hoffmann A, Kirchmair J, Makarov V, Nietzsche S, Schmidtke M, Rollinger JM (2016) Discovery of prenylated flavonoids with dual activity against influenza virus and *Streptococcus pneumoniae*. Sci Rep 6: 27156.

Grundmann A, Kuznetsova T, Afiyatullov SS, Li S-M (2008) FtmPT2, an *N*-prenyltransferase from *Aspergillus fumigatus*, catalyses the last step in the biosynthesis of fumitremorgin B. Chembiochem 9:2059-2063

Grundmann A, Li S-M (2005) Overproduction, purification and characterization of FtmPT1, a brevianamide F prenyltransferase from *Aspergillus fumigatus*. Microbiology 151:2199-2207

Guo Z, Li X, Li J, Yang X, Zhou Y, Lu C, Shen Y (2016) Licoflavonol is an inhibitor of the type three secretion system of *Salmonella enterica* serovar Typhimurium. Biochem Biophys Res Commun 477:998-1004

Hamerski D, Schmitt D, Matern U (1990) Induction of two prenyltransferases for the accumulation of coumarin phytoalexins in elicitor-treated *Ammi majus* cell suspension cultures. Phytochemistry 29:1131-1135

Haynes SW, Gao X, Tang Y, Walsh CT (2013) Complexity generation in fungal peptidyl alkaloid biosynthesis: A two-enzyme pathway to the hexacyclic MDR export pump inhibitor ardeemin. ACS Chem Biol 8:741-748

Hegarty JM, Yang H, Chi NC (2013) UBIAD1-mediated vitamin K2 synthesis is required for vascular endothelial cell survival and development. Development 140:1713-1719

Heide L (2009a) Prenyl transfer to aromatic substrates: genetics and enzymology. Curr Opin Chem Biol 13:171-179

Heide L (2009b) The aminocoumarins: biosynthesis and biology. Nat Prod Rep 26:1241-1250

Hossain MM, Kawamura Y, Yamashita K, Tsukayama M (2006) Microwave-assisted regioselective synthesis of natural 6-prenylpolyhydroxyisoflavones and their hydrates with hypervalent iodine reagents. Tetrahedron 62:8625-8635

Hu L-H, Sim K-Y (2000) Sampsoniones A-M, a unique family of caged polyprenylated benzoylphloroglucinol derivatives, from *Hypericum sampsonii*. Tetrahedron 56:1379-1386

Jost M, Zocher G, Tarcz S, Matuschek M, Xie X, Li S-M, Stehle T (2010) Structure-function analysis of an enzymatic prenyl transfer reaction identifies a reaction chamber with modifiable specificity. J Am Chem Soc 132:17849-17858

Kato H, Yoshida T, Tokue T, Nojiri Y, Hirota H, Ohta T, Williams RM, Tsukamoto S (2007) Notoamides A-D: prenylated indole alkaloids isolated from a marine-derived fungus, *Aspergillus* sp. Angew Chem Int Ed Engl 46:2254-2256

REFERENCES

Kato N, Suzuki H, Takagi H, Asami Y, Kakeya H, Uramoto M, Usui T, Takahashi S, Sugimoto Y, Osada H (2009) Identification of cytochrome P450s required for fumitremorgin biosynthesis in *Aspergillus fumigatus*. Chembiochem 10:920-928

Koes RE, Quattrocchio F, Mol JNM (1994) The flavonoid biosynthetic pathway in plants: Function and evolution. BioEssays 16:123-132

Kremer A, Li S-M (2008) Tryptophan aminopeptidase activity of several indole prenyltransferases from *Aspergillus fumigatus*. Chem Biol 15:729-738

Kremer A, Li S-M (2010) A tyrosine *O*-prenyltransferase catalyses the first pathway-specific step in the biosynthesis of sirodesmin PL. Microbiology 156:278-286

Kremer A, Westrich L, Li S-M (2007) A 7-dimethylallyltryptophan synthase from *Aspergillus fumigatus*: overproduction, purification and biochemical characterization. Microbiology 153:3409-3416

Kumano T, Richard SB, Noel JP, Nishiyama M, Kuzuyama T (2008) Chemoenzymatic syntheses of prenylated aromatic small molecules using *Streptomyces* prenyltransferases with relaxed substrate specificities. Bioorg Med Chem 16:8117-8126

Kuzuyama T, Noel JP, Richard SB (2005) Structural basis for the promiscuous biosynthetic prenylation of aromatic natural products. Nature 435:983-987

Lee DYW, Liu Y (2003) Molecular structure and stereochemistry of silybin A, silybin B, isosilybin A, and isosilybin B, isolated from *Silybum marianum* (Milk Thistle). J Nat Prod 66:1171-1174

Li C-S, Li X-M, An C-Y, Wang BG (2014) Prenylated indole alkaloid derivatives from marine sediment-derived fungus *Penicillium paneum* SD-44. Helv Chim Acta 97:1440-1444

Li H, Ban Z, Qin H, Ma L, King AJ, Wang G (2015a) A heteromeric membrane-bound prenyltransferase complex from hop catalyzes three sequential aromatic prenylations in the bitter acid pathway. Plant Physiol 167:650-659

Li S, Lowell AN, Yu F, Raveh A, Newmister SA, Bair N, Schaub JM, Williams RM, Sherman DH (2015b) Hapalindole/ambiguine biogenesis is mediated by a cope rearrangement, C-C bond-forming cascade. J Am Chem Soc 137:15366-15369

Li S-M (2010) Prenylated indole derivatives from fungi: structure diversity, biological activities, biosynthesis and chemoenzymatic synthesis. Nat Prod Rep 27:57-78

Li S-M (2011) Genome mining and biosynthesis of fumitremorgin-type alkaloids in ascomycetes. J Antibiot 64:45-49

Liebhold M, Li S-M (2013) Regiospecific benzylation of tryptophan and derivatives catalyzed by a fungal dimethylallyl transferase. Org Lett 15:5834-5837

Liebhold M, Xie X, Li S-M (2012) Expansion of enzymatic Friedel-Crafts alkylation on indoles: Acceptance of unnatural beta-unsaturated allyl diphospates by dimethylallyl-tryptophan synthases. Org Lett 14:4884-4885

REFERENCES

Liebhold M, Xie X, Li S-M (2013) Breaking cyclic dipeptide prenyltransferase regioselectivity by unnatural alkyl donors. Org Lett 15:3062-3065

Liu M, Hansen PE, Wang G, Liu Q, Dong J, Yin H, Qian Z, Yang M, Miao J (2015) Pharmacological profile of xanthohumol, a prenylated flavonoid from hops (*Humulus lupulus*). Molecules 20:754-779

Ma J, Zuo D, Song Y, Wang B, Huang H, Yao Y, Li W, Zhang S, Zhang C, Ju J (2012) Characterization of a single gene cluster responsible for methylpendolmycin and pendolmycin biosynthesis in the deep sea bacterium *Marinactinospora thermotolerans*. Chembiochem 13:547-552

Magnuson R, Solomon J, Grossman AD (1994) Biochemical and genetic characterization of a competence pheromone from *B. subtilis*. Cell 77:207-216

Mai P, Zocher G, Ludwig L, Stehle T, Li S-M (2016) Actions of tryptophan prenyltransferases toward fumiquinazolines and their potential application for the generation of prenylated derivatives by combining chemical and chemoenzymatic syntheses. Adv Synth Catal 358:1639-1653

Maiya S, Grundmann A, Li S-M, Turner G (2006) The fumitremorgin gene cluster of *Aspergillus fumigatus*: identification of a gene encoding brevianamide F synthetase. Chembiochem 7:1062-1069

McIntosh JA, Donia MS, Nair SK, Schmidt EW (2011) Enzymatic basis of ribosomal peptide prenylation in cyanobacteria. J Am Chem Soc 133:13698-13705

Mercado-Marin EV, Garcia-Reynaga P, Romminger S, Pimenta EF, Romney DK, Lodewyk MW, Williams DE, Andersen RJ, Miller SJ, Tantillo DJ, Berlinck RGS, Sarpong R (2016) Total synthesis and isolation of citrinalin and cyclopiamine congeners. Nature 509:318-324

Metzger U, Schall C, Zocher G, Unsöld I, Stec E, Li S-M, Heide L, Stehle T (2009) The structure of dimethylallyl tryptophan synthase reveals a common architecture of aromatic prenyltransferases in fungi and bacteria. Proc Natl Acad Sci U S A 106:14309-14314

Mireku EA, Mensah MLK, Mensah AY (2016) Prenylated indole alkaloids from the stem bark of *Hexalobus monopetalus*. Phytochemistry Lett 16:108-114

Mori T, Zhang L, Awakawa T, Hoshino S, Okada M, Morita H, Abe I (2016) Manipulation of prenylation reactions by structure-based engineering of bacterial indolactam prenyltransferases. Nat Commun 7:10849

Munakata R, Olry A, Karamat F, Courdavault V, Sugiyama A, Date Y, Krieger C, Silie P, Foureau E, Papon N, Grosjean J, Yazaki K, Bourgaud F, Hehn A (2016) Molecular evolution of parsnip (*Pastinaca sativa*) membrane-bound prenyltransferases for linear and/or angular furanocoumarin biosynthesis. New Phytol 211:332-344

Mundt K, Li S-M (2013) CdpC2PT, a reverse prenyltransferase from *Neosartorya fischeri* with distinct substrate preference from known *C2*-prenyltransferases. Microbiology 159:2169-2179

REFERENCES

Mundt K, Wollinsky B, Ruan HL, Zhu T, Li S-M (2012) Identification of the verruculogen prenyltransferase FtmPT3 by a combination of chemical, bioinformatic and biochemical approaches. Chembiochem 13:2583-2592

Nagalingam SV, Wai-Ling K, Teng-Jin K (2016) Structural derivatization of clusianone and *In vitro* cytotoxicity evaluation targeting respiratory carcinoma cells. Planta Med Lett 3:e10-e13

Nakagawa K, Hirota Y, Sawada N, Yuge N, Watanabe M, Uchino Y, Okuda N, Shimomura Y, Suhara Y, Okano T (2010) Identification of UBIAD1 as a novel human menaquinone-4 biosynthetic enzyme. Nature 468:117-121

Nguyen HN, Kim JH, Hyun WY, Nguyen NT, Hong SW, Lee H (2013) TTG1-mediated flavonols biosynthesis alleviates root growth inhibition in response to ABA. Plant Cell Rep 32:503-514

Noike M, Liu C, Ono Y, Hamano Y, Toyomasu T, Sassa T, Kato N, Dairi T (2012) An enzyme catalyzing *O*-prenylation of the glucose moiety of fusicoccin A, a diterpene glucoside produced by the fungus *Phomopsis amygdali*. Chembiochem 13:566-573

O'Brien M, Nielsen KF, O'Kiely P, Forristal PD, Fuller HT, Frisvad JC (2006) Mycotoxins and other secondary metabolites produced in vitro by *Penicillium paneum* Frisvad and *Penicillium roqueforti* Thom isolated from baled grass silage in Ireland. J Agric Food Chem 54:9268-9276

Ohmomo S, Utagawa T, Abe M (1977) Identification of roquefortine C produced by *Penicillium roqueforti*. Agric Biol Chem 41:2097-2098

Okada M, Sato I, Cho SJ, Iwata H, Nishio T, Dubnau D, Sakagami Y (2005) Structure of the *Bacillus subtilis* quorum-sensing peptide pheromone ComX. Nature Chem Biol 1:23-24

Okada M, Sugita T, Akita K, Nakashima Y, Tian T, Li C, Mori T, Abe I (2016) Stereospecific prenylation of tryptophan by a cyanobacterial post-translational modification enzyme. Org Biomol Chem 14:9639-9644

Okada M, Yamaguchi H, Sato I, Tsuji F, Qi J, Dubnau D, Sakagami Y (2007) Acid labile ComX pheromone from *Bacillus mojavensis* RO-H-1. Biosci Biotechnol Biochem 71:1807-1810

Okada Y, Ito K (2001) Cloning and analysis of valerophenone synthase gene expressed specifically in lupulin gland of hop (*Humulus lupulus* L.). Biosci Biotechnol Biochem 65:150-155

Okada Y, Sano Y, Kaneko T, Abe I, Noguchi H, Ito K (2004) Enzymatic reactions by five chalcone synthase homologs from hop (*Humulus lupulus* L.). Biosci Biotechnol Biochem, 68:1142-1145

Ozaki T, Mishima S, Nishiyama M, Kuzuyama T (2009) NovQ is a prenyltransferase capable of catalyzing the addition of a dimethylallyl group to both phenylpropanoids and flavonoids. J Antibiot 62:385-392

REFERENCES

Ozaki T, Nishiyama M, Kuzuyama T (2013) Novel tryptophan metabolism by a potential gene cluster that is widely distributed among actinomycetes. J Biol Chem 288:9946-9956

Pandey RP, Parajuli P, Koffas MAG, Sohng JK (2016) Microbial production of natural and non-natural flavonoids: Pathway engineering, directed evolution and systems/synthetic biology. Biotechnol Adv 34:634-662

Paniego NB, Zuurbier KWM, Fung SY, van der Heijden R, Schefer JJC, Verpoorte R (1999) Phlorisovalerophenone synthase, a novel polyketide synthase from hop (*Humulus lupulus* L.) cones. Eur J Biochem 262:621-616

Piccinelli AL, Cuesta-Rubio O, Chica MB, Mahmood N, Pagano B, Pavone M, Barone V, Rastrelli L (2005) Structural revision of clusianone and 7-*epi*-clusianone and anti-HIV activity of polyisoprenylated benzophenones. Tetrahedron 61:8206-8211

Pockrandt D, Ludwig L, Fan A, König GM, Li S-M (2012) New insights into the biosynthesis of prenylated xanthones: XptB from *Aspergillus nidulans* catalyses an *O*-prenylation of xanthones. Chembiochem 13:2764-2771

Pojer F, Wemakor E, Kammerer B, Chen H, Walsh CT, Li S-M, Heide L (2003) CloQ, a prenyltransferase involved in clorobiocin biosynthesis. Proc Natl Acad Sci U S A 100:2316-2321

Powell KA, Ramer SW, Del Cardayré S.B., Stemmer WP, Tobin MB, Longchamp PF, Huisman GW (2001) Directed Evolution and Biocatalysis. Angew Chem Int Ed Engl 40:3948-3959

Qi J, Porco JA (2007) Rapid access to polyprenylated phloroglucinols via alkylative dearomatization-annulation: total synthesis of (±)-Clusianone 1. J Am Chem Soc 129:12682-12683

Raju R, Piggott, AM, Huang XC, and Capon R J (2011) Nocardioazines: a novel bridged diketopiperazine scaffold from a marinederived bacterium inhibits p-glycoprotein. Org. Lett. 13, 2770-2773.

Rank C, Phipps RK, Harris P, Frisvad JC, Gotfredsen CH, Larsen TO (2006) *epi*-Aszonalenins A, B, and C from *Aspergillus novofumigatus*. Tetrahedron Lett 47:6099-6102

Robins JG, Kim KJ, Chinn AJ, Woo JS, Scheerer JR (2016) Intermolecular Diels–Alder cycloaddition for the construction of bicyclo[2.2.2]diazaoctane dtructures: formal synthesis of brevianamide B and premalbrancheamide. J Org Chem 81:2293-2301

Rudolf JD, Poulter CD (2013) Tyrosine *O*-prenyltransferase SirD catalyzes *S*-, *C*-, and *N*-prenylations on tyrosine and tryptophan derivatives. ACS Chem Biol 8:2707-2714

Saleh O, Gust B, Boll B, Fiedler H-P, Heide L (2009a) Aromatic prenylation in phenazine biosynthesis: dihydrophenazine-1-carboxylate dimethylallyltransferase from *Streptomyces anulatus*. J Biol Chem 284:14439-14447

REFERENCES

Saleh O, Haagen Y, Seeger K, Heide L (2009b) Prenyl transfer to aromatic substrates in the biosynthesis of aminocoumarins, meroterpenoids and phenazines: The ABBA prenyltransferase family. Phytochemistry 70:1728-1738

Sales L, Pezuk JA, Borges KS, Brassesco MS, Scrideli CA, Tone LG, dos Santos MH, Ionta M, de Oliveira JC (2015) Anticancer activity of 7-epiclusianone, a benzophenone from *Garcinia brasiliensis*, in glioblastoma. BMC Complement Altern Med 15:393

Sandhar HK, Kumar B, Prasher S, Tiwari P, Salhan M, Sharma P (2011) A review of phytochemistry and pharmacology of flavonoids. Intern Pharm Sci 1:25-41

Sasaki K, Mito K, Ohara K, Yamamoto H, Yazaki K (2008) Cloning and characterization of naringenin 8-prenyltransferase, a flavonoid-specific prenyltransferase of *Sophora flavescens*. Plant Physiol 146:1075-1084

Sasaki K, Tsurumaru Y, Yamamoto H, Yazaki K (2011) Molecular characterization of a membrane-bound prenyltransferase specific for isoflavone from *Sophora flavescens*. J Biol Chem 286:24125-24134

Schneider P, Weber M, Hoffmeister D (2008) The *Aspergillus nidulans* enzyme TdiB catalyzes prenyltransfer to the precursor of bioactive asterriquinones. Fungal Genet Biol 45:302-309

Schuller JM, Zocher G, Liebhold M, Xie X, Stahl M, Li S-M, Stehle T (2012) Structure and catalytic mechanism of a cyclic dipeptide prenyltransferase with broad substrate promiscuity. J Mol Biol 422:87-99

Schultz AW, Lewis CA, Luzung MR, Baran PS, Moore BS (2010) Functional characterization of the cyclomarin/cyclomarazine prenyltransferase CymD directs the biosynthesis of unnatural cyclic peptides. J Nat Prod 73:373-377

Schultz AW, Oh DC, Carney JR, Williamson RT, Udwary DW, Jensen PR, Gould SJ, Fenical W, Moore BS (2008) Biosynthesis and structures of cyclomarins and cyclomarazines, prenylated cyclic peptides of marine actinobacterial origin. J Am Chem Soc 130:4507-4516

Seeger K, Flinspach K, Haug-Schifferdecker E, Kulik A, Gust B, Fiedler HP, Heide L (2011) The biosynthetic genes for prenylated phenazines are located at two different chromosomal loci of *Streptomyces cinnamonensis* DSM 1042. Microb Biotechnol 4:252-262

Shen G, Huhman D, Lei Z, Snyder J, Sumner LW, Dixon RA (2012) Characterization of an isoflavonoid-specific prenyltransferase from *Lupinus albus*. Plant Physiol 159:70-80

Shimizu S, Yamamoto Y, Inagaki J, Koshimura S (1982a) Antitumor effect and structure-activity relationship of asterriquinone analogs. Gann 73:642-648

Shimizu S, Yamamoto Y, Koshimura S (1982b) Antitumor activity of asterriquinones from *Aspergillus* fungi. IV. An attempt to modify the structure of asterriquinones to increase the activity. Chem Pharm Bull (Tokyo) 30:1896-1899

REFERENCES

Shimizu Y, Shi SL, Usuda H, Kanai M, Shibasaki M (2010) Catalytic asymmetric total synthesis of *ent*-Hyperforin. Angew Chem Int Ed 49:1103-1106

Simpkins NS, Pavlakos L, Weller MD, Male L (2013) The cascade radical cyclisation approach to prenylated alkaloids: synthesis of stephacidin A and notoamide B. Org Biomol Chem 11:4957-4970

Socolsky C, Salamanca E, Giménez A, Borkosky SA, Bardón A (2016) Prenylated acylphloroglucinols with leishmanicidal activity from the fern *Elaphoglossum lindbergii*. J Nat Prod 79:98-105

Song C, Ring L, Hoffmann T, Huang FC, Slovin J, Schwab W (2016a) Acylphloroglucinol biosynthesis in strawberry fruit. Plant Physiol 169:1656-1670

Song X, Diao J, Ji J, Wang G, Guan C, Jin C, Wang Y (2016b) Molecular cloning and identification of a flavanone 3-hydroxylase gene from Lycium chinense, and its overexpression enhances drought stress in tobacco. Plant Physiol Biochem 98:89-100

Steffan N, Grundmann A, Afiyatullov A, Ruan H, Li S-M (2009) FtmOx1, a non heme Fe(II) and alpha-ketoglutarate-dependent dioxygenase, catalyses the endoperoxide formation of verruculogen in *Aspergillus fumigatus*. Org Biomol Chem 7:4082-4087

Steffan N, Unsöld IA, Li S-M (2007) Chemoenzymatic synthesis of prenylated indole derivatives by using a 4-dimethylallyltryptophan synthase from *Aspergillus fumigatus*. Chembiochem 8:1298-1307

Steyn PS (1971) Austamide, a new toxic metabolite from *Aspergillus ustus*. Tetrahedron Lett 36:3331-3334

Sunassee SN, Davies-Coleman MT (2012) Cytotoxic and antioxidant marine prenylated quinones and hydroquinones. Nat Prod Rep 29:513-535

Sunderhaus JD, McAfoos TJ, Finefield JM, Kato H, Li S, Tsukamoto S, Sherman DH, Williams RM (2013) Synthesis and bioconversions of notoamide T: a biosynthetic precursor to stephacidin A and notoamide B. Org Lett 15:22-25

Takahashi S, Takagi H, Toyoda A, Uramoto M, Nogawa T, Ueki M, Sakaki Y, Osada H (2010) Biochemical characterization of a novel indole prenyltransferase from *Streptomyces* sp. SN-593. J Bacteriol 192:2839-2851

Tanaka N, Mamemura T, Shibazaki A, Gonoi T, Kobayashi J (2011) Yojironins E-I, prenylated acylphloroglucinols from *Hypericum yojiroanum*. Bioorg Med Chem Lett 21:5393-5397

Tanaka N, Otani M, Kashiwada Y, Takaishi Y, Shibazaki A, Gonoi T, Shiro M, Kobayashi J (2010) Petiolins J–M, prenylated acylphloroglucinols from *Hypericum pseudopetiolatum* var. *kiusianum*. Bioorg Med Chem Lett 20:4451-4455

Tang MC, Zou Y, Watanabe K, Walsh C, Tang Y (2017) Oxidative cyclization in natural product biosynthesis. Chem Rev DOI: 10.1021/acs.chemrev.6b00478

REFERENCES

Tanner ME (2015) Mechanistic studies on the indole prenyltransferases. Nat Prod Rep 32:88-101

Tarcz S, Ludwig L, Li S-M (2014a) AstPT catalyses both reverse *N1*- and regular *C2*-prenylation of a methylated bisindolyl benzoquinone. Chembiochem 15:108-116

Tarcz S, Xie X, Li S-M (2014b) Substrate and catalytic promiscuity of secondary metabolite enzymes: *O*-prenylation of hydroxyxanthones with different prenyl donors by a bisindolyl benzoquinone *C*- and *N*-prenyltransferase. RSC Adv 4:17986-17992

Tello M, Kuzuyama T, Heide L, Noel JP, Richard SB (2008) The ABBA family of aromatic prenyltransferases: broadening natural product diversity. Cell Mol Life Sci 65:1459-1463

Tian WJ, Yu Y, Yao XJ, Chen HF, Dai Y, Zhang XK, Yao XS (2014) Norsampsones A-D, four new decarbonyl polycyclic polyprenylated acylphloroglucinols from *Hypericum sampsonii*. Org Lett 16:3448-3451

Tischer S, Metz P (2007) Selective C-6 prenylation of flavonoids *via* europium(III)-catalyzed claisen rearrangement and cross-metathesis. Adv Synth Catal 349:147-151

Tsai HF, Wang H, Gebler JC, Poulter CD, Schardl CL (1995) The *Claviceps purpurea* gene encoding dimethylallyltryptophan synthase, the committed step for ergot alkaloid biosynthesis. Biochem Biophys Res Commun 216:119-125

Tsukamoto S, Kato H, Greshock TJ, Hirota H, Ohta T, Williams RM (2009a) Isolation of notoamide E, a key precursor in the biosynthesis of prenylated indole alkaloids in a marine-derived fungus, *Aspergillus* sp. J Am Chem Soc 131:3834-3835

Tsukamoto S, Kawabata T, Kato H, Greshock TJ, Hirota H, Ohta T, Williams RM (2009b) Isolation of antipodal (-)-versicolamide B and notoamides L-N from a marine-derived *Aspergillus* sp. Org Lett 11:1297-1300

Tsukano C, Siegel DR, Danishefsky SJ (2007) Differentiation of nonconventional "carbanions"—the total synthesis of nemorosone and clusianone. Angew Chem Int Ed 46:8840-8844

Tsurumaru Y, Sasaki K, Miyawaki T, Uto Y, Momma T, Umemoto N, Momose M, Yazaki K (2012) HlPT-1, a membrane-bound prenyltransferase responsible for the biosynthesis of bitter acids in hops. Biochem Biophys Res Commun 417:393-398

Unsöld IA, Li S-M (2005) Overproduction, purification and characterization of FgaPT2, a dimethylallyltryptophan synthase from *Aspergillus fumigatus*. Microbiology 151:1499-1505

Van Cleemput M, Cattoor K, De Bosscher K., Haegeman G, De Keukeleire D, Heyerick A (2009) Hop (*Humulus lupulus*)-derived bitter acids as multipotent bioactive compounds. J Nat Prod 72:1220-1230

van de Schans MGM, Ritschel T., Bovee TF, Sanders MG, de Waard P, Gruppen H, Vincken JP (2015) Involvement of a hydrophobic pocket and helix11 in determining the modes of action of prenylated flavonoids and isoflavonoids in the human estrogen receptor. Chembiochem 16:2668-2677

REFERENCES

Wakana D, Hosoe T, Itabashi T, Nozawa K, Okada K, Takaki GMdC, Yaguchi T, Fukushima K, Kawai KI (2006) Isolation of isoterrein from *Neosartorya fischeri*. Mycotoxins 56:3-6

Wallwey C, Li S-M (2011) Ergot alkaloids: structure diversity, biosynthetic gene clusters and functional proof of biosynthetic genes. Nat Prod Rep 28:496-510

Wang R, Chen R, Li J, Liu X, Xie K, Chen D, Peng Y, Dai J (2016) Regiospecific prenylation of hydroxyxanthones by a plant flavonoid prenyltransferase. J Nat Prod 79:2143-2147

Wang R, Chen R, Li J, Liu X, Xie K, Chen D, Yin Y, Tao X, Xie D, Zou J, Yang L, Dai J (2014) Molecular characterization and phylogenetic analysis of two novel regio-specific flavonoid prenyltransferases from *Morus alba* and *Cudrania tricuspidata*. J Biol Chem 289:35815-35825

Wätjen W, Weber N, Lou YJ, Wang ZQ, Chovolou Y, Kampkötter A, Kahl R, Proksch P (2007) Prenylation enhances cytotoxicity of apigenin and liquiritigenin in rat H4IIE hepatoma and C6 glioma cells. Food Chem Toxicol 45:119-124

White MD, Payne KA, Fisher K, Marshall SA, Parker D, Rattray NJ, Trivedi DK, Goodacre R, Rigby SE, Scrutton NS, Hay S, Leys D (2015) UbiX is a flavin prenyltransferase required for bacterial ubiquinone biosynthesis. Nature 522:502-506

Williams RM, Stocking EM, Sanz-Cervera JF (2000) Biosynthesis of prenylated alkaloids derived from tryptophan. Topics Curr Chem 209:97-173

Winkelblech J, Fan A, Li S-M (2015a) Prenyltransferases as key enzymes in primary and secondary metabolism. Appl Microbiol Biotechnol 99:7379-7397

Winkelblech J, Li S-M (2014) Biochemical investigations of two 6-DMATS enzymes from *Streptomyces* revealing novel features of L-tryptophan prenyltransferases. Chembiochem 15:1030-1039

Winkelblech J, Liebhold M, Gunera J, Xie X, Kolb P, Li S-M (2015b) Tryptophan *C5*-, *C6*- and *C7*-prenylating enzymes displaying a preference for C-6 of the indole ring in the presence of unnatural dimethylallyl diphosphate analogues. Adv Synth Catal 357:975-986

Wollinsky B, Ludwig L, Xie X, Li S-M (2012) Breaking the regioselectivity of indole prenyltransferases: identification of regular *C3*-prenylated hexahydropyrrolo[2,3-b]indoles as side products of the regular *C2*-prenyltransferase FtmPT1. Org Biomol Chem 10:9262-9270

Woodside AB, Huang Z, Poulter CD (1988) Trisammonium geranyl diphosphate. Org Synth 66:211-215

Wu S-B, Long C, Kennelly EJ (2014) Structural diversity and bioactivities of natural benzophenones. Nat Prod Rep 31:1158-1174

Yamamoto Y, Kiriyama N, Shimizu S, Koshimura S (1976a) Antitumor activity of asterriquinone, a metabolic product from *Aspergillus terreus*. Gann 67:623-624

REFERENCES

Yamamoto Y, Nishimura K, Kiriyama N (1976b) Studies on the metabolic products of *Aspergillus terreus*. I. Metabolites of the strain IFO 6123. Chem Pharm Bull 24:1853-1859

Yang X, Yang J, Jiang Y, Yang H, Yun Z, Rong W, Yang B (2016) Regiospecific synthesis of prenylated flavonoids by a prenyltransferase cloned from *Fusarium oxysporum*. Sci Rep 6: 24819

Yazaki K, Sasaki K, Tsurumaru Y (2009) Prenylation of aromatic compounds, a key diversification of plant secondary metabolites. Phytochemistry 70:1739-1745

Yin S, Yu X, Wang Q, Liu XQ, Li S-M (2013) Identification of a brevianamide F reverse prenyltransferase BrePT from *Aspergillus versicolor* with a broad substrate specificity towards tryptophan-containing cyclic dipeptides. Appl Microbiol Biotechnol 97:1649-1660

Yin W-B, Cheng J, Li S-M (2009a) Stereospecific synthesis of aszonalenins by using two recombinant prenyltransferases. Org Biomol Chem 7:2202-2207

Yin W-B, Grundmann A, Cheng J, Li S-M (2009b) Acetylaszonalenin biosynthesis in *Neosartorya fischeri*: Identification of the biosynthetic gene cluster by genomic mining and functional proof of the genes by biochemical investigation. J Biol Chem 284:100-109

Yin W-B, Ruan H-L, Westrich L, Grundmann A, Li S-M (2007) CdpNPT, an *N*-prenyltransferase from *Aspergillus fumigatus*: overproduction, purification and biochemical characterisation. Chembiochem 8:1154-1161

Yin W-B, Xie X-L, Matuschek M, Li S-M (2010a) Reconstruction of pyrrolo[2,3-*b*]indoles carrying an α-configured reverse *C3*-dimethylallyl moiety by using recombinant enzymes. Org Biomol Chem 8:1133-1141

Yin W-B, Yu X, Xie X-L, Li S-M (2010b) Preparation of pyrrolo[2,3-*b*]indoles carrying a ß-configured reverse *C3*-dimethylallyl moiety by using a recombinant prenyltransferase CdpC3PT. Org Biomol Chem 8:2430-2438

Yu H, Liebhold M, Xie X, Li S-M (2015a) Tyrosine *O*-prenyltransferases TyrPT and SirD displaying similar behavior toward unnatural alkyl or benzyl diphosphate as their natural prenyl donor dimethylallyl diphosphate. Appl Microbiol Biotechnol 99:7115-7124

Yu Q, Ravu RR, Xu QM, Ganji S, Jacob MR, Khan SI, Yu BY (2015b) Antibacterial prenylated acylphloroglucinols from *Psorothamnus fremontii*. J Nat Prod 78:2748-2753

Yu X, Yang A, Lin W, Li S-M (2012a) Friedel-Crafts alkylation on indolocarbazoles catalyzed by two dimethylallyltryptophan synthases from *Aspergillus*. Tetrahedron Lett 53:6861-6864

Yu X, Li S-M (2011) Prenylation of flavonoids by using a dimethylallyltryptophan synthase 7-DMATS from *Aspergillus fumigatus*. Chembiochem 12:2280-2283

Yu X, Li S-M (2012) Prenyltransferases of the dimethylallyltryptophan synthase superfamily. Methods Enzymol 516:259-278

REFERENCES

Yu X, Liu Y, Xie X, Zheng X-D, Li S-M (2012b) Biochemical characterization of indole prenyltransferases: Filling the last gap of prenylation positions by a 5-dimethylallyltryptophan synthase from *Aspergillus clavatus*. J Biol Chem 287:1371-1380

Yu X, Xie X, Li S-M (2011) Substrate promiscuity of secondary metabolite enzymes: prenylation of hydroxynaphthalenes by fungal indole prenyltransferases. Appl Microbiol Biotechnol 92:737-748

Yu X, Zocher G, Xie X, Liebhold M, Schütz S, Stehle T, Li S-M (2013) Catalytic mechanism of stereospecific formation of *cis*-configured prenylated pyrroloindoline diketopiperazines by indole prenyltransferases. Chem Biol 20:1492-1501

Zelová H, Hanáková Z, Čermáková Z, Šmejkal K, Dalí Acqua S, Babula P, Cvačka J, Hošek J. (2014) Evaluation of anti-inflammatory activity of prenylated substances isolated from *Morus alba* and *Morus nigra*. J Nat Prod 77:1297-1303

Zhang JJ, Yang J, Liao Y, Yang XW, Ma JZ, Xiao QL, Yang LX, Xu G (2014) Hyperuralones A and B, new acylphloroglucinol derivatives with intricately caged cores from *Hypericum uralum*. Org Lett 16:4912-4915

Zhang P, Li XM, Wang JN, Li X, Wang BG (2015) Prenylated indole alkaloids from the marine-derived fungus *Paecilomyces variotii*. Chinese Chem Lett 26:316

Zhao W, Zhuang Y, Bai Y, Bi H, Liu T, Ma Y (2016) Biosynthesis of phlorisovalerophenone and 4-hydroxy-6-isobutyl-2-pyrone in *Escherichia coli* from glucose. Microb Cell Fact 15:149

Zocher G, Saleh O, Heim JB, Herbst DA, Heide L, Stehle T (2012) Structure-based engineering increased the catalytic turnover rate of a novel phenazine prenyltransferase. PLoS One 7:e48427

Zou H-X, Xie X, Zheng X-D, Li S-M (2011) The tyrosine *O*-prenyltransferase SirD catalyzes *O*-, *N*-, and *C*-prenylations. Appl Microbiol Biotechnol 89:1443-1451

Zou H-X, Xie X-L, Linne U, Zheng X-D, Li S-M (2010) Simultaneous *C7*- and *N1*-prenylation of cyclo-L-Trp-L-Trp catalyzed by a prenyltransferase from *Aspergillus oryzae*. Org Biomol Chem 8:3037-3044

Zou Y, Zhan Z, Li D, Tang M, Cacho RA, Watanabe K, Tang Y (2015) Tandem prenyltransferases catalyze isoprenoid elongation and complexity generation in biosynthesis of quinolone alkaloids. J Am Chem Soc 137:4980-4983

Acknowledgements

Firstly, I would like to express my deepest and sincere gratitude to Prof. Dr. Shu-Ming Li for accepting me as his PhD student and for his excellent supervision, guidance, and care during the past three years over the course of this thesis. I have learned not only the knowledge on biochemistry and molecular biology, but also scientific thinking, hard-working, and high efficiency on arrangement of works from him, which I could benefit for my whole life.

I am grateful to Prof. Dr. Peter Kolb for acting as second referee and examiner.

I would like to thank Dr. Xiulan Xie, Dr. Regina Ortmann and Stefan Newel for taking NMR spectra as well as Rixa Kraut and Nina Zitzer for taking mass spectra. I would also like to thank Buvac Drázen for preparing media and Dr. Dieter Kreusch and Sabine Burgers for ordering chemicals as well as lab supplies and maintenance of laboratory equipment.

My deep and special thanks go to Dr. Aili Fan for her friendship and support in both my personal and official life. And also my deep and special thanks to Florian Kindinger and Huili Yu for the guidance patiently and sharing their ideas with me for my gene deletion project. I would like to express my special gratitude to Linus Naumann for translating the summary part of this dissertation, Lindsay Coby for proofreading the summary, and Dr. Wen-Xuan Wang and Dr. Gang Li for proofreading this dissertation. Thanks to Dr. Katija Backhaus, Viola Wohlgemuth, Kirsten Brockmeyer, Elisabeth Hühner, Kristin Malin Öqvist, and Jing Liu for expanding my biological horizon. Thanks to Lena Ludwig, Dr. Aili Fan, Dr. Julia Winkelblech, Bastian Kemmerich, Jonas Nies, Jie Fan, Peter Mai, Lena Mikulski, and Ge Liao for sharing experience with me for HPLC maintenance.

I also want to thank all my current and former colleagues in the institute, including Julia Wohl, Victoria Werner, Thang Son Ta, Johanna Schäfer, Jennifer Robinson, Lennart Poppe, Agus Chahyadi, Dr.Soheil Pezeshki, Nina Gerhards, Alexander Frehse, Huomiao Ran, Liujuan Zheng, Dr. Xia Yu, Dr. Sylwia Tarcz, Dr. Beate Wollinsky, Dr. Daniel Pockrandt, Dr. Carsten Wunsch, Dr. Kathrin Mundt, and Dr. Mike Liebhold for the great and wonderful time. In the meantime, I would also like to express my thanks to the short-term communication Professors and students in our institute for the wonderful sightseeing together.

My special thanks also to my friends Xiao-Hong Tan, Jing-Wei Sun, Songya Zhang, Xiao-Wei Han, Han Han, Yan Zhou, Chen Shi, An-Ning Zhang, Biao Ouyang, Hou-Hu Song, Cheng-Cheng Song, Si-Yan Yu, Jing Zhao, Dr. Hui-Yan Lin, Dr. Hui-Qin Chen, Dr. Jie Li, and Xia Li for their motivational pushes and support.

I deeply thank my family, for their love, encouragement, and unconditional support over all the years.

At last, thanks for the China Scholarship Council (CSC) for financial support.

Erklärung

ERKLÄRUNG

Ich, Kang Zhou, versichere, dass ich meine Dissertation

„Anwendungen von pilzlichen Prenyltransferasen in der Chemoenzymatischen Synthese"

selbständig, ohne unerlaubte Hilfe angefertigt und mich dabei keiner anderen als der von mir ausdrücklich bezeichneten Quellen bedient habe. **Alle vollständig oder sinngemäß übernommenen Zitate sind als solche gekennzeichnet.**

Die Dissertation wurde in der jetzigen oder einer ähnlichen Form noch bei keiner anderen Hochschule eingereicht und hat noch keinen sonstigen Prüfungszwecken gedient.

Marburg, den..........................

....
(Unterschrift mit Vor- und Zuname)

Page 180 (Curriculum vitae) contains personal data. It is therefore not part of the online-publication of this thesis.